Lappeenranta
University of Technology

Eveliina Repo

EDTA- AND DTPA-FUNCTIONALIZED SILICA GEL AND CHITOSAN ADSORBENTS FOR THE REMOVAL OF HEAVY METALS FROM AQUEOUS SOLUTIONS

Thesis for the degree of Doctor of Science (Technology) to be presented
with due permission for public examination and criticism in the
Auditorium in MUC, Mikkeli University Consortium, Mikkeli, Finland on
the 5th of August, 2011 at noon.

Acta Universitatis
Lappeenrantaensis 437

Supervisor Professor Mika Sillanpää
Department of Energy and Environmental Technology
Laboratory of Green Chemistry
Lappeenranta University of Technology
Mikkeli, Finland

Reviewers Professor Roman Zarzycki
Department of Environmental
Engineering Systems
Technical University of Lodz
Poland

Professor Rui Alfredo da Rocha Boaventura
Department of Chemical Engineering
University of Porto
Portugal

Opponent Professor Roman Zarzycki
Department of Environmental
Engineering Systems
Technical University of Lodz
Poland

ISBN 978-952-265-107-5
ISBN 978-952-265-108-2 (PDF)
ISSN 1456-4491
Lappeenrannan teknillinen yliopisto
Digipaino 2011

ABSTRACT

Eveliina Repo
EDTA- and DTPA-functionalized silica gel and chitosan adsorbents for the removal of heavy metals from aqueous solutions
Lappeenranta 2011
p. 104
Acta Universitatis Lappeenrantaensis 437
Diss. Lappeenrannan teknillinen yliopisto
ISBN 978-952-265-107-5, ISBN 978-952-265-108-2 (PDF), ISSN 1456-4491

Adsorbents functionalized with chelating agents are effective in removal of heavy metals from aqueous solutions. Important properties of such adsorbents are high binding affinity as well as regenerability. In this study, aminopolycarboxylic acid, EDTA and DTPA, were immobilized on the surface of silica gel, chitosan, and their hybrid materials to achieve chelating adsorbents for heavy metals such as Co(II), Ni(II), Cd(II), and Pb(II).

New knowledge about the adsorption properties of EDTA- and DTPA-functionalized adsorbents was obtained. Experimental work showed the effectiveness, regenerability, and stability of the studied adsorbents. Both advantages and disadvantages of the adsorbents were evaluated. For example, the EDTA-functionalized chitosan-silica hybrid materials combined the benefits of the silica gel and chitosan while at the same time diminishing their observed drawbacks.

Modeling of adsorption kinetics and isotherms is an important step in design process. Therefore, several kinetic and isotherm models were introduced and applied in this work. Important aspects such as effect of error function, data range, initial guess values, and linearization were discussed and investigated. The selection of the most suitable model was conducted by comparing the experimental and simulated data as well as evaluating the correspondence between the theory behind the model and properties of the adsorbent. In addition, modeling of two-component data was conducted using various extended isotherms. Modeling results for both one- and two-component systems supported each other.

Finally, application testing of EDTA- and DTPA-functionalized adsorbents was conducted. The most important result was the applicability of DTPA-functionalized silica gel and chitosan in the capturing of Co(II) from its aqueous EDTA-chelate. Moreover, these adsorbents were efficient in various solution matrices. In addition, separation of Ni(II) from Co(II) and Ni(II) and Pb(II) from Co(II) and Cd(II) was observed in two- and multimetal systems. Lastly, prior to their analysis, EDTA- and DTPA-functionalized silica gels were successfully used to preconcentrate metal ions from both pure and salty waters.

Keywords: water treatment, chelating agent, heavy metals, adsorption isotherm, adsorption kinetics, modeling

UDC 661.183:628.16:663.63:544.723:546.4:546.7:546.8

PREFACE

The research work for this PhD-thesis was conducted at the Laboratory of Green Chemistry (formerly Laboratory of Applied Environmental Chemistry, University of Eastern Finland) in Mikkeli during February 2007 - March 2011.

I am highly grateful for my supervisor Professor Mika Sillanpää for providing me the opportunity to carry out this study and for the support during the whole course of this work. In addition, I would like to thank Dr. Jolanta Warchol for the valuable guidance in experimental work, data analysis, and preparation of manuscripts. For the financial support, I gratefully acknowledge the Finnish Funding Agency for Technology and Innovation (Tekes), Environmental Science and Technology Graduate School (EnSTe), and Mikkeli University Consortum (MUC).

I express my gratitude to Professor Roman Zarzycki and Professor Rui Alfredo da Rocha Boaventura, the reviewers of this thesis, for their constructive comments.

I would like to thank Professor Risto Harjula, Dr. Risto Koivula, and M.Sc. Leena Malinen from the University of Helsinki for the great co-operation during this project. I also gratefully acknowledge Dr. Tonni Kurniawan, Dr. Amit Bhatnagar, and Professor Roman Petrus for their contribution as co-authors. Furthermore, I would like to acknowledge Dr. Mary Metzler and Dr. Shannon Kuismanen for the language revisions.

I am very grateful for the staff of the Laboratory of Green Chemistry for all the support and help. Most of all I would like to thank Heikki Särkkä for his priceless help during my work. In addition, I would like to thank Erasmus students Karina and Marcin for being my extra hands in the laboratory.

Finally, I would like to thank my family for everything. My deepest gratitude goes to my parents for their support during my entire life. Especially, they encouraged me to reach for the higher education and enabled my studies right from the beginning. I would also like to thank my sister, Anna-Kaisa, for showing me an example when selecting the study place after high school and all the guidance during my studies. My special thanks go to my sister, Päivikki, for being my closest friend and best possible listener during the recent years. I also thank my brother, Pekka, for helping me whenever I needed. Furthermore, I am highly grateful for all my friends for being in my life.

Last but not least I would like to express my gratitude to Jarno for his understanding and support.

A profound interest and enthusiasm for research and science made this work possible.

Mikkeli, August, 2011

Eveliina Repo

LIST OF PUBLICATIONS

I Repo, E., Kurniawan, T.A., Warchol, J.K., Sillanpää, M.E.T., Removal of Co(II) and Ni(II) ions from contaminated water using silica gel functionalized with EDTA and/or DTPA as chelating agents, J. Hazard. Mater. 171 (2009) 1071-1080.

II Repo, E., Warchol, J.K., Kurniawan, T.A., Sillanpää, M.E.T., Adsorption of Co(II) and Ni(II) by EDTA- and/or DTPA-modified chitosan: kinetic and equilibrium modeling, Chem. Eng. J.161 (2010) 73-82.

III Repo, E., Warchoł, J.K., Bhatnagar, A., Sillanpää, M., Heavy metals adsorption by novel EDTA-modified chitosan-silica hybrid materials, J. Colloid. Int. Sci. 358 (2011) 261-267.

IV Repo, E., Petrus, R., Sillanpää, M., Warchoł, J.K., Equilibrium studies on the adsorption of Co(II) and Ni(II) by modified silica gels: one-component and binary systems, Chem. Eng. J. (2011) DOI: 10.1016/j.cej.2011.06.019 (in press).

V Repo, E., Malinen, L.K., Koivula, R., Harjula, R., Sillanpää, M., Capture of Co(II) from its aqueous EDTA-chelate by DTPA-modified silica gel and chitosan, J. Hazard. Mater. 187 (2011) 122-132.

The author's contribution in the publications

I The author carried out all experiments, analyzed the data, and prepared the first draft of the manuscript.

II The author carried out all experiments, analyzed the most of the data, and prepared the first draft of the manuscript.

III The author carried out most of the experiments, analyzed data, and prepared the first draft of the manuscript.

IV The author planned and supervised most of the experiments. Data was analyzed and the manuscript prepared together with the co-authors.

V The author carried out all experiments, analyzed data, and prepared the first draft of the manuscript.

TABLE OF CONTENTS

NOMENCLATURE

List of symbols

A	Surface area	cm^2
A_E	Elovich model parameter	mmol/min g
A_T	Temkin maximum binding energy	L/mmol
a_T	Toth adsorptive potential constant	mmol/L
b	Langmuir constant (gas/solid adsorption)	
B_{DR}	Dubinin-Radushkevich constant	$mmol^2/J^2$
B_E	Elovich model parameter	g/mmol
b_T	Temkin constant	-
B_T	Temkin constant related to the heat of adsorption	J/mol
C	Intraparticle diffusion constant	mmol/g
C_e	Equilibrium concentration	mmol/L or mg/L
C_i	Initial concentration	mmol/L or mg/L
E_{ads}	Mean free energy of the adsorption	J/mmol
E_{des}	Activation energy of desorption	J/mol
G	Standard Gibbs free energy	J or J/mol
k_1	Pseudo-first-order rate constant	1/min
k_2	Pseudo-second-order rate constant	g/mmol min
K_{ads}	Equilibrium constant of adsorption	mmol/L
K_d	Distribution ratio	mL/g
k_{dif}	Diffusion rate constant	$mmol/g\ min^{1/2}$
k_{des}	Rate of desorption from fully covered surface	mol/cm^2s
$k_{des\infty}$	Rate constant of desorption at infinite T	mol/cm^2s
K_{eq}	Thermodynamic equilibrium constant of adsorption	L/mmol
K_{BiL}	BiLangmuir affinity constant	$(mmol/g)/(L/mmol)^{1/nF}$
K_F	Freundlich affinity constant	L/mmol
K_{FS}	Fritz-Schlunder affinity constant	L/mmol
K_L	Langmuir affinity constant	L/mmol
K_{RP}	Redlich-Peterson affinity constant	L/mmol
K_S	Sips affinity constant	L/mmol or
M	Molecular mass	g/mol
m	Weight of the adsorbent	g
m_T	Toth heterogeneity factor	-

n	Quantity of material / Number of data points	mol / -
N	Primary hydration number	-
n_F	Freundlich heterogeneity factor	-
n_{FS}	Fritz-Schlunder heterogeneity factor	-
n_{Gen}	General adsorption heterogeneity factor	-
n_{RP}	Redlich-Peterson heterogeneity factor	-
n_S	Sips heterogeneity factor	-
m_{FS}	Fritz-Schlunder heterogeneity factor	-
P	Pressure	Pa
p	Number of parameters	-
Q	Heat of adsorption	J/mol
q_e	Equilibrium adsorption capacity	mmol/g
q_m	Maximum adsorption capacity	mmol/g
q_t	Adsorption capacity at time t	mmol/g
R^2	Coefficient of determination/correlation coefficient	-
R_{ads}	Rate of adsorption on bare surface	mol/cm^{2}s
R_{des}	Rate of desorption from the surface	mol/cm^{2}s
R_g	Ideal gas constant	8.314 J/Kmol
R_H	Hydrated radius	Å
R_s	Collision rate of molecules to the surface	mol/cm^{2}s
S	Entropy	J/K or J/molK
T	Temperature	K or ^{o}C
U	Internal energy	J or J/mol
V	Volume of the solution	L or cm^3
α	Striking coefficient, phase	-
β	Phase	-
χ^2	Non-linear reduced chi-square	-
ε	Polanyi potential	J/mmol
γ	Surface tension	J/cm^2
Γ	Surface excess	mol/cm^2
μ	Chemical potential	J/mol
θ	Fractional coverage	-
σ	Plane interface	-

Abbreviations

AN-DVB	Acrylonitrile-divinylbenzene
APCA	Aminopolycarboxylic acid
APTES	(3-aminopropyl)triethoxysilane
ARE	The average relative error
calc	Calculated
CE	Capillary electrophoresis
DTPA	Diethylenetriaminepentaacetic acid
EABS	The sum of absolute errors
EDAC	1-ethyl-3-(3-dimethylaminopropyl)carbodiimide
EDTA	Ethylenediaminetetraacetic acid
EPR	Electron paramagnetic resonance
ERRSQ	The sum of the square of the errors
ESR	Electron spin resonance
exp	Experimental
FTIR	Fourier transform infrared spectroscopy
HAc	Acetic acid
HEDP	1-hydroxyethylene-1,1-diphosphonic acid
HYBRID	The hybrid error function
ICP-MS	Inductively coupled plasma mass spectrometry
ICP-OES	Inductively coupled plasma optical emission spectrometry
IDA	Iminodiacetic acid
LDH	Layered double hydroxide
ME	Mean error
MPSD	Marquardt's percent standard deviation
NTA	Nitrilotriacetic acid
PAMAM	Polyamidoamine
PBA	Polybenzylamine
PS	Polystyrene
PS1	Pseudo-first-order
PS2	Pseudo-second-order
PVA	Polyvinylalcohol
SBA-15	Mesoporous silica
SEM	Scanning electron microscope
SNE	Sum of normalized errors
TEOS	Tetraethylorthosilicate
XRD	X-Ray diffraction

1 INTRODUCTION

1.1 Basic concepts and theory of adsorption

Adsorption is a process in which a component accumulates at the common boundary of two phases. The accumulating component from the gas or liquid phase is called adsorbate and the adsorbing material the adsorbent [1]. Over the past thirty years adsorption technology has become a major unit operation used in petrochemical industries, production of industrial gases, and air and water purification [2]. Modeling of adsorption equilibrium as well as kinetics, however, has become more and more important for a fast and successful process design [3]. Therefore, the first section of this work concentrates on the basic concepts and principles of the adsorption phenomena as well as theoretical isotherm and kinetic models.

1.1.1 Chemisorption and physisorption

There are different ways to categorize adsorption. One of them is chemical and physical adsorption [4]. Basically, the difference between these two processes is a binding mechanism. For example, nitrogen gas binding on the solid surface at 77 K is physisorption and metal binding by surface chelating groups, chemisorption. Characteristics of chemisorption and physisorption are compared in Table 1.

Table 1. Comparison of chemisorption and physisorption [4].

	Chemisorption	Physisorption
Type of interaction	Covalent bond	Van der Waals, hydrogen bonding, hydrophobic interactions
Heat of the adsorption (kcal/mol)	10-100	5-10
Effect of temperature	Occurs at wide temperature range	Occurs at low temperatures
Reversibility	Irreversible or reversible	Irreversible
Layer forming	Only monolayers	Mono- or multilayers

1.1.2 Adsorption, ion-exchange, and surface complexation/chelation

In general, sorption processes can be divided into adsorption and ion-exchange. While in adsorption a component directly binds onto the surface, in ion-exchange a component from the fluid phase exchanges places with a component bound to the surface. Usually, exchanging components have a similar charge.

In some cases, however, drawing the line between adsorption and ion-exchange is complicated. Usually, the sorption process is dependent on the pH. This means that for example acidic surface groups can be protonated at low pH, but protons can still be replaced by cations through the ion-exchange mechanism. On the other hand, at higher pH, surface groups can be negatively charged and then directly adsorb dissolved cations. Sorption materials that can bind target compounds by both adsorption and ion-exchange are for example complexing/chelating resins with three dimensional ligands [5]. Instead of using either of these two sorption terms, a concept of surface complexation or chelation can be applied. In this study, however, the term adsorption is generally used to describe the surface binding phenomena of metal ions by chelating agents.

1.1.3 Electric double-layer and zeta-potential

Particles in liquids or suspensions are usually charged because of the ionizable groups on the particle surfaces. The charge of the particle is important factor in determining its adsorption properties. A particle with a certain surface charge is surrounded by the ions with the opposite charge (countercharge). These ions as well as solvent molecules nearby are in thermal motion, which causes the dispersion of the countercharge forming a diffusion layer (Figure 1) [6,7].

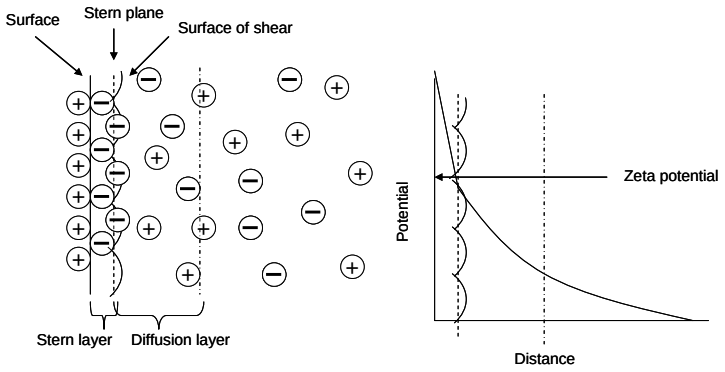

Figure 1. Planes, layers, and the electrostatic potential near a charged particle [modified from refs. 6 and 7].

The surface charge of the particles is determined by applying electric field and measuring particle mobility. The particles move to the direction of oppositely charged electrode. Counter ions closest to the particle surface tend to pull particles to the other direction, however, and some of the counter ions will move with the particle. These counter ions constitute the Stern layer as observed in Figure 1.

The electrostatic potential between the surface and closest counter ions changes more rapidly than the potential through the diffusion layer (Figure 1). The surface, which separates the bound charge and diffusion charge around the particle, marks where the particle and solution move in opposite directions. It is called the surface of share. The electrostatic potential on that surface is called the zeta potential, which can be measured from the movement of particles. When the absolute value of the zeta potential is higher than 25 V, the system is stable. In an unstable system, repulsive forces between the particles are not strong enough to keep particles dispersed and aggregation occurs [6].

1.1.4 Thermodynamics of adsorption

The fundamental method examining the thermodynamics of surface phenomena was presented by Young and then developed by Gibbs over a hundred years ago [8]. The basic concepts of the method are: (i) a dividing surface, until which the properties of the phases are assumed to be identical and where all extensive parameters change abruptly, (ii) the idealized reference system,

in which volume and shape are the same as in a real system and other properties constant up to the selected dividing surface, and (iii) excess thermodynamic quantities, which describe the difference between extensive quantities in real and reference systems.

Figure 2 shows the equilibrium between two phases separated by a surface plane (fracture surface). In this system the fundamental equations of thermodynamics give [9]:

$$dU^{\sigma} = TdS^{\sigma} - \gamma dA^{\sigma} + \sum_{i=1}^{N} \mu_i dn_i^{\sigma} \quad (1)$$

where U (J) is internal energy, T (K) is temperature, S (J/K) is entropy, γ (J/cm^2) is surface tension, A (cm^2) is surface area, μ (J/mol) is chemical potential, and n (mol) is the quantity of material.

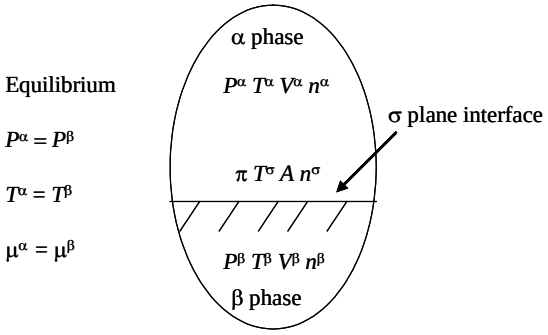

Figure 2. Equilibrium between phases α and β separated by a plane interface σ (P is pressure (Pa) and V is volume (cm^3)) [modified from ref. 10].

Integration with constant T, A and μ_i followed by differentiation and subtraction from the original form (Eq. 1) yields the fundamental equation (2) at constant temperature:

$$-A\mathrm{d}\gamma + \sum_{i=1}^{N} n_i^{\sigma}\mathrm{d}\mu_i = 0 \tag{2}$$

For a two-phase system, this takes a form:

$$A\mathrm{d}\gamma = n_1^{\sigma}\mathrm{d}\mu_1 + n_2^{\sigma}\mathrm{d}\mu_2 \quad \rightarrow \quad \mathrm{d}\gamma = \Gamma_1\mathrm{d}\mu_1 + \Gamma_2\mathrm{d}\mu_2 \tag{3}$$

where Γ is surface excess (moles of the component adsorbed/cm^2). Gibbs adsorption isotherm is derived from the equation (3) by placing the Gibbs dividing plane so that the surface excess of liquid phase is zero ($\Gamma_1 = 0$):

$$\Gamma_2 = -\left(\frac{\mathrm{d}\gamma}{\mathrm{d}\mu_2}\right)_T = \left(\frac{\mathrm{d}\gamma}{R_\mathrm{g}T^{\sigma}\mathrm{d}\ln a_2}\right) = \frac{a_2}{R_\mathrm{g}T^{\sigma}}\left(\frac{\mathrm{d}\gamma}{\mathrm{d}a_2}\right) \tag{4}$$

where a is activity and R_g the universal gas constant. Eq. (4) is one of the most important equations in the surface science and can be used as a basis for the derivation of the Henry's law as well as the famous Langmuir isotherm [10].

1.1.5 Adsorption isotherms for one-component systems

An adsorption isotherm describes the amount of component adsorbed on the adsorbent surface versus the adsorbate amount in the fluid phase at equilibrium. The fitting of adsorption isotherm equations is one of the main stages in data-analysis. The most commonly used adsorption isotherms are still the Langmuir and Freundlich models even though they were first introduced over 90 years ago [11-13].

Theoretical adsorption isotherms have originally been derived for the gas phase adsorption [10] and these equations were later applied with some modifications on the liquid-solid systems. For example, the simplest isotherm equation, Langmuir isotherm, is derived in this

section using the kinetic theory of gas as well as thermodynamic approach. Other isotherm models are presented directly for liquid-solid adsorption without derivation.

Langmuir isotherm

The assumptions of the Langmuir model are: (i) homogeneous surface, when adsorption energy of all adsorption sites is constant, (ii) adsorption of adsorbates is localized, and (iii) each of the adsorption sites can accommodate only one adsorbate. Kinetic theory of gas gives that the rate (R_s, mol/cm^{2}s) of which a component collide on the surface is:

$$R_s = \frac{P}{\sqrt{2\pi M R_g T}} \tag{5}$$

where P is pressure (Pa), M molecular mass of the gas (kg/mol), R_g the universal gas constant, and T temperature (K). When gas molecules strike on the surface, a fraction of them will be adsorbed. In an ideal case this fraction would be unity, but Langmuir presented that a striking coefficient α, which accounts for non-perfect striking, should be added into the equation to obtain rate of the adsorption on bare surface:

$$R_{ads} = \frac{\alpha P}{\sqrt{2\pi M R_g T}} \tag{6}$$

When a gas molecule collides to the occupied adsorption site, it will reflect back to the gas phase very quickly. Therefore, the rate of the adsorption on the occupied surface can be written as:

$$R_a = \frac{\alpha P}{\sqrt{2\pi M R_g T}}(1-\theta) \tag{7}$$

where θ is a fractional coverage. The rate of desorption is the desorption rate from fully occupied surface (k_{des}) multiplied by a fractional coverage.

$$R_{\mathrm{des}} = k_{\mathrm{des}}\theta = k_{\mathrm{des}\infty}\exp\left(-\frac{E_{\mathrm{des}}}{R_{\mathrm{g}}T}\right)\theta \tag{8}$$

where E_{des} is the activation energy for desorption and $k_{\mathrm{des}\infty}$ a rate constant of desorption at infinite temperature. The Langmuir isotherm can be obtained by equating the rates of the adsorption and desorption (Eq. 7 and 8):

$$\theta = \frac{bP}{1+bP} \tag{9}$$

where

$$b = \frac{\alpha\exp\left(Q/R_{\mathrm{g}}T\right)}{k_{\mathrm{des}\infty}\sqrt{2\pi MR_{\mathrm{g}}T}} \tag{10}$$

Parameter b is called affinity constant and Q is the heat of the adsorption, which is equal to the activation energy of desorption. Thus, when b is higher, surface is covered more with adsorbates and when Q increases, the adsorbed amount increases due to the higher energy barrier adsorbates have to overcome to be evaporated back into the gas phase [10].

In liquid-solid system, pressure is replaced by equilibrium concentration (C_{e}) and b by the Langmuir affinity constant K_{L}. Furthermore, when both of the sides of Eq. (9) are multiplied by q_{m} (mmol/g, maximum adsorption capacity), the Langmuir equation is transformed to:

$$q_{\mathrm{e}} = \frac{q_{\mathrm{m}}K_L C_{\mathrm{e}}}{1+K_L C_{\mathrm{e}}} \tag{11}$$

where q_e (mmol/g) is adsorption capacity at equilibrium ($\theta \times q_{\mathrm{m}}$). The affinity constant K_{L} (L/mmol) does not have a similar definition than in the gas-solid adsorption, but it still describes how strong the interactions between the adsorbate and surface are. At low concentrations, the Langmuir isotherm follows the Henry's law *i.e.* adsorption capacity is linearly proportional to the adsorbate concentration in the solution. At high concentrations, the Langmuir isotherm approaches a constant capacity value [14].

Thermodynamic approach for the derivation of the Langmuir isotherm is based on the equilibrium equation of binding of adsorbate A to surface site S.

$$\mathrm{A} + \mathrm{S} \overset{K}{\leftrightarrow} \mathrm{AS} \qquad K_{\mathrm{eq}} = \frac{[\mathrm{A}][\mathrm{S}]}{[\mathrm{AS}]} \tag{12}$$

where K_{eq} is a thermodynamic equilibrium constant. The mass balance equation in this case is:

$$[\mathrm{S}_{\mathrm{tot}}] = [\mathrm{S}] + [\mathrm{AS}] \tag{13}$$

where $[\mathrm{S}_{\mathrm{tot}}]$ is a total amount of surface sites. By combining equations (12) and (13) and assuming that there are no changes of [AS] with respect of time one will obtain:

$$[\mathrm{AS}] = \frac{([\mathrm{S}_{\mathrm{tot}}]/K_{\mathrm{eq}})[\mathrm{A}]}{1 + [\mathrm{A}]/K_{\mathrm{eq}}} \tag{14}$$

which can be arranged to equation (11). The Langmuir model is a very commonly used isotherm equation mostly because it can be linearized and therefore easily fitted to the experimental data [13]. Most of the adsorption materials, however, have heterogeneous surface, which is taken into account in many other isotherm equations.

Freundlich isotherm

As the Langmuir isotherm, the Freundlich isotherm [11] contains only two parameters and is the simplest isotherm that takes the surface heterogeneity into account [13,14]. The Freundlich isotherm is given as:

$$q_{\mathrm{e}} = K_{\mathrm{F}} C_{\mathrm{e}}^{1/n_{\mathrm{F}}} \tag{15}$$

where K_{F} ((mmol/g)/(L/mmol)^{nF}) and n_{F} are the Freundlich adsorption constants. The Freundlich isotherm is one of the earliest empirical isotherms applied for describing adsorption equilibrium. It can be used for heterogeneous surfaces and for multilayer adsorption. The linearized form of

this equation is often used, but generally the Freundlich isotherm lacks the thermodynamic basis since not approaching the Henry's law at low concentrations [14].

Sips isotherm (Langmuir-Freundlich)

The Sips isotherm is a combination of the Langmuir and Freundlich isotherms and can be derived using either equilibrium or thermodynamic approach [15]:

$$q_e = \frac{q_m (K_S C_e)^{n_S}}{1 + (K_S C_e)^{n_S}} \tag{16}$$

where K_S (L/mmol) is the affinity constant and n_S describes the surface heterogeneity. When n_S equals unity, the Sips isotherm returns to the Langmuir isotherm and predicts homogeneous adsorption. On the other hand, deviation of n_S value from the unity indicates heterogeneous surface [16]. At high concentrations, the Sips isotherm approaches to a constant value and at low concentrations Freundlich type equation [14].

Redlich-Peterson isotherm

The Redlich-Peterson isotherm [17] also combines the features of the Langmuir and Freundlich models:

$$q_e = \frac{q_m K_{RP} C_e}{1 + (K_{RP} C_e)^{n_{RP}}} \tag{17}$$

where K_{RP} and n_{RP} are the Redlich-Peterson constants. There are some discrepancies in literature about the definitions of the Redlich-Peterson parameters. In some cases they are said to be constants without any physical meaning [14,18-21] and in some cases their meaning is assigned to be similar to the Sips model [13,22-24]. In this study the latter definition is used.

Toth isotherm

The Toth isotherm [25] is an empirical equation, which was derived to improve the Langmuir model fittings at both low and high concentration limits. The Toth model assumes an asymmetrical quasi-Gaussian energy distribution and is useful in the cases of heterogeneous adsorption [26-28].

$$q_e = \frac{q_m C_e}{(a_T + C_e^{\,m_T})^{\frac{1}{m_T}}} \tag{18}$$

where a_T is adsorptive potential constant (mmol/L) and m_T Toth's heterogeneity factor.

Temkin isotherm

The Temkin isotherm explicitly takes into account the interactions between adsorbent and adsorbate. It is based on the uniformly distributed binding energies up to some maximum energy. The Temkin isotherm states that heat of the adsorption decreases linearly with the increasing adsorbate coverage [27,28].

$$q_e = \frac{R_g T}{b_T} \ln(A_T C_e) \tag{19}$$

where $R_g T/b_T = B_T$ (J/mol) is related to the heat of the adsorption and A_T (L/mmol) is the equilibrium binding constant i.e. maximum binding energy. R_g is the universal gas constant.

General adsorption isotherm (Biosorption model)

The general adsorption isotherm was derived by Liu et al. [29] according to the thermodynamics of adsorption (see the Langmuir case).

$$q_e = \frac{q_m C_e^{\,n_{Gen}}}{K_{ads} + C_e^{\,n_{Gen}}} \tag{20}$$

in which

$$K_{ads} = \left[\exp\left(\frac{\Delta G^0}{RT}\right)\right]^{n_{Gen}} = \left(\frac{1}{K_{eq}}\right)^{n_{Gen}} \tag{21}$$

where ΔG^0 (J/mol) is the change in standard Gibbs free energy, K_{eq} is a thermodynamic equilibrium constant, and n_{Gen} is a positive constant. When $n_{Gen} = 1$, the equation reduces to the Langmuir equation and when equilibrium concentration (C_e) in the liquid phase is much lower

than the constant K_{ads}, equation becomes the Freundlich isotherm. The Sips isotherm can also be derived from the general adsorption equation [29].

Dubinin-Radushkevich isotherm

The Dubinin-Radushkevich isotherm is based on the potential theory and assumes a Gaussian energy distribution.

$$q_e = q_m \exp\left(- B_{DR}\varepsilon^2\right) \tag{22}$$

where ε is the Polanyi potential given by:

$$\varepsilon = RT \ln\left(1 + \frac{1}{C_e}\right) \tag{23}$$

A constant B_{DR} (mmol^2/J^2) is related to the mean free energy E_{ads} of the adsorption per molecule when it is transferred to the surface from infinity of the bulk phase.

$$E_{ads} = \frac{1}{\sqrt{2B_{DR}}} \tag{24}$$

Besides of Eq. (22) a modified form of the Dubinin-Radushkevich isotherm can be found in the literature [13].

Fritz-Schlunder isotherm

Increasing the amount of estimated parameters make isotherm equations more flexible leading generally better fitting results. The following empirical four-parameter isotherm equation was proposed by Fritz and Schlunder [19,30]:

$$q_e = \frac{q_m K_{FS} C_e^{\ n_{FS}}}{1 + K_{FS} C_e^{\ m_{FS}}} \tag{25}$$

where K_{FS} (L/mmol) corresponds to the Langmuir affinity constant and n_{FS} and m_{FS} describe the heterogeneity of the surface. This kind of models, however, should be carefully used since the physical meaning of the parameters is not clear.

BiLangmuir isotherm (Two-site Langmuir)

The heterogeneity of the adsorption system can be taken into account by assuming two or more different surface active sites that follow a Langmuir type behavior [31]. The BiLangmuir model (two-site Langmuir model) is the simplest four-parameter isotherm incorporating two Langmuir equations:

$$q_e = \frac{q_{m1} K_{BiL1} C_e}{1 + K_{BiL1} C_e} + \frac{q_{m2} K_{BiL2} C_e}{1 + K_{BiL2} C_e} \tag{26}$$

where q_{m1} (mmol/g) is the maximum adsorption capacity of the first active site and K_{BiL1} (L/mmol) the adsorption energy related to that active site. Similarly q_{m2} and K_{BiL2} are the corresponding parameters related to the second adsorption site. It should be noted that both of the active sites are homogeneous and can bind only one adsorbate at a time according to the assumptions of the simple Langmuir model.

Other isotherms

Some other empirical three-parameter models, although less commonly used, are for example the Khan [19,32], Koble-Carrigan [19,33], and Jossens [18,34] isotherms. A three-parameter Radke-Prausnitz isotherm [19,35] has thermodynamic basis. Also quite rarely applied four-parameter models are the Weber-van Vliet [18,36], Vieth-Sladek [21,37], and Marczewski-Jaroniec [38] isotherms.

Isotherm shape

Four different isotherm shapes are commonly observed (Figure 3) [39,40]. The C-type isotherm is a line passing through the origin (Figure 3a). It refers to a system were the ratio between the concentration of the compound in solution and adsorbed on the solid is the same at whole concentration range. In practice, this kind of isotherm can only be obtained for a narrow range of concentrations or low concentrations.

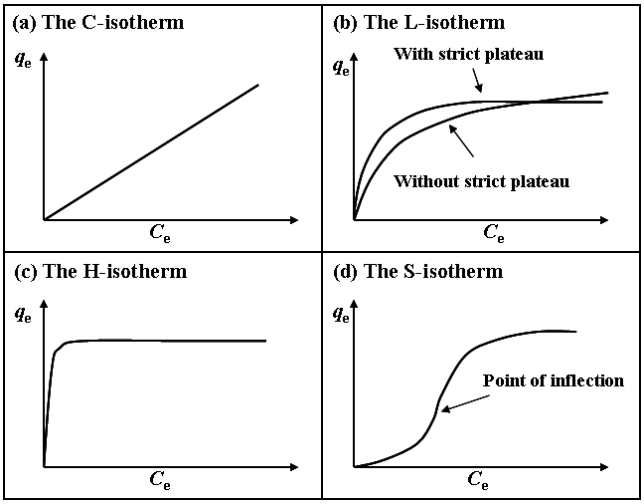

Figure 3. The main types of isotherm curves [modified from refs. 39,40].

The L-type isotherm proposes a progressive saturation of the solid with or without of a strict plateau (Figure 3b). Most of the isotherm equations are of this type. The H-type isotherm is a special case of the L-type isotherm (Figure 3c) with a very high initial slope indicating strong adsorbate–adsorbent interactions [41]. Finally, the S-type isotherm, although quite rarely observed, shows a low adsorption affinity at low adsorbate concentrations and enhanced adsorption after the point (point of inflection, Figure 3d) at which some adsorption has already occurred.

1.1.6 Adsorption isotherms for two-component systems

Adsorption isotherms introduced in the previous section are applicable for systems containing only one adsorbing compound. This is rarely the case, however, in real systems. Therefore, many of the one-component isotherms have been extended to be applicable for the simultaneously adsorption of more than one adsorbate. For the simplicity, in this section, extended isotherms are presented for two-component systems.

Langmuir type 1 isotherm

The simplest extended isotherm, the Langmuir type 1 isotherm, is derived from the assumption that two adsorbates compete for the same adsorption sites [42]:

$$q_{e1} = \frac{q_{m1} K_{L1,1} C_{e1}}{1 + K_{L1,1} C_{e1} + K_{L1,2} C_{e2}} \tag{27}$$

$$q_{e2} = \frac{q_{m2} K_{L1,2} C_{e2}}{1 + K_{L1,1} C_{e1} + K_{L1,2} C_{e2}} \tag{28}$$

where q_{e1} and q_{e2} are amount of components 1 and 2 adsorbed at equilibrium, q_{m1} and q_{m2} are their maximum adsorption capacities, $K_{L1,1}$ and $K_{L1,2}$ affinity constants of the adsorbent for components 1 and 2, respectively and C_{e1} and C_{e2} the concentrations of the components in the solution at equilibrium.

Langmuir type 2 isotherm

The Langmuir type 2 isotherm assumes that the adsorption is uncompetitive phenomenon [42,43]:

$$q_{e1} = \frac{q_{m1}\left(K_{L2,1} C_{e1} + K_{L2,3} C_{e1} C_{e2}\right)}{1 + K_{L2,1} C_{e1} + K_{L2,2} C_{e2} + K_{L2,3} C_{e1} C_{e2}} \tag{29}$$

$$q_{e2} = \frac{q_{m2}\left(K_{L2,2} C_{e2} + K_{L2,3} C_{e1} C_{e2}\right)}{1 + K_{L2,1} C_{e1} + K_{L2,2} C_{e2} + K_{L2,3} C_{e1} C_{e2}} \tag{30}$$

where $K_{L2,3}$ (L/mmol) is the affinity constant for the simultaneous bonding of two components by the same adsorption site and other parameters have the same meaning as in the Langmuir type 1 model.

Langmuir type 3 isotherm

The Langmuir type 3 isotherm is based on the concept that one component can be attached onto both free and occupied adsorption sites [42,43]:

$$q_{e1} = \frac{q_{m1}\left(K_{L3,1}C_{e1} + K_{L3,2}K_{L3,3}C_{e1}C_{e2}\right)}{1 + K_{L3,1}C_{e1} + K_{L3,2}C_{e2} + \left(K_{L3,1}K_{L3,3} + K_{L3,2}K_{L3,4}\right)C_{e1}C_{e2}} \quad (31)$$

$$q_{e2} = \frac{q_{m2}\left(K_{L3,2}C_{e2} + K_{L3,1}K_{L3,4}C_{e1}C_{e2}\right)}{1 + K_{L3,1}C_{e1} + K_{L3,2}C_{e2} + \left(K_{L3,1}K_{L3,3} + K_{L3,2}K_{L3,4}\right)C_{e1}C_{e2}} \quad (32)$$

where $K_{L3,3}$ (L/mmol) is the equilibrium constant for the bonding of component 1 with the binding site occupied with component 2 and $K_{L3,4}$ (L/mmol) is the equilibrium constant for the bonding of component 2 with the binding site occupied with component 1. Other parameters have the same meaning than in the Langmuir type 1 model. It should be noted that also the extended Langmuir models assume that all the binding sites are similar as a simple Langmuir case [42].

Extended Sips isotherm

The binary form of Sips isotherm is given by [43,44]:

$$q_{e1} = \frac{q_{m1}\left(K_{S1}C_{e1}\right)^{nS1}}{1 + \left(K_{S1}C_{e1}\right)^{nS1} + \left(K_{S2}C_{e2}\right)^{nS2}} \quad (33)$$

$$q_{e2} = \frac{q_{m2}\left(K_{S2}C_{e2}\right)^{nS2}}{1 + \left(K_{S1}C_{e1}\right)^{nS1} + \left(K_{S2}C_{e2}\right)^{nS2}} \quad (34)$$

where K_{S1} and K_{S2} (L/mmol) are analogous to the Langmuir affinity constant and n_{S1} and n_{S2} are the heterogeneity constants. Similarly as in the case of the one-component Sips model, deviation of $n_{S1/S2}$ from unity indicates heterogeneous adsorption.

Extended Redlich-Peterson isotherm

The Redlich-Peterson model [43] was also extended to cover multi-component systems. This model is purely mathematical but may describe the experimental data very well.

$$q_{e1} = \frac{q_{RP1}K_{RP1}C_{e1}}{1 + K_{RP1}\left(C_{e1}\right)^{nRP1} + K_{RP2}\left(C_{e2}\right)^{nRP2}} \quad (35)$$

$$q_{e2} = \frac{q_{RP2} K_{RP2} C_{e2}}{1 + K_{RP1} (C_{e1})^{nRP1} + K_{RP2} (C_{e2})^{nRP2}} \quad (36)$$

where n_{RP} reflects the heterogeneity of the adsorbent surface.

Extended BiLangmuir model

In the case of two component systems, the extended BiLangmuir model is given as:

$$q_{e1} = \frac{q_{m1,1} K_{BiL1,1} C_{e1}}{1 + K_{BiL1,1} C_{e1} + K_{BiL2,1} C_{e2}} + \frac{q_{m1,2} K_{BiL1,2} C_{e1}}{1 + K_{BiL1,2} C_{e1} + K_{BiL2,2} C_{e2}} \quad (37)$$

$$q_{e2} = \frac{q_{m2,1} K_{BiL2,1} C_{e2}}{1 + K_{BiL1,1} C_{e1} + K_{BiL2,1} C_{e2}} + \frac{q_{m2,2} K_{BiL2,2} C_{e2}}{1 + K_{BiL1,2} C_{e1} + K_{BiL2,2} C_{e2}} \quad (38)$$

where $q_{m1,1}$ and $q_{m1,2}$ are the maximum adsorption capacities of the component 1 on adsorption sites 1 and 2 and $K_{BiL1,1}$ and $K_{BiL1,2}$ are adsorption energies related to the adsorption of the component 1 on adsorption sites 1 and 2. Accordingly, $q_{m2,1}$, $q_{m2,2}$, $K_{BiL2,1}$, and $K_{BiL2,2}$ are corresponding parameters related to the adsorption of component 2. In this model, both competitive ions can be adsorbed on either of the sites and only monolayer adsorption is possible. Kaczmarski *et al.* [45] presented a quite similar form of the extended BiLangmuir model than above, but with the assumption that only one of the active sites was totally available for the both components.

1.1.7 Important aspects in isotherm modeling

The linear forms of the Langmuir and Freundlich equations are still frequently applied. The isotherm parameters can be easily determined from the slope and intercept of the linear plots. For three or four parameter models, linearization in ordinary manner is not longer possible and non-linear regression is applied in modeling. This is done by minimizing the error distribution between experimental and predicted adsorption isotherms. Different error functions can be used in minimization. Furthermore, important aspects in non-linear regression are the experimental data range and initial guess values. These are discussed below.

Error functions

Non-linear regression involves minimization of the error distribution between experimental and predicted adsorption isotherms usually by minimizing or maximizing the used error function depending on its definition. Table 2 shows the most commonly used error functions. Roughly, these can be divided into equations that account for the amount of parameters (p) and those that do not. Moreover, in most of the error functions the deviation between the experimental and simulated q_e values is divided by the experimental q_e to decrease weighting towards high concentration data [14].

Table 2. The list of error functions [14,27].

Error function	Definition
The coefficient of determination, correlation coefficient (R^2)	$\frac{\left(q_{e,exp}-\overline{q_{e,calc}}\right)^2}{\sum\left(q_{e,exp}-\overline{q_{e,calc}}\right)^2+\left(q_{e,exp}-q_{e,calc}\right)^2}$
The sum of the square of the errors (ERRSQ)	$\sum_{i=1}^{n}\left(q_{e,exp}-q_{e,calc}\right)_i^2$
The hybrid error function (HYBRID)	$\sum_{i=1}^{n}\left(\frac{\left(q_{e,exp}-q_{e,calc}\right)^2}{q_{e,exp}}\right)_i$ or $\frac{100}{n-p}\sum_{i=1}^{n}\left(\frac{\left(q_{e,exp}-q_{e,calc}\right)^2}{q_{e,exp}}\right)_i$
Marquardt's percent standard deviation (MPSD)	$\sum_{i=1}^{n}\left(\frac{q_{e,exp}-q_{e,calc}}{q_{e,exp}}\right)_i^2$ or $100\sqrt{\frac{1}{n-p}\sum_{i=1}^{n}\left(\frac{q_{e,exp}-q_{e,calc}}{q_{e,exp}}\right)_i^2}$
The average relative error (ARE), Mean error (ME)	$\sum_{i=1}^{n}\left\lvert\frac{q_{e,exp}-q_{e,calc}}{q_{e,exp}}\right\rvert_i$ or $\frac{100}{n}\sum_{i=1}^{n}\left\lvert\frac{q_{e,exp}-q_{e,calc}}{q_{e,exp}}\right\rvert_i$
The sum of absolute errors (EABS)	$\sum_{i=1}^{n}\left\lvert q_{e,exp}-q_{e,calc}\right\rvert_i$
Non-linear reduced chi-square (χ^2)	$\frac{1}{n-p}\sum_{i=1}^{n}\frac{\left(q_{e,exp}-q_{e,calc}\right)_i^2}{q_{e,calc}}$

n = number of data points, p = number of parameters of the isotherm equation, exp = experimental/measured, calc = calculated/estimated.

Several authors have introduced the comparison of different error functions. In the case of metal ion adsorption on peat the best correlation between simulated and experimental data was obtained using HYBRID and MPSD [14], of which the former was applicable for two parameter isotherms and the latter for three. HYBRID function was also appropriate in modeling of arsenic adsorption on iron oxide coated cement [46], basic dye adsorption by kudzu [47], and dye adsorption by

cationized starch-based material [48]. EABS function provided the best approximation for Cu(II) adsorption on chitosan [49] and the R^2 for the basic red 9 adsorption on activated carbon [50]. For adsorption of methylene blue on activated carbon R^2 function gave the closest fit to the experimental data for three parameter models and MPSD for two-parameter models [51]. Previous examples show that the applicability of different error functions is clearly case dependent.

Besides using error functions in fitting procedure, these functions are more often used in evaluation of goodness of fit [52]. The sum of normalized errors (SNE) is presented to provide a meaningful way to find the best fitting isotherm. This alone, however, should also not be used for selecting the optimum isotherm. In addition, the extent of which the theory behind the model and determined adsorbent properties converges should carefully be evaluated [51].

Data range

Limited discussion exists in the literature on how the data range affects isotherm fittings. After a literature survey, it can be stated that in over 80% of the studies fitting of isotherms and error analysis have been done using only eight or less experimental points. It is obvious that in these cases critical data might be missing from the isotherm curves. If high enough concentrations are not used in the experimental studies, the applied isotherm model may propose maximum adsorption capacity far from the true value. In addition, if all the experimental points lie in the initial part (linear range) or plateau of the isotherm curve the deviations between different isotherm models may not be observable. Therefore, proper experimental data should contain points from the concentration range that covers the whole isotherm. Even a wide experimental data range is used, however, minor changes in the data points may lead to notable changes in the fitting results [53].

Initial guess values

In most of the cases in literature, authors do not state how they have selected the initial values for non-linear fittings. The reason may be that a selection of the initial values has not affected the fitting results. Trial and error approach is supposed to be adequate [13]. Convergence difficulties, however, may arise when the initial guesses are set far from their true values [54]. To optimize the iteration procedure Ncibi [52] used the values obtained from linear fittings as initial

guesses for non-linear regressions. It is also reasonable to use the experimentally obtained q_m as an initial guess whenever possible. Kinniburgh [13] stated that in the case of the BiLangmuir model, initial guesses of the other K_{BiL} and q_m should be taken from the fit of the simple Langmuir model. On the whole, to ensure the best fitting result, it is reasonable to test a few sets of initial guesses in non-linear regression.

Linear and non-linear fitting

The most commonly applied method in the fitting of models to the experimental data is the least squares regression combined with linearization of adsorption isotherms. Linear fitting of the two-parameter Langmuir and Freundlich isotherms is often used due to the simplicity of the method. A lot of literature, however, states that a better way to obtain fitting parameters is non-linear regression [50-52,55-59]. This is attributed to the change of the error distribution caused by linearization [13]. Moreover, the Langmuir isotherm can be linearized in four different ways (Table 3) resulting in different parameter estimations [55,57,58].

Table 3. Linear forms of the Langmuir isotherm [55,57,58].

Isotherm	Linear form	Plot
Langmuir-lin1	$\frac{C_e}{q_e} = \frac{1}{q_m} C_e + \frac{1}{K_L q_m}$	$\frac{C_e}{q_e}$ vs. C_e
Langmuir-lin2	$\frac{1}{q_e} = \left(\frac{1}{K_L q_m}\right)\frac{1}{C_e} + \frac{1}{q_m}$	$\frac{1}{q_e}$ vs. $\frac{1}{C_e}$
Langmuir-lin3	$q_e = q_m - \left(\frac{1}{K_L}\right)\frac{q_e}{C_e}$	q_e vs. $\frac{q_e}{C_e}$
Langmuir-lin4	$\frac{q_e}{C_e} = K_L q_m - K_L q_e$	$\frac{q_e}{C_e}$ vs. q_e

When the non-linear form of the isotherm equation is fitted, the least squares problem can be solved either as a general unconstrained optimization problem (Microsoft Excel Solver) or an iterative algorithm such as the Gauss-Newton or Levenberg-Marquardt algorithm (Matlab, Origin, some special software) [60,61]. The benefit of the non-linear regression over the linear one is that it does not assume an equal error distribution for all the values of x [55]. Hence, non-linear fitting is generally a better choice for parameter estimation.

Lastly, it should be noted that the lack of the both linear and non-linear regression is an assumption that the independent variable (x) is error free. This assumption can lead to a wrong set of estimated parameters. To overcome this El-Khaiary [61] used orthogonal distance regression in modeling and found it to be a better method. Unfortunately, this procedure has not been widely applied.

Two-component systems

Besides the above discussion, a few special aspects need to be emphasized in the modeling of two-component systems. First, these systems are more complicated when the fitting as well as interpretation of the results can be difficult. The experimental data range should also include a large amount of points measured in different concentrations and different ratios of target components. This causes more experimental work. Therefore, some of the authors have fitted the two-component models to the experimental data by taking all the parameters from the one-component modeling results [42,44,62]. Despite this method being quite successful in some cases, it is important to note that equation parameters can be affected by the competing ions [63]. Moreover, when one-component parameters are not utilized, the two-component modeling involves the adjusting of 4 to 8 parameters. This can lead to a situation where experimental data is well fitted with the model, but the model does not conform the actual physical behavior of the system [3]. As in the case of one-component modeling different two-component isotherms can be compared using an error analysis. To justify the obtained results, however, the theory behind a model and experimentally observed properties of adsorption system should be carefully compared [51]. It is also reasonable to compare the results of one- and two-component modeling.

1.1.8 Kinetics of adsorption

Before reaching the equilibrium state, several steps affect the adsorption process [64,65]. First of all, the component to be adsorbed has to move from the bulk phase to the vicinity of the adsorbent surface. Secondly, the properties of the solution close to the adsorbing particles differ from the bulk phase (diffusion and Stern layer, Figure 1) and the adsorbates have to travel through this region to reach the surface. This is called a film diffusion or boundary diffusion. Furthermore, most of the adsorbents have porous structure and therefore, diffusion of the

adsorbates in macro/meso/micropores can have a major impact on the rate of the adsorption. Finally, after reaching the active site, adsorbate is bound to it via a chemical reaction or physical interactions. This step can be generally called as a surface reaction.

As was depicted above, adsorption is not a simple one step process. Usually, the effect of travel in the solution is eliminated by vigorous mixing, but the contribution of all the other stages should be investigated. Therefore, different kinetic models have been developed to predict the rate determining step of the adsorption. Similarly, as in the case of adsorption isotherms (Langmuir, Freundlich), adsorption kinetics has most often been fitted by the two simplest models: pseudo-first- and pseudo-second-order equations. These models were originally proposed empirically and have only recently been examined on their theoretical basis [66].

Besides of the pseudo kinetic models, which assume that the adsorption is governed by the surface reaction, a variety of diffusion based models have been derived [64]. Especially in the case of porous adsorbents, diffusion can greatly affect the adsorption rate, which is discussed in the end of this section.

Pseudo-first-order model

Legergren proposed the simplest empirical kinetic model at the end of 19th century [67]. The model was also called the pseudo-first-order (PS1) model due to the fact that it was associated with the kinetics of one-site adsorption governed by the rate of the surface reaction. The equation is given as:

$$\frac{dq}{dt} = k_1(q_e - q) \tag{39}$$

By integrating above equation at the boundary conditions q=0 at t=0 and q=q_t at t=t, one will obtain a linear form of the PS1 model:

$$\ln(q_e - q_t) = \ln q_e - k_1 t \tag{40}$$

where q_t and q_e are the adsorption capacity (mmol/g) at time t and at equilibrium respectively, while k_1 represents the PS1 rate constant (1/min). For fitting of experimental data, however, it is

better to use the non-linear equation rearranged from eq. (40). This is because for the linear fitting the left hand side q_e (term $\ln(q_e-q_t)$) has to be taken from the experimental data when there are actually two values for q_e in Eq. (40).

Earlier the PS1 model was derived for special cases such as ion-exchange by natural zeolites [68,69] and biosorption by aerobic granular sludge [70]. General analytical derivation was presented by Azizian [71] for high solution concentrations. Based on his derivation, k_1 was a combination of adsorption and desorption rate constants and a linear function of the initial concentration of adsorbate. Liu and Liu [15], however, denoted that Azizian's assumptions about the first order adsorption and desorption reactions with respect to the available and occupied adsorption sites, were not justified. They also stated that this derivation was only valid for pure solutions, which is rarely the case in the real systems. Moreover, the dependence of k_1 on the initial concentration of adsorbate has not always been observed even if PS1 model has been well fitted [64].

Finally, Rudzinski and Plazinski [72] derived a general kinetic equation based on the Statistical Rate Theory and showed that the PS1 model was a special case of this new equation. Similarly to Azizian's approach, this was achieved by assuming high solution concentration, which essentially remained constant during the kinetic experiment. The PS1 rate constant was determined as a function of initial concentration of the adsorbate and the energy of the adsorption.

It should be noted that even if most of the derivations of PS1 model were achieved from the assumption that the surface reaction governs the adsorption process, mathematically equivalent equations have also been obtained for film or pore diffusion [68,73]. Based on this, Plazinski *et al.* [65] suggested that the PS1 model is a general formula describing the experimental data measured not too far from the equilibrium. Authors also proved this point by investigating the properties of mechanism independent general rate equation.

Pseudo-second-order model

The PS1 model was generalized to two-site-occupancy adsorption to form a pseudo-second-order (PS2) equation:

$$\frac{dq}{dt} = k_2 (q_e - q)^2 \tag{41}$$

where k_2 is the PS2 rate constant (g/mmol min) and $k_2 q_e^2$ represents the initial sorption rate. An integration of Eq. (41) at the boundary conditions, q = 0 at t=0 and q=q_t at t=t, gives a linear form:

$$\frac{t}{q_t} = \frac{1}{k_2 q_e^2} + \frac{t}{q_e} \tag{42}$$

Azizian [71] derived the PS2 model using classical theory of adsorption/desorption by assuming a low initial concentration of adsorbate. Based on this derivation, k_2 was a complicated function of the initial concentration of adsorbate, its equilibrium surface capacity as well as the rates of the adsorption and desorption. Later on Azizian's assumptions were debated by Liu and Liu [15], who stated that his derivation was applicable in the initial stage of the adsorption (small value of t) and did not necessarily require the assumption of a low initial concentration.

The direct mathematical derivation of the PS2 model could not be done using the Statistical Rate Theory. Convergence of the general model derived by Rudzinski and Plazinski [72] and the PS2 model, however, was nearly perfect in certain conditions indicating that the PS2 model was a special case of this general equation.

The PS2 model has also been assigned to a special case of the more general rate law [74] or the Langmuir kinetic model [75]. In addition, it has been noted that this model is able to estimate experimental q_e values quite well and is not very sensitive for the influence of the random errors [65]. The latter is also one of the reasons the second-order model is usually better fitted on the experimental data than the first-order model.

Elovich model

The Elovich model was proposed by Roginsky and Zeldovich in the early 1930's:

$$q_t = \frac{1}{B_E} \ln(1 + A_E B_E t) \tag{43}$$

where A_E (mmol/min g) and B_E (g/mmol) are the Elovich constants. These constants were related to the rate of the chemisorption and surface coverage, respectively [76,77].

Interpretations of the Elovich equation are usually connected to the heterogeneous surfaces. This assumption was also used by Rudzinski and Plazinski when they derived an Elovich-like equation using the Statistical Rate Theory [72,73,78]. One interesting observations the authors made [78] was that the PS2 model and Elovich-type model were essentially identical when the surface coverage of the adsorbate was lower than 0.7 times the equilibrium coverage.

Intraparticle diffusion model

Weber and Morris [64] proposed that a plot of the adsorption capacity vs. the square root of contact time should give a straight line if the pore-diffusion was the rate limiting step of the adsorption process. The most commonly applied pore-diffusion model is the intraparticle diffusion model:

$$q = k_{dif} t^{1/2} (+ C) \tag{44}$$

where k_{dif} (mmol/gmin$^{1/2}$) is the rate constant of intraparticle diffusion and C (mmol/g) represents the thickness of the boundary layer.

In many studies, the plot of the intraparticle diffusion model has shown multi-linearity, which has been assigned the following diffusion steps during the adsorption process [64,79,80]: (i) an external surface adsorption or film diffusion, (ii) a gradual adsorption, where intraparticle diffusion is controlled, and (iii) a slow diffusion of the adsorbates from larger pores to micropores. Different linear portions can also be assigned to diffusion into macropores, then mesopores and finally into micropores [80].

Ho *et al*. [64] presented some more criteria to confirm the diffusion mechanism. The constant k_{dif} should vary linearly with reciprocal particle diameter and the product of k_{dif} and the adsorbent mass should vary linearly with the adsorbent mass. Moreover, the rate of the reaction governed by surface reaction depends more on the temperature than the diffusion governed process.

Other kinetic models

Plenty of different kinetic models have been derived for adsorption processes. Besides those presented above, these include for example: Langmuir kinetics [65], Freundlich kinetics [81], the modified PS1 model [82], different forms of the PS2 model [83], the Bangham diffusion model [20,84], the particle diffusion model [64,68], and the Ritchie equation [83,85]. Previous models, however, are rarely applied and therefore not discussed further.

Linear or non-linear fittings

Kinetic modeling is usually done by the linear fitting of PS1 and PS2 models (Eq. 40 and 42). After comparing the linear and non-linear methods several authors concluded that the non-linear method is a better way to estimate the model parameters [86-88]. When comparing the linear forms of pseudo-equations Plazinski *et al*. [65] noted that the linear PS2 model tends to "smooth" the experimental data due to the contribution of inherent errors in t/q_t not dependent on the system's closeness to equilibrium. In the case of the PS1 model, however, errors in $\ln(q_e\text{-}q_t)$ are inversely proportional to the $(q_e\text{-}q_t)$ when most of the scattering in experimental data ($\ln(q_e\text{-}q_t)$ vs. t) ought to occur close to equilibrium. In addition, to conduct linear fitting, q_e in this term is taken from the experimental data and can differ from the estimated value (right hand side q_e in Eq. 40).

1.2 Adsorbents functionalized with chelating agents

In order to remove heavy metals from contaminated waters, it is very important to strongly bind metal ions on the adsorbent surface. The surfaces of most natural (for example zeolites) and synthetic (for example activated carbon) adsorption materials are covered by functional groups such as hydroxyls, sulfonics, phosphates, amines etc. Bonds between these simple surface groups and metal cations, however, are not usually strong. Therefore, surface functionalization with high affinity binding groups has attained a lot of attention in recent years. Amongst them are for example chelating agents such as aminopolycarboxylic acids (APCAs): iminodiacetic acid (IDA), nitrolotriacetic acid (NTA), ethylenediaminetetraacetic acid (EDTA), and diethylenetriamine-pentaacetic acid (DTPA) (Figure 4).

1.2.1 Properties of aqueous aminopolycarboxylic acids and their metal chelates

The structures and properties of the group of APCAs are extensively reviewed in literature [89-91]. In this work a focus will be in those that are often applied in surface functionalization (IDA, NTA, EDTA, and DTPA, (Figure 4)).

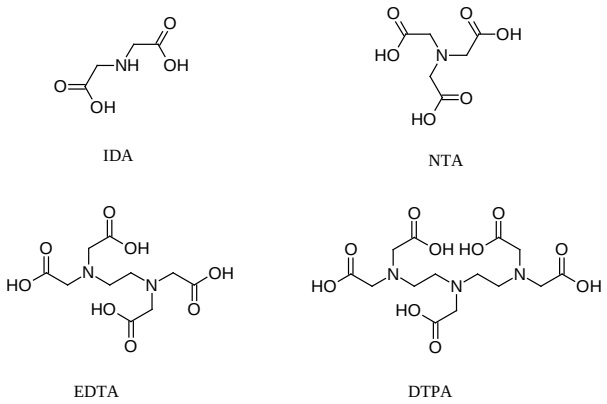

Figure 4. Structures of the most common APCAs.

APCAs are widely used in many industrial processes or products (i) to prevent metal precipitation, (ii) to inhibit catalytic activity of metal ions, (iii) to remove metal ions, or (iv) to keep metal ions in the solution [91]. All of this is possible because APCAs form very stable chelates with metals. Moreover, the higher the number of carboxyl groups in the structure of APCA the higher the stability of the formed chelate (Table 4).

Table 4. pK values for some metal APCA chelates [92].

	$Me(II)IDA_2^{2-}$	Me(II)IDA	$Me(II)HIDA^{+}$
Co(II)	12.3	6.97	
Ni(II)	14.3	8.19	
Cu(II)	16.3	10.6	
Zn(II)	12.4	7.03	
Cd(II)	9.99	5.7	
Pb(II)		7.45	10.4
	$Me(II)NTA_2^{4-}$	$Me(II)NTA^{-}$	Me(II)HNTA
Co(II)	14.97	11.66	
Ni(II)	16.93	12.79	
Cu(II)	18.04	14.28	16.1
Zn(II)	14.88	11.84	
Cd(II)	15.11	11.04	
Pb(II)	13.44	12.76	15.33
	$Me(II)EDTA^{2-}$	$Me(II)HEDTA^{-}$	Me(II)H2EDTA
Co(II)	18.16	21.59	23.49
Ni(II)	20.11	23.64	24.74
Cu(II)	20.49	24.02	26.23
Zn(II)	18	21.43	22.83
Cd(II)	18.1	21.43	23.23
Pb(II)	19.71	22.54	24.44
	$Me(II)DTPA^{3-}$	$Me(II)HDTPA^{2-}$	$Me(II)_2DTPA^{-}$
Co(II)	20.95	26.53	25.98
Ni(II)	22.25	28.53	29.13
Cu(II)	23.35	28.79	31.43
Zn(II)	20.35	26.59	26.12
Cd(II)	21.15	26.61	24.74
Pb(II)	20.95	26.76	25.65

The high stability of metal APCA chelates can be attributed to the multidentate binding of APCA to the metal center. Both carboxyl and amine groups participate in chelation. For example NTA forms octahedral chelates with divalent metal ions. In these structures metal is coordinated via all carboxyl groups, nitrogen, and two water molecules [93]. In most studies, EDTA chelates with divalent metals are reported as quinquedentate where one of the carboxyl groups is free and one water molecule is coordinated to the metal center. Sexidentate structures may be important at high ionic strength [94]. Octahedral structures have been determined for the Cu(II)DTPA and Pb(II)DTPA chelates with more distorted structure of the latter one due to the bigger ionic radius of Pb(II) [95]. These structures have shown metal coordination via three nitrogen and three carboxyl groups with two free carboxyl groups. Similar structures are proposed for Zn(II) and

Cd(II)DTPA chelates with some additional alternatives, where only one carboxyl group is free and coordination of metal occurs via two nitrogen and four carboxyl groups [96].

Considerable concern about the environmental effects of APCAs has arisen in recent decades. Especially, EDTA and DTPA have the highest concentration compared to the other measurable synthetic organic compounds in both drinking and surface waters [97]. Moreover, a generally presented conclusion is that they are not eliminated by conventional biological and physico-chemical water treatment methods although some contradictory results exist [98]. Therefore, utilization of these chelating agents in aqueous form should be limited or more efficient water treatment methods applied. One possible solution, however, could be the use of these chelating agents as immobilized form to prevent their release in to the environment, but still take advantage of their beneficial properties.

Before introducing some APCA-functionalized chelating adsorbents some of their features need to be highlighted. These arise from the difference between surface bound ligands and their dissolved analogies in the liquid phase. Immobilized ligands are insoluble, they have a limited set of conformations, a more irregular distribution, high volume concentration, and are sterically unequivalent. All of this influences the adsorption properties of the chelating resins [5]. Moreover, when successfully immobilized on the solid adsorbent, chelating agent can have higher adsorption efficiency compared to their aqueous form [99].

1.2.2 IDA- and NTA-functionalized adsorbents

IDA and NTA are the simplest APCAs containing two and three carboxyl groups. IDA- and NTA-functionalized adsorbents have been widely studied during the recent decades. Only some of the materials will be introduced here (Table 5) because the experiments being conducted using EDTA- and DTPA-functionalized adsorbents. NTA-functionalization has, for example, been applied for chitosan [100], silica polyamine composites [101], and melamine-formaldehyde [102]. In addition, commercial NTA Superflow chelating resin is available [103]. Besides of a variety of commercial IDA-functionalized chelating resins [104] some self-prepared materials are IDA-functionalized silica gel [105], acrylonitrile-divinylbenzene (AN-DVB) [104,106,107], and polybenzylamine (PBA) [108].

Table 5. IDA- and NTA-functionalized adsorbents.

Chelating adsorbent	Surface coverage (mmol/g)	Metal	pH	q_m (mmol/g)	Reference
NTA-chitosan	1.45	Cu(II)	-	1.53	[100]
NTA-silica-poly(allylamine) composite	1.36	Co(II) Ni(II) Zn(II)	3	0.35 0.55 0.25	[101]
NTA-silica-poly(ethyleneimine) composite	0.79	Co(II) Ni(II) Zn(II)	3	0.7 0.75 0.6	[101]
NTA-melamine-formaldehyde	0.67	Cu(II)	6	0.47	[102]
IDA-silica gel	1.22	Co(II) Ni(II) Cu(II) Zn(II)	5.5	1.0 1.1 1.23 0.63	[105]
IDA-AN-DVB	-	Co(II) Ni(II) Cu(II)	5	2.51 2.81 3.26	[106]
IDA-AN-DVB	-	Cd(II) Pb(II)	5.5	0.99 0.69	[104]
IDA-PBA	-	Cu(II) Cd(II) Pb(II)	5	1.72 0.61 1.12	[108]
Amberlite IRC-748 (commercial IDA resin)	-	Cu(II) Cd(II) Pb(II)	5	1.69 0.61 1.13	[108]

Table 5 shows that the adsorption capacity of different NTA- and IDA-functionalized materials varies greatly depending on the supporting material. In addition, the order of adsorption capacities does not follow the order of the stability constants (Table 4), which is discussed more in the next section. It should also be noted that some self-prepared materials are more efficient adsorbents than commercial ones [106].

Finally, it is important to consider the binding mechanism of metal ions on chelating agents, when they are attached on the solid support. Unfortunately, authors have not usually investigated the surface structures of immobilized metal IDA/NTA-chelates. As an example, the structure of metal chelates formed on IDA-AN-DVB was studied by Fourier transform infrared spectroscopy (FTIR), X-Ray diffraction (XRD), and electron paramagnetic resonance (EPR). A tetrahedral structure, where metal ions were coordinated through one amine and two carboxyl groups, was proposed [107].

1.2.3 EDTA-functionalized adsorbents

Various materials from biomass to inorganic oxides have been functionalized with EDTA. The popularity of EDTA arises from its strong metal chelating ability, local availability, and low price. Table 6 shows the metal adsorption properties of EDTA-functionalized adsorbents.

Silica gel is an amorphous form of silicon dioxide where silicon atoms are linked together via oxygen atoms with siloxane bonds. Silica gel surface contains hydroxyl groups that can be further functionalized using a familiar silanization procedure [99,109]. Silica gel has various advantages as an inorganic support compared, for example, to organic polymeric resins. These include good selectivity, no swelling, rapid adsorption, and good mechanical stability. EDTA can be attached on the silica support by first using the amine group containing silylating agents ((3-aminopropyl)triethoxysilane, APTES) and then reacting surface bound amine groups with EDTA anhydride in a mixture of ethanol and acetic acid [110]. Table 6 shows relatively low adsorption capacities for metal ions by EDTA-silica gels, which can be attributed to the experimental conditions such as short contact time (1 h) and acidic media.

Chitosan can be prepared from chitin, one of the nature's most abundant biopolymers. Chitosan contains primary amino groups, which can be further functionalized with different organic ligands. In the synthesis of EDTA-chitosan, chitosan is reacted with EDTA anhydride in acetic acid/MeOH solution [111-113]. When EDTA is used as such, the formation of amide bonds between amino groups and EDTA carboxyl groups can be mediated using carbodiimides [114]. A complete functionalization of amino groups by EDTA leading to the adsorbents with very high adsorption capacities has been reported in the literature [111-113].

The same authors, who first prepared EDTA-functionalized chitosan, also tested a similar synthesis for polyallylamine. Adsorption properties of these two adsorbents were, however, quite different and they suggested that in the case of modified polyallylamine, carboxyl groups did not effectively participate in the chelate formation [113].

Silica polyamine composites have been functionalized with EDTA using a synthetic route similar to that of amino functionalized silica gel. A higher amount of available primary amino groups of composite materials, however, has enabled a better surface coverage of EDTA groups compared to that of silica gel [115].

Most of the commercial ion-exchange resins are based on the crosslinked polystyrene (PS). The high loading capacity (0.5–3 mmol/g) and low cost of PS make it a good support for solid phase synthesis [116]. Polystyrene based EDTA-resins were prepared by at first introducing ethylenediamine in styrene-divinylbenzene copolymer and then increasing the amount of carboxyl groups using chloroacetate [117,118]. The mechanical strength of the PS-EDTA resin was improved by wrapping it up by polyvinylalcohol (PVA) beads [119]. This material was an effective adsorbent for Zn(II).

Polyamidoamine (PAMAM) dendrimers are branched, well-defined synthetic nanoscale materials, consisting of globular macromolecules with three covalently bonded components: core, interior branch cells, and terminal branch cells. PAMAM dendrimers with amino terminal groups have previously been used for Cu(II) removal [120]. The difficult recycling process of pure dendrimers, however, has prompted researchers to design PAMAM based inorganic-organic hybrid materials. Mesoporous silica such as SBA-15 was used as a support for dendrimer structures prior to functionalization with EDTA [121].

Plenty of natural and low-cost materials have also been utilized as supports for EDTA functionalities. These are for example saw dust and sugarcane bagasse [122], mercerized cellulose and sugarcane bagasse [123], rice husk [124], maize husk [125], maize cob [126], biomass of baker's yeast [127], and carbon cloth [128]. Some of these modified adsorbents have shown very high adsorption capacities, for example mercerized cellulose and sugarcane bagasse [123]. The authors stated that mercerization (treatment with 5 M NaOH) made hydroxyl groups of raw materials more susceptible to esterification with EDTA anhydride thus increasing the surface coverage of EDTA groups.

Finally, layered double hydroxide interchelated with EDTA (MgFe-LDH-EDTA) have been tested for Cu(II) and Pb(II) adsorption [129]. The high stability constant of Cu(II)EDTA chelate (Table 4) could explain a very high adsorption capacity obtained for Cu(II) (Table 6).

Table 6. EDTA-functionalized adsorbents.

Matrices functionalized with EDTA	Surface coverage (mmol/g)	Metal	pH	q_m (mmol/g)	Reference
Silica gel	0.30	Co(II) Ni(II) Cu(II)	1	≈ 0.01 ≈ 0.06 ≈ 0.07	[110]
Chitosan	≈ 5.9	Pb(II) Ni(II)	2 2	1.5 2.1	[112] [113]
Polyallylamine	-	Ni(II)	2	2.0	[113]
Silica-poly(allylamine) composite	0.76	Co(II) Ni(II) Cu(II) Zn(II)	3	0.47 0.55 0.58 0.48	[115]
Silica-poly(ethyleneimine) composite	0.56	Co(II) Ni(II) Cu(II) Zn(II)	3	0.46 0.45 0.50 0.46	[115]
PS	-	Cu(II) Pb(II)	6	0.66 0.15	[118]
PS-PVA	-	Zn(II)	6	0.59	[119]
PAMAM-SBA-15	-	Ni(II) Cu(II) Zn(II) Pb(II)	4	0.21* 0.21* 0.15* 0.03*	[121]
Sawdust	0.79	Zn(II)	6.2	1.22	[122]
Sugarcane bagasse	0.81	Zn(II)	6.2	1.61	[119]
Mercerized sugarcane bagasse[a]	1.04	Cu(II) Cd(II) Pb(II)	5.3	1.46 1.33 1.61	[123]
Mercerized cellulose[a]	0.64	Cu(II) Cd(II) Pb(II)	5.3	1.05 1.00 1.12	[120]
Maize husk	-	Zn(II) Cd(II) Pb(II)	7.5	≈ 0.54 ≈ 0.27 ≈ 0.15	[125]
Maize cob	-	Co(II) Cu(II)	7.5	≈ 0.87 ≈ 0.82	[126]
Biomass	-	Cu(II) Pb(II)	6	1.02 0.93	[127]
Carbon cloth	-	Co(II) Ni(II) Cu(II) Zn(II) Cd(II) Pb(II)		0.80 0.96 0.70 0.40 0.35 0.09	[128]
MgFe-LDH-EDTA	-	Cu(II) Pb(II)	5.5	≈ 5 ≈ 0.2	[129]

*Competitive conditions, total adsorption capacity: 0.6 mmol/g

Table 6 shows that the type of the supporting material greatly affects adsorption performances of different materials although pH can play a significant role as well. Furthermore, the adsorption capacities of different metals do not follow any particular trend comparable to the results presented in Table 5. The order of stability constants of aqueous EDTA chelates is Cu>Ni>Pb>Co>Cd>Zn (Table 4) suggesting that Zn(II) should have the lowest capacity. The hydrated radius (R_H) on its behalf follows the order of Pb>Cd>Zn>Co>Cu>Ni and the primary hydration number the opposite order: Ni>Cu>Co>Zn>Cd>Pb [130]. Therefore, both the type of the supporting material and the metal ion properties affect the adsorption capacity of the immobilized EDTA. Almost all the results in Table 6, however, were obtained for one-component systems. Experiments performed in multi-metal solutions may provide better information about the true differences between different metals.

As with IDA/NTA-functionalized adsorbents, most of the authors do not give suggestions of exact structures of metal EDTA-chelates formed on the surface. The metal chelate formed on EDTA-silica gel was proposed to have an ideal octahedral structure without any convincing evidence. The authors only observed chelate formation between EDTA functionalized silica gel and Cu(II) from variations of diffuse reflectance spectra and electron spin resonance (ESR) analysis [110]. Pereira *et al*. [122] suggested a quinquedentate structure for Me(II)EDTA chelate immobilized on sawdust and sugarcane bagasse without any characterization of metal loaded adsorbent. Coordination of metals with EDTA immobilized on biomass was confirmed by XPS-analysis, which showed bonds between metal and nitrogen as well as carboxyl groups [127]. IR-measurements also suggested the coordination through both amino and carboxyl groups [117] Finally, EDTA-functionalized mercerized cellulose and sugarcane bagasse reportedly adsorbed three metals per every two EDTA surface groups, but the binding mechanism was not discussed [123].

1.2.4 DTPA-functionalized adsorbents

Similarly to EDTA, DTPA can be attached on the silica support by first using silylating agents (APTES) and then reacting surface bound amine groups with DTPA anhydride [110]. The synthesis of DTPA functionalized chitosan is also similar to that of EDTA-chitosan [111-113]. For silica gel, DTPA coverage was much higher than EDTA coverage (Tables 6 and 7). Despite

this, the adsorption capacities of metals were much lower for DTPA-silica gel. This was attributed to the lower chelating ability of the immobilized DTPA. For chitosan, a considerably lower surface coverage was obtained for DTPA than for EDTA. This was explained by a steric hindrance of bulky DTPA molecules or the crosslinking of DTPA groups [113]. Adsorption capacities of these two modified chitosans, however, were similar (Tables 6 and 7).

Little literature is available on DTPA-functionalized adsorbents. The latest examples are melamine-formaldehyde-DTPA [131] and melamine-DTPA [132] chelating resins. The first one was prepared by heat treatment of a homogeneous slurry of melamine, DTPA, and formaldehyde and the second one by a heat-treatment of melamine and DTPA dissolved in dimethylsulfoxide. The adsorption capacities of these melamine based adsorbents were not as high as those obtained for DTPA-chitosan (Table 7), but comparable with many of the EDTA-functionalized adsorbents (Table 6).

Table 7. DTPA-functionalized adsorbents.

Matrices functionalized with DTPA	Surface coverage (mmol/g)	Metal	pH	Maximum adsorption capacity (mmol/g)	Reference
Silica gel	1.29	Cu(II)	1	0.006	[110]
Chitosan	≈ 1.3	Pb(II)	2	1.8	[112]
		Ni(II)	2	2.0	[113]
Polyallylamine	-	Ni(II)	2	1.4	[113]
Melamine-formaldehyde	0.93	Co(II)	5	0.29*	[131]
		Cu(II)		0.23*	
		Zn(II)		0.23*	
		Cd(II)		0.16*	
Melamine	-	Ni(II)	-	0.66	[132]
		Cu(II)		0.63	

*****Competitive conditions, total adsorption capacity: 0.91 mmol/g

The structures of aqueous metal DTPA-chelates are more complex than those of EDTA leading to difficult determination of the structures of immobilized DTPA-chelates. Octahedral chelate formation was suggested for Cu(II) and Co(II) based on the color change of melamine-formaldehyde-DTPA chelating resin after treatment with solutions containing corresponding metal ions [131]. In a recent study, density functional theory calculations indicated the octahedral

structure of Ni(II) and Cu(II) chelates on DTPA-functionalized melamine with coordination of metal center to three carboxyl and three amine groups [132].

Generally, comparison of Tables 5, 6, and 7 shows that higher adsorption capacities are obtained for the adsorbents with smaller ligands. This can be attributed to the steric hindrance of bigger ligands decreasing the surface coverage [112].

1.3 Applications of functionalized adsorbents

Functionalization of adsorbents with different organic groups may change the adsorbent properties into the desirable direction. Functional group addition may increase the adsorption capacity, make adsorbent more selective, or increase the stability of the adsorbent. In the case of resins functionalized with chelating agents, the main applications are the removal of heavy metals from contaminated waters, separation of different metals, or preconcentration of metal ions prior to their analysis.

1.3.1 Removal of metals from different solution matrices

In principle, most of the synthesized adsorbents are first tested in pure solutions containing only one target metal. Real waters to be treated, however, contain various metals as well as salts, acids, and different organic species. Therefore, the adsorption performance of novel adsorbents should also be tested in different solution matrices.

The benefits of APCA-functionalized adsorbents are their selectivity toward heavy metals due to their high affinity surface groups. Therefore, they can show high adsorption efficiencies in the presence of various interfering species. Wood sawdust and sugarcane bagasse modified with EDTA were able to remove 89-92% of Zn(II) from real electroplating wastewater [122]. Three different commercial IDA-bearing chelating resins were used to remove Ni(II) from the acid leached fly ash samples [133]. In this study, however, precipitation of Al(III) and Fe(III) was conducted before a successful Ni(II) adsorption (adsorption capacity 1.3 mmol/g). IDA-functionalized glycidyl methacrylate effectively adsorbed Cr(III), Cu(II), Cd(II), and Pb(II) in the presence of high content of Ca(II) and Mg(II) as well as NTA as aqueous organic species [134]. Furthermore, in a recent study IDA-functionalized Purolite S-920 resin was used to remove

metals complexed by 1-hydroxyethylene-1,1-diphosphonic acid (HEDP) from industrial effluents [135].

One of the most important organic compounds found in water matrices is EDTA. EDTA containing wastewaters are problematic since the metals chelated by it do not effectively adsorb on the adsorption resins and also EDTA enhances the transportation of metals from disposal sites in soils. Ion-exchange has been presented as the most promising solution for the metal removal in the presence of EDTA [136]. Most of the studies are based on anion-exchange, however, when the whole metal EDTA chelate is bound on the adsorbent surface [136,137]. Due to the possible leaching of metal EDTA chelates a better way would be the use of strong cation-exchangers that are able to capture metal ion from its aqueous chelate. Only a few cation-exchangers, however, have been applied for this purposes and evidence of the actual separation of metal and EDTA have not been reported [138,139]. From APCA-functionalized adsorbents material with surface group that forms more stable chelates with metals than EDTA would be preferred. Based on the stability constants of aqueous species (Table 4), DTPA-functionalized adsorbents could provide the solution, but none of the materials presented in Table 7 have not been tested for this application.

1.3.2 Separation of metals by chelating adsorbents

The reuse of metals collected from wastewater requires their separation from each other. Conventional separation methods for metals are precipitation and liquid phase extraction. Compared to those, however, solid-phase extraction using chelating resins offers several advantages such as high recovery and enrichment factors, low consumption of organic solvents, and repeated uses [140].

Particularly at low pH range metal ions are separated by many of the APCA-functionalized adsorbents [110,113]. Different commercial IDA-functionalized resins were found to be selective sorbents for Ni(II) and Co(II) in the simulated pressure acid leach liquor containing Al(III), Fe(III), Zn(II), Mn(II), Mg(II), and Cu(II) [141]. Using EDTA- and DTPA-functionalized chitosans, Co(II) (0.2 mM) could be separated from the solution containing 93 mM of Al(III) and Ni(II) from the solution containing the same amount of Ni(II) and Co(II) (1.7 mM) [113]. The separation of Co(II) from Ni(II) is important for example in hydrometallurgy

[142]. In addition, the separation of Ni(II) from the excess of Al(III) by modified chitosans [111] and from Fe(II), Co(II), and Zn(II) by EDTA-functionalized silica-poly(allylamine) composite material [115] has been reported. Shiraishi *et al*. [110] showed the separation of Cu(II), Ni(II), VO^{2+}, Zn(II), Co(II), and Mn(II) using EDTA-silica gel.

1.3.3 Preconcentration of trace amounts of metals using chelating adsorbents

Determination of trace amounts of metals from environmental samples is highly important. The analysis equipments such as the inductively coupled plasma mass spectrometry (ICP-MS), however, are very sensitive for matrix effects and high concentrations of salts, for example, considerably decrease their detection limits. Preconcentrating metals by chelating resins is the most promising technique to obtain reliable and repeatable results in metal analysis.

Prior to ICP-MS analysis, commercial IDA-functionalized Muromac A-1 chelating resin was successfully used to preconcentrate 15 rare earth elements from seawater [143]. For similar equipment, over 85% recovery of most of the trace metals (10 different) from three kinds of seawater samples was obtained using Chelex 100 (also IDA-functionalized) packed minicolumn as a preconcentration unit [144]. The benefit of the APCA-functionalized chelating adsorbents is that they can selectively bind trace amounts of heavy metals in the presence of high amounts of salts. For NTA Superflow resin almost 100% recovery was obtained for Cu(II) and Fe(III) at pH range 2-6 from 100 μm metal solutions. For Co(II), Ni(II), Zn(II), and Cd(II), however, pH above 5 was required for their total recovery [103].

2 OBJECTIVES AND STRUCTURE OF THE WORK

Study of heavy metal adsorption by EDTA/DTPA-functionalized adsorbents

The first aim of this work was to study general adsorption properties of EDTA/DTPA-functionalized silica gel and chitosan materials from pure metal solutions in different experimental conditions (Papers **I**-**III**). The effect of pH, contact time, and metal concentration as well as regenerability of the spent adsorbents was investigated. Moreover, one of the objectives was to suggest reaction mechanisms describing the adsorption processes.

Modeling of adsorption isotherms and kinetics

The aim of the modeling part was to find the isotherm and kinetic equations that could describe the obtained experimental data. Furthermore, it was important to verify the applicability of the model by comparing the properties of adsorbents with the theories behind the models. Besides work presented in Papers **I**-**V**, some additional modeling was conducted to compare all the isotherm models presented in sections 1.1.5 and 1.1.6 as well as investigate the effect of error function. Linear and non-linear regression was also compared. Paper **IV** in this work is almost purely theoretical and presents the fitting results of one- and two-component isotherms to very extensive experimental data range.

Application study of EDTA/DTPA-functionalized adsorbents

In application testing the main interest was to test DTPA-functionalized silica gel and chitosan in capturing Co(II) from its aqueous EDTA-chelate (Paper **V**). In the same study the effect of various solution matrices was investigated. Separation of metals was studied in two-component (Papers **II** and **IV**) and multimetal systems (Paper **III**). Finally, some previously unpublished data about the applicability of EDTA- and DTPA-silica gel as preconcentrating adsorbents is presented.

3 MATERIALS AND METHODS

3.1 Synthesis of EDTA/DTPA-functionalized adsorbents

Syntheses of EDTA/DTPA-functionalized adsorbents are described in detail in Papers **I**, **II**, and **III**. Briefly, silica gel (particle sizes 5-20, 40-63, and 63-200 μm) was at first modified with amino groups by silanization method after which the surface bound amino groups were let to react with EDTA or DTPA anhydride in a mixed ethanol and acetic acid solution (Figure 5a and Paper **I**). Chitosan was reacted with EDTA or DTPA anhydride in methanol containing 10% of acetic acid (Figure 5b and Paper **II**). Finally chitosan-silica hybrid materials (Chi:TEOS 2:60, 2:30, and 2:15, Figure 6) were prepared by the sol gel method following a similar EDTA-functionalization as in the case of chitosan (Paper **III**).

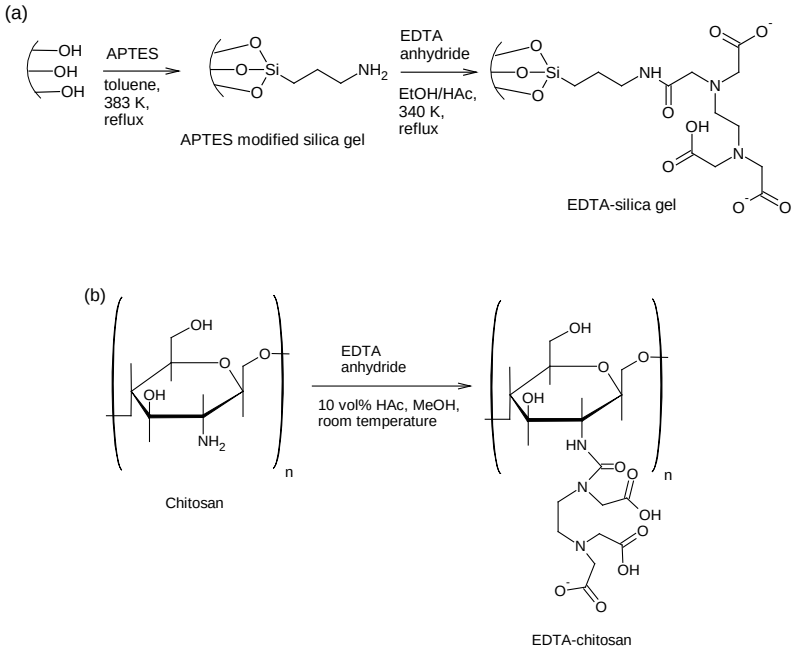

Figure 5. Synthesis of (a) EDTA-silica gel and (b) EDTA-chitosan.

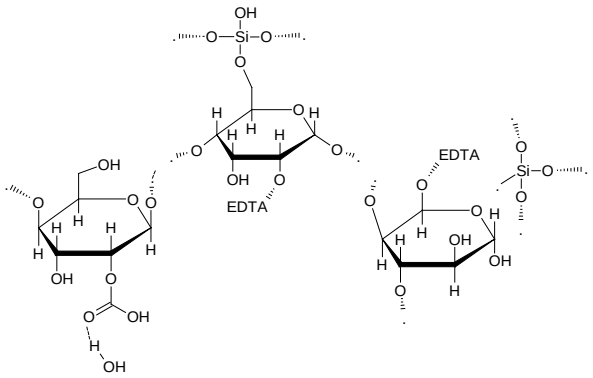

Figure 6. A possible structure of the chitosan-silica hybrid materials.

3.2 Characterization of functionalized adsorbents

Elemental analysis was conducted for determining the surface coverage of EDTA and DTPA (Papers **I** and **II**). A specific surface area and total pore volume of the adsorbents were determined with Autosorb-1-C surface area and pore size analyzer (Quantachrome, the UK). Zetasizer Nano Series model ZEN 3600 (Malvern, the UK) was employed to measure isoelectric points. The surface morphology was examined using a Hitachi S-4100 scanning electron microscope (SEM). Fourier transform infrared spectroscopy (FTIR) type Nicolet Nexus 8700 (USA) was used to identify the surface groups of the synthesized adsorbents.

3.3 Adsorption and desorption experiments

Adsorption and desorption experiments are described in detail in Papers **I-V**. Briefly, solution containing metal ions was mixed with adsorbent (dose: 2 g/L) for a designed time after which the solid was separated from the solution. The equilibrium adsorption capacity (q_e, mmol/g) was calculated as follows:

$$q_e = \frac{(C_i - C_e)}{m} V \tag{45}$$

where C_i and C_e are the initial and the equilibrium concentrations (mmol/L), while m and V are the weight of the adsorbent (g) and the volume of the solution (L). The distribution ratio (K_d, mL/g), which describes the distribution of adsorbate between the solution and the adsorbent at equilibrium, was calculated using the following equation.

$$K_d = 1000 \frac{mL}{L} \times \frac{q_e}{C_e} \quad (46)$$

In desorption experiments conducted by batch mode, 1 or 2 M HNO_3 was used to remove metal ions from the adsorbent surface after which the adsorbent was reused (see Papers **I**, **II**, and **V**).

3.4 Analysis of solutions

The metal concentrations in the solutions were determined using an inductively coupled plasma optical atomic emission spectrometry (ICP-OES) model iCAP 6300 (Thermo Electron Corporation, USA). The used wavelengths for different metals were: Co(II): 228.616 nm, Ni(II): 231.605 nm, Cd(II): 226.502 nm, and Pb(II): 220.353 nm. The specifiation of Co(II)EDTA and EDTA was determined by capillary electrophoresis (CE) measurements (Beckman Coulter, USA). The detailed description of CE analysis is presented in Paper **V**.

3.5 Preconcentration experiments

Preconcentration experiments were conducted by pumping (flow rate: 0.5 mL/min) 500 mL of the solution containing 1 μg/L of metals through columns filled with EDTA- or DTPA-silica gel (bed volume: 3.5 cm^3). After rinsing with 50 mL of water, metals were desorbed from the adsorbent surfaces using ca. 5 mL of 2 M HNO_3 with a flow rate of 1 mL/min. ICP analysis was performed from the concentrated sample. Experiments were conducted from the multimetal solutions using both pure water and 3% NaCl as matrix.

3.6 Modeling of adsorption kinetics and isotherms

Modeling of adsorption kinetics was conducted using Origin software version 8.0 (Microcal Software, Inc.). Both linear and non-linear regression was applied. Modeling of adsorption isotherms was done by non-linear regression using Origin software (Papers **I**-**III** and **V**)) or self-made program (Papers **II** and **IV**). Both of the methods used the Levenberg-Marquardt algorithm for optimizing. The first method was based on the minimizing of ERRSQ error function and the second one minimizing of both ERRSQ and MPSD error functions.

4 RESULTS AND DISCUSSION

4.1 Characterization of EDTA/DTPA-functionalized adsorbents

Important characteristics of adsorption materials are their specific surface areas and surface morphologies. Silica gel is a mesoporous material with high surface area. After surface modification surface area and total pore volume of silica gel decreased due to the pore blocking by functional groups. Furthermore, modification with larger molecules enhanced the pore blocking (Figure 3 and Table 3 in Paper **I**). The low surface areas of functionalized chitosans indicated their non-porous structure (Section 3.1 in Paper **II**). Surface properties of EDTA-functionalized chitosan-silica hybrid materials resembled those of modified silica gels except they had lower surface areas and higher pore volumes and pore diameters. The surface area increased with the increasing silicon content, but the parameters related to the pore properties did not follow this trend. Comparison of the unmodified and modified hybrid materials (Table 1 in Paper **III**) showed the expected decrease of the surface area comparable to the case of silica gel (Table 3 in Paper **I)**. This could not be attributed to the pore blocking, however, due to the increase in pore volume and size after modification. Hence, the changes of surface areas were most likely due to the loss of some silicon during the synthesis. Table 8 compares the surface properties of the studied EDTA/DTPA-functionalized adsorbents.

Table 8. Properties of EDTA/DTPA-functionalized adsorbents

Adsorbent	Particle size (μm)	Specific surface area (m^2/g)[b]	Total pore volume (cm^3/g)[b]	Average pore diameter (Å)[b]	Si content (%)[b]	Surface coverage of EDTA/DTPA (mmol/g)[b]
EDTA-silica gel	40-63	384	0.48	49	-	0.32
DTPA-silica gel	40-63	328	0.41	49	-	0.23
EDTA-chitosan	100-200[a]	0.71	0.0018	610	-	1.40
DTPA-chitosan	100-200[a]	0.36	0.0007	552	-	0.96
EDTA-Chi:TEOS 2:60	5-50[a]	226	0.69	122	73.4	-
EDTA-Chi:TEOS 2:30	5-50[a]	209	0.90	158	70.0	-
EDTA-Chi:TEOS 2:15	5-50[a]	169	0.55	131	54.6	-

[a]Approximated from SEM-images
[b]Data collected from Papers I-III.

SEM-images presented in Figure 7 show the differences between the surface morphology of studied adsorbents. As Table 8 demostrates, modified silica gel and hybrid materials had mesoporous surface morphology compared to modified chitosans, which had quite a smooth surface. Comparison of hybrid materials with different ratios of chitosan and silica (Figure 1 in Paper **III**) showed that material with the highest chitosan content had more grain coalescence than others, which was attributed to the crosslinking between chitosan groups close to each other [114].

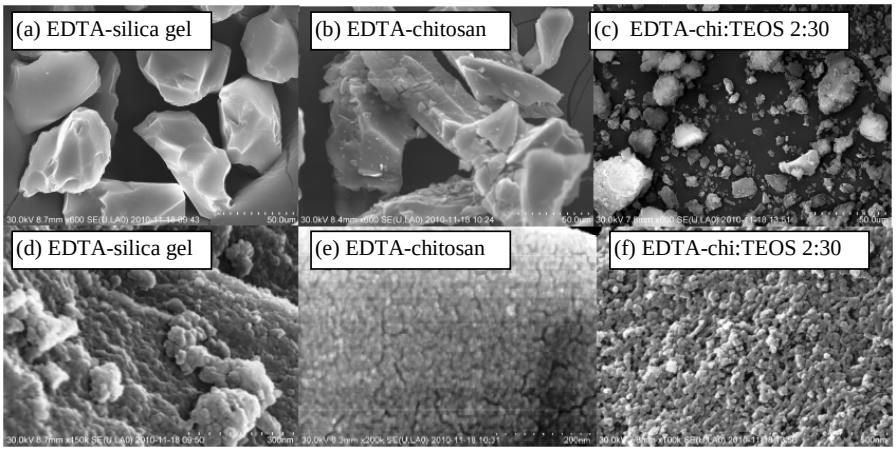

Figure 7. SEM-images for EDTA-functionalized adsorbents.

Surface coverages of EDTA and DTPA of modified adsorbents were determined by elemental analysis (Table 8 and Papers **I** and **II**). EDTA-chitosan obtained the highest coverage, which can be attributed to the highest amount of primary amino groups on its surface. For hybrid materials neither the elemental analysis nor calculating the coverages from the silicon content gave reasonable results (values well below 0.1 mmol/g were obtained). This might be attributed to the release of some silicon during the EDTA-functionalization step, when comparison of modified and unmodified materials gave incorrect results. However, it is evident from Tables 6 and 7 that many of the papers do not present the surface coverages of EDTA or DTPA functionalized adsorbents. Thus, it is possible that other authors have also confronted some difficulties in determining these.

A useful tool for analyzing the type of functional groups on the adsorbent surface is FTIR-spectroscopy. The FTIR-spectra of modified silica gel and chitosan are presented in Figure 8 and those of hybrid materials in Figure S1 in Paper **III**. Table 9 summarizes the identified absorption bands [107,127].

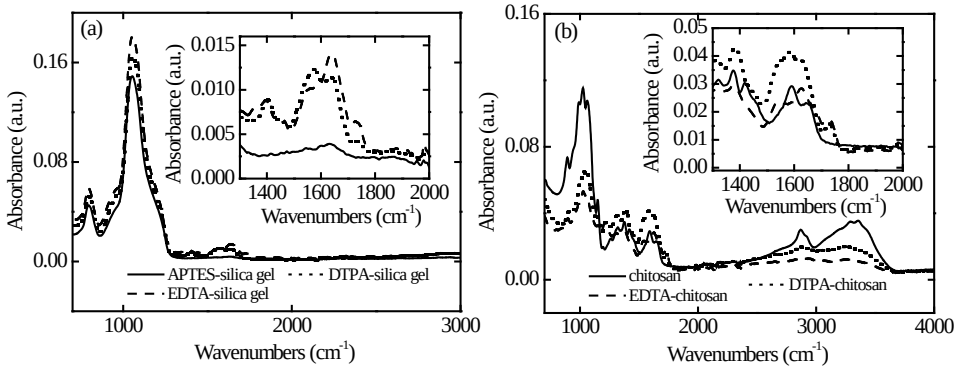

Figure 8. FTIR-spectra for EDTA/DTPA-functionalized (a) silica gel and (b) chitosan.

Table 9. Identification of the absorption bands of EDTA/DTPA-functionalized adsorbents.

	EDTA-silica gel	DTPA-silica gel	EDTA-chitosan	DTPA-chitosan	EDTA-Chi:TEOS 2:60	EDTA-Chi:TEOS 2:30	EDTA-Chi:TEOS 2:15
OC–N, amide III	1319	1321	1309	1311	1315	1311	1319
—COO^-	1398	1398	1377	1379	1389	1389	1387
C=O in —COOH	1441	1440	1418	1423	1433	1433	1433
Vibrations of N–H bond, amide II band, —COO^-	1543	1554	1549	1551	1560	1543	1549
C=O bond in amide group (amide I band)	1635	1632	1628	1622	1634	1635	1632
C=O in —COOH	1724	1728	1726	1730	1730	1734	1734

The presence of bands related to amide bond and carboxyl groups confirmed the functionalization of silica gel and chitosan materials with EDTA or DTPA. Furthermore, comparison of the spectra of unmodified and EDTA/DTPA-functionalized chitosans (Figure 8b) clearly showed that the band between 3000 and 3400 cm^{-1}, assigned to the stretching of OH-groups and overlapping stretching of NH_2-groups, significantly decreased after EDTA/DTPA-immobilization. This

suggests a high functionalization degree of primary amino groups also observed earlier by Inoue *et al.* [112] and Nagib *et al.* [111]. According to Figure 8b some of the NH_2-groups, however, remained on the chitosan surface after chelate binding, which is discussed later on. Moreover, it should be noted that the bands related to the NH_2- and OH-groups were not as intense for aminopropyl-functionalized silica gel (Figure 8a) or chitosan-silica hybrid materials (Figure S1 in Paper **III)**.

Furthermore, FTIR spectra after metal binding was measured and chelation mechanism confirmed from the change of bands at 1309-1319 cm^{-1}, 1543-1554 cm^{-1}, and 1622-1635 cm^{-1} (Figures 9 and 10) [107]. The bands at 1418-1441 cm^{-1} and 1724-1734 cm^{-1}, however, did not disappear completely after metal binding indicating that some free –COOH–groups remained on the surface. The results are in agreement with the formation of quinquedentate [94,122] and octahedral [95,132] structures of metal EDTA and DTPA surface chelates.

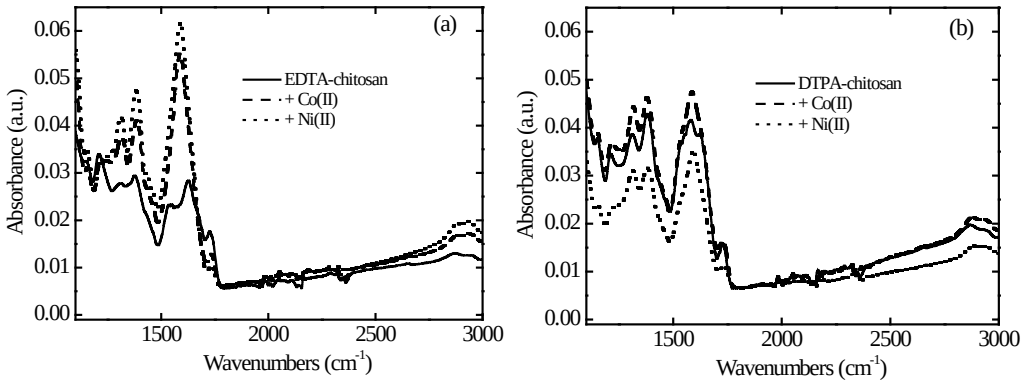

Figure 9. Effect of Co(II) and Ni(II) adsorption on FTIR-spectra of (a) EDTA-chitosan and (b) DTPA-chitosan (unpublished data).

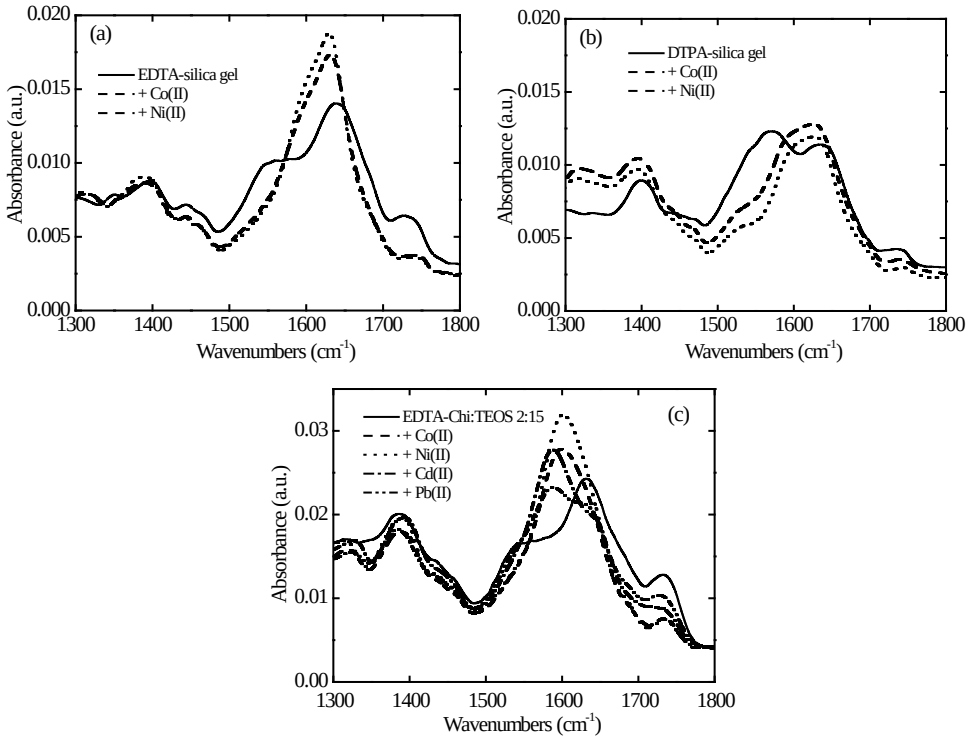

Figure 10. Effect of metal adsorption on FTIR-spectra of (a) EDTA-silica gel (b) DTPA-silica gel, and (c) EDTA-Chi:TEOS 2:15 (unpublished data).

4.2 Adsorption of heavy metals by EDTA/DTPA-functionalized adsorbents

4.2.1 Effect of pH

Acidity of the solution affects the solubility (ionization) of the metal ions and concentration of the counter ions of the surface groups (in this case H^+) [119]. These significantly influence the adsorption process and therefore pH should be optimized to ensure the best adsorption efficiency. Figure 11 shows the effects of pH on the adsorption of Co(II) by EDTA-functionalized adsorbents. It can be seen that adsorption efficiency increased with the increasing pH for all the adsorbents. The similar trend was observed for almost all the EDTA/DTPA-functionalized

materials presented in Tables 6 and 7. The limiting behavior at low pH can be attributed to the competition between protons and metal ions for the available adsorption sites [115]. Zeta-potential measurements showed that the surface charge of the EDTA/DTPA-functionalized silica gels increased as the pH decreased (Figure 2 in Paper **I**) suggesting repulsive forces between surface and metal cations in acidic media.

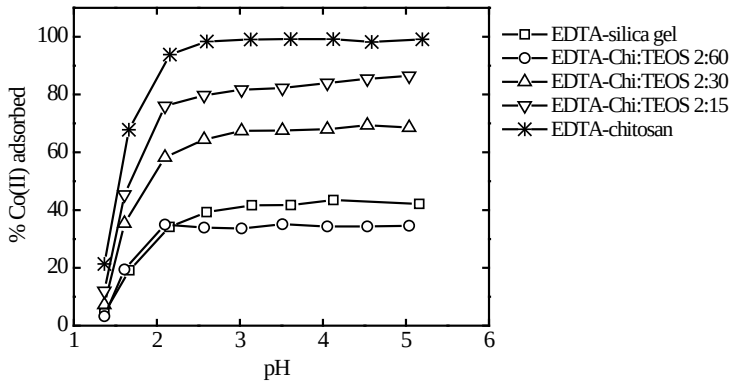

Figure 11. Effect of pH on adsorption of Co(II) by EDTA-functionalized adsorbents. Experiments repeated using the initial Co(II) concentration of 1.3 mM. Dose: 2 g/L.

Comparison between different materials suggests that higher chitosan content increased the adsorption efficiency of the material at low pH (see also Figure 3b in Paper **III**). For example, at pH 2 81% of maximum capacity was obtained for EDTA-silica gel, 87% for EDTA-Chi:TEOS 2:15, and 95% for EDTA-chitosan. It is possible that the chitosan matrix, which is more electronegative (electronegativity of carbon: 2.5) than the silica gel matrix (electronegativity of silicon: 1.7) increased the acidity of the EDTA carboxyl groups making them more available for metal adsorption at low pH range. Moreover, the chelating ability of immobilized EDTA-groups at a low pH has also been observed elsewhere and assigned to the inductive effects that decrease pK_a values of EDTA carboxyl groups [122].

In Paper **II** (Figure 2b)**,** it was observed that EDTA/DTPA-functionalized chitosans showed a clear adsorption maximum for Co(II) at pH range from 2 to 2.5 at low metal concentrations (17 μM). This was attributed to the crosslinking effect between carboxyl groups of

chelating agents and the surface. At higher concentrations fast metal binding occurred before crosslinking and adsorption capacity remained similar after pH 2. On the other hand, a similar effect was not seen in modified silica gels possibly due to their rigid structure as well as a lower amount of primary amino groups preventing corsslinking (see FTIR spectra in Figure 8).

The type of the target metal significantly influenced the pH curves (Papers **I**-**III**). Ni(II) started to adsorb at a lower pH range than Co(II) and at pH as low as 1 around 90% Ni(II) removal was obtained for EDTA-chitosan from a 100 mg/L solution (Figure 2 in Paper **II**). This indicates that EDTA/DTPA-functionalized adsorbents could be used to separate Ni(II) from Co(II) at a low pH, which could be applied in hydrometallurgy, for example [142]. The Cd(II) adsorption had a pH behavior similar to Co(II) and Pb(II) to Ni(II) (Figure 3a in Paper **III**). Better adsorption efficiencies of Ni(II) and Pb(II) over Co(II) and Cd(II) can be explained by the higher stabilities of their EDTA- and DTPA-chelates forming at low pH (see Table 4 and Appendix I).

4.2.2 Effect of contact time

Figure 12 shows the effect of contact time on the adsorption of Co(II) by EDTA/DTPA-functionalized adsorbents. At the initial adsorption stage, the adsorbent surface contained a lot of available active sites for metal binding and fast adsorption took place. After this adsorption slowed down due to the decrease of concentration of metals in solutions phase as well as a possible location of active sites in the positions that were not easily available (for example inside the pores).

For all the EDTA-functionalized adsorbents a contact time of 6 h was sufficient to attain equilibrium at high metal concentrations (1.3 mM). More differences were seen at lower metal concentrations (Figure 12b), for which EDTA-chitosan showed the fastest adsorption. This can be attributed to the highest surface coverage of EDTA on the chitosan surface creating active sites that were easily available for metal binding. In the case of EDTA-Chi-TEOS 2:60 and EDTA-silica gel the smaller size of the former (see Table 8 and Figure 7) led to faster adsorption, which was also evident for the modified silica gels of different particle sizes (Figure 7 in Paper **I**).

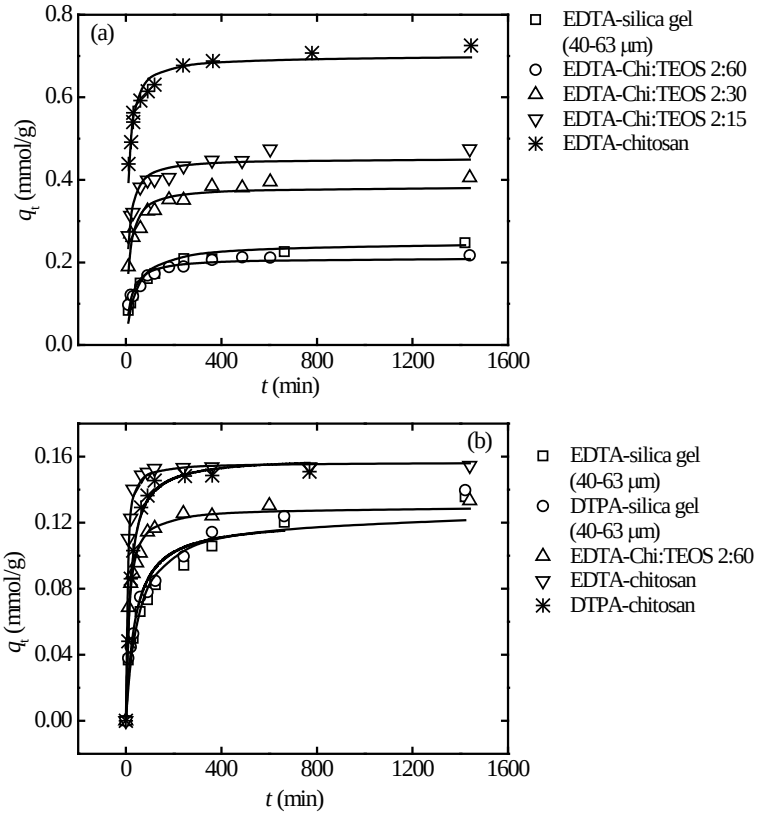

Figure 12. Effect of contact time on adsorption of Co(II) by EDTA/DTPA-functionalized adsorbents. Results collected from Papers **I**-**III** and **V**. Dose: 2 g/L, pH: 2 for modified chitosans and pH: 3 for other adsorbents, Co(II) concentration: (a) 1.3 mM and (b) 0.3 mM.

For modified silica gels, the effect of contact time was not significant when EDTA- and DTPA-functionalized materials were compared (Figure 12b). Differences between EDTA- and DTPA-chitosan were clear (Figure 12b, Figure 4 in Paper **II**), however, and slower adsorption on DTPA-chitosan was attributed to the crosslinking caused by bulky DTPA-groups [111] and lower surface coverage of DTPA.

4.2.3 Effect of initial metal concentration

Adsorption isotherms were measured by varying only the initial metal concentrations. Comparisons of different EDTA-functionalized materials are shown in Figure 13. The highest adsorption capacity was obtained for EDTA-chitosan, which was expected due to its highest ligand loading. Furthermore, the adsorption capacity for hybrid adsorbents increased as the chitosan content increased. The adsorption efficiencies of EDTA-silica gel and EDTA-Chi:TEOS 2:60 were, however, similar.

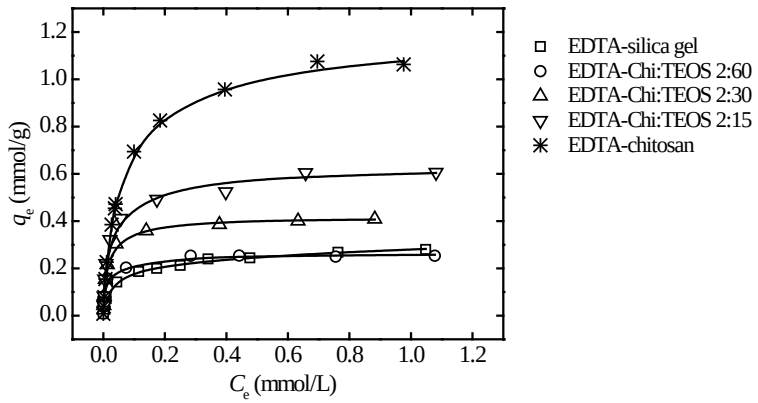

Figure 13. Effect of initial metal concentration on the adsorption of Co(II) by EDTA-functionalized adsorbents. Dose: 2 g/L, pH: 2 for EDTA-chitosan and pH: 3 for other adsorbents. Results collected from Papers **I-III**

Table 10 further summarizes the adsorption efficiencies. It is interesting to note that even if the modified chitosans showed the highest adsorption efficiency at high concentrations they gave lower efficiency at concentrations below 0.17 mM (10 mg/L). A similar effect was seen in the pH experiments (see section 4.2.1) and can be attributed to the enhanced interactions of carboxylic groups and chitosan surface at low metal concentrations (crosslinking effect).

Table 10. Comparison of adsorption efficiencies of EDTA/DTPA-functionalized adsorbents.

			Co(II) conc. 0.17 mM	Co(II) conc. 0.85 mM	Co(II) conc. 1.7 mM
Adsorbent	pH	q_m (mmol/g)[a]	% of Co(II) adsorbed	% of Co(II) adsorbed	% of Co(II) adsorbed
EDTA-silica gel	3	0.34	97.4	58.7	35.5
DTPA-silica gel	3	0.27	99.0	62.7	31.6
EDTA-chitosan	2	1.07	98.0	96.6	93.8[b]
DTPA-chitosan	2	0.83	95.5	93.3	85.9
EDTA-Chi:TEOS 2:60	3	0.25	98.6	64.3	30.2
EDTA-Chi:TEOS 2:30	3	0.42	98.2	83.9	55.6
EDTA-Chi:TEOS 2:15	3	0.63	98.4	93.5	67.7

[a]Data collected from Papers **I**, **II**, and **III**
[b]99.2% at pH 3

Comparison of Table 10 to Tables 6 and 7 shows that our EDTA- and DTPA-silica gels had considerably higher adsorption efficiencies than those obtained by Shiraishi *et al.* [110] despite their equal or higher coverage of functional groups. This discrepancy can be explained at least partly by the different experimental conditions. Shiraishi *et al*. used only 1 hour equilibrium time and pH 1 where they also observed the highest adsorption performance. This was not the case in this study and therefore, it is possible that the materials prepared by Shiraishi *et al*. differed from those synthesized in our work.

EDTA- and DTPA-chitosan were also synthesized earlier by Inoue *et al.* [113]. They obtained somewhat higher adsorption capacities compared to this work, which was attributed to the differences between the starting materials (Paper **II**). The adsorption performances of EDTA-chitosan silica hybrid adsorbents were comparable to many of those presented in Table 6. Especially, EDTA-Chi:TEOS 2:15 clearly showed a higher adsorption capacity compared to conventionally functionalized silica gel. This novel hybrid adsorbent, having a rigid structure (see section 4.3 and Figure S2 in Paper **III**), seemed to combine the beneficial properties of both silica gel and chitosan.

4.2.4 Adsorption mechanism

Papers **I** and **II** present the suggested adsorption mechanisms for EDTA-silica gel and -chitosan. Furthermore, FTIR-measurements confirmed that metals were bound on the surface by chelation

(Figures 9 and 10). In the case of EDTA- and DTPA-functionalized silica gels (pH 3), the release of protons during the adsorption was approximately one to every adsorbed metal ion, which for Co(II) adsorption can be explained by the following reaction equation:

$$SiO_2\text{-}NH\text{-}HEDTA^{2-} + Co^{2+} \leftrightarrow SiO_2\text{-}NH\text{-}Co(II)EDTA^{-} + H^{+} \quad (47)$$

The above mechanism is also supported by the zeta-potential measurements, which showed that the surface carried a negative charge after metal binding (Figure 2 in Paper **I**). For modified chitosans the solution pH was not significantly affected by metal adsorption. The mechanism derived from the speciation calculations, however, showed that some protons should have appeared in the solution due to the adsorption (see Section 3.3 in Paper **II**). This discrepancy was explained by the binding of released protons by free amino groups on the chitosan surface [145].

In contrast to these results, EDTA-functionalized chitosan-silica hybrid materials showed a release of two protons for every adsorbed metal ion at a pH range from 3 to 5. Therefore, the following reaction is suggested:

$$SiO_2\text{-}NH\text{-}H_2EDTA^{-} + Co^{2+} \leftrightarrow SiO_2\text{-}NH\text{-}Co(II)EDTA^{-} + 2H^{+} \quad (48)$$

Unlike for modified chitosans, released protons were not able to bind on the surface, because the hybrid chitosan-silica network (Figure 6) did not contain any free amino groups after EDTA-immobilization (see Figure S1 in Paper **III** and ref. [146]). On the whole, however, the surface reactions are better considered as chelation rather than ion-exchange due to the uncertainty of the true amount of protons released for every metal ion absorbed. In addition, for example at neutral conditions, all the carboxyl groups of the immobilized chelating agents should be in their ionic form when ion-exchange is not longer possible.

Finally, it is important to note that speciation calculations based on the aqueous species may not be directly applicable for the surface bound chelates [5]. Therefore, the mechanisms presented in this work are only suggestions based on the best available information.

4.3 Stability and regenerability of the EDTA/DTPA-functionalized adsorbents

Stability of the different adsorbents was investigated by regeneration experiments (Papers **I**, **II** and **V**) and by analyzing the silicon leaching after the adsorption experiments (Papers **I** and **III**). Regeneration performed by 1 or 2 M HNO_3 did not significantly change the adsorption efficiency of EDTA/DTPA-functionalized silica gels or chitosans (Table 10 in Paper **I** and Table 1 in Paper **II**), indicating a very high stability. Moreover, the leaching of silicon from EDTA/DTPA-silica gels was significantly lower than that from the intermediate synthetic product APTES-silica gel (Figure 5 in Paper **I**), which was attributed to the stabilization of the materials by the surface bound chelating agents. The silicon leaching from EDTA-Chi:TEOS 2:60 was slightly higher than from EDTA-silica gel (Figure 2 in Paper **III**). Considerably lower leaching observed for EDTA-Chi:TEOS 2:30 and 2:15, however, confirmed their stability. Finally, comparison of the swelling of studied adsorbents showed increasing rigidity of the hybrid materials over the modified chitosan (see Figure S2 in Paper **III**), which can be attributed to the networking between silica and chitosan moieties (see Figure 6 and ref. [146]).

4.4 Modeling adsorption kinetics

4.4.1 Pseudo-second-order model

As presented in section 1.1.8 the PS2 model suggests that the adsorption rate is governed by the surface reaction. In papers **I** and **II** we applied linear fittings of both PS1 and PS2 models and found that the PS2 model sufficiently described the adsorption kinetics of modified silica gels and chitosans. In papers **III** and **V** non-linear regression was used instead. For comparison, both linear and non-linear fittings of PS2 model were conducted for Co(II) adsorption by all the studied adsorbents and results are shown in Table 11. For clarity, Table 11 shows results only for one initial concentration of Co(II) for each of the adsorbent and the results obtained for the other studied metals (Papers **I-III**) and Co(II)EDTA complex (Paper **V**) are not presented.

Table 11. Comparison of linear and non-linear regression of PS2 model for Co(II) adsorption by EDTA/DTPA-functionalized adsorbents. Dose: 2 g/L, pH: 2 for functionalized chitosans and pH: 3 for the other adsorbents. Uncertainty of the parameters obtained by Origin. Total differential used for linear equations.

			linear			*non-linear*		
Adsorbent	C_0 (mmol/L)	$q_{e,exp}$ (mmol/g)	q_e (mmol/g)	k_2 (g/mmol min)	R^2	q_e (mmol/g)	k_2 (g/mmol min)	R^2
EDTA-silica gel 5-20[a]	1.31	0.25	0.25 ± 0.01	0.36 ± 0.09	1.000	0.27 ± 0.01	1.03 ± 0.11	0.992
EDTA-silica gel 40-63[a]	1.31	0.26	0.27 ± 0.01	0.06 ± 0.02	0.999	0.25 ± 0.01	0.11 ± 0.02	0.957
EDTA-silica gel 63-200[a]	1.31	0.24	0.24 ± 0.01	0.05 ± 0.02	0.999	0.22 ± 0.01	0.09 ± 0.02	0.960
DTPA-silica gel 5-20[a]	1.31	0.24	0.24 ± 0.01	0.54 ± 0.24	1.000	0.24 ± 0.01	1.27 ± 0.12	0.997
DTPA-silica gel 40-63[a]	1.31	0.27	0.27 ± 0.01	0.06 ± 0.03	0.998	0.24 ± 0.01	0.15 ± 0.03	0.958
DTPA-silica gel 63-200[a]	1.31	0.26	0.26 ± 0.01	0.06 ± 0.02	1.000	0.24 ± 0.01	0.11 ± 0.02	0.955
EDTA-chitosan[a]	1.64	0.70	0.70 ± 0.01	0.27 ± 0.08	1.000	0.71 ± 0.01	0.16 ± 0.02	0.993
DTPA-chitosan[a]	1.64	0.71	0.72 ± 0.01	0.03 ± 0.01	1.000	0.70 ± 0.02	0.03 ± 0.01	0.989
EDTA-Chi:TEOS 2:60[b]	1.21	0.22	0.22 ± 0.01	0.17 ± 0.04	1.000	0.21 ± 0.01	0.26 ± 0.05	0.963
EDTA-Chi:TEOS 2:30[b]	1.15	0.41	0.41 ± 0.01	0.10 ± 0.02	1.000	0.38 ± 0.01	0.22 ± 0.04	0.964
EDTA-Chi:TEOS 2:15[b]	1.15	0.44	0.44 ± 0.01	0.11 ± 0.03	0.999	0.42 ± 0.01	0.22 ± 0.03	0.976

[a]Linear data taken from Papers **I** and **II**, non-linear data recalculated
[b]Non-linear data taken from Paper **III**, linear data recalculated

Both linear and non-linear fittings provided similar q_e values, which were also close to those obtained experimentally. In most cases, however, non-linear fitting provided rate constants around two times higher than linear fitting. In addition, the correlation coefficients were lower for non-linear fitting, indicating that the PS2 model might not be the best one for describing kinetic data. The differences between linear and non-linear fitting results may arise from the appearance of variable *t* on the both sides of Eq. (42). Despite that, calculated PS2 rate constants correlated well with the observations achieved in section 4.2.2 predicting the highest rate constants for the smaller particles and the highest ligand loading owing EDTA-chitosan. On the other hand, low adsorption kinetics for DTPA-chitosan can be attributed to its crosslinked structure.

In Paper **V**, the PS2 model was also applied to Co(II)EDTA adsorption by DTPA-silica gel and –chitosan at different temperatures. The first interesting observation was that we obtained

greatly improved non-linear fitting results for chelated Co(II) than for free Co(II) in the case of DTPA-silica gel (Figure 3a and Table 2 in Paper **V**), which was attributed to the direct chemical reaction of Co(II)EDTA with the outermost DTPA surface groups. Free Co(II) was able to diffuse inside the mesoporous structure of modified silica gel, however, which worsened the PS2 fitting. A clear increase of the PS2 rate constants with increasing temperature also supported the PS2 model applicability for Co(II)EDTA adsorption [64].

4.4.2 Intraparticle diffusion model

Intraparticle diffusion model (Eq. 44) was used in this study since most of the studied adsorbents had a mesoporous structure. Results for modified chitosan and hybrid materials can be found in Papers **II**, **III**, and **V**. For comparison, diffusion rate constants were determined for the modified silica gels as well and are compared to the other studied adsorbents in Table 12. As in Table 11, only results for one initial Co(II) concentration for each of the adsorbent are shown.

Table 12. Diffusion rate constants obtained from intraparticle diffusion plots for Co(II) adsorption by EDTA/DTPA-functionalized adsorbents. Dose: 2 g/L, pH: 2 for functionalized chitosans and pH: 3 for the other adsorbents. Uncertainty of the parameters obtained by Origin.

Adsorbent	C_0 (mmol/ L)	$k_{dif,1}$ (mmol/g $min^{1/2}$)	$k_{dif,2}$ (mmol/g $min^{1/2}$)	$k_{dif,3}$ (mmol/g $min^{1/2}$)	$k_{dif,4}$ (mmol/g $min^{1/2}$)
EDTA-silica gel 5-20[a]	1.31	0.056 ± nd	0.0054 ± 0.0016	0.0012 ± 0.0001	0.00014 ± 0.00004
EDTA-silica gel 40-63[a]	1.31	0.022 ± 0.002	0.0077 ± 0.0006	0.0019 ± 0.0001	0.00001 ± 0.00001
EDTA-silica gel 63-200 [a]	1.31	0.018 ± 0.001	0.0052 ± 0.0001	0.0020 ± 0.0001	0.00070 ± 0.00010
DTPA-silica gel 5-20 [a]	1.31	0.057 ± nd	0.0176 ± 0.0008	0.0027 ± 0.0002	0.00015 ± 0.00006
DTPA-silica gel 40-63 [a]	1.31	0.023 ± 0.003	0.0059 ± 0.0005	0.0018 ± 0.0002	0.00081 ± 0.00045
DTPA-silica gel 63-200 [a]	1.31	0.023 ± 0.001	0.0071 ± 0.0002	0.0023 ± 0.0001	0.00040 ± 0.00014
EDTA-chitosan[b]	1.64	0.118 ± nd	0.0583 ± 0.0010	0.0003 ± 0.0001	
DTPA-chitosan[b]	1.64	0.054 ± 0.010	0.0188 ± 0.0018	0.0025 ± 0.0006	
EDTA-Chi:TEOS 2:60[b]	1.21	0.044 ± nd	0.0104 ± 0.0013	0.0039 ± 0.0004	0.00047 ± 0.00018
EDTA-Chi:TEOS 2:30[b]	1.15	0.060 ±0.001	0.0113 ± 0.0039	0.0048 ± 0.0008	0.00076 ± 0.00001
EDTA-Chi:TEOS 2:15[b]	1.15	0.071 ± nd	0.0247 ± 0.0029	0.0050 ± 0.0005	0.00003 ± 0.00001

[a]Calculated for comparison [b]Taken from Papers **II** and **III,** nd = not determined, line drawn from the origin to the first experimental point.

In Table 12, the first diffusion constant ($k_{dif,1}$) can be attributed to the boundary layer or external film diffusion and the remaining constants to the diffusion in macro/meso/micro pores [80]. The $k_{dif,1}$ visibly increased with decreasing particle size in modified silica gels, which can be attributed to the smaller diffusion layer thickness of smaller particles [147]. Furthermore, a linear relationship was seen between the concentration and $k_{dif,1}$ (see Papers **II**, **III**, and **V**), which is consistent with the concept of surface "film diffusion" [148]. For hybrid materials, the fastest external film diffusion occured for the material with the highest ligand loading. In addition, the higher amount of active sites seemed to accerelate pore diffusion. Comparison of diffusion rate constants of modified silica gels and hybrid materials suggests that faster diffusion inside the pores was accomplished for materials with larger pore sizes (see Table 8).

In Paper **II**, we assigned different regions of intraparticle diffusion plots obtained for EDTA- and DTPA-chitosan to diffusion in meso- and micropores. The SEM-images obtained later, however, showed the non-porous structure of modified chitosans (Figure 7e) and measurements of surface properties a possible presence of macropores (Table 8). Therefore, the diffusion constant $k_{dif,2}$ in this case should instead be assigned to the diffusion of metals in macropores or in regions, where active sites were harder to reach by metal ions due to the crosslinking between surface groups (see sections 4.2.1, 4.2.2).

Besides these observations, significance of pore diffusion was seen in the adsorption of Co(II)EDTA chelates by DTPA-functionalized silica gel and chitosan (Paper **V**). These results indicated that the large Co(II)EDTA molecules could not diffuse inside the mesopores of DTPA-silica gel as in the case of free Co(II) ions. For DTPA-chitosan, however, intraparticle diffusion plots showed different linear regions indicating diffusion also in the interior parts (macropores, crosslinked sections) of the adsorbent.

4.5 Modeling adsorption isotherms

4.5.1 One-component systems

In Papers **I**-**V** the studied isotherm models were Langmuir, Freundlich, Sips, Redlich-Peterson, and BiLangmuir. To further compare different models we also tested other isotherm equations

presented in section 1.1.5. Furthermore, to study the effect of linearization, four different linear forms of Langmuir model (Table 3) were applied. Modeling results for Co(II) adsorption by EDTA- and DTPA-silica gels are shown in Figures 14 and 15 and Tables 13 and 14.

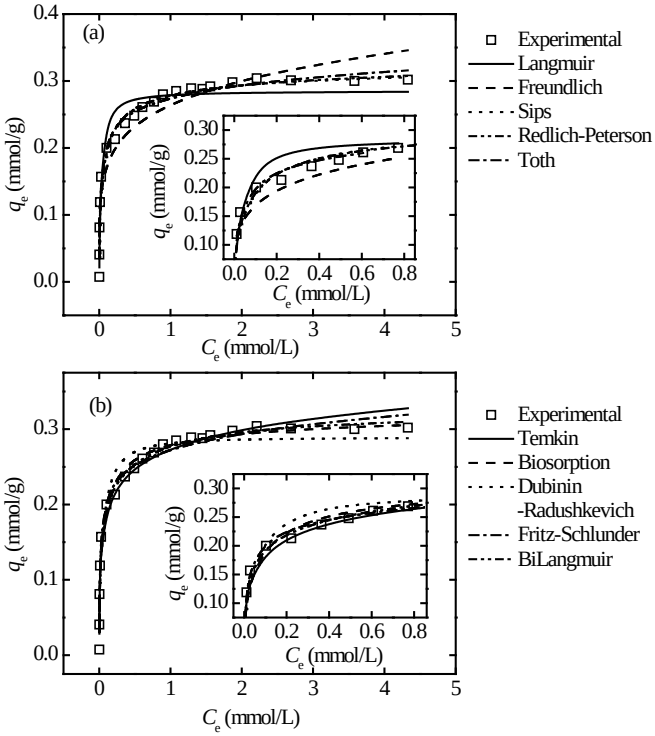

Figure 14. Fitting results of different isotherms for Co(II) adsorption by EDTA-silica gel 40-63 μm. Dose: 2 g/L, pH: 3, Co(II) concentration: 0.017-5.1 mM. Most of the isotherms simulated for comparison (see Table 13).

Figure 14 shows that many of the isotherm models appeared to fit to the experimental data well. Clear deviations were seen in the Langmuir, Freundlich, Temkin, and Dubinin-Radushkevich models. The poor fittings of the Langmuir and Freundlich models were also seen in Papers **I** and **II**. By comparing the predicted q_m values and magnitudes of selected error functions, the best fitting model appeared to be the BiLangmuir model. It was also observed that the Sips and general adsorption models gave overlapping curves. This is because the general adsorption

isotherm can be rearranged to the Sips equation [29]. Furthermore, it was noticed that Fritz-Schlunder model was poorly fitted at high concentrations (Figure 14b) even though the equations with a higher amount of parameters are generally better fitted. In this case a higher amount of adjustable parameters seemed to increase weighting towards low concentration range (small ME, see Tables 13 and 14). From linearized Langmuir models, the fourth form seemed to offer the closest approximation to the non-linear regression. The best linear plot was obtained using the first form, however, and the curve drawn based on the estimated parameters gave the best apparent fit to the experimental data amongst all of the other forms of Langmuir model (Figure 15). El-Khaiary also presented similar observations [61].

The differences between linearized Langmuir models are due to the different weighting of the data points [61]. For example, the second linear model did not give any reasonable results, because the lowest q_e values (ie. high $1/q_e$) had extreme weights resulting in highly biased estimation. In the first and fourth form the *x*- and *y*-axis were no longer independent, strengthening the correlation. The fourth model with q_e/C_e as the *y*-axis gave higher values and thus higher weighting at low concentrations, however, while the first model with C_e/q_e as the *y*-axis gave higher values and weighting at high concentrations. The latter led to a better apparent fit of the model. Moreover, it seems that the non-linear regression of the Langmuir model was also weighted towards low q_e values (Figure 15).

Table 13. Fitting results of different isotherms for Co(II) adsorption by EDTA-silica gel 40-63 μm. $q_{m,exp}$ = 0.30 mmol/g. Uncertainty of the parameters obtained by Origin. Total differential used for linear equations.

Equilibrium model	q_m (mmol/g)	K (L/mmol)	n		χ^2	R^2	ME (%)
Langmuir	0.29 ± 0.01	41.98 ± 8.19			0.0035	0.949	18.93
Langmuir-lin1	0.31 ± 0.01	14.90 ± 2.25			0.0219	0.999[a]/ 0.900[b]	16.02
Langmuir-lin2	1.00 ± 0.29	5.42 ± 102.72			0.2894	0.720[a]/ -[b]	156.17
Langmuir-lin3	0.27 ± 0.01	66.18 ± 11.30			0.0034	0.637[a]/ 0.929[b]	24.42
Langmuir-lin4	0.29 ± 0.09	43.44 ± 7.41			0.0032	0.637[a]/ 0.947[b]	19.73
Freundlich		0.0007 ± 0.0005[d]	5.43 ± 0.55		0.0066	0.910	62.37
Sips	0.33 ± 0.01	5.46 ± 1.63	0.57 ± 0.06		0.0026	0.981	29.59
Redlich-Peterson[c]	0.28 ± 0.01	82.22 ± 13.87	0.91 ± 0.01		0.0016	0.994	21.80
General adsorption	0.33 ± 0.01	0.18 ± 0.05[e]	0.57 ± 0.06		0.0026	0.981	29.60
	q_m (mmol/g)	a_T (mmol/L)	n_T				
Toth	0.35 ± 0.02	9.95 ± 1.51	0.44 ± 0.06		0.0022	0.984	26.58
	q_m (mmol/g)	B_{DR} (mmol^2/J^2)					
Dubinin–Radushkevich	0.29 ± 0.01	0.0089 ± 0.0007			0.0025	0.967	24.53
	A_T (L/mmol)	B_T (J/mmol)					
Temkin	1439 ± 306	0.038 ± 0.001			0.0021	0.980	25.56
	q_m (mmol/g)	K_{FS} (L/mmol)	n_{FS}	m_{FS}			
Fritz-Schlunder	0.27 ± 0.01	436.51 ± 501.21	1.30 ± 0.21	1.19 ± 0.22	0.0014	0.987	17.22
	q_{m1} (mmol/g)	K_{BiL1} (L/mmol)	q_{m2} (mmol/g)	K_{BiL2} (L/mmol)			
BiLangmuir[c]	0.19 ± 0.02	110.67 ± 22.92	0.13 ± 0.01	1.88 ± 0.75	0.0015	0.996	20.83

[a]R^2 value of linear fitting. [b]R^2 value calculated after non-linear fitting using parameters obtained from linear fitting.
[c]Data from Paper IV, other results simulated for comparison.
[d]Unit: (mmol/g)/(L/mmol)^{nF} [e]Unit: mmol/L

Table 14. Fitting results of different isotherms for Co(II) adsorption by DTPA-silica gel 40-63 μm. $q_{m,exp}$ = 0.28 mmol/g. Uncertainty of the parameters obtained by Origin. Total differential used for linear equations.

Equilibrium model	q_m (mmol/g)	K (L/mmol)	n		χ^2	R^2	ME (%)
Langmuir	0.28 ± 0.01	57.93 ± 8.84			0.0021	0.963	12.53
Langmuir-1[a]	0.30 ± 0.01	17.31 ± 3.22			0.0223	0.999[a]/ 0.906[b]	15.23
Langmuir-2[a]	0.57 ± 0.76	15.99 ± 22.77			0.1007	0.868[a]/ -[b]	78.29
Langmuir-3[a]	0.27 ± 0.01	77.70 ± 10.18			0.0019	0.744[a]/ 0.955[b]	15.04
Langmuir-4[a]	0.28 ± 0.07	57.48 ± 8.04			0.0021	0.725[a]/ 0.959[b]	13.17
Freundlich		0.00039 ± 0.00033[d]	5.83 ± 0.62		0.0067	0.903	57.47
Sips	0.31 ± 0.01	7.71 ± 1.85	0.60 ± 0.05		0.0016	0.989	20.39
Redlich-Peterson[c]	0.27 ± 0.01	97.93 ± 11.68	0.92 ± 0.01		0.0009	0.997	12.01
General adsorption	0.31 ± 0.01	0.13 ± 0.03[e]	0.60 ± 0.05		0.0016	0.989	20.39
	q_m (mmol/g)	a_T (mmol/L)	n_T				
Toth	0.32 ± 0.01	12.58 ± 1.55	0.47 ± 0.05		0.0012	0.992	17.16
	q_m (mmol/g)	B_{DR} (mmol^2/J^2)					
Dubinin–Radushkevich	0.28 ± 0.01	0.049 ± 0.003			0.0014	0.982	17.34
	A_T (L/mmol)	B_T (J/mmol)					
Temkin	2324 ± 522	0.035 ± 0.001			0.0015	0.981	18.68
	q_m (mmol/g)	K_{FS} (L/mmol)	n_{FS}	m_{FS}			
Fritz-Schlunder	0.27	93.29	0.99	0.92	0.0002	0.993	12.20
	q_{m1} (mmol/g)	K_{BiL1} (L/mmol)	q_{m2} (mmol/g)	K_{BiL2} (L/mmol)			
BiLangmuir[c]	0.19 ± 0.01	137.37 ± 23.39	0.12 ± 0.01	2.78 ± 0.91	0.0008	0.998	11.69

[a]R^2 value of linear fitting. [b]R^2 value calculated after non-linear fitting using parameters obtained from linear fitting.
[c]Data from Paper IV, other results simulated for comparison.
[d]Unit: (mmol/g)/(L/mmol)^{nF} [e]Unit: mmol/L

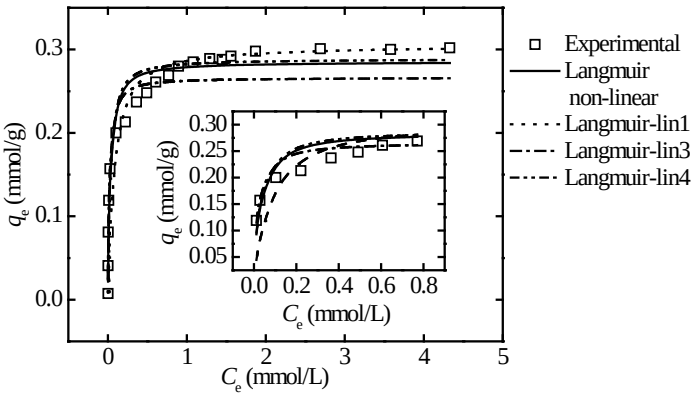

Figure 15. Fitting results of the linear and non-linear Langmuir models for Co(II) adsorption by EDTA-silica gel 40-63 μm. Dose: 2 g/L, pH: 3, Co(II) concentration: 0.017-5.1 mM (Unpublished data simulated for comparison).

Even if the BiLangmuir model gave the best approximation for the experimental isotherm curves, the applicability of the equation should be verified. As presented in section 1.1.5 the BiLangmuir model assumes that the adsorbent surface has two different active sites with different affinities. In Paper **I**, the high affinity sites were assigned to the EDTA- or DTPA-groups and low affinity sites to primary amino groups of APTES-functionalities. This was justified by comparing the amount of determined surface coverages of chelating agents and the total amount of metals adsorbed. In Paper **V**, however, the model fits to the equilibrium curves measured at a higher pH (pH 4) indicated that the amount of high energy active sites was much lower than the amount of low energy active sites. Based on this, the interpretations presented in Paper **I** were reconsidered and the low and high energy active sites assigned to the different speciations of EDTA and DTPA surface groups (see Papers **IV** and **V**). The latter was supported by speciation calculations, which gave similar relations for the two most abundant speciations compared to the relations of q_{m1} and q_{m2} values obtained from the BiLangmuir model (Papers **IV** and **V**). Furthermore, the surface coverages calculated based on the elemental analysis did not necessarily give the most reliable results, which was seen in the case of the hybrid materials (see section 4.1). Therefore, the experimental verification presented in Paper **I** can be questioned. Lastly, it should be noted that speciation calculations that are considered for aqueous species are not directly applicable for

immobilized chelates. Therefore, as with the acidity of the carboxyl groups [122], stability constants of surface bound chelates can also differ from those of aqueous chelates causing different speciation distributions.

For modified chitosans, the Sips model gave the best fitting results for both Co(II) and Ni(II) (Papers **II** and **V**). This suggested a heterogeneous adsorption and can be assigned to the crosslinking effect as well as some amount of functionalities (other than chelating groups) such as -NH_2 and -OH on the adsorbent surface (see FTIR-spectra in Figure 8). The isotherm curves were slightly S-shaped, which can be attributed to the lower affinity of surface groups towards metal ions at low concentrations. A crosslinking effect (see sections 4.2.1, 4.2.2), which was enhanced at low concentrations and inhibited due to the fast metal chelation at high concentrations, might have played an important role in the adsorption phenomena on modified chitosans.

We observed that fitting results for hybrid materials were more related to the type of metal than the type of material (Paper **III**). Adsorption isotherms of Co(II) and Cd(II) were better fitted by the BiLangmuir model and those of Ni(II) and Pb(II) by the Sips model (except Ni(II) adsorption on Chi:TEOS 2:60). The latter suggested a more heterogeneous adsorption for Ni(II) and Pb(II) compared to the two other metals. This was supported by the Ni(II) adsorption on modified chitosans observations, which showed higher heterogeneity for Ni(II) adsorption compared to that of Co(II) (Table 4 in Paper **II**). At pH 2, Ni(II)EDTA prefers the speciation with one negatively charged carboxyl group (Appendix IA). Paper **II** suggested that this group participated in the binding of another Ni(II) ion thus increasing a system heterogeneity. At pH 3, however, all the studied metals form EDTA-chelates with negatively charged carboxyl groups (Appendix IA). In this case, a lower heterogeneity for Co(II) and Cd(II) adsorption can be assigned to a lower affinity of carboxylates and amino-bearing groups towards these cations than towards Ni(II) and Pb(II) [92]. Lastly, it should be noted that a similar heterogeneity as above was not seen for EDTA- and DTPA-silica gels most likely due to their rigid structure and lower surface coverage of functional groups.

Effect of error function

The effect of error functions was discussed in section 1.1.7. Most of the modeling in this work was conducted by minimizing ERRSQ error function, because it is programmed in the Origin software. For the comparison, however, simple simulations with the Excel Solver were used to test all error functions presented in Table 2.

Figure 16 shows that the BiLangmuir fits using error functions other than MPSD and ARE were rather similar. ERRSQ and R^2 gave exactly the same results followed by EABS and χ^2 (Table 15). The poor fittings obtained with MPSD and ARE arises from their weighting towards low concentrations. Therefore, ME values shown in Table 15 are low for these functions. Similar results are presented in Table 4 in Paper **II** and Tables 3 and 4 in Paper **IV**. Tables 3 and 4 in Paper **IV** also show that the MPSD error function predicted that both of the actives sites on functionalized silica gels were similar thus turning the BiLangmuir model into a simple one-component Langmuir isotherm. In conclusion, the use of ERRSQ error function throughout this study seems to be a proper choice.

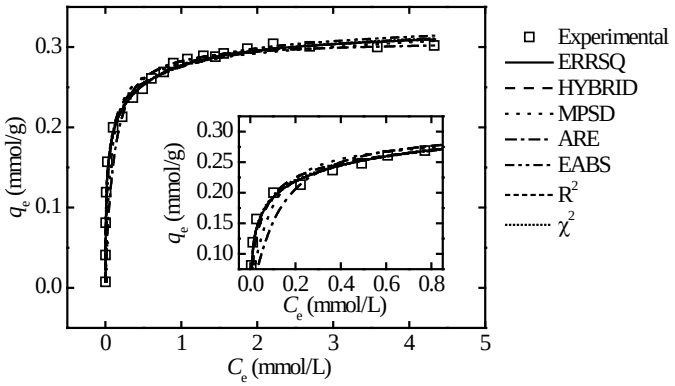

Figure 16. Effect of the error function on the BiLangmuir fits for Co(II) adsorption by EDTA-silica gel 40-63 μm. Dose: 2 g/L, pH: 3, Co(II) concentration: 0.017-5.1 mM (Unpublished data simulated for comparison).

Table 15. Effect of the error function on the BiLangmuir model parameters for Co(II) adsorption by EDTA/DTPA-silica gel 40-63 μm (Unpublished data simulated for comparison).

Equilibrium model	q_{m1} (mmol/g)	K_{BiL1} (L/mmol)	q_{m2} (mmol/g)	K_{BiL2} (L/mmol)	χ^2	R^2	ME (%)
EDTA-silica gel							
ERRSQ	0.19	110.55	0.13	1.89	0.0015	0.992	20.88
HYBRID	0.23	52.21	0.10	0.90	0.0029	0.980	16.17
MPSD	0.28	20.62	0.07	0.15	0.0155	0.930	15.02
ARE	0.01	55.67	0.30	10.62	0.0349	0.883	15.02
EABS	0.20	100.00	0.13	1.56	0.0015	0.991	19.71
R^2	0.19	110.55	0.13	1.89	0.0015	0.992	20.88
χ^2	0.21	93.82	0.12	1.43	0.0015	0.991	19.43
DTPA-silica gel							
ERRSQ	0.19	136.85	0.12	2.78	0.0008	0.996	11.76
HYBRID	0.22	83.27	0.09	1.36	0.0010	0.992	10.36
MPSD	0.28	39.55	0.00	21.21	0.0049	0.959	12.10
ARE	0.24	68.27	0.08	0.78	0.0014	0.988	10.18
EABS	0.22	100.00	0.09	1.54	0.0008	0.994	10.62
R^2	0.19	136.85	0.12	2.78	0.0008	0.996	11.76
χ^2	0.20	117.13	0.11	2.15	0.0007	0.995	11.12

Effect of data range

In Paper **IV**, it was observed that the error between simulated and experimental data was highest at low concentrations. Therefore, simulations for the BiLangmuir model were conducted by omitting the first equilibrium point (Table 16), which considerably improved the MPSD and ARE fittings. Other error functions were less affected by the change of the data range, although ME values in these cases also decreased significantly.

Table 16. Effect of the error function on the BiLangmuir model parameters for Co(II) adsorption by EDTA/DTPA-silica gel 40-63 μm. First equilibrium point omitted from simulations (Unpublished data simulated for comparison).

Equilibrium model	q_{m1} (mmol/g)	K_{BiL1} (L/mmol)	q_{m2} (mmol/g)	K_{BiL2} (L/mmol)	χ^2	R^2	ME (%)
EDTA-silica gel							
ERRSQ	0.18	138.58	0.14	2.16	0.0002	0.996	2.98
HYBRID	0.19	117.86	0.13	1.78	0.0002	0.995	2.90
MPSD	0.21	101.10	0.12	1.35	0.0003	0.994	3.03
ARE	0.19	122.23	0.13	1.88	0.0002	0.995	2.80
EABS	0.20	100.00	0.13	1.56	0.0004	0.993	2.98
R^2	0.18	138.58	0.14	2.16	0.0002	0.996	2.98
χ^2	0.19	122.93	0.13	1.84	0.0002	0.995	2.88
DTPA-silica gel							
ERRSQ	0.18	159.10	0.12	3.20	0.0001	0.996	1.92
HYBRID	0.18	152.49	0.12	3.01	0.0001	0.996	1.86
MPSD	0.19	146.04	0.12	2.75	0.0001	0.996	1.81
ARE	0.20	131.64	0.11	2.45	0.0001	0.995	1.67
EABS	0.22	100.00	0.09	1.54	0.0003	0.993	2.77
R^2	0.18	159.10	0.12	3.20	0.0001	0.996	1.92
χ^2	0.19	152.13	0.12	3.02	0.0001	0.996	1.85

It is also interesting to compare the BiLangmuir model fittings of Papers **I** and **IV**, due to the higher amount of experimental points measured in the latter. Around a 10 to 15% differences was seen in the predicted $q_{m1/2}$ values, while the differences between $K_{BiL1/2}$ values ranged from 25 to 50%. Therefore, as Cernik *et al.* proposed earlier [53], small changes in the experimental points may noticeably influence the fitting results. It should be noted, however, that the used data range did not change the type of the best fitted model or the relations of simulated $q_{m1/2}$ and $K_{BiL1/2}$ values and therefore fitting results in Papers **I** and **IV** rather support each other.

Effect of initial guess values

Effect of initial guess values was investigated in Paper **IV**. The initial guesses for the three-parameter Redlich-Peterson model did not affect the simulation results (see section 4.1 in Paper **IV**). The four-parameter BiLangmuir model, however, gave a worse fit when the initial guesses of $q_{m1/2}$ were not set close to those obtained experimentally (Figure 3 and Tables 3 and 4 in Paper **IV**). Therefore, it can be concluded that the higher amount of estimated parameters makes the isotherm model more sensitive to the initial guesses and use of experimentally obtained q_m values gives a proper initialization for the simulations.

4.5.2 Two-component systems

Two-component experimental data was obtained using solutions containing different ratios of Co(II) and Ni(II) (Papers **II** and **IV**). It was observed that both modified silica gels and chitosans had significantly higher affinities towards Ni(II) than Co(II), which was attributed to the higher stability constants of Ni(II) chelates (see section 3.5.3 in Paper **II** and Figure 4 in Paper **IV**). Extended forms of Sips (Paper **II**), Redlich-Peterson (Paper **IV**), and BiLangmuir model (Paper **IV**) were applied, but for comparison Figures 17 and 18 and Tables 17 and 18 also show the results obtained for the different extended Langmuir models (Eq. 27-32). In addition, all the simulations were performed by omitting the one-component data (not done in Paper **IV**) because all the parameters were assumed to be affected by another component in the solution. Therefore, also none of the parameters were fixed.

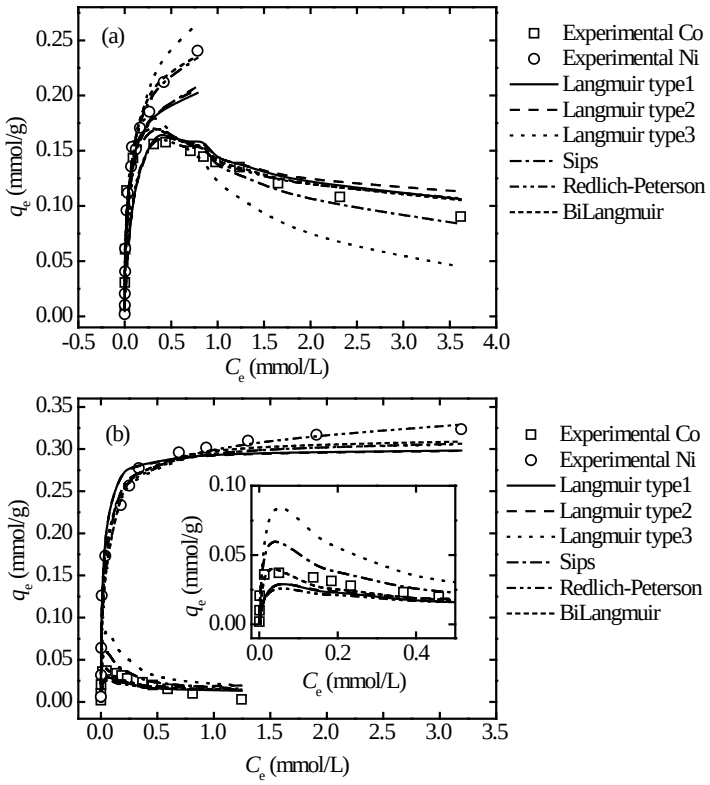

Figure 17. Two-component model fits for Co(II) and Ni(II) adsorption by EDTA-silica gel 40-63 μm. Dose: 2 g/L, pH: 3, Co(II):Ni(II) ratio (a) 3:1 and (b) 1:3. (Unpublished data simulated for comparison).

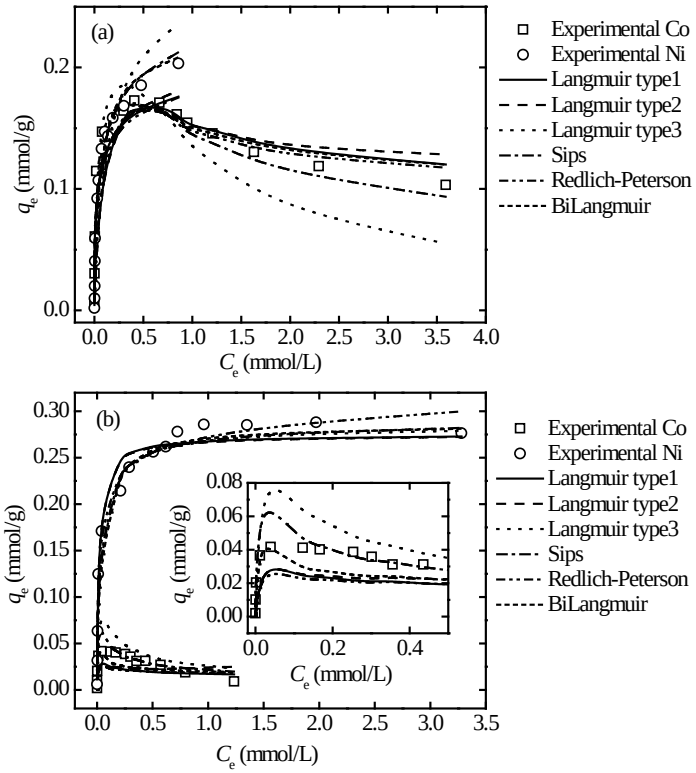

Figure 18. Two-component model fits for Co(II) and Ni(II) adsorption by DTPA-silica gel 40-63 μm. Dose: 2 g/L, pH: 3, Co(II):Ni(II) ratio (a) 3:1 and (b) 1:3. (Unpublished data simulated for comparison).

Table 17. Two-component model parameters for Co(II) and Ni(II) adsorption by EDTA-silica gel 40-63 μm (Unpublished data simulated for comparison). Uncertainty of the parameters obtained by Origin.

	q_{m1}	$K_{L1,1}$	q_{m2}	$K_{L1,2}$			χ^2	R^2	ME (%)
Langmuir type1	0.31 ±.0.01	10.31 ± 0.94	0.31 ±.0.01	89.39 ± 7.00			0.0144	0.970	36.3
	q_{m1}	$K_{L2,1}$	q_{m2}	$K_{L2,1}$	$K_{L2,3}$		χ^2	R^2	ME (%)
Langmuir type2	0.31 ±.0.01	10.76 ± 0.96	0.31 ± 0.01	91.54 ± 7.13	1.35 ± 1.40		0.0144	0.970	38.6
	q_{m1}	$K_{L3,1}$	q_{m2}	$K_{L3,2}$	$K_{L3,3}$	$K_{L3,4}$	χ^2	R^2	ME (%)
Langmuir type3	0.23 ±.0.01	52.82 ± 5.29	0.38 ±.0.01	61.75 ± 5.17	0.31 ± 0.21	5.55 ± 0.64	0.0087	0.960	38.99
	q_{m1}	K_{S1}	q_{m2}	K_{S2}	n_{S1}	n_{S2}	χ^2	R^2	ME (%)
Sips	0.32 ±.0.01	14.54 ± 1.80	0.32 ±.0.01	68.79 ± 5.02	0.65 ± 0.02	0.90 ± 0.03	0.0037	0.980	37.44
	q_{m1}	K_{RP1}	q_{m2}	K_{RP2}	n_{RP1}	n_{RP2}	χ^2	R^2	ME (%)
Redlich-Peterson	0.35 ±.0.03	11.69 ± 2.16	0.22 ±.0.01	165.34 ± 23.98	1.01 ± 0.03	0.93 ±.0.01	0.0132	0.973	40.34

	$q_{m1,1}$	$K_{BiL1,1}$	$q_{m1,2}$	$K_{BiL1,2}$	$q_{m2,1}$	$K_{BiL2,1}$	$q_{m2,2}$	$K_{BiL2,2}$	χ^2	R^2	ME (%)
BiLangmuir	0.25 ±.0.01	64.16 ± 13.14	0.01 ±.0.02	0.52 ± 0.19	0.11 ±.0.01	412.48 ± 90.49	0.22 ±.0.01	15.28 ± 1.87	0.0048	0.981	37.10

q_m (mmol/g), K (L/mmol)

Table 18. Two-component model parameters for Co(II) and Ni(II) adsorption by DTPA-silica gel 40-63 μm (Unpublished data simulated for comparison). Uncertainty of the parameters obtained by Origin.

	q_{m1}	$K_{L1,1}$	q_{m2}	$K_{L1,2}$			χ^2	R^2	ME (%)
Langmuir type1	0.31 ± 0.01	11.00 ± 1.25	0.29 ± 0.01	73.26 ± 6.92			0.0144	0.969	35.63
	q_{m1}	$K_{L2,1}$	q_{m2}	$K_{L2,1}$	$K_{L2,3}$		χ^2	R^2	ME (%)
Langmuir type2	0.30 ± 0.01	10.56 ± 1.31	0.31 ± 0.05	90.91 ± 7.18	1.67 ± 1.35		0.0142	0.970	36.41
	q_{m1}	$K_{L3,1}$	q_{m2}	$K_{L3,2}$	$K_{L3,3}$	$K_{L3,4}$	χ^2	R^2	ME (%)
Langmuir type3	0.25 ± 0.01	39.59 ± 5.30	0.35 ± 0.01	46.19 ± 5.18	0.25 ± 0.13	4.18 ± 0.37	0.0064	0.968	30.83
	q_{m1}	K_{S1}	q_{m2}	K_{S2}	n_{S1}	n_{S2}	χ^2	R^2	ME (%)
Sips	0.34 ± 0.01	14.07 ± 2.31	0.30 ± 0.01	51.72 ± 4.42	0.61 ± 0.02	0.88 ± 0.02	0.0026	0.984	29.66
	q_{m1}	K_{RP1}	q_{m2}	K_{RP2}	n_{RP1}	n_{RP2}	χ^2	R^2	ME (%)
Redlich-Peterson	0.41 ± 0.05	10.23 ± 1.96	0.20 ± 0.02	127.46 ± 22.89	1.08 ± 0.05	0.93 ± 0.02	0.0135	0.972	38.87

	$q_{m1,1}$	$K_{BiL1,1}$	$q_{m1,2}$	$K_{BiL1,2}$	$q_{m2,1}$	$K_{BiL2,1}$	$q_{m2,2}$	$K_{BiL2,2}$	χ^2	R^2	ME (%)
BiLangmuir	0.25 ± 0.01	87.33 ± 19.30	0.00 ± 0.01	0.88 ± 0.29	0.08 ± 0.01	399.25 ± 90.67	0.22 ± 0.01	16.41 ± 2.29	0.0037	0.983	31.58

q_m (mmol/g), K (L/mmol)

Figures 17 and 18 show that the extended Redlich-Peterson and BiLangmuir models gave the best apparent fits for the experimental two-component data (see Paper **IV**). Based on the statistical analysis, all the models gave rather similar results (Tables 17 and 18). Langmuir types 1 and 2, Sips, and Redlich-Peterson models predicted higher or similar maximum adsorption capacity for Co(II) compared to that of Ni(II), however, which was not observed experimentally. Furthermore, the poor fit of the Langmuir model to the one-component data indicates that the assumption of similar active sites being related to all the extended Langmuir models is not valid in this case.

The applicability of the extended BiLangmuir model was further supported by modeling results obtained for one-component systems and $K_{BiLi,j}$ values suggesting considerably higher binding affinities for Ni(II) than for Co(II). The only discrepancy was that the extended BiLangmuir model predicted lower adsorption capacity for the higher affinity binding groups for

Ni(II) adsorption. The overall complexity of the system might have caused this. Furthermore, for such a wide experimental data range used in modeling, large ME values were expectable. This may be due to the high errors obtained for the lowest concentrations (see for example Figure 6 in Paper **IV**). In addition, the uncertainties related to the affinity parameters (*K*) were significant.

In Paper **IV** we also studied the effect of the amount of fixed parameters in the two-component modeling. For both extended Redlich-Peterson and BiLangmuir models the best approximation was obtained when all the parameters were estimated (see Tables 5 and 6 in Paper **IV**). Obviously, the higher amount of adjustable parameters gave more flexibility in the simulations [149]. Moreover, it is evident from Figures 17 and 18 that competing conditions affected clearly the adsorption capacities of the studied metal ions.

Less equilibrium points were measured in the two-component adsorption on EDTA- and DTPA-functionalized chitosan (Paper **II**). The obtained data, however, was well fitted with the extended Sips model also supported by the one-component modeling results. Interestingly, a clear synergistic behavior was observed for modified chitosans *i.e.* adsorption capacity of Ni(II) was higher in the two-component systems than in one-component system. This can be explained by the positive synergy of chelation and electrostatic interactions that may have taken place with the surface groups [63]. Despite the complexity of the two-component systems and modeling result interpretations, the results presented in this section emphasize the importance of comparison of the one- and two-component modeling results.

4.6 Application testing of EDTA/DTPA-functionalized adsorbents

4.6.1 Capture of Co(II) from its aqueous EDTA chelate

Based on the higher stability constant of metal DTPA-chelates, DTPA-functionalized silica gel and chitosan were tested for Co(II) capture from its aqueous EDTA chelate (Paper **V)**. The adsorption efficiencies obtained for DTPA-silica gel and –chitosan ranged from 93 to 96% for solutions where all the Co(II) ions were chelated by EDTA. Moreover, CE measurements (Figures 6 and 7 in Paper **V**) showed that the amount of released EDTA correlated well with the amount of adsorbed Co(II) suggesting that Co(II)EDTA chelates were actually disintegrated during the adsorption process. The results were highly promising since Co(II) specific adsorbent

CoTreat developed for the removal of radioactive ^{60}Co loses its adsorption capability in the presence of EDTA [150].

4.6.2 Adsorption of Co(II) from different solution matrices

In Paper **V**, we also studied how Co(II) removal was affected by different solution matrices. The matrix compositions were selected based on applications for the treatment of wastewaters originating from the operation of nuclear power plants (Table 1 in Paper **V**). Results showed that DTPA-chitosan was a better adsorbent than DTPA-silica gel in various solution compositions even though DTPA-silica gel showed higher adsorption efficiency in pure metal solutions (at low Co(II) concentrations). For example, over 90% Co(II) removal was observed for the DTPA-chitosan in simulated decontamination solutions containing iron, nitric acid, and EDTA as well as in the presence of excess of oxalate, iron, and calcium (Table 1 and Figure 2 in Paper **V**).

4.6.3 Adsorption tests from multi-metal solutions

Besides the two-component experiments for modified silica gels and chitosans showing the separation of Ni(II) and Co(II), adsorption properties of the modified hybrid materials were tested in the solutions containing Co(II), Ni(II), Cd(II), and Pb(II) (Figures 7 and S4 and Table 6 in Paper **III**). Adsorption efficiency followed the order: Pb(II)>Ni(II)>Cd(II)≈Co(II) for EDTA-Chi:TEOS 2:60 and 2:30 and Pb(II)≈Ni(II)>Cd(II)≈Co(II) for EDTA-Chi:TEOS 2:15. Otherwise, excluding the Pb(II) and Ni(II) order, observed selectivity could be explained by the stability constants of metal EDTA chelates (Table 4). It was suggested that the properties of surface bound EDTA differed from its dissolved form [5] and, for example, the lowest hydration number of Pb(II) [130] enhanced the Pb(II) surface chelation.

4.6.4 Preconcentration studies

Preconcentration is one of the important chelating adsorbents applications. Especially, a reliable metal analysis from seawater samples requires preconcentration to increase the sensitivity of the method and separate the analyte from the complex matrix solution [103]. Based on the promising regeneration results preconcentration of trace amount of metals was tested using columns filled

with EDTA- or DTPA-silica gel. Table 19 shows the measured concentrations after preconcentration as well as determination limits of ICP-OES for each of the studied metals.

Table 19. Preconcentration studies using EDTA/DTPA-functionalized silica gel (Unpublished data).

	Determination limit in water (μg/L)	Real concentration (μg/L)	Determined after preconcentration using EDTA-silica gel (μg/L)	Determined after preconcentration using DTPA-silica gel (μg/L)
Mixed metal solution in water				
Co(II)	5.2	1.0	1.0	1.2
Ni(II)	2.5	1.0	1.0	1.1
Cd(II)	1.9	1.0	1.4	1.3
Pb(II)	12.4	1.0	1.0	1.0
Mixed metal solution in 3% NaCl				
	Determination limit in 3% NaCl (μg/L)	Real concentration (μg/L)	Determined after preconcentration using EDTA-silica gel (μg/L)	Determined after preconcentration using DTPA-silica gel (μg/L)
Co(II)	10.2	1.0	1.0	1.1
Ni(II)	7.5	1.0	1.0	1.0
Cd(II)	3.2	1.0	1.7	1.6
Pb(II)	21.8	1.0	1.0	1.0

Table 19 shows that the determination limits of ICP-OES cannot give reliable results for metal concentrations of 1.0 μg/L and the presence of NaCl further increases the determination limits. After preconcentration all metals, except Cd(II), could be determined with high accuracy. Especially the determination limit of Pb(II) was not very good even in pure water, emphasizing the importance of preconcentration.

For commercial IDA-chelating resin Chelex-100, 96.3, 95.2, 89.0, and 89.3% recoveries were obtained for Co(II), Ni(II), Cd(II), and Pb(II) from 1.0 μg/L solutions in salty matrix using ICP-MS [144]. Table 19 shows that for EDTA- and DTPA-silica gels recoveries were 100% in most cases, indicating their potential as preconcentrating chelating resins.

5 CONCLUSIONS AND FURTHER RESEARCH

Adsorption materials functionalized with chelating agents can be considered as effective, selective, and regenerable adsorbents for heavy metals. Depending on the supporting material, the adsorption properties of chelating adsorbents may vary significantly. In this study silica gel, chitosan, and chitosan silica hybrid materials were used as supports for EDTA- and DTPA-functionalities. The supporting material affected the surface coverage of the chelating agents and therefore the adsorption capacity of metals on the synthesized adsorbents. The influence of the pH and initial concentration of metal ions was, however, also different for adsorbents with different composition. For example, for modified chitosans, crosslinking played a significant role when a metal concentration was low and the pH was higher than 2.5. EDTA-functionalized chitosan-silica hybrid materials combined the beneficial properties of silica gel (rigidity) and chitosan (high surface coverage). Overall, the studied adsorbents showed very good stability by either lasting several regeneration cycles or releasing insignificant amount of silicon during the adsorption experiments.

Adsorption mechanisms were suggested based on the speciation calculations and the amount of protons released during the adsorption. Overall, the chelation mechanism was proposed as dominant, which was further supported by the FTIR-analysis of metal loaded adsorbents.

Both surface coverage and porosity of the chelating adsorbent affected the adsorption kinetics. Therefore, applied kinetic models were the pseudo-second-order model and intraparticle diffusion model. In pure metal solutions pore diffusion was significant for adsorbents with mesoporous structures and intraparticle model plots revealed several diffusion steps affecting the adsorption process. Surface reaction *i.e.* chelation was, however, important for non-porous/macroporous chitosans and for the adsorption of Co(II) chelated by EDTA on mesoporous DTPA-silica gel because the large molecules were not able to diffuse inside the pores of the adsorbent. Furthermore, the adsorption rate increased with increasing surface coverage and decreasing particle size.

Modeling of adsorption isotherms is important because it can give information about the adsorbent surface properties and the adsorption mechanism. Modeling is one of the central steps in process design. In this study, various isotherm models were tested to find the best fitting equations.

Error analysis, comparison of experimental and simulated maximum adsorption capacities, as well as comparison of the properties of adsorbents on isotherm theories were performed to ensure establishment of an optimal isotherm model. The BiLangmuir model suggesting two different active sites on the adsorbent surface was found to be best fitted for modified silica gels. Some uncertainties existed in the type of functionalities of active sites, however, and finally the best suggestion was that these were different speciations of EDTA- or DTPA-groups. Sips model fittings and slightly S-shaped isotherms indicated a heterogeneous adsorption on modified chitosans. This was attributed to the possible crosslinking effects and some amount of amino and hydroxyl groups, besides chelating agents on the surfaces of modified chitosans. Interestingly, EDTA-functionalized hybrid materials showed isotherm dependency on the type of metal rather than material type. More heterogeneous adsorption of Ni(II) and Pb(II) over Co(II) and Cd(II) was attributed to their higher affinities towards surface groups enabling different kinds of binding mechanisms. Overall, the modeling of isotherms revealed the dependency of the fitting results on the error function, initial guess values, and experimental data range.

Two-component modeling applied to simultaneous adsorption of Co(II) and Ni(II) suggested the fitting of the extended BiLangmuir model for modified silica gels and the extended Sips isotherm for modified chitosans. Both results were supported by the one-component modeling results. The higher amount of adjustable parameters allowed the best fitting results due to the increased flexibility of the equation. Basically, it was suggested that all the parameters were affected by the competing conditions and therefore differed from the one-component-based parameters. A lot of deviations between simulated and experimental data were seen at low concentrations.

In application testing, DTPA-silica gel and -chitosan were found as effective adsorbents for Co(II) in the presence of EDTA. Especially, DTPA-chitosan worked very well in various solution matrices containing different acids and salts as well as iron. Experiments in multi-metal

systems showed separation of Ni(II) from Co(II) and Ni(II) and Pb(II) from Co(II) and Cd(II). In addition, preconcentration studies suggested that EDTA/DTPA-silica gels could be used to preconcentrate trace amount of metals from salty waters.

By keeping eye on the future studies, the adsorption properties of EDTA/DTPA-functionalized materials should be further studied in various solution matrices such as real wastewater samples. This would be important prior to scaling up the process. In the industrial scale, the applications of novel adsorbents could, for example, be in hydrometallurgy and mining industry.

Also, the capture of Co(II) from its aqueous EDTA chelate is a potential application worth further investigation using newly developed adsorbents with strong cation exchange properties. Besides Co(II)EDTA, the capture of other metal ions such as Ni(II), Cd(II), Pb(II), Cu(II), and Zn(II) from their EDTA-chelates should be studied.

As was seen in the literature survey and the experimental work of this study the substrate to be functionalized significantly influences the properties of the adsorbent. Therefore, it would be important to test different substrates for EDTA- and DTPA-functionalities. Moreover, the two most interesting and topical groups of substrates would be low-cost materials, such as cellulose, and nanomaterials, such as carbon nanotubes. Besides changing the substrate, different chelating agents should also be tested. Attractive chelating agents with high metal binding affinities are, for example, amino polyphosphonates.

Finally, use of EDTA- and DTPA-functionalized adsorbents in preconcentration of various trace and rare elements from different solution matrices is important. Similar procedures could be further applied, for example, for the recovery of valuable metals.

REFERENCES

1. Sposito, G., *Surface Chemistry of Natural Particles*, Oxford University Press (2004) p. 3.
2. Zhou, L., Adsorption : *Progress in Fundamental and Application Research* : *Selected Reports at the 4th Pacific Basin Conference on Adsorption Science and Technology*, World Scientific (2007) p.3.
3. Asnin L, Kaczmarski K, Guiochon G. Empirical development of a binary adsorption isotherm based on the single-component isotherms in the framework of a two-site model. *J. Chrom. A.* 1138 (2007) 158-168.
4. Krishnamurthy, N., Vallinayagam, P., Madhavan, D., *Engineering Chemistry*, Prentice-Hall Of India Pvt. Ltd., New Delhi (2007) pp. 58-59.
5. Muraviev, D., *Ion Exchange*, New York, USA, Mercel Dekker (2000) pp. 267-344.
6. Colloidal Dynamics Pty Ltd., 1999, *Electroacoustics Tutorials*, *Zeta Potential*, *Colloidal Dynamics Leaders In Colloid Measurement*, Autralia.
7. Pan, R., Liew, K., *Handbook of Nanophysics*, *Nanoparticles and quantum Dots*, ed. Sattler, K.D., Taylor and Francis/CRC Press, Boca Raton (2010) pp. 18-2 - 18-3.
8. Dadashev, R.Kh. *Thermodynamics of Surface Phenomena*, Cambridge International Science Publishing (2008) p. 1.
9. Erbil, H.Y. *Surface Chemistry of Solid and Liquid Interfaces*; Blackwell Publishing: Oxford, UK (2006) pp. 91-100.
10. Do, D. D. *Adsorption Analysis: Equilibria and Kinetics*, Imperial College Press, Vol. 2, (1998) pp. 13-34.
11. Freundlich, H.M.F. Over the adsorption in solution, *Zeitschrift für Physikalische Chemie* 57 (1906) 385-470.
12. Langmuir, I., The adsorption of gases on plane surfaces of glass, mica, and platinum, *J. Am. Chem. Soc.* 40 (1918) 1361-1368.
13. Kinniburgh D.G., General purpose adsorption isotherms, *Environ Sci. Technol*. 20 (1986) 895-904.

14. Ho Y.S., Porter J.F., McKay G., Equilibrium isotherm studies for the sorption of divalent metal ions onto peat: copper, nickel and lead single component systems, *Water Air Soil Pollut.* 141 (2002) 1-33.
15. Liu, Y., Liu, Y-J, Biosorption isotherms, kinetics and thermodynamics, *Sep. Pur. Tech.* 61 (2008) 229-242.
16. Guo, L., Li, G., Liu, J., Yin, P., Li, Q., Adsorption of aniline on cross-linked starch sulfate from aqueous solution, *Ind. Eng. Chem. Res*. 48 (2009) 10657-10663.
17. Redlich, O., Peterson, D.L., A useful adsorption isotherm, *J. Phys Chem*. 63 (1959) 1024-1029.
18. Hamdaoui, O., Naffrechoux, E., Modeling of adsorption isotherms of phenol and chlorophenols onto granular activated carbon Part I. Two-parameter models and equations allowing determination of thermodynamic parameters, *J. Hazard. Mater*. 147 (2007) 381-394.
19. Basha, S., Murthy, Z.V.B., Jha, B., Sorption of Hg(II) from aqueous solutions onto Carica papaya: application of isotherms, *Ind. Eng. Chem. Res*. 47 (2008) 980-986.
20. Mane, V.S., Mall, I.D., Srivastava, V.C., Kinetic and equilibrium isotherm studies for the adsorptive removal of Brilliant Green dye from aqueous solution by rice husk ash, *J. Environ. Manage*. 84 (2007) 390-400.
21. Kumar, K.V., Porkodi, K., Relation between some two- and three-parameter isotherm models for the sorption of methylene blue onto lemon peel, *J. Hazard. Mater*. 138 (2006) 633-635.
22. Hameed, B.H., Tan, I.A.W., Ahmad, A.L., Adsorption isotherm, kinetic modeling and mechanism of 2,4,6-trichlorophenol on coconut husk-based activated carbon, *Chem. Eng. J.* 144 (2008) 235-244.
23. Peric, J., Trgo, M., Vukojevic Medvidovic, N., Removal of zinc, copper and lead by natural zeolite – comparison of adsorption isotherms, *Water Res.* 38 (2004) 1893-1899.
24. Gedik, K., Imamoglu, I., Affinity of Clinoptilolite-based zeolites towards removal of Cd from aqueous solutions, *Sep. Pur. Technol*. 43 (2008) 1191-1207.
25. Toth, J., State equations of the solid gas interface layer, *Acta Chem. Acad. Hung.* 69 (1971) 311-317.

26. Allen, S.J., Mcka,y G., Porter, J.F., Adsorption isotherm models for basic dye adsorption by peat in single and binary component systems, *J. Colloid Interface Sci*. 280 (2004) 322-333.
27. Foo, K.Y., Hameed, B.H., Insights into the modeling of adsorption isotherm systems, *Chem. Eng. J*. 156 (2010) 2-10.
28. Kundu, S., Gupta, A.K., Arsenic adsorption onto iron oxide-coated cement (IOCC): regression analysis of equilibrium data with several isotherm models and their optimization, *Chem. Eng. J*. 122 (2006) 93-106.
29. Liu, Y., Xu, H., Tay, J-H., Derivation of a general adsorption isotherm model, *J. Environ. Eng.* 131 (2005) 1466-1468.
30. Fritz, W., Schluender, E.U., Simultaneous adsorption equilibria of organic solutes in dilute aqueous solutions on activated carbon, *Chem. Eng. Sci.* 29 (1974) 1279-1282.
31. Karthikeyan, K.G., Tshabalala, M.A., Wang, D., Kalbasi, M., Solution chemistry effects on orthophosphate adsorption by cationized solid wood residues, *Environ. Sci. Technol.* 38 (2004) 904-911.
32. Khan, A.R., Ataullah, R., Al-Haddad, A., Equilibrium adsorption studies of some aromatic pollutants from dilute aqueous solutions on activated carbon at different temperatures, *J. Colloid Interface Sci.* 194 (1997) 154-165.
33. Koble, R.A., Corrigan, T.E., Adsorption isotherms for pure hydrocarbons, *Ind. Eng. Chem.* 44 (1952) 383-387.
34. Jossens, L., Prausnitz, J.M., Fritz, E.U., Myers, A.L., Thermodynamics of multi-solute adsorption from dilute aqueous solutions, *Chem. Eng. Sci*. 33 (1978) 1097-1106.
35. Radke, C. J., Prausnitz, J.M., Adsorption of organic solutes from dilute aqueous solution of activated carbon, *Ind. Eng. Chem. Fundam*. 11 (1972) 445-450.
36. van Vliet, B.M., Weber, W.J., Hozumi, H., Modeling and prediction of specific compound adsorption by activated carbon and synthetic adsorbents, *Water Res.* 14 (1980) 1719-1817.
37. Vieth, W.R., Sladek, K.J., A model for diffusion in a glassy polymer, *J. Colloid Sci.*, 20 (1965) 1014-1033.
38. Deryło-Marczewska, A., Marczewski, A.W., Effect of adsorbate structure on adsorption from solutions, *Appl. Surf. Sci.* 196 (2002) 264-272.

39. Giles, C.H., Smith, D., Huitson, A., A general treatment and classification of the solute adsorption isotherm. I. Theoretical, *J. Colloid Interface Sci*. 47 (1974) 755-765.
40. Limousin, G., Gaudet, J.-P., Charlet, L., Szenknect, S., Barthe, V., Krimissa, M., Sorption isotherms: A review on physical bases, modeling and measurement, *Appl. Geochem*. 22 (2007) 249-275.
41. Covelo, E.F., Vega, F.A., Andrade, M.L., Simultaneous sorption and desorption of Cd, Cr, Cu, Ni, Pb and Zn in acid soils. I. Selectivity sequences, *J. Hazard. Mater*. 147 (2007. 852-861.
42. Apiratikul, R., Pavasant, P., Sorption isotherm model for binary component sorption of copper, cadmium, and lead ions using dried green macroalga, Caulerpa lentillifera. *Chem. Eng. J.* 119 (2006) 135-145.
43. Kumar, D., Singh, A., Gaur, J.P., Mono-component versus binary isotherm models for Cu(II) and Pb(II) sorption from binary metal solution by the green alga Pithophora oedogoni., *Bioresour. Technol.* 97 (2008) 8280-8287.
44. Al-Asheh S, Banat F, Al-Omari R, Duvnjak Z. Predictions of binary sorption isotherms for the sorption of heavy metals by pine bark using single isotherm data, *Chemosphere* 41 (2000) 659-665.
45. Kaczmarski K, Zhou D, Gubernak M, Guiochon G. Equivalent models of indanol isomers adsorption on cellulose tribenzoate, *Biotechnol. Prog*. 19 (2003) 455-463.
46. Kundu, S., Gupta, A.K., Arsenic adsorption onto iron oxide-coated cement (IOCC): regression analysis of equilibrium data with several isotherm models and their optimization, *Chem. Eng. J.* 122 (2006), pp. 93-106.
47. Allen, S.J., Gan, Q., Matthews, R., Johnson, P.A., Comparison of optimised isotherm models for basic dye adsorption by kudzu, *Bioresour. Technol*. 88 (2003) 143-152.
48. Gimbert, F., Morin-Crini, N., Renault, F., Badot, P.M., Crini, G., Adsorption isotherm models for dye removal by cationized starch-based material in a single component system: error analysis, *J. Hazard. Mater.* 157 (2008) 34-46.
49. Ng, J.C.Y. Cheung, W.H., McKay G., Equilibrium studies of the sorption of Cu(II) ions onto chitosan, *J. Colloid Interface Sci*. 255 (2002) 64-74.

50. Kumar, K.V., Porkodi, K., Rocha, F., Comparison of various error functions in predicting the optimum isotherm by linear and non-linear regression analysis for the sorption of basic red 9 by activated carbon, *J. Hazard. Mater.* 150 (2008) 158-165.
51. Kumar, K.V., Porkodi, K., Rocha, F., Isotherms and thermodynamics by linear and non-linear regression analysis for the sorption of methylene blue onto activated carbon: comparison of various error functions, *J. Hazard. Mater*. 151 (2008) 794-804.
52. Ncibi, M.C., Applicability of some statistical tools to predict optimum adsorption isotherm after linear and non-linear regression analysis, *J. Hazard. Mater*. 153 (2008) 207-212.
53. Cernik, M., Borkovec, M., Westall, J.C., Regularized least-Squares methods for the calculation of discrete and continuous affinity distributions for heterogeneous sorbents, *Environ. Sci. Technol.* 29 (1995) 413-425.
54. Bothwell, M.K., Walker, L.P., Evaluation of parameter estimation methods for estimating cellulose binding constants, *Biores. Technol.* 53 (1995) 21-29.
55. Kumar, K.V., Comparative analysis of linear and non-linear method of estimating the sorption isotherm parameters for malachite green onto activated carbon, *J. Hazard. Mater*. B136 (2006) 197-202.
56. Ho, Y.S., Chiu, W.T., Wang, C.C., Regression analysis for the sorption isotherms of basic dyes on sugarcane dust, *Bioresour. Technol*. 96 (2005) 1285-1291.
57. Kumar, K.V., Sivanesan, S., Prediction of optimum sorption isotherm: comparison of linear and non-linear method, *J. Hazard. Mater*. 126 (2005) 198-201.
58. Subramanyan, B., Das, A., Linearized and non-linearized isotherm models comparative study on adsorption of aqueous phenol solution in soil, *Int. J. Environ. Sci. Tech*. 6 (2009) 633-640.
59. Lai, Y.L., Annadurai, G., Huang, F.C., Lai, L.F., Biosorption of Zn(II) on the different Ca-alginate beads from aqueous solution, *Bioresour Technol* 99 (2008) 6480-6487.
60. Maeder, M., Zuberbüehler, A.D., Nonlinear least-squares fitting of multivariate absorption data, *Anal. Chem*. 62 (1990) 2220-2224.
61. El-Khaiary, M.I., Least-squares regression of adsorption equilibrium data: comparing the options, *J. Hazard. Mater*. 158 (2008), pp. 73-87.

62. Papageorgiou, S.K., Katsaros, F.K., Kouvelos, E.P., Kanellopoulos, N.K., Prediction of binary adsorption isotherms of Cu^{2+}, Cd^{2+} and Pb^{2+} on calcium alginate beads from single adsorption data, *J. Hazard. Mater*. 162 (2009) 1347-1354.
63. Vieira, R.S., Guibal, E., Silva, E.A., Beppu, M.M., Adsorption and desorption of binary mixtures of copper and mercury on natural and crosslinked chitosan membranes, *Adsorption* 13 (2007) 603-611.
64. Ho, Y.S., Ng, J.C.Y., McKay, G., Kinetics of pollutant sorption by biosorbents: review. *Sep Purif Methods* 29 (2000) 189–232.
65. Plazinski, W., Rudzinski, W., Plazinska, A., Theoretical models of sorption kinetics including a surface reaction mechanism: a review, *Adv. Colloid Interface Sci*. 152 (2009) 2-13.
66. Azizian, S., Bashiri, H., Adsorption kinetics at the solid/solution interface: statistical rate theory at initial times of adsorption and close to equilibrium, *Langmuir* 24 (2008) 11669-11676.
67. Lagergren, S., "Zur Theorie Der Sogenannten Adsorption Geloster Stoffe, Kungliga Svenska Vetenskapsakademiens," Handlingar, 24 (1898) 1-39.
68. Boyd, G.E., Adamson Jr, A.W., Myers, L.S., The exchange adsorption of ions from aqueous solutions by organic zeolites, *J. Am. Chem. Soc*. 69 (1947) 2836-2848.
69. Blanchard, G., Maunaye, M., Martin, G., Removal of heavy metals from waters by means of natural zeolites, *Water Res.* 18 (1984) 1501-1507.
70. Liu, Y., Yang, S., Xu, H., Woon, K., Lin, Y., Tay, J., Biosorption kinetics of cadmium (II) on aerobic granular sludge, *Process Biochem*. 38 (2003) 997-1002.
71. Azizian, S., Kinetic models of sorption: a theoretical analysis, *J. Colloid Interf. Sci*. 276 (2004) 47-52.
72. Rudzinski, W., Plazinski, W., Kinetics of solute adsorption at solid/solution interfaces: a theoretical development of the empirical pseudo-first and pseudo-second order kinetic rate equations, based on applying the statistical rate theory of interfacial transport, *J. Phys. Chem. B* 110 (2006) 16514-16525.
73. Rudzinski, W., Plazinski, W., Studies of the kinetics of solute adsorption at solid/solution interfaces: on the possibility of distinguishing between the diffusional and the surface

reaction kinetic models by studying the pseudo-first order kinetics special features of the initial adsorption kinetics, *J. Phys. Chem. C* 111 (2007) 15100-15110.

74. Özer, A., Removal of Pb(II) ions from aqueous solutions by sulphuric acid-treated wheat bran, *J. Hazard. Mater.* 141 (2007) 753-761.
75. Liu, Y., Shen, L., From Langmuir kinetics to first- and second-order rate equations for adsorption, *Langmuir* 24 (2008) 11625-11630.
76. Teng, H., Hsieh, C., Activation energy for oxygen chemisorption on carbon at low temperatures, *Ind. Eng. Chem. Res* 38 (1999) 292-297.
77. Cheung, C.W., Porter, J.F., Mckay, G., Sorption kinetics analysis for the removal of cadmium ions from effluents using bone char, *Water Res.* 35 (2001) 605-612.
78. Rudzinski, W., Plazinski, W., On the applicability of the pseudo-second order equation to represent the kinetics of adsorption at solid/solution interfaces: a theoretical analysis based on the statistical rate theory, *Adsorption* 15 (2009) 181-192.
79. Wu, F.C., Tseng, R.L., Juang, R.S., Initial behavior of intraparticle diffusion model used in the description of adsorption kinetics, *Chem. Eng. J.* 153 (2009) 1-8.
80. Cheung, W.H., Szeto, Y.S., McKay, G., Intraparticle diffusion processes during acid dye adsorption onto chitosan, *Bioresour. Technol*. 98 (2007) 2897-2904.
81. Weng, C.-H., Tsai, C.-Z., Chu, S.-H., Sharma Y.C., Adsorption characteristics of copper(II) onto spent activated clay, *Sep. Purif. Technol*. 54 (2007) 187-197.
82. Yang, X., Al-Duri, B., Kinetic modeling of liquid-phase adsorption of reactive dyes on activated carbon, *J. Colloid. Interface Sci.* 287 (2005) 25-34.
83. Ho, Y.S., Review of second-order models for adsorption systems, *J. Hazard. Mater*. 136 (2006) 681-689.
84. Aharoni, C., Sideman, S., Hoffer, E., Adsorption of sulphate ions by colloidion-coated alumina *J. Chem. Technol. Biotechnol*, 29 (1979) 404-412.
85. Ritchie, A.G., Alternative to the Elovich equation for the kinetics of adsorption of gases on solids, *J. Chem. Soc., Faraday Trans*. I 73 (1977) 1650-1653.
86. Kumar K.V., Siranesan, S., Selection of optimum sorption kinetics: comparison of linear and non-linear method, *J. Hazard. Mater. B* 136 (2006) 277-279.

87. Ho, Y.S., Second-order kinetic model for the sorption of cadmium onto tree fern: a comparison of linear and non-linear methods, *Water Res.* 40 (2006) 119-125.
88. Borah, J.M., Das, M.R., Mahiuddin, S., Influence of anions on the adsorption kinetics of salicylate onto [alpha]-alumina in aqueous medium *J. Colloid Interface Sci*. 316 (2007) 260-267.
89. Nowack, B., VanBriesen, J.M., Chelating agents in the environment. In: B. Nowack and J.M. VanBriesen, Editors, *Biogeochemistry of Chelating Agents. ACS Symposium Series, American Chemical Society*, Washington, DC (2005) pp. 1-18.
90. Nowack, B., Environmental chemistry of aminopolycaboxylate chelating agents, *Environ. Sci. Technol*. 36 (2002) 4009–4016.
91. Bucheli-Witschel M., Egli, T., Environmental fate and microbial degradation of aminopolycarboxylic acids, *Microbiol. Rev*. 25 (2001) 69-106.
92. Smith, R.M., Martell, A.E., Motekaitis, R.J., NIST standard reference database 46.6. National Institute of Standards and Technology, U.S. Department of Commerce, Gaithersburg, MD (2007).
93. Piszczek, L., Ignatowicz, A., Kielbasa, J., Application of cyclic voltammetry for stoichiometry determination of Ni(II), Co(II), and Cd(II) complex compounds with polyaminopolycarboxylic acids, *J. Chem. Educ*. 65 (1988) 171-173.
94. Nowack, B., Sigg, L., Adsorption of EDTA and metal-EDTA complexes onto goethite, *J. Colloid Interface Sci.* 177 (1996) 106-121.
95. Silva, V.L., Carvalho, R. Freitas, M.P., Tormena, C.F., Melo, W.C., Spectrometric and theoretical investigation of the structures of Cu and Pb/DTPA complexes, *Struct. Chem*. 18 (2007) 605-609.
96. Silva, V.L., Carvalho, R., Freitas, M.P., Tormena, C.F., Melo, W.C., Structural determination of Zn and Cd–DTPA complexes: MS, infrared, 13C NMR and theoretical investigation, *Spectrochim. Acta, Part A* 68 (2007) 1197-1200.
97. Nörtemann, B., Biodegradation of chelating agents: EDTA, DTPA, PDTA, NTA, and EDDS. In: Nowack B, VanBriesen JM (eds) *Biogeochemistry of chelating agents, ACS symposium series 910*, American Chemical Society, Washington, DC, 2005, pp 150-170.

98. Sillanpää, M., Environmental fate of EDTA and DTP A, Rev. Environ. Contam. Toxicol. 152 (1997) 85-111.
99. Jal, P.K., Patel, S. Mishra, B.K., Chemical modification of silica surface by immobilization of functional groups for extractive concentration of metal ions, *Talanta* 62 (2004) 1005-1028.
100. Tikhonov, V.E., Radigina, L.A., Yamskov, Y.A., Metal-chelating chitin derivatives via reaction of chitosan with nitrilotriacetic acid, *Carbohydr. Res.* 290 (1996) 33-41.
101. Hughes, M.A., Wood, J., Rosenberg, E., Polymer structure and metal ion selectivity in silica polyamine composites modified with sodium chloroacetate and nitriloacetic acid (NTA) anhydride, *Ind. Eng. Chem. Res.* 47 (2008) 6765-6774.
102. Baraka, A., Hall, P.J., Heslop, M.J., Melamine-formaldehyde-NTA chelating gel resin: synthesis, characterization and application for copper(II) ion removal from synthetic wastewater, *J. Hazard. Mater.* 140 (2007) 86-94.
103. Lohan, M.C., Aguliar-Islas, A.M., Franks, R.P., Bruland, K.W., Determination of iron and copper in seawater at pH 1.7 with a new commercially available chelating resin, NTA Superflow, *Anal. Chim. Acta* 530 (2005) 121-129.
104. Dinu, M.V., Dragan, E.S., Trochimczuk, A.W., Sorption of Pb(II), Cd(II) and Zn(II) by iminodiacetate chelating resins in non-competitive and competitive conditions, *Desalination* 249 (2009) 374-379.
105. El-Nahhal, I.M., Zaggout, F.R., Nassar, M.A., El-Ashgar, N.M., Maquet, J., Babonneau, F., Chehimi, M.M., Synthesis, characterization and applications of immobilized iminodiacetic acid-modified silica, *J. Sol–Gel Sci. Technol.* 28 (2003) 255-265.
106. Dinu, M.V., Dragan, E.S., Heavy metals adsorption on some iminodiacetate chelating resins as a function of the adsorption parameters, *React. Funct. Polym.* 68 (2008), pp. 1346-1354.
107. Dragan, E.S., Dinu, M.V., Lisa, G., Trochimczuk, A.W., Study on metal complexes of chelating resins bearing iminodiacetate groups, *Eur. Pol. J.* 45 (2009) 2119-2130.
108. Ling, P., Liu, F., Li, L., Jing, X., Yin, B., Chen, K., Li, A., Adsorption of divalent heavy metal ions onto IDA-chelating resins: Simulation of physicochemical structures and elucidation of interaction mechanisms, *Talanta* 81 (2010) 424-432.

109. Sharma, R.K., Mittal, S., Koel, M., Analysis of trace amounts of metal ions using silica-based chelating resins: a green analytical method, *Crit. Rev. Anal. Chem*. 33 (2003) 183-197.
110. Shiraishi, Y., Nishimura, G., Hirai, T., Komasawa, I., Separation of transition metals using inorganic adsorbents modified with chelating ligands, *Ind. Eng. Chem. Res*. 41 (2002) 5065-5070.
111. Nagib, S., Inoue, K., Yamaguchi, T., Tamaru, T., Recovery of Ni from a large excess of Al generated from spent hydrodesulfurization catalyst using picolylamine type chelating resin and complexane types of chemically modified chitosan, *Hydrometallurgy* 51 (1999) 73–85.
112. Inoue, K., Ohto, K., Yoshizuka, K., Yamaguchi, T., Tanaka, T., Adsorption of lead(II) ion on complexane types of chemically modified chitosan, *Bullet. Chem. Soc. Japan* 70 (1997) 2443-2447.
113. Inoue, K., Yoshizuka, K., Ohto, K., Adsorptive separation of some metal ions by complexing agent types of chemically modified chitosan, *Anal. Chim. Acta* 388 (1999) 209-218.
114. Bernkop-Schnurch, A., Krajicek, M.E., Mucoadhesive polymers as platforms for peroral peptide delivery and absorption: synthesis and evaluation of different chitosan–EDTA conjugates, *J. Control. Release* 50 (1998) 215-223.
115. Hughes, M., Rosenberg, E., Characterization and applications of poly-acetate modified silica polyamine composites, *Sep. Sci. Technol*. 42 (2007) 261-283.
116. Sucholeiki, I., New developments in solid phase synthesis supports, *Mol. Divers*. 4 (1999) 25-30.
117. Yang, L.Q., Li, Y.F., Wang, L.Y., Zhang, Y., Ma, X.J., Ye, Z.F., Preparation and adsorption performance of a novel bipolar PS-EDTA resin in aqueous phase, *J. Hazard. Mater*. 180 (2010) 98-105.
118. Wang, L.Y., Yang, L.Q., Li, Y.F., Zhang, Y., Ma, X.J., Ye, Z.F., Study on adsorption mechanism of Pb(II) and Cu(II) in aqueous solution using PS-EDTA resin, *Chem. Eng. J*. 163 (2010) 364-372.
119. Zhang, Y., Li, Y.F., Yang, L.Q., Ma, X.J., Wang, L.Y., Ye, Z.F., Characterization and adsorption mechanism of Zn^{2+} removal by PVA/EDTA resin in polluted water, *J. Hazard. Mater*. 178 (2010) 1046-1054.

120. Diallo, M.S., Christie, S., Swaminathan, P., Johnson, J.J., Goddard 3rd, W.A., Dendrimer enhanced ultrafiltration. 1. Recovery of Cu(II) from aqueous solutions using PAMAM dendrimers with ethylene diamine core and terminal NH_2 groups, *Environ. Sci. Technol.* 39 (2005) 1366-1377.

121. Jiang, Y., Gao, Q., Yu, H., Chen, Y., Deng, F., Intensively competitive adsorption for heavy metal ions by PAMAM-SBA-15 and EDTA-PAMAMSBA-15 inorganic–organic hybrid materials, *Micropor. Mesopor. Mater.* 103 (2007) 316-324.

122. Pereira, F.V., Gurgel, L.V.A., Gil, L.F., Removal of Zn^{2+} from aqueous single metal solutions and electroplating wastewater with wood sawdust and sugarcane bagasse modified with EDTA dianhydride (EDTAD*), J. Hazard. Mater.* 176 (2010) 856-863.

123. Karniz Júnior, O., Gurgel, L.V.A., Freitas, R.P., Gil, L.F., Adsorption of Cu(II), Cd(II), and Pb(II) from aqueous single metal solutions by mercerized cellulose and mercerized sugarcane bagasse chemically modified with EDTA dianhydride (EDTAD), *Carbohydr. Polym.* 77 (2009) 643-650.

124. Ong, S-T, Lee, W-N, Keng, P-S, Lee, S-L, Hung, Y-T, Ha, S-T, Equilibrium studies and kinetics mechanism for the removal of basic and reactive dyes in both single and binary systems using EDTA modified rice husk, *Int. J. Phys. Sci*. 5 (2010) 582-595.

125. Igwe, C., Abia, A.A., Equilibrium sorption isotherm studies of Cd(II), Pb(II) and Zn(II) ions detoxification from waste water using unmodified and EDTA-modified maize husk, *Electr. J. Biotechnol.* 10 (2007) 536-548.

126. Igwe, C., Abia, A.A., Adsorption kinetics and intraparticulate diffusivities for bioremediation of Co (II), Fe (II) and Cu (II) ions from waste water using modified and unmodified maize cob, *Int. J. Phys. Sci*. 2 (2007) 119-127.

127. Yu, J., Tong, M., Sun, X., Li, B., Enhanced and selective adsorption of Pb^{2+} and Cu^{2+} by EDTAD-modified biomass of baker's yeast, *Biores. Technol*. 99 (2008) 2588-2593.

128. Afkhami, A., Madrakian, T., Amini, A., Karimi, Z., Effect of the impregnation of carbon cloth with ethylenediaminetetraacetic acid on its adsorption capacity for the adsorption of several metal ions, *J. Hazard. Mater.* 150 (2008) 408-412.

129. Gasser, M.S., Aly, H.F., Kinetic and adsorption mechanism of Cu(II) and Pb(II) on prepared nanoparticle layered double hydroxide intercalated with EDTA, *Colloids Surfaces A* 336 (2009) 167-173.
130. Trivedi, P., Axe, L., Predicting divalent metal sorption to hydrous Al, Fe, and Mn oxides, *Environ Sci Technol* 35 (2001) 1779-1784.
131. Baraka, A., Hall, B.J., Heslop, M.J., Preparation and characterization of melamine–formaldehyde–DTPA chelating resin and its use as an adsorbent for heavy metals removal from wastewater, *React. Funct. Polym.* 67 (2007) 585-600.
132. Zhao, X., Song, L., Zhang, Z., Wang, R., Fu, J., Adsorption investigation of MA-DTPA chelating resin for Ni(II) and Cu(II) using experimental and DFT methods, *J. Molec. Struct.* 986 (2011) 68-74.
133. Seggiani, M., Vitolo, S., D'Antone, S., Recovery of nickel from Orimulsion fly ash by iminodiacetic acid chelating resin, *Hydrometallurgy* 81 (2006) 9-14.
134. Wang, Ch. Ch., Chen, Ch. Y., Chang, Ch. Y., Synthesis of chelating resins with iminodiacetic acid and its wastewater treatment application, *J. Appl. Polym. Sci.* 84 (2002) 1353-1362.
135. Kołodyska, D., Cu(II), Zn(II), Ni(II), and Cd(II) complexes with HEDP removal from industrial effluents on different ion exchangers, *Ind. Eng. Chem. Res.*, 49 (2010) 2388-2400.
136. Kołodyńska, D., Hubicka, H., Hubicki, Z., Sorption of heavy metal ions from aqueous solutions in the presence of EDTA on monodisperse anion exchangers, *Desalination* 227 (2008) 150-166.
137. Wang, C.-C., Wang, C.-C., Adsorption characteristics of metal complexes by chelated copolymers with amino group, *React. Func. Polym.* 66 (2006) 343-356.
138. Kołodyńska, D., Skwarek, E., Hubicki, Z., Janusz, W., Effect of adsorption of Pb(II) and Cd(II) ions in the presence of EDTA on the characteristics of electrical double layers at the ion exchanger/NaCl electrolyte solution interface. *J. Colloid Interface Sci.* 33 (2009) 448-456.
139. Juang, R.S., Wang, Y.C., Effect of added complexing anions on cation exchange of Cu(II) and Zn(II) with a strong-acid resin, *Ind. Eng. Chem. Res.* 41 (2002) 5558-5564.

140. Bari, F., Begun, N., Jamaludin, S.B., Hussin, K., Extraction and separation of Cu(II), Ni(II) and Zn(II) by sol–gel silica immobilized with Cyanex 272, *Hydrometallurgy* 96 (2009) 140-147.
141. Mendes, F.D., Martins, A.H., Selective sorption of nickel and cobalt from sulphate solutions using chelating resins, *Int. J. Miner. Process.* 74 (2004), pp. 359-371
142. Flett, D.S., Cobalt-nickel separation in hydrometallurgy: a review, *Chem. Sustain. Dev.* 12 (2004) 81-91.
143. Hirata, S., Kajiya, T., Aihara, M., Honda. H., Shikino, O., Determination of rare earth elements in seawater by on-line column preconcentration inductively coupled plasma mass spectrometry, *Talanta* 58 (2002) 1185-1194.
144. Rahmi, D., Zhu, Y., Fujimori, E., Umemura, T., Haraguchi, H., Multielement determination of trace metals in seawater by ICP-MS with aid of down-sized chelating resin-packed minicolumn for preconcentration, *Talanta* 72 (2007) 600-606.
145. Juang R.-S., Wu, F.-C., Tseng, R.-L., Adsorption removal of copper(II) using chitosan from simulated rinse solutions containing chelating agents, Water Res. 33 (1999) 2403-2409.
146. Rashidova, S.Sh., Shakarova, D.Sh., Ruzimuradov, O.N., Satubaldieva, D.T., Zalyalieva, S.V., Shpigun, O.A., Varlamov, V.P., Kabulov, B.D., Bionanocompositional chitosan-silica sorbent for liquid chromatography, *J. Chromatograph. B* 800 (2004) 49-53.
147. Guibal, E., Jansson-Charrier, M., Saucedo, I., Le Cloirec, P., Enhancement of metal ion sorption performance of chitosan. Effect of the structure on the diffusion properties, *Langmuir* 11 (1995) 591-598.
148. Helfferich, F., *Ion Exchange*, Dover, New York (1995) p. 285.
149. Pagnanelli, F., Trifoni, M., Becolchini, F., Esposito, A., Toro, L., Veglio, F., Equilibrium biosorption studies in single and multi-metal systems, Process Biochem. 37 (2001) 115-124.
150. Malinen, L.K., Koivula, R., Harjula, R., Removal of radiocobalt from EDTA-complexes using oxidation and selective ion exchange. *Water Sci. Technol*. 60 (2009) 1097-101.

APPENDICES

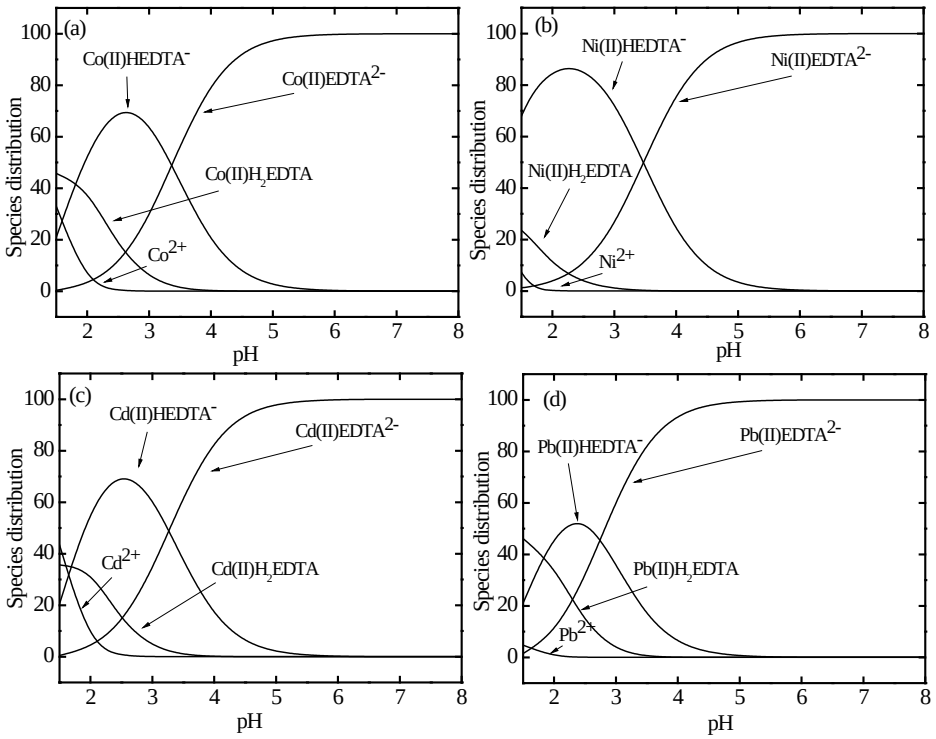

Appendix IA. Species distribution in Me(II)EDTA 1:2 solutions calculated by Visual MINTEQ software ver. 2.53.

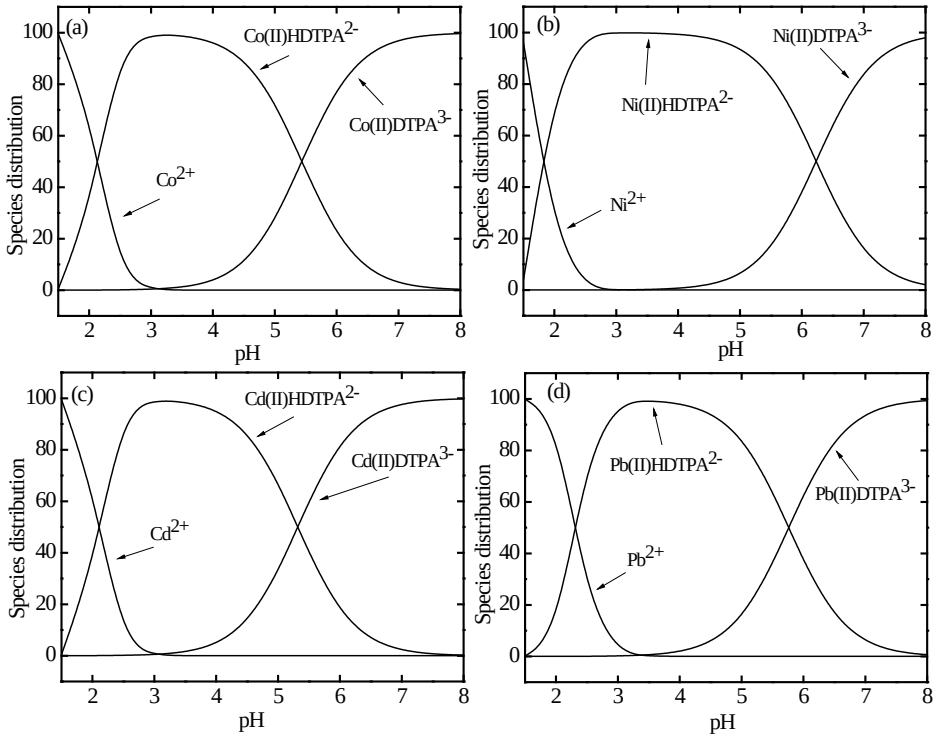

Appendix IB. Species distribution in Me(II)DTPA 1:2 solutions calculated by Visual MINTEQ software ver. 2.53.

Paper I

Removal of Co(II) and Ni(II) ions from contaminated water using silica gel functionalized with EDTA and/or DTPA as chelating agents

Eveliina Repo, Tonni Agustiono Kurniawan, Jolanta K.Warchol, Mika E.T. Sillanpää

Journal of Hazardous Materials 171 (2009) 1071–1080

Journal of Hazardous Materials 171 (2009) 1071–1080

Contents lists available at ScienceDirect

Journal of Hazardous Materials

journal homepage: www.elsevier.com/locate/jhazmat

Removal of Co(II) and Ni(II) ions from contaminated water using silica gel functionalized with EDTA and/or DTPA as chelating agents

Eveliina Repo[a,*], Tonni Agustiono Kurniawan[a], Jolanta K. Warchol[b], Mika E.T. Sillanpää[a]

[a] Laboratory of Applied Environmental Chemistry (LAEC), Department of Environmental Science, The University of Kuopio, Patteristonkatu 1, FI-50100 Mikkeli, Finland
[b] Rzeszów University of Technology, Department of Water Purification and Protection, 6 Powstańców Warszawy Street, 35-959 Rzeszów, Poland

ARTICLE INFO

Article history:
Received 9 April 2009
Received in revised form 3 June 2009
Accepted 22 June 2009
Available online 27 June 2009

Keywords:
Adsorption
Environmental protection
Heavy metal removal
Surface modification
Wastewater treatment

ABSTRACT

In this study, the removal of Co(II) and Ni(II) ions from contaminated water was investigated using silica gel materials functionalized with both ethylenediaminetetraacetic acid (EDTA) and diethylenetriaminepentaacetic acid (DTPA). The modified adsorbents were characterized using elemental analysis, surface area and pore size analysis, and zeta potential analysis. The adsorption and regeneration studies were conducted in batch mode. The optimum conditions for the removal of both metals at an initial concentration of 10 mg/L were 2 g/L of dose, pH 3, 50 rpm of agitation speed and 4 h of contact time. The removal of Co(II) and Ni(II) by EDTA- and/or DTPA-modified silica gels was substantially higher than that by their unmodified form. The maximum Co(II) and Ni(II) uptakes by the EDTA-modified silica gel were 20.0 and 21.6 mg/g, comparable to their adsorption capacities by DTPA-modified silica gel (Co(II): 16.1 mg/g; Ni(II): 16.7 mg/g). At the same concentration of 10 mg/L, the removal of both metals by the modified adsorbents ranged from 96% to 99%. The two-site Langmuir model was representative to simulate adsorption isotherms. The kinetics of Co(II) and Ni(II) adsorption by modified silica gels followed pseudo-second-order.

1. Introduction

Heavy metals such as Co(II) and Ni(II) are commonly found in contaminated water from storage battery, catalyst and nuclear industries [1,2]. These metals are toxic, not biodegradable, and often accumulate in food chain. If ingested beyond the permitted level, their toxicities cause health disorders such as allergy or damage internal organs [3–6]. Therefore, their removal from contaminated water is required prior to discharge.

At concentrations higher than 100 mg/L, the removal of heavy metals can be accomplished by chemical precipitation. This conventional method, however, is ineffective and produces a huge amount of toxic sludge [4]. At lower concentrations, the removal of metals is better achieved by adsorption. This technology may be able to generate treated effluents that contain an acceptable effluent limit of target metals. Due to state-of-the-art of adsorption technology, the development of new adsorbents has intensified in recent years.

Recently, organic polymers chemically modified with functional groups such as amine, carboxylic and phosphate have been employed to facilitate metal removal from an aquatic environment [7]. In spite of having a high amount of active sites for metal binding, their drawbacks include swelling, slow kinetics, irreversible adsorption of target compounds and loss of mechanical stability [8,9]. To overcome these problems, inorganic materials may be employed to provide viable solutions.

One of the potential inorganic materials that could be used in water treatment is silica gel. This material can be chemically modified with different functional groups by a silanization method to improve its removal performance. In addition, other advantages of silica gel are local availability, high surface area of about 600 m^2/g and high thermal resistance [8,9].

Preliminary studies reported that functionalized silica gels could effectively remove trace elements such as Cu, Zn, Fe, Cd, Pb, and Mn from contaminated water [8,9]. However, all of the silica-bound ligands could not reverse the metal binding and the regeneration of spent adsorbent became complicated [10,11]. To address this problem, in the present study, silica gel was functionalized with metal chelating agents such as ethylenediaminetetraacetic acid (EDTA) and diethylenetriaminepentaacetic acid (DTPA) prior to their use as adsorbents. The chelating agents were anticipated to have the ability to form stable structures with target metals and reverse the metal binding after being treated chemically.

The aim of this study was to investigate the performance of silica gel modified with EDTA and DTPA for the removal of Co(II) and Ni(II) from contaminated water. Effects of pertinent factors such as pH and contact time on the metal removal by the adsorbents were studied. The Langmuir, Freundlich and two-site Langmuir models were employed to simulate their adsorption isotherms. The

* Corresponding author. Tel.: +358 15 355 3707; fax: +358 15 355 6363.
E-mail address: Eveliina.repo@uku.fi (E. Repo).

0304-3894/$ – see front matter © 2009 Elsevier B.V. All rights reserved.
doi:10.1016/j.jhazmat.2009.06.111

Table 1
Physical properties of unmodified silica gel.

Properties	Silica gel		
Diameter (μm)	5–20	40–63	63–200
Pore volume (g/cm^3)	0.84	0.90	0.84
Surface area (m^2/g)	540	580	540

adsorption mechanisms of metal removal by the adsorbents are also presented.

2. Materials and methods

2.1. Materials

As-received silica gel type LiChroPrep®, supplied by Merck (Finland), was provided in powder form. Its physical properties are presented in Table 1. All chemicals used in this study were of analytical grade and supplied by the same company. Stock solutions of 1000 mg/L were periodically prepared by dissolving appropriate amounts of Co(II) and Ni(II) nitrate salts in double deionized water. Working solutions ranging from 1 to 400 mg/L of Co(II) or Ni(II) were prepared from the stock solutions. Adjustment of pH was undertaken using 0.1 M NaOH and 0.1 M HNO_3.

2.2. Methods

2.2.1. Chemical modification of silica gels

Silica gel was refluxed with 6 M HCl for 3 h. After washing, the gel was dried in an oven at 200 °C for 24 h. To form functional groups on its surface, about 15 mL of aminopropyl-triethoxysilane (APTES) and 50 g of silica gel were added into 300 mL of toluene and magnetically stirred at 200 rpm for 16 h. After filtration, the resulting aminopropyl silica gel (APSG) was washed with 150 mL toluene and 150 mL acetone and then dried in an oven 105 °C for 4 h. The surface-bound amino groups were then reacted with 25 g of EDTA anhydride in 188 mL of a mixed ethanol and acetic acid (1:1) solution at 76 °C for 16 h (Fig. 1) [12,13].

Functionalization of the gel with DTPA was undertaken by reacting 17.5 g DTPA anhydride with 6.5 g APSG in 136 mL of mixed ethanol/acetic acid. After complete reaction, the yellowish product was filtrated and washed with 4 M NH_4OH, 1:1 mixture of ethanol/acetic acid, water and methanol [14]. Finally the modified silica gels (EDSG and DTSG) were dried in an oven at 105 °C for 6 h. The same method was also performed to functionalize silica gels with different particle sizes. The formation of functional groups on their surface was studied using a FTIR-spectroscopy type Nicolet Nexus 8700 (USA). The presence of peaks at wavelength ranging from 1630 to 1400 cm^{-1} on EDSG and DTSG indicated the formation of carboxylic groups on the surface of the adsorbents.

2.2.2. Characterization of the modified silica gels

For elemental analysis, the Kjeldahl and sulfuric acid–dichromate methods were employed according to the Standard Methods to determine the amount of nitrogen and organic carbon respectively in the modified silica gels [15]. The results were used to determine the surface coverage of APTES, EDTA, and DTPA on the adsorbents. Autosorb-1-C surface area and pore size analyzer (Quantachrome, The UK) were used to determine the surface properties of the adsorbents before and after modification. Zetasizer Nano Series model ZEN 3600 (Malvern, the UK) was employed to measure their isoelectric points before and after metal adsorption. The zeta potential measurements were performed in 0.1 M NaCl.

2.2.3. Batch adsorption studies

Batch experiments were conducted at ambient temperature using the optimum conditions of all pertinent factors such as dose, pH, agitation speed, and contact time. Subsequent adsorption experiments were carried out with only optimized parameters. Agitation of the system under investigation was carried out on a rotary shaker type ST5 (CAT M.Zipperer GmbH, Staufen, Germany). At the designated time, the adsorbent was separated from aqueous solution using 0.45 μm polypropylene syringe filter.

Adsorption isotherm tests were carried out at ambient temperature in a mixture of 0.02 g of an adsorbent and 0.01 L of solution containing Co^{2+} and/or Ni^{2+} with varying concentration from 1 to 400 mg/L.

2.2.4. Chemical analysis

After dilution with 2% HNO_3, the samples were analyzed by an inductively coupled plasma optical atomic emission spectrometry (ICP-OES) model iCAP 6300 (Thermo Electron Corporation, USA). Changes in the metal concentrations due to adsorption were analyzed at wavelengths of 228.616 nm (for Co^{2+}) and 231.605 nm (for Ni^{2+}). The minimum detectable concentrations of both Co(II) and Ni(II) ions by this equipment were 0.4 and 0.8 μg/L respectively. The quantity of the adsorbed metal per unit mass of modified silica gel (mg/g) was calculated as follows:

$$q_e = \frac{C_i - C_e}{M} V \quad (1)$$

where C_i and C_e are the initial and the equilibrium concentrations (mg/L), while M and V represent the weight of the adsorbent (g) and the volume of the solution (L) respectively.

2.2.5. Regeneration studies

After treatment, the exhausted adsorbent containing the adsorbed metal was collected for regeneration. Initially the adsorbent was loaded by the metal ions by mixing around 0.5 g of EDSG or DTSG with 0.02 L of 250 mg/L Co(II) or Ni(II) solution. After attaining an equilibrium, the spent adsorbent was separated from the solution using centrifuge. Metal ions were eluted by mixing the adsorbent with 0.01 L of 2 M HNO_3. Treated effluents were collected and chemically analyzed for metal determination. The regeneration

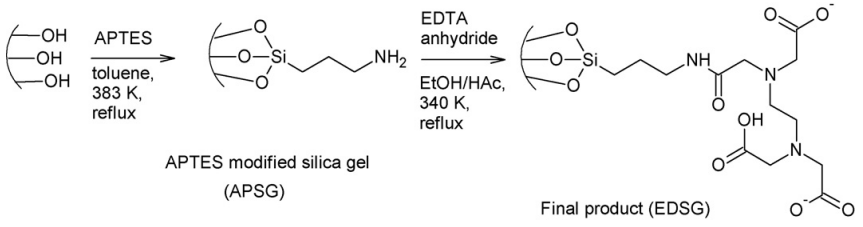

Fig. 1. Synthesis route of EDSG [13].

Table 2
Elemental analysis and calculated surface coverage of EDTA and DTPA.

Adsorbents (mmol/g)	Particle size (μm)	C (mmol/g)	N (mmol/g)	EDTA/DTPA
Unmodified silica gel	63–200	0.16	<0.05	–
EDSG	5–20	7.7	1.6	0.25
	40–63	7.6	1.7	0.32
	63–200	8.3	2.0	0.22
DTSG	5–20	7.7	1.7	0.19
	40–63	7.5	1.7	0.23
	63–200	8.3	1.9	0.15

efficiency (*%RE*) of the adsorbent was calculated using Eq. (2):

$$\%RE = \frac{q_r}{q_0} \times 100 \quad (2)$$

where q_0 and q_r are the adsorption capacities of the adsorbents before and after regeneration respectively.

2.2.6. Statistical analysis

All the experiments were conducted in duplicate under identical conditions. The coefficient of variation was mostly less than 1%. If the variation of metal removal by the adsorbent exceeded 5%, an identical run would be undertaken and closer data points were used. To determine the margin of error, a confidence interval (CI) of 95% was calculated for each set of the samples by using SPSS 17.00 Windows version and the obtained data were analyzed using *t*-test and/or ANOVA test. Differences were considered statistically significant when $p \leq 0.05$ for the analysis of variance (ANOVA) or *t*-tests.

3. Results and discussion

3.1. Characterization of the modified silica gels

To identify changes after surface modification, the modified adsorbents were thoroughly characterized using elemental analysis, surface area and pore size analysis, as well as zeta potential measurements. The values of EDTA and DTPA loadings were calculated by subtracting the amount of nitrogen and carbon obtained for APSG from the ones obtained for EDSG or DTSG. The data presented in Table 2 are the average values calculated from the amount of carbon and nitrogen in modified silica gels. The average values for EDTA and DTPA surface coverages were 0.26 and 0.18 mmol/g respectively. There was no significant correlation between the particle size and surface coverage of the adsorbents. This could be attributed to similar surface areas of raw silica gel used (Table 1).

Substantially higher ligand loadings (0.58–0.74 mmol/g) were obtained for silica polyamino composites modified by EDTA [14]. In addition, ligand loadings of 5.9 and 1.3 mmol/g were obtained for the EDTA- and DTPA-modified chitosan [16,17]. The higher surface coverages of these materials compared to those of modified silica gels obtained in this study were due to the higher amount of amino groups available for binding EDTA and/or DTPA. The amounts of amino groups in silica polyamino composites and chitosan were 4 and 5.9 mmol/g respectively, while the amount of APTES groups on the surface of silica gel was 1.5 mmol/g. In addition, not all the surface-bound amino groups completely reacted with EDTA or DTPA in spite of the excess of the anhydrides used in the synthesis. This could be attributed to the steric hindrances caused by bulky organic groups such as DTPA [16].

The isoelectric point determined by zeta potential measurements for both EDSG and DTSG was found to be at pH 4, while it ranged between pH 1 and 2 for unmodified silica gels (Fig. 2). The difference of silica gel in the modified and unmodified forms was observed at an acidic pH range, where the surface charge of modified material was more positive than that of unmodified form. In addition, the surface charge of the modified silica gels changed from positive to negative as a function of pH. This could be due to the release of protons from the surface. Changes in the values of isoelectric point observed after metal binding indicated the stability of the surface-bound metal chelate.

The results of the surface properties of EDSG and DTSG measured are presented in Table 3. The table shows that the specific surface area and the total pore volume of the particles of 5–20 μm were slightly larger than those of 40–63 and 63–200 μm particles. The specific surface area and the total pore volume decreased after the formation of organic groups on the surface (Table 1). This could be attributed to the reduced pore sizes and pore blocking of the modified adsorbents. The pore size distribution was affected by the size of the attached organic group and the size of the particle (Fig. 3). After surface modification, the amount of smaller pores increased, while that of larger pores decreased due to the formation of functional groups inside the pores.

3.2. Pertinent factors affecting on the removal of heavy metals by modified silica gels

3.2.1. Effects of pH

To maximize the removal of heavy metals by the adsorbents, knowledge of an optimum pH is important. pH affects not only the surface charge of adsorbent, but also the degree of ionization and

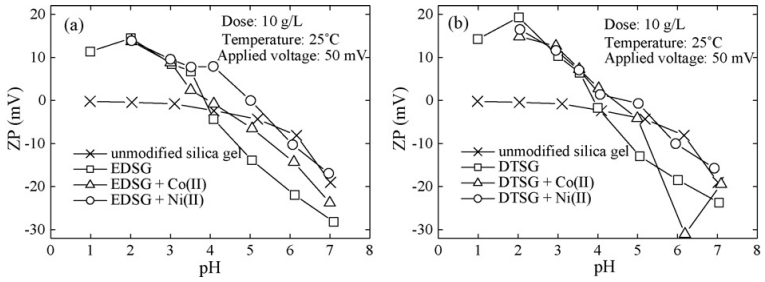

Fig. 2. Zeta potentials as a function of pH in 0.1 M NaCl.

Table 3
Surface properties of modified silica gels.

Adsorbents	Particle size (μm)	Specific surface area (m^2/g)	Total pore volume (cm^3/g)
EDSG	5–20	386	0.47
	40–63	384	0.48
	63–200	297	0.33
DTSG	5–20	367	0.45
	40–63	328	0.41
	63–200	309	0.34

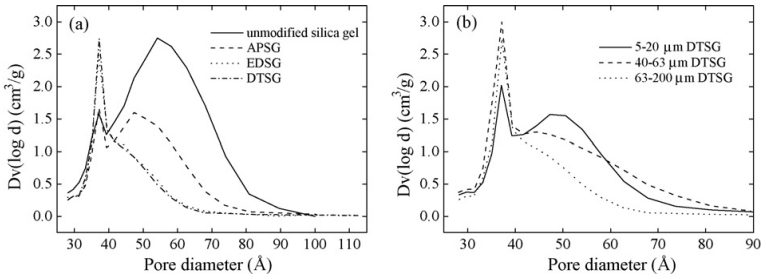

Fig. 3. Pore size distribution. (a) Effects of the functional group for 63–200 μm particles; (b) Effects of the particle size for DTSG.

speciation of adsorbate during reaction. To study the effects of H^+ concentrations on metal removal, the solution pH was varied from 1 to 7. The effects of pH on the adsorption of Co(II) and Ni(II) by the modified silica gels are presented in Fig. 4.

It is apparent from the figure that the extent of Co(II) and Ni(II) removal was dependent on pH. The maximum metal adsorption was attained at pH ranging from 2 to 3, close to the isoelectric point of the EDSG and DTSG. This could be attributed to the decrease in the positive surface charge, thus lowering electrostatic repulsions between the surface of the adsorbent and metal ions [18]. While at pH ranging from 4 to 7, the metal uptake was limited by the ligand loading and the stability of the surface-bound chelate [14]. To maximize metal removal, subsequent adsorption tests were carried out at pH 3.0 as the optimum pH.

When pH was varied from 1 to 7, it was noticed that the leaching of the functional groups from the surface of the materials increased at a higher pH. This effect was studied by measuring the Si concentration in the solution before and after experiments (Fig. 5). The amount of Si released from the surface was around 0.4% and 0.6% for EDSG and DTSG respectively. For comparison, Fig. 5 shows that almost tenfold amount of Si released in the solution from APSG at the same conditions. The leaching of the grafted APTES groups from the silica gel surfaces was attributed to the nucleophilic attack of the end amino group to the Si–O–Si bond, thus breaking down the bond [19]. Thus, it is suggested that the EDTA and DTPA groups protected the surface of silica gels from leaching.

3.2.2. Effects of functional group

Fig. 4 presents that unmodified silica gel had a substantially lower metal removal (1.4 mg/g) than modified silica gels (15.9 mg/g) at the same initial Co(II) concentration of 80 mg/L. This suggests that the chelating groups played predominant roles in improving the metal adsorption by the modified adsorbents. Fig. 6a illustrates the equilibrium state of Co(II) and Ni(II) adsorption on 63–200 μm of EDSG and DTSG particles.

The differences in the adsorption capacities of EDSG and DTSG were due to the amount of ligands attached on the surface as well as the stability of the surface-bound metal chelates, as reflected by their stability constants (K). During equilibrium, the DTPA formed more stable chelates with both metals [$\log K = 19.15$ for Co(II); $\log K = 20.17$ for Ni(II)] than the EDTA did [$\log K = 16.26$ for Co(II); $\log K = 18.52$ for Ni(II)] [20]. Thus, the surface-bound DTPA chelates

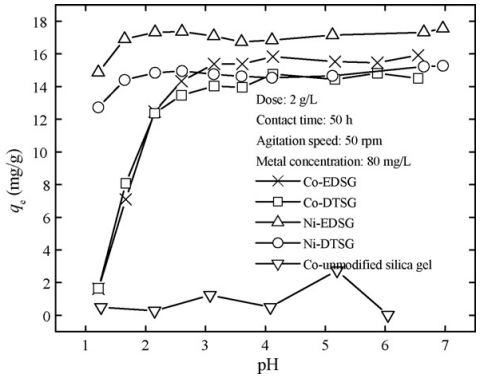

Fig. 4. Removal of Ni(II) and Co(II) as a function of pH.

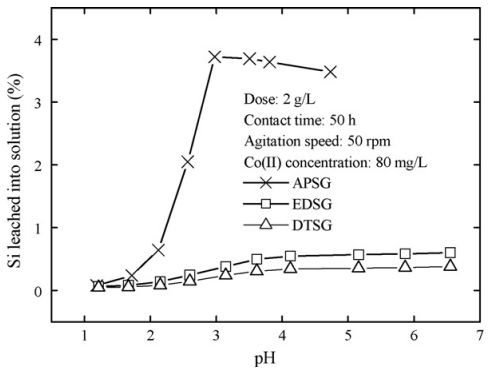

Fig. 5. Leaching of silicon into solution as a function of pH.

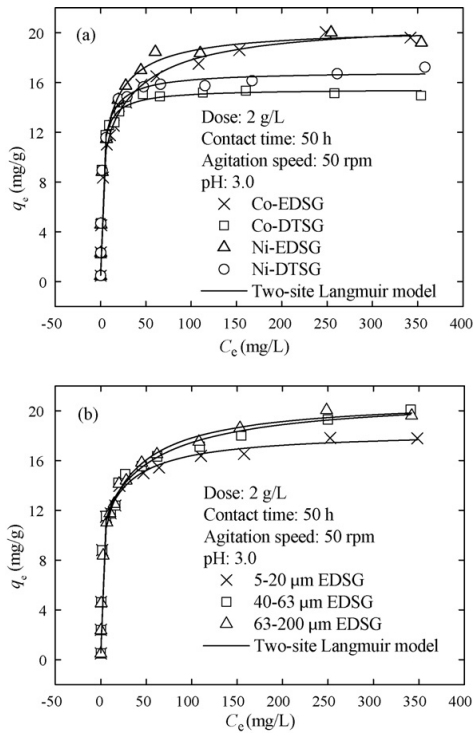

Fig. 6. Equilibrium data of metal adsorption on EDSG and DTSG. (a) Effects of the functional group; (b) Effects of the particle size for Co(II) adsorption on EDSG.

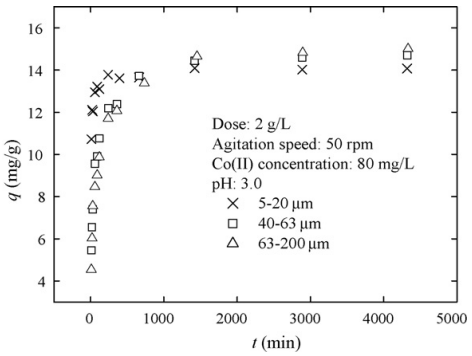

Fig. 7. Effects of contact time on Co(II) adsorption by EDSG.

were anticipated to be more stable than the corresponding EDTA chelates, while Ni(II) chelates were more stable than Co(II) ones.

The optimum uptake of Co(II) by the EDSG was slightly higher (q_m = 20.0 mg/g) than that by the DTSG (q_m = 16.1 mg/g), while the maximum adsorption capacities of Ni(II) by the EDSG and the DTSG were 21.6 and 16.7 mg/g respectively. The uptake of the metals by EDSG was higher because of its higher surface coverage (Table 2). The EDSG employed in this study also demonstrated a higher adsorption capacity for Ni(II) compared to the corresponding material (6.3 mg/g) used in another study undertaken by Shiraishi et al. [13]. The adsorption capacities of EDTA-functionalized silica polyamine composites were 26 mg/g for Co(II) and 32 mg/g for Ni(II) [14], substantially lower than those obtained by EDTA- and DTPA-modified chitosan for Ni(II), which was about 120 mg/g [16,17]. Better adsorption performances of previous materials compared to those of EDSG and DTSG in this study are likely due to their higher amount of available functional groups for metal binding (see Section 3.1).

It should also be noticed that at a lower concentration of 10 mg/L, EDSG and DTSG bound Co(II) more effectively than Ni(II) regardless of their stability constants. In this case, the immobilization of chelating agents might have contributed to their binding properties.

3.2.3. Effects of particle size

To study the effects of particle size on metal removal, silica gel particles with different sizes were functionalized with EDTA and/or DTPA ligands. The equilibrium curves for Co(II) adsorption on the EDSG are depicted in Fig. 6b. It was observed that the maximum adsorption capacities of 40–63 and 63–200 μm particles were slightly higher than that of 5–20 μm particles. Similar results were obtained for the DTSG. Normally, smaller particles have higher adsorption performance than larger ones due to their higher surface area. By increasing the particle surface area, it is possible to increase the adsorption rate of the metals. However, in this study, particle size did not significantly affect the extent of metal removal by the modified adsorbents, as they had similar surface area and coverage for metal adsorption, as suggested by the BET surface area measurement (Table 3).

3.2.4. Effects of contact time

The removal of Co(II) and Ni(II) by the adsorbents was also studied as a function of contact time. The contact time was varied from 10 to 4320 min. Fig. 7 shows that the removal rate of Co(II) by the EDSG was rapid in the first 120 min, then gradually decreased, until the metal adsorption attained an equilibrium. This indicated the ease of the target metal in diffusing through the pores of adsorbents at the initial stage of adsorption. Within 4 h of contact time, about 91% of maximum Co(II) removal by the 5–20 μm particles of EDSG was attained. This stemmed from the fact that a large number of vacant active surface sites were still available for adsorption during the initial stage and that after a lapse of time, the remaining vacant surface sites were occupied by the adsorbed metal. This suggests that the nature of the adsorbent and its available adsorption sites affected the time required to attain equilibrium. Considering that there was no significant increase of metal removal beyond 4 h, this contact time was sufficient to attain equilibrium conditions, as reflected by the data in Fig. 7. However, due to the minor increase in the adsorption capacity after 24 h, a contact time of 50 h was selected for all the equilibrium tests.

3.3. Removal of Co(II) and Ni(II) at different concentrations

The technical applicability of the adsorbents depends on their performance at varying metal concentrations. Table 4 shows the removal efficiency of Co(II) and Ni(II) at varying doses of the EDSG and the DTSG at different metal concentrations. When an optimum dose was employed, the modified silica gels were effective to remove target metals at both low and high concentrations with their removal efficiency over 96%. This finding suggests that the tested adsorbents were relatively promising for water treatment applications.

3.4. Adsorption mechanism of heavy metal by the adsorbent

Since the surface of silica gel contains functional groups such as carboxylic, hydroxyl, amine, and carbonyl, it was assumed that the physico-chemical interactions that might have occurred during

Table 4
Adsorption performance of unmodified and modified silica gels at different concentrations at pH 3.0.

Type of adsorbent	Co(II)			Ni(II)		
	Initial metal concentration (mg/L)	Dose (g/L)	Metal removal (%)	Initial metal concentration (mg/L)	Dose (g/L)	Metal removal (%)
Unmodified silica gel	1	2	9.2	–	–	–
	80	2	3.0	–	–	–
EDSG	1	2	98.2	1	2	97.0
	10	2	97.4	10	2	97.2
	80	2	43.5	80	2	46.1
	250	25	96.3	250	25	99.5
DTSG	1	2	99.1	1	2	96.5
	10	2	99.0	10	2	96.7
	80	2	40.3	80	2	39.4
	250	25	98.6	250	25	99.4

metal removal by the adsorbent could be expressed as follows:

$$M^{n+} + n(-SiOHY) \leftrightarrows (-SiOY)_n M \uparrow + nH^+ \quad (3)$$

where (–SiOHY) represents the surface functional group of modified silica gels with EDTA symbolized by Y and n is the coefficient of the reaction component, depending on the oxidation state of metal ions, while M^{n+} and H^+ are the heavy metal (Ni^{2+} or Co^{2+}) and the hydrogen ions respectively.

On the basis of thermodynamic data [21], EDTA has various species distribution represented by H_nEDTA^{n-4}, where n ranges from 0 to 5. The calculation of the EDTA species distribution using the MINEQL software [22,23] showed that negatively charged H_2EDTA^{2-} (85%) and $HEDTA^{3-}$ (15%) are the predominant species at pH 3, where most of the experiments were undertaken. Based on the experimental data, it is proposed that the metal removal by the modified silica gels could be presented as follows:

$$[SiO–H–H_iEDTA]^{i-2}{}_{(aq)} + M^{2+}{}_{(aq)} \leftrightarrows [SiO–M–H_iEDTA]^{i-1}\uparrow_{(s)} + H^+{}_{(aq)} \quad (4)$$

where $[SiO–H–H_iEDTA]^{i-2}$ represents the EDTA-modified silica gel and i is the number of hydrogen ions complexed with EDTA ranging from 0 to 3, while M^{2+} is the divalent metal cation.

Eq. (4) suggests that the metal adsorption on the surface of the adsorbent was attributed to columbic forces between the positive charge of the heavy metal and the negative surface charge of the adsorbent. Based on the attractive electrostatics interaction between the electron-donating nature of the oxygen-containing functional groups on the surface of the adsorbent (Lewis base) and the electron-accepting nature of the heavy metal ions (Lewis acid), the ion exchange mechanism of Ni(II) or Co(II) might also have contributed to the metal removal by the EDTA-modified silica gel. At an acidic pH range, the functional groups of the modified adsorbents are protonated, thus facilitating ion exchange to take place.

In this regard, an Ni(II) or Co(II) ion might attach itself to three adjacent hydroxyl, carboxylic, and amine groups of the adsorbent, which might have donated the lone pairs of delocalized p-electrons to the surface to the metal ion to form surface oxide compounds $[SiO–M–H_iEDTA]^{i-1}$. Nowack and Sigg [24] reported that the structures of the Co(II) and Ni(II) EDTA chelates in the aqueous phase are quinquedentate, where three carboxylic groups are involved in metal binding and that one of the coordination sites is occupied by a water molecule.

Eq. (4) also indicates that as solution pH increased to 6.0 or the concentration of H^+ decreased (to 10^{-6} M), the adsorption reaction shifted from left to right, which resulted in the production of more oxygenated metal complex $[SiO–M–H_iEDTA]^{i-1}$ on the surface of the adsorbent or a higher metal removal. During equilibrium, it was found that pH decreased after metal adsorption. This suggests that the adsorbent was hydrophilic. The amount of protons released into the solution corresponded to the amount of EDTA/DTPA groups on the surface (Table 5). This finding was confirmed by zeta potential measurements, which showed changes in the isoelectric points after metal loading (Fig. 2).

3.5. Adsorption kinetics

To investigate the adsorption kinetics of heavy metals onto the adsorbents, two kinetic models (pseudo-first-order and pseudo-second-order) were employed to simulate the experimental data. The pseudo-first-order kinetic model is commonly used to predict adsorption kinetics. This assumes that the rate of change of solute uptake with time is directly proportional to difference in saturation concentration.

To distinguish a kinetic equation based on the adsorption capacity of an adsorbent, the equation for the pseudo-first-order kinetics

Table 5
Correlation between proton release during adsorption and the amount of EDTA or DTPA groups obtained experimentally and from modeling.

Adsorbent	Particle size (μm)	Metal	Ratio of protons released and metals adsorbed	Ratio of surface coverage of EDTA or DTPA and metals adsorbed[a]	q_{m2}/q_m from two-site Langmuir model[b]
EDSG	5–20	Co	1.32	0.83	0.68
	40–63	Co	0.76	0.94	0.59
	63–200	Co	0.78	0.66	0.51
	63–200	Ni	0.89	0.67	0.58
DTSG	5–20	Co	0.89	0.75	0.74
	40–63	Co	0.86	0.84	0.55
	63–200	Co	0.58	0.60	0.66
	63–200	Ni	0.5	0.51	0.59

[a] The amount of metals adsorbed represents the total amount of functional groups on the surface.
[b] q_{m2} is the amount of EDTA or DTPA and q_m the total amount of functional groups.

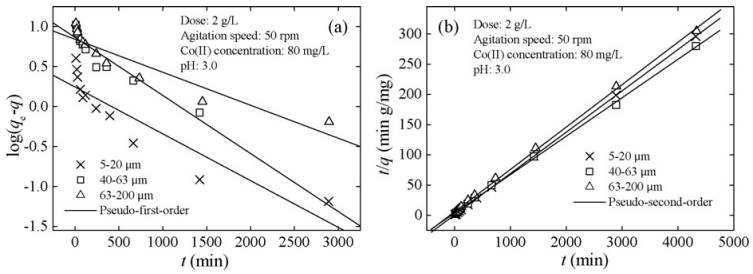

Fig. 8. Adsorption kinetics of Co(II) on EDSG.

is presented as follows [25]:

$$\frac{dq}{dt} = k_1(q_e - q) \tag{5}$$

By integrating this particular equation at the boundary conditions $q = 0$ at $t = 0$ and $q = q_t$ at $t = t$, this can be transformed into a logarithmic function as follows:

$$\log(q_e - q_t) = \log q_e - \frac{k_1 t}{2.303} \tag{6}$$

where q_t and q_e are the adsorption capacity at time t (mg/g) and at equilibrium respectively, while k_1 represents the pseudo-first-order rate constant (min^{-1}). The plot of $\log(q_e - q_t)$ versus t is depicted in Fig. 8a, while other parameters are presented in Tables 6 and 7.

Fig. 8a and Tables 6 and 7 show that the pseudo-first-order model was not applicable for the adsorption of Co(II) and Ni(II) by all the adsorbents, as indicated by their lower correlation coefficients than those of pseudo-second-order kinetics. Yang et al. [25] also reported their similar findings. Generally, pseudo-first-order do not fit well with the whole range of contact time and is applicable only for the initial stage of adsorption [26].

The kinetic data of metal adsorption by the adsorbents were then simulated by pseudo-second-order. The equation of this model is presented as follows:

$$\frac{dq}{dt} = k_2(q_e - q)^2 \tag{7}$$

An integration of Eq. (7) at the boundary conditions, $q = 0$ at $t = 0$ and $q = q_t$ at $t = t$, would give:

$$\frac{t}{q_t} = \frac{1}{k_2 q_e^2} + \frac{t}{q_e} \tag{8}$$

where k_2 is the rate constant of the pseudo-second-order (g/mg min), while q_e represents the amount of metal adsorbed (mg/g) at equilibrium.

By plotting (t/q_t) versus t (Fig. 8b), the rate constants k_2 and correlation coefficients can be calculated. Fig. 8b and Tables 6 and 7 show that the pseudo-second-order kinetic model correlated better with the experimental data than the pseudo-first-order did. Hence, it was more representative than the latter to simulate the adsorption of Co(II) and Ni(II) onto all types of the tested adsorbents. Furthermore, the obtained rate constants (k_2) were the highest for the smallest particles. This could be due to the larger amount of particles involved in the adsorption, thus enabling the metal ions to be adsorbed more quickly.

3.6. Adsorption isotherm

In addition to adsorption kinetics, isotherm studies were undertaken to simulate the metal uptake by adsorbents. Adsorption isotherm defines the relationship between the amount of adsorbate adsorbed per unit mass of adsorbent (equilibrium adsorption capacity, q_e) at constant temperature and adsorbate's concentration at equilibrium conditions (C_e). The Langmuir and the Freundlich isotherms are the most frequently used models to represent the equilibrium data of adsorption from aqueous solution.

Table 6
Kinetic parameters for Co(II) and Ni(II) adsorption on EDSG.

Particle size	Type of metal	C_0 (mg/L)	$q_{e,exp}$ (mg/g)	Pseudo-first-order			Pseudo-second-order		
				q_e (mg/g)	k_1 (1/min)	R^2	q_e (mg/g)	k_2 (g mg/min)	R^2
40–63	Co	20	8.765	4.838	0.00115	0.807	8.865	0.00113	0.999
40–63	Co	80	15.435	6.027	0.00092	0.798	15.723	0.00105	0.999
5–20	Co	80	14.600	1.760	0.00138	0.655	14.620	0.00603	1.000
63–200	Co	80	14.223	6.971	0.00092	0.827	14.265	0.00084	0.999
40–63	Ni	20	9.203	4.526	0.00115	0.703	9.285	0.00138	0.999
40–63	Ni	80	18.463	9.570	0.00138	0.851	18.657	0.00071	0.999

Table 7
Kinetic parameters for Co(II) and Ni(II) adsorption on DTSG.

Particle size	Type of metal	C_0 (mg/L)	$q_{e,exp}$ (mg/g)	Pseudo-first-order			Pseudo-second-order		
				q_e (mg/g)	k_1 (1/min)	R^2	q_e (mg/g)	k_2 (g mg/min)	R^2
40–63	Co	20	9.093	4.907	0.00115	0.930	9.174	0.00112	0.999
40–63	Co	80	15.844	6.126	0.00069	0.706	15.625	0.00103	0.998
5–20	Co	80	14.077	1.132	0.00138	0.647	14.085	0.00960	1.000
63–200	Co	80	15.322	6.497	0.00115	0.647	15.385	0.00104	1.000
40–63	Ni	20	9.167	5.335	0.00092	0.937	9.242	0.00093	0.998
40–63	Ni	80	16.199	7.328	0.00115	0.899	16.181	0.00103	0.999

3.6.1. Langmuir isotherm

The Langmuir isotherm assumes that adsorption occurs at specific homogeneous sites within the adsorbent without any interaction between the adsorbed substances [27]. The non-linear form of the Langmuir isotherm can be expressed as follows:

$$q_e = \frac{q_m K_L C_e}{1 + K_L C_e} \quad (9)$$

where q_e and C_e are the adsorption capacity (mg/g) and the equilibrium concentration of the adsorbate (mg/L) respectively, while q_m and K_L represent the maximum adsorption capacity of adsorbents (mg/g) and the energy of the adsorption (L/mg). The plot of the Langmuir isotherm is illustrated in Fig. 9, while the Langmuir constants are presented in Tables 8 and 9. In spite of having correlation coefficients higher than 0.95, Fig. 9 shows that the equilibrium data did not fit well with the Langmuir isotherm. Moreover, this model did not correspond to the experimentally obtained values of $q_{m,exp}$. This suggests that homogeneous adsorption might not have occured at the surface of the silica gel.

3.6.2. Freundlich isotherm

The Freundlich model assumes a heterogeneous adsorption surface with sites that have different energies of adsorption [27]. Its non-linear form can be represented as follows:

$$q_e = K_F C_e^{1/n_F} \quad (10)$$

where K_F and n_F are the Freundlich adsorption isotherm constants. Fig. 9 illustrates the Freundlich plot of the Co(II) adsorption, while the Freundlich constants are presented in Tables 8 and 9. The '*n*' values are higher than 1, indicating that the adsorption was favorable. Thus, the adsorption of Co(II) and Ni(II) by all types of adsorbents represents a favorable uptake. However, the Freundlich model was not representative enough to simulate the equilibrium data, as reflected by the low correlation coefficients (Tables 8 and 9).

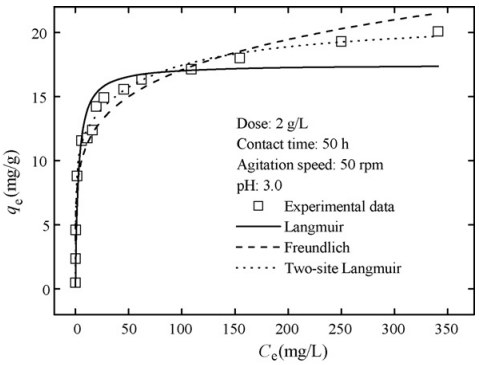

Fig. 9. Adsorption isotherms of Co(II) on EDSG.

3.6.3. Two-site Langmuir isotherm

For further modeling study, the two-site Langmuir model, which assumes that the surface contains two different active sites with different affinities toward target compounds, was also employed [28]. The model presented in Eq. (11) was plotted against the equilibrium data.

$$q_e = \frac{q_{m1} K_{L1} C_e}{1 + K_{L1} C_e} + \frac{q_{m2} K_{L2} C_e}{1 + K_{L2} C_e} \quad (11)$$

Table 8
Isotherm constants of EDSG for Co(II) and Ni(II).

Model	Particle size (μm)	Type of metal	$q_{m,exp}$ (mg/g)	q_m (mg/g)	K_L (L/mg)	n	R^2
Langmuir	5–20	Co	17.80	16.206	0.755		0.959
	40–63	Co	20.09	17.550	0.504		0.948
	63–200	Co	20.05	18.483	0.209		0.952
	63–200	Ni	19.62	18.516	0.383		0.968
Freundlich	5–20	Co	17.80		110419	5.859	0.920
	40–63	Co	20.09		30213	5.264	0.936
	63–200	Co	20.05		13997	4.978	0.935
	63–200	Ni	19.62		29874	5.195	0.892

Model	Particle size (μm)	Metal	$q_{m,exp}$ (mg/g)	q_{m1} (mg/g)	K_{L1} (L/mg)	q_{m2} (mg/g)	K_{L2} (L/mg)	R^2
Two-site Langmuir	5–20	Co	17.80	5.951	0.0198	12.501	1.395	0.998
	40–63	Co	20.09	8.935	0.0114	12.684	1.481	0.998
	63–200	Co	20.05	10.364	0.0234	10.636	1.222	0.998
	63–200	Ni	19.62	8.615	0.0394	11.747	1.209	0.996

Table 9
Isotherm constants of DTSG for Co(II) and Ni(II).

Model	Particle size (μm)	Type of metal	$q_{m,exp}$ (mg/g)	q_m (mg/g)	K_L (L/mg)	n	R^2
Langmuir	5–20	Co	14.99	14.233	3.351		0.968
	40–63	Co	16.03	15.340	0.621		0.954
	63–200	Co	15.16	14.662	1.336		0.976
	63–200	Ni	16.97	16.112	0.750		0.980
Freundlich	5–20	Co	14.99		10874378	7.716	0.847
	40–63	Co	16.03		7.344	6.268	0.887
	63–200	Co	15.16		2360844	7.134	0.827
	63–200	Ni	16.97		179497	6.075	0.871

Model	Particle size (μm)	Metal	$q_{m,exp}$ (mg/g)	q_{m1} (mg/g)	K_{L1} (L/mg)	q_{m2} (mg/g)	K_{L2} (L/mg)	R^2
Two-site Langmuir	5–20	Co	14.99	3.991	0.113	11.109	5.443	0.998
	40–63	Co	16.03	7.784	0.0562	9.364	3.176	0.999
	63–200	Co	15.16	5.326	0.113	10.167	3.401	0.996
	63–200	Ni	16.97	6.815	0.0958	9.931	2.306	0.997

Table 10
Regeneration of EDSG and DTSG for Co(II) and Ni(II) by 2 M HNO_3.

No.	Types of Adsorbent	Adsorption capacity of Co		Regeneration efficiency (%)	Adsorption capacity of Ni		Regeneration efficiency (%)
		Before regeneration (mg/g)	After regeneration (mg/g)		Before regeneration (mg/g)	After regeneration (mg/g)	
1	EDSG	9.47	9.37	98.92	9.96	9.95	99.91
3	EDSG	9.47	9.37	98.88	9.96	9.95	99.91
6	EDSG	9.47	9.37	98.87	9.96	9.95	99.92
1	DTSG	9.70	9.51	98.00	9.94	9.93	99.90
3	DTSG	9.70	9.47	97.59	9.94	9.94	99.96
6	DTSG	9.70	9.56	97.41	9.94	9.94	99.99

Fig. 9 and Tables 8 and 9 show that the two-site Langmuir model was applicable to the measured equilibrium data with a correlation coefficient of 0.99. This suggests that the active sites having a low affinity toward metal ions were APTES groups and that those with high affinity were EDTA and/or DTPA groups. The obtained K values supported this finding, considering that for both EDSG and DTSG, the other K (related to APTES groups) was smaller than the others (related to EDTA and DTPA). Furthermore, the values of q_{m2} (q_{m2} is the adsorption capacity related to EDTA and DTPA) well correlated to the experimentally obtained coverage of EDTA or DTPA groups (Table 5). This confirms the applicability of the two-site Langmuir model for the removal of Co(II) and Ni(II) by the modified silica gels.

3.7. Regeneration of spent adsorbents

To reuse the spent adsorbents, after they had become completely saturated, metal desorption from the surface of modified silica gels was conducted using 2 M HNO_3 solution. Encouraging results presented in Table 10 were obtained for different adsorbents at the same conditions (metals concentration: 250 mg/L; dose of adsorbent: 25 g/L; volume of regenerant: 0.01 L). The table indicates that HNO_3 could effectively regenerate all the adsorbents with regeneration efficiencies ranging from 98% to 100%. After the first cycle of regeneration, the adsorption capacities of the adsorbents for Co(II) and Ni(II) decreased to less than 1%. These results are relatively promising, as the spent adsorbents could be regenerated for subsequent use, thus improving their cost-effectiveness and reducing operational cost in water treatment applications.

4. Conclusions

It is evident that the EDTA- and/or the DTPA-modified silica gels were effective for Co(II) and Ni(II) removal from contaminated water. The maximum metal uptake by the EDSG was slightly higher (q_m = 20.0 mg/g for Co(II) and q_m = 21.6 mg/g for Ni(II)) than that by the DTSG (q_m = 16.1 mg/g for Co(II) and q_m = 16.7 mg/g for Ni(II)). At a lower concentration of 10 mg/L, the removal of Co(II) and Ni(II) by the modified silica gels ranged from 95% to 98%. The stability of the EDSG and the DTSG was relatively better than silica gel modified by the APTES groups. Moreover, modified silica gels could be regenerated for subsequent use with regeneration efficiencies ranging from 98% to 100%. The two-site Langmuir model was representative to simulate the adsorption isotherms, suggesting the presence of two different functional groups on the surface of modified silica gels. The kinetics of Co(II) and Ni(II) adsorption by the modified silica gels followed pseudo-second-order model.

Acknowledgments

The authors are grateful to the European Commission (Brussels) for the Marie Curie Research Fellowship for Transfer of Knowledge (No. MTKD-CT-2006-042637) and Finnish Funding Agency for Technology and Innovation (TEKES) for financial support.

References

[1] S. Babel, T.A. Kurniawan, Low-cost adsorbents for heavy metals uptake from contaminated water: a review, J. Hazard. Mater. 97 (2003) 219–243.
[2] A. Dyer, J.K. Abou-Jamous, Zeolites for nuclear waste treatment: Co, Ni and Zn uptake into synthetic faujasite X. II. Effect of the presence of large cations on the leaching of Co, Ni and Zn radioisotopes, J. Radioanal. Nucl. Chem. 224 (1997) 59–66.
[3] S. Rengaraj, S.-H. Moon, Kinetics of adsorption of Co(II) removal from water and wastewater by ion exchange resins, Water Res. 36 (2002) 1783–1793.
[4] N. Akhtar, J. Iqbal, M. Iqbal, Removal and recovery of nickel(II) from aqueous solution by loofa sponge-immobilized biomass of *Chlorella sorokiniana*: characterization studies, J. Hazard. Mater. 108 (2004) 85–94.
[5] T.G. Kazi, N. Jalbani, N. Kazi, M.B. Arain, M.K. Jamali, H.I. Afridi, G.A. Kandhro, A.S. Raja, A.Q. Shah, R. Ansari, Estimation of toxic metals in scalp hair samples of chronic kidney patient, Biol. Trace Elem. Res. 125 (2009) 16–27.
[6] T.G. Kazi, N. Jalbani, N. Kazi, M.K. Jamali, M.B. Arain, H.I. Afridi, G.A. Kandhro, Z. Pirzado, Evaluation of toxic metals in blood ad urine samples of chronic renal failure patients, before and after dialysis, Ren. Fail. 30 (2008) 737–745.
[7] G. Crini, Recent developments in polysaccharide-based materials used as adsorbents in. wastewater treatment, Prog. Polym. Sci. 30 (2005) 38–70.
[8] P.K. Jal, S. Patel, B.K. Mishra, Chemical modification of silica surface by immobilization of functional groups for extractive concentration of metal ions, Talanta 62 (2004) 1005–1028.
[9] K. Sharma, S. Mittal, M. Koel, Analysis of trace amounts of metal ions using silica-based chelating resins: a green analytical method, Crit. Rev. Anal. Chem. 33 (3) (2003) 183–198.
[10] T. Seshadri, A. Kettrupt, Synthesis and characterization of silica gel ion-exchanger bearing 2-amino-1-cyclopentene-1-dithio-carboxylic acid (ACDA) as chelating compound, Fresen. Z. Anal. Chem. 310 (1982) 1–5.
[11] D.E. Leyden, G.H. Luttrell, Preconcentration of trace metals using chelating groups immobilized via silylation, Anal. Chem. 47 (1975) 1612–1617.
[12] M. Tülü, K.E. Geckeler, Synthesis and properties of hydrophilic polymers. Part 7. Preparation, characterization and metal complexation of carboxy-functional polyesters based on poly (ethylene glycol), Polym. Int. 48 (1999) 909–914.
[13] Y. Shiraishi, G. Nishimura, T. Hirai, I. Komasawa, Separation of transition metals using inorganic adsorbents modified with chelating ligands, Ind. Eng. Chem. Res. 41 (2002) 5065–5070.
[14] M. Hughes, E. Rosenberg, Characterization and applications of poly-acetate modified silica polyamine composites, Sep. Sci. Technol. 42 (2007) 261–283.
[15] Standard Methods for the Examination of Water and Wastewater, 21st ed., American Public Health Association, Washington DC (US), 2005.
[16] S. Nagib, K. Inoue, T. Yamaguchi, T. Tamaru, Recovery of Ni from a large excess of Al generated from spent hydrodesulfurization catalyst using picolylamine type chelating resin and complexane types of chemically modified chitosan, Hydrometallurgy 51 (1999) 73–85.
[17] K. Inoue, K. Yoshizuka, K. Ohto, Adsorptive separation of some metal ions by complexing agent types of chemically modified chitosan, Anal. Chim. Acta 388 (1999) 209–218.
[18] Z. Reddad, C. Gerente, Y. Andres, P. Le Cloirec, Adsorption of several metal ions onto a low-cost biosorbent: kinetic and equilibrium studies, Environ. Sci. Technol. 36 (2002) 2067–2070.
[19] M. Etienne, A. Walcarius, Analytical investigation of the chemical reactivity and stability of aminopropyl-grafted silica in aqueous medium, Talanta 59 (2003) 1173–1188.
[20] A.E. Martell, R.M. Smith, Critical Stability Constants, vol. 1. Amino acids, Plenum Press, New York, 1974.
[21] A.E. Martell, R.M. Smith, R.J. Motekaitis, NIST Critically Selected Stability Constants of Metal Complexes database Version 3.0, Texas A&M, Texas, 1997.
[22] J.P. Gustafsson, Visual MINTEQ ver 2.53, 2007.
[23] J.C. Westall, J.L. Zacahri, F.M.M. Morel, MINEQL: A Computer Programme for the Calculation of Chemical Equilibrium Composition of Aqueous Systems, Technical Note No. 18, Massachusetts Institute of Technology, Cambridge, MA, 1976.

[24] B. Nowack, L.J. Sigg, Adsorption of EDTA and metal–EDTA complexes onto goethite, Colloids Int. Sci. 177 (1996) 106–121.
[25] J. Yang, J. Peng, J. Jia, H. Fang, Adsorption of carbon disulfide (CS_2) in water by different types of activated carbon—equilibrium, dynamics, and mathematical modeling, J. Environ. Eng. 133 (2007) 294–302.
[26] G. McKay, Y.S. Ho, The sorption of lead ions on peat, Water Res. 33 (1999) 578–584.
[27] S.J. Allen, G. Mckay, J.F. Porter, Adsorption isotherm models for basic dye adsorption by peat in single and binary component systems, J. Colloids Interface Sci. 280 (2004) 322–333.
[28] K.G. Karthikeyan, M.A. Tshabalala, D. Wang, M. Kalbasi, Solution chemistry effects on orthophosphate adsorption by cationized solid wood residues, Environ. Sci. Technol. 38 (2004) 904–911.

Paper II

Adsorption of Co(II) and Ni(II) by EDTA- and/or DTPA-modified chitosan: Kinetic and equilibrium modelling

Eveliina Repo, Jolanta K. Warchol, Tonni Agustiono Kurniawan, Mika E.T. Sillanpää

Chemical Engineering Journal 161 (2010) 73–82

Chemical Engineering Journal 161 (2010) 73–82

Contents lists available at ScienceDirect

Chemical Engineering Journal

journal homepage: www.elsevier.com/locate/cej

Adsorption of Co(II) and Ni(II) by EDTA- and/or DTPA-modified chitosan: Kinetic and equilibrium modeling

Eveliina Repo[a,*], Jolanta K. Warchol[c], Tonni Agustiono Kurniawan[a,1], Mika E.T. Sillanpää[a,b,1]

[a] Laboratory of Applied Environmental Chemistry (LAEC), The University of Eastern Finland, Patteristonkatu 1, FI-50100 Mikkeli, Finland
[b] Faculty of Technology, Lappeenranta University of Technology, Patteristonkatu 1, FI-50100 Mikkeli, Finland
[c] Rzeszów University of Technology, Department of Water Purification and Protection, 6 Powstanïców Warszawy Street, 35-959 Rzeszów, Poland

ARTICLE INFO

Article history:
Received 10 February 2010
Received in revised form 14 April 2010
Accepted 15 April 2010

Keywords:
Modified chitosan
Adsorption isotherm
Metal removal
EDTA
DTPA
Binary system

ABSTRACT

The aim of the present study was to investigate the adsorption properties of surface modified chitosans in the aqueous solutions containing Co(II) and/or Ni(II) ions. For this purpose, the ligands of ethylenediaminetetraacetic acid (EDTA) or diethylenetriaminepentaacetic acid (DTPA) were immobilized onto polymer matrices of chitosan. Adsorption of Co(II) and Ni(II) by prepared adsorbents was investigated in batch techniques. The effects of pH, functional group, contact time, and the concentration of metals were studied. Metal uptake by EDTA-chitosan was 63.0 mg g^{-1} for Co(II) and 71.0 mg g^{-1} for Ni(II) and by DTPA-chitosan 49.1 mg g^{-1} for Co(II) and 53.1 mg g^{-1} for Ni(II). The adsorption efficiency of studied adsorbents ranged from 93.6% to 99.5% from 100 mg L^{-1} Co(II) and/or Ni(II) solution, when the adsorbent dose was 2 g L^{-1} and solution pH 2.1. The kinetics of Co(II) and Ni(II) on both of the modified chitosans followed the pseudo-second-order model but the adsorption rate was also influenced by intraparticle diffusion. The equilibrium data was best described by the Sips isotherm and its extended form was also well fitted to the two-component data obtained for systems containing different ratios of Co(II) and Ni(II). Nevertheless, the obtained modeling results indicated relatively homogenous system for Co(II) and heterogeneous system for Ni(II) adsorption.

1. Introduction

The increasing level of toxic metals such as Co(II) and Ni(II) that are discharged into the environment as industrial wastes, represent a serious threat to human health, living resources, and ecological systems [1]. Co(II) is present in the wastewater of nuclear power plants and many other industries such as mining, metallurgical, electroplating, paints, pigments, and electro-engineering [2]. Ni(II) is widely used in silver refineries, electroplating, zinc base casting, and storage battery industries [3].

Various technologies have been applied to remove Co(II) and Ni(II) from waste streams. These include chemical precipitation [4], chemical oxidation/reduction [5], and electrochemical treatment [6]. However, all of the above methods have disadvantages making them less technically appealing in wastewater treatment. Precipitation is ineffective and produces a lot of sludge, chemical reduction/oxidation requires extra chemicals and electrochemical treatment has high operating costs [7,8].

One of the most effective methods for the removal of Co(II) and Ni(II) from wastewater streams is adsorption. Activated carbon has been the most popular material in wastewater treatment for heavy metal removal. However, the high cost of this material makes its application less economically attractive in industrial scale [9]. Cation-exchange resins used for Co(II) and Ni(II) removal can produce treated effluents that contain metals less than the required discharge limits [10]. However, commercial resins remain expensive materials [7]. To reduce the operational costs, the search for alternative adsorbents has intensified in recent years. For example, natural bentonite [2], orange peel [11], chitosan [12–15], and anaerobic granular sludges [16,17] have been tested for heavy metal removal. However, these materials have usually low adsorption capacities in as-received forms. To improve their performance, non-conventional materials such as chitosan needs to be modified chemically.

Due to the reactivity of amine groups and stable chelation, chitosan can be functionalized to improve its adsorption properties [15]. Chemical modification of chitosan with chelating agents such as ethylenediaminetetraacetic acid (EDTA) and diethylenetriaminepentaacetic acid (DTPA), which form very strong chelates with metal ions [18,19] may produce adsorbents with excellent metal binding properties. The environmental fate of these chelating agents has received attention, but, when immobilized, EDTA and

* Corresponding author. Tel.: +358 15 355 3707; fax: +358 15 355 6363.
E-mail address: eveliina.repo@uef.fi (E. Repo).
[1] Tel.: +358 15 355 3707; fax: +358 15 355 6363.

1385-8947/$ – see front matter © 2010 Elsevier B.V. All rights reserved.
doi:10.1016/j.cej.2010.04.030

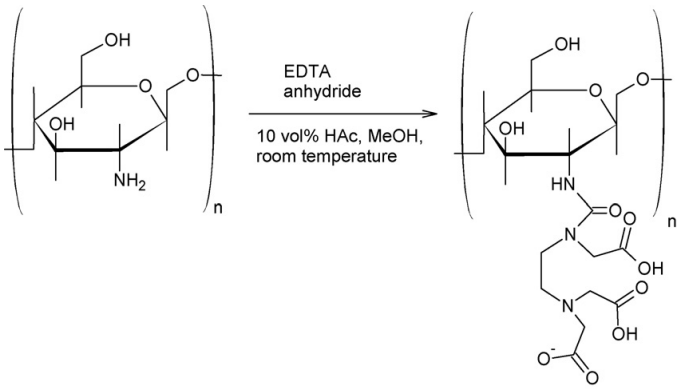

Fig. 1. Synthesis of EDTA-chitosan.

DTPA are not expected to be environmentally critical compounds [20]. Inoue et al. studied quite extensively adsorption of metals such as Cd, Fe, Cu, Ni, Co, and Zn by EDTA- and DTPA-chitosans [21,22]. However, their work lacked of simulation modeling of adsorption kinetics and isotherms of the adsorbents as well as adsorption mechanism and regeneration studies. Therefore, the aim of this study was to investigate the adsorption properties of these promising materials in more detail.

In the previous study, we investigated the applicability of EDTA- and/or DTPA-modified silica gels to remove Co(II) and Ni(II) from contaminated water at optimized conditions [23]. In this work, EDTA- and DTPA-chitosans were used to adsorb Co(II) and Ni(II) from aqueous solutions. The effects of variables including the type of chelating agent, metal concentration, and pH on the adsorption capacity, selectivity and desorption properties of the modified chitosan were considered. To investigate the mechanism of adsorption the gathered experimental data was fitted to kinetic and equilibrium models. Furthermore, equilibrium behavior of modified chitosans was investigated in Co(II)/Ni(II) two-component systems and obtained data modeled using binary isotherm selected based on the modeling results of one-component systems.

2. Methods

2.1. Materials

Chitosan flakes >85% deacetylated supplied by Sigma–Aldrich had molecular weight ranging from 190,000 to 375,000 g mol^{-1} and viscosity of 200–2000 MPa. All other chemicals used in this study were of analytical grade and supplied by Merck (Finland). Stock solutions of 1000 mg L^{-1} were prepared by dissolving appropriate amounts of Co(II) and Ni(II) nitrate salts in double deionized water. Working solutions ranging from 1 to 200 mg L^{-1} of Co(II) or Ni(II) were prepared by diluting the stock solutions. Adjustment of pH was carried out using 0.1 M NaOH and 0.1 M HNO_3.

2.2. Synthesis of EDTA- and/or DTPA-modified chitosan

To improve its reactivity, chitosan was functionalized with EDTA and/or DTPA according to Nagib et al. [22] (Fig. 1). About 10 g of chitosan was dissolved in 200 mL of 10% (v/v) acetic acid and then diluted five times with methanol. Afterwards, approximately 60 g of EDTA anhydride synthesized according to Tülü and Geckeler [24] suspended in methanol was added and the mixture was stirred vigorously for 24 h in room temperature. After filtration the precipitation was mixed with ethanol (AA) and subsequently stirred for another 16 h. Then the precipitation was washed with NaOH solution (pH 11) to remove unreacted EDTA. Finally, EDTA-modified chitosan was washed with deionized water, 0.1 M HCl, again deionized water, and ethanol. The final product was dried in an oven at 40 °C for 48 h and stored in a desiccator. Using the same method, the chitosan was functionalized with DTPA.

2.3. Characterization of modified chitosans

The formation of additional functional groups on chitosan surface after modification with EDTA and/or DTPA was studied using a FTIR-spectroscope type Nicolet Nexus 8700 (USA). Kjeldahl method was employed to determine the amount of nitrogen in the modified chitosans [25] and the results were used to determine the surface coverage of EDTA and DTPA on the adsorbents. The specific surface area and total pore volume of modified chitosans were measured with Autosorb-1-C surface area and pore size analyzer (Quantachrome, the UK).

2.4. Batch adsorption tests

Applicability of modified chitosans for Co(II) and Ni(II) removal was studied using batch experiments in a reaction mixture of 0.01 g of adsorbent and 0.005 L of metal solution containing Co^{2+} and/or Ni^{2} at concentrations ranging from 1 to 200 mg L^{-1}. To study adsorption equilibrium in binary systems, solutions containing Co(II) and Ni(II) at ratios of 1:1, 2:1, and 1:2, where total concentration of metals varied from 1 to 500 mg L^{-1}, were used. The effect of pH was studied at metal concentration of 100 mg L^{-1} in the pH range of 1–7. Alkalic solutions were not used to avoid the hydroxide formation (Visual MINTEQ ver. 2.53). The effect of contact time was studied at metal concentrations of 20 and 100 mg L^{-1}. Agitation was undertaken using a rotary shaker type ST5 (CAT M.Zipperer GmbH, Staufen, Germany). At designated contact time, the adsorbent was separated from the solution using 0.45 μm polypropylene syringe filter. After dilution with 2% HNO_3, the metal concentrations in the filtrates were analyzed by an inductively coupled plasma optical atomic emission spectrometry (ICP-OES) model iCAP 6300 (Thermo Electron Corporation, USA). Co(II) was analyzed at a wavelength of 228.616 nm, while Ni(II) was detected at 231.605 nm. The detection limits for Co(II) and Ni(II) were 0.4 and 0.8 μg L^{-1}, respectively. The adsorption capacities (mg g^{-1}) of modified chitosans were calculated as follows:

$$q_e = \frac{C_i - C_e}{M} V \quad (1)$$

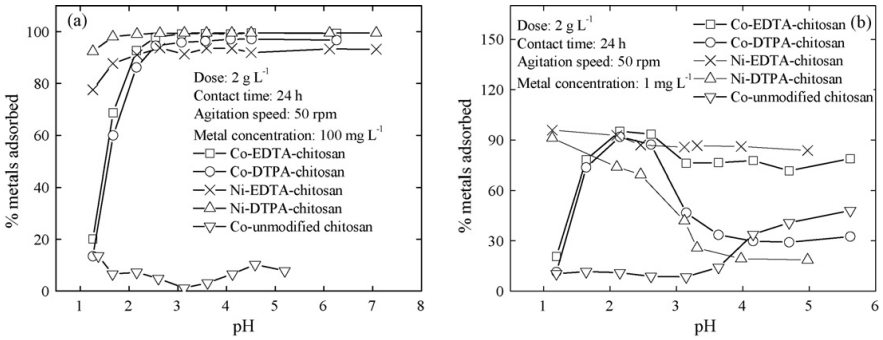

Fig. 2. Effects of pH on adsorption of Co(II) and Ni(II) by unmodified and modified chitosans.

where C_i and C_e are the initial and the equilibrium concentrations, respectively (mg L^{-1}), while M (g) and V (L) represent the weight of the adsorbent and the volume of the solution, respectively.

2.5. Regeneration studies

To evaluate their reusability, regeneration of the spent adsorbents were performed in acidic conditions. At first adsorbents were loaded by metal ions by mixing around 0.08 g of the adsorbent with 0.02 L of 100 mg L^{-1} Co(II) or Ni(II) solution. Regeneration studies were performed using higher dose to make separation procedure easier. After attaining equilibrium, the spent adsorbent was separated from the solution by centrifuge. Metal ions were eluted using 2 M HNO_3. The regeneration efficiency (%RE) of the adsorbent was calculated using Eq. (2):

$$\%\,\mathrm{RE} = \frac{q_r}{q_0} \times 100 \quad (2)$$

where q_0 and q_r are the adsorption capacities of the adsorbents (mg g^{-1}) before and after regeneration, respectively.

2.6. Statistical analysis

All the experiments were conducted in duplicate under identical conditions. The coefficient of variation was mostly less than 1%. If the variation of the metal removal by the adsorbent exceeded 5%, an identical run was undertaken and the closer data point used. To determine the margin of error, a confidence interval of 95% was calculated for each set of the samples using Origin software version 8.0 (Microcal Software, Inc.). The obtained data were then analyzed using t-test and/or ANOVA test. Differences were considered statistically significant when $p \leq 0.05$ for the analysis of variance (ANOVA) or t-tests.

3. Results and discussion

3.1. Characterization of modified chitosans

The presence of additional functional groups on the surface of modified chitosans was studied using FTIR spectroscopy. Absorption peaks of the carbonyl groups of amides and carboxylic groups were observed at 1629 and 1729 cm^{-1}, respectively [22]. Surface coverage of EDTA and DTPA was calculated based on the difference between the amount of nitrogen in unmodified (42.1 g kg^{-1}) and modified chitosans (81.2 and 82.6 g kg^{-1}) obtained from elemental analysis. Coverages were 1.4 and 0.96 mmol g^{-1} for EDTA- and DTPA-modified chitosan, respectively. These values are considerable lower than those presented by Nagib et al. [22] (around 5.9 and 1.3 mmol g^{-1} for EDTA- and DTPA-functionalized chitosan). This is probably due to the different type of chitosan used in synthesis. However, the surface concentrations obtained in this study were well correlated to the amount of metals adsorbed (see Section 3.2.2), which supports the results of elemental analysis.

The specific surface area and the total pore volume of the EDTA-chitosan were $0.71 \pm 0.09\ m^2\ g^{-1}$ and $1.76 \pm 0.09 \times 10^{-3}\ cm^3\ g^{-1}$, respectively. For DTPA-chitosan substantially lower values were obtained ($0.36 \pm 0.06\ m^2\ g^{-1}$ and $0.74 \pm 0.05 \times 10^{-3}\ cm^3\ g^{-1}$). These results suggested that DTPA formed crosslinks between the amino groups of chitosan moieties more effectively than EDTA thus reducing the surface area and the total pore volume of modified adsorbent. Furthermore, the specific surface area and the total pore volume of the unmodified chitosan were $5.9 \pm 0.1\ m^2\ g^{-1}$ and $11.8 \pm 0.1 \times 10^{-3}\ cm^3\ g^{-1}$, respectively, indicating that the surface modification reduced significantly the area and pore sizes.

3.2. Pertinent factors affecting on the removal of Co(II) and Ni(II) by modified chitosans

3.2.1. Effects of pH

In adsorption, pH affects protonation of surface groups and speciation of metal ions in the solution. Therefore, optimal pH needs to be determined to maximize the removal of target metals. Fig. 2a shows the adsorption performance of chitosan materials as a function of pH. At high initial concentration metal removal increased only when pH changed from 1 to 2.5 reaching an asymptotic value (Fig. 2a) and at low initial concentration it reached a maximum at pH around 2.1 for Co(II) and at 1.1 for Ni(II) (Fig. 2b). pH 2.1 was selected for further experiments because the adsorption at pH as low as 1.1 was not effective at high initial concentration.

It is worthwhile to consider more carefully the effect of pH at low metal concentrations because in 1 mg L^{-1} metal solution a quite significant decrease of adsorption efficiency as a function of pH was observed for DTPA-chitosan (Fig. 2b). This could be due to the speciation of DTPA. Calculations with MINEQL software (Visual MINTEQ ver. 2.53) show that the dominant forms of DTPA at pH 3 to pH 5 are H_3DTPA^{-2} and H_2DTPA^{-3}. Negatively charged carboxyl groups may interact with positively charged surface amino groups and therefore crosslink with surface before bind metal ions that are found a relatively small amount in the solution. At higher metal concentrations chelation of metals is fast and crosslinking do not occur in the same extent as at lower metal concentrations (Fig. 2a). For EDTA-chitosan crosslinking is less effective most likely due to the fact that EDTA molecule is shorter. Therefore, a drop of adsorption efficiency as a function of pH at low metal concentrations is not significant in the case of EDTA-chitosan.

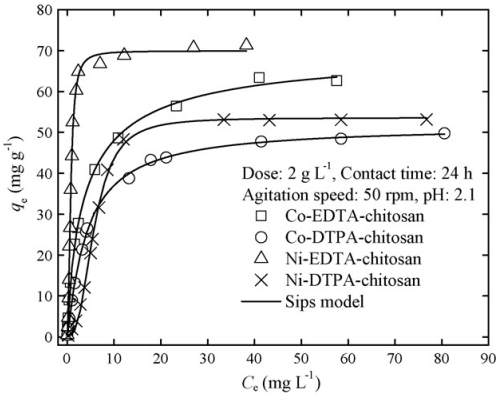

Fig. 3. Adsorption isotherms for Co(II) and Ni(II) adsorption by modified chitosans.

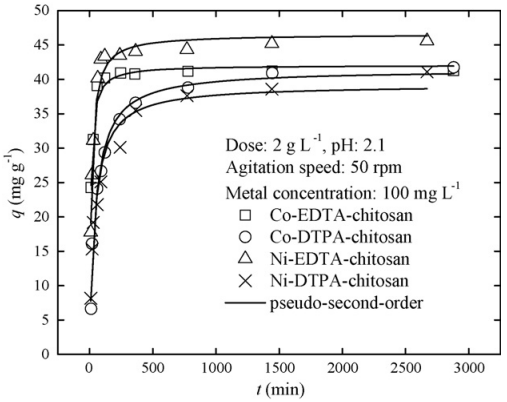

Fig. 4. Effect of contact time on Co(II) and Ni(II) adsorption by modified chitosans.

Finally, Fig. 2a shows that the removal of Ni(II) occurred at lower pH than adsorption of Co(II), which is in agreement with the earlier studies [23,26]. These results indicated that at low pH region EDTA- and DTPA-functionalized chitosans could be used for specific adsorption of Ni(II) in the presence of Co(II) (Section 3.5.3).

3.2.2. Effects of functional group

Fig. 2 shows that chemical modification of chitosan improved remarkably its adsorption performance. The removal of Co(II) by unmodified chitosan at 100 mg L^{-1} of initial concentration was only 5%, while EDTA- and DTPA-modified chitosan could almost completely remove the metal at the same operational conditions. As presented in Fig. 3, the maximum adsorption capacities of Co(II) and Ni(II) by EDTA-chitosan were 63.0 and 71.0 mg g^{-1} and by DTPA-chitosan 49.1 and 53.1 mg g^{-1}, respectively. Using the surface coverages of EDTA and DTPA, it was calculated that 72–86% of EDTA surface groups and 89–94% of DTPA surface groups were occupied by metal ions. The reason for unoccupied surface groups is most likely the crosslinking effect making some of the functionalities unable for metal binding.

In 100 mg L^{-1} metal solution the adsorption efficiency of EDTA-modified chitosan (dose: 2 g L^{-1}) was 99.2% for Co(II) and 99.5% for Ni(II). The same dose of DTPA-chitosan removed 96.7% of Co(II) and 93.6% of Ni(II) at the similar operational conditions. A higher metal removal by EDTA-chitosan could be attributed to a crosslinked structure of DTPA-chitosan (Inoue et al. [21], Section 3.1) and lower surface coverage of DTPA compared to EDTA. In addition, the higher maximum adsorption capacity of Ni(II) compared to that of Co(II) by both adsorbents was probably due to the higher stability constants of Ni(II) chelates (log K = 18.52 for EDTA and log K = 20.17 for DTPA) compared to the corresponding Co(II) chelates (log K = 16.26 for EDTA and log K = 19.15 for DTPA) [27].

In another study, Nagib et al. [22] obtained twice higher adsorption capacities for Ni(II) for both EDTA- and DTPA-functionalized chitosans. This may be due to the fact that chitosan raw materials used were different. However, the modified chitosans in this study demonstrated substantially higher adsorption capacities than similarly functionalized silica gels [23] or silica polyaminocomposites [28]. More importantly, EDTA- and DTPA-functionalized chitosans were effective adsorbents at pH ranging from 2 to 3 suggesting that they could be used in the treatment of acidic wastewater for example from electroplating industry [11].

3.2.3. Effects of contact time

The effects of contact time on the removal of Co(II) and Ni(II) by EDTA- and DTPA-modified chitosan are depicted in Fig. 4. Initially the metal uptake was fast due to the many vacant adsorption sites. For EDTA-chitosan, all the active sites were occupied by target metals within 4 h after which the adsorption rate gradually decreased and became constant at equilibrium. However, Fig. 4 shows that DTPA-chitosan needed 12 h to attain equilibrium conditions where the concentration of adsorbate in the bulk solution was in dynamic balance with that at the interface. It is possible that some of the adsorption sites of DTPA-chitosan were not as easily obtained as others due to the crosslinking (see Section 3.1). This was also seen from the slower kinetics of metal adsorption by DTPA-chitosan compared to that of EDTA-chitosan (Section 3.5.1). Due to the differences between EDTA- and DTPA-chitosans and the small increase of the adsorption capacity after 12 h of

Table 1
Regeneration of EDTA- and DTPA-chitosan for Co(II) and Ni(II) by 2 M HNO_3.

Type of adsorbent	No. of cycles	Adsorption capacity of Co(II)		Regeneration efficiency (%)	Adsorption capacity of Ni(II)		Regeneration efficiency (%)
		Before regeneration (mg g^{-1})	After regeneration (mg g^{-1})		Before regeneration (mg g^{-1})	After regeneration (mg g^{-1})	
EDTA-chitosan	1	22.96	22.66	98.73	24.35	24.34	99.99
	3	22.96	22.70	98.91	24.35	24.17	99.23
	6	22.96	22.83	99.46	24.35	24.34	99.96
	10	22.96	22.73	99.01	24.35	24.33	99.94
DTPA-chitosan	1	22.71	22.18	97.64	24.16	24.07	99.59
	3	22.71	22.49	99.02	24.16	24.10	99.73
	6	22.71	22.59	99.48	24.16	24.16	99.96
	10	22.71	22.63	99.64	24.16	24.07	99.60

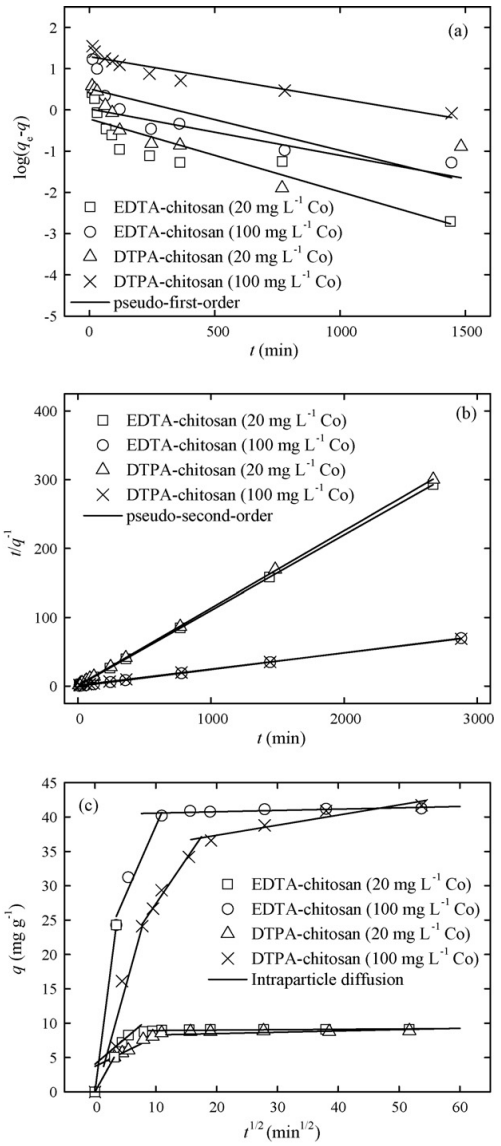

Fig. 5. Kinetic modeling of Co(II) adsorption by modified chitosans. pH: 2.1, dose: 2 g L^{-1}, and agitation speed: 50 rpm.

mixing, contact time of 24 h was selected for all the equilibrium tests.

3.3. Adsorption mechanism

On the basis of thermodynamic data [29], EDTA is represented by various species of general formula H_nEDTA^{n-4} where n ranges from 0 to 5. The calculation using the MINEQL software showed that negatively charged H_3EDTA^- (41%) and uncharged H_4EDTA (35%) were the predominant species at pH 2.1, where most of the experiments were conducted. Based on this, it is proposed that the metal removal by the modified chitosans could be presented as follows [23]:

$$RH_iEDTA^{i-3} + M^{2+} \rightleftarrows M(RHEDTA) + (i-1)H^+ \quad (3)$$

where R represents the chitosan and i is the number of hydrogen ions complexed with EDTA ranging from 2 to 3, while M^{2+} is a metal ion.

According to the above mechanism at least one proton should be released into the solution upon metal binding. However, experimentally observed amount of released protons was only half of expected against every adsorbed metal ion. This indicated that some of the protons were also bound to the surface and following protonation mechanism of free amino groups was suggested:

$$RNH_2 + H^+ \rightleftarrows RNH_3{}^+ \quad (4)$$

A protonation constant ($\log K_p$) of above reaction is 6.3 [30] indicating that all of the free amino groups were protonated at pH 2.1. This explains the observation that the pH did not decrease during the adsorption as much it was expected based on the reaction (3).

From the above and characterization of the modified chitosans, it was found that the chitosan surface contained some free amino groups after synthesis. Therefore, a part of the metal ions could bind on the surface also via amino groups. Earlier it has been presented that two OH groups and one amino group of chitosan are grabbed by metal ion and rest of the coordination sites are occupied by water molecules [30]:

$$RNH_2 + M^{2+} \rightleftarrows M(RNH_2)^{2+} \quad (5)$$

However, the metal binding by surface amino groups was probably highly inhibited at pH 2.1 due to the competition of protons (Eq. (4)) as could be seen in the case of unmodified chitosan (Fig. 2 [26]). Therefore, it is suggested that the metal binding occurred mainly via surface chelation by EDTA and DTPA groups. This was also supported by the similar amount of metals adsorbed vs. the amount of chelating surface groups.

3.4. Regeneration studies

Regeneration of the spent adsorbent is necessary to restore its original adsorption capacity and it enables valuable metals to be recovered from wastewater streams for reuse. In this study, Co(II) and Ni(II) were desorbed from EDTA- and DTPA-chitosans using 2 M HNO_3. Table 1 suggests that the regeneration efficiency of both adsorbents was almost complete for both metals. These results indicate the suitability of HNO_3 as the regenerant for both adsorbents. It should also be noticed that unmodified chitosan is not stable in 2 M HNO_3 [13,14]. Therefore, it seems that the modification of chitosan with EDTA and/or DTPA stabilized chitosan to resist acidic regenerant.

3.5. Simulative modeling of adsorption data

3.5.1. Modeling of adsorption kinetics

Modeling of adsorption kinetics was conducted by using the pseudo-first-order and pseudo-second-order models. These originally empirical models have been used extensively to describe the sorption kinetics. Recently, also theoretical backgrounds for these models have been studied by Azizian [31] using the classical Theory of Activated Adsorption/Desorption and Rudzinski and Plazinski [32,33] using the Statistical Rate Theory. The pseudo-first-order model is expressed as [34]:

$$\log(q_e - q_t) = \log(q_e) - \frac{k_1}{2.303}t \quad (6)$$

Table 2
Pseudo-first-order, pseudo-second-order, and intraparticle diffusion model parameters for Co(II) and Ni(II) adsorption by modified chitosans.

		EDTA-chitosan				DTPA-chitosan			
Metal	C_0 (mg L^{-1})	$q_{e,exp}$ (mg g^{-1})	q_e (mg g^{-1})	k_1 (min^{-1})	R^2	$q_{e,exp}$ (mg g^{-1})	q_e (mg g^{-1})	k_1 (min^{-1})	R^2
Pseudo-first-order									
Co(II)	20	9.12	0.61	0.0041	0.787	8.89	2.10	0.0714	0.893
	100	41.25	3.25	0.00346	0.703	41.73	14.49	0.00115	0.733
Ni(II)	20	9.48	0.69	0.00253	0.607	7.77	2.83	0.00276	0.847
	100	45.59	7.59	0.00230	0.631	42.23	19.91	0.00115	0.887

		EDTA-chitosan				DTPA-chitosan			
Metal	C_0 (mg L^{-1})	$q_{e,exp}$ (mg g^{-1})	q_e (mg g^{-1})	k_2 (g mg^{-1} min^{-1})	R^2	$q_{e,exp}$ (mg g^{-1})	q_e (mg g^{-1})	k_2 (g mg^{-1} min^{-1})	R^2
Pseudo-second-order									
Co(II)	20	9.12	9.12	0.0338	1.000	8.89	8.90	0.0125	0.999
	100	41.25	41.32	0.00459	1.000	41.73	42.37	0.00044	0.999
Ni(II)	20	9.48	9.49	0.02539	1.000	7.77	7.83	0.00390	0.999
	100	45.59	45.66	0.00171	1.000	42.23	42.37	0.00036	0.998

		EDTA-chitosan			DTPA-chitosan		
Metal	C_0 (mg L^{-1})	$k_{id,1}$ (mg g^{-1} min$^{-1/2}$)	$k_{id,2}$ (mg g^{-1} min$^{-1/2}$)	$k_{id,3}$ (mg g^{-1} min$^{-1/2}$)	$k_{id,1}$ (mg g^{-1} min$^{-1/2}$)	$k_{id,2}$ (mg g^{-1} min$^{-1/2}$)	$k_{id,3}$ (mg g^{-1} min$^{-1/2}$)
Intraparticle diffusion model							
Co(II)	20	2.043	0.751	0.0059	1.594	0.433	0.035
	100	6.933	3.438	0.019	3.196	1.105	0.147
Ni(II)	20	1.723	1.390	0.0048	0.828	0.196	0.023
	100	5.626	4.494	0.058	3.309	1.008	0.198

The pseudo-second-order rate equation is:

$$\frac{t}{q_t} = \frac{1}{k_2 q_e^2} + \frac{1}{q_e} t \tag{7}$$

where q_t and q_e (mg/g) are the adsorption capacity at time t and at equilibrium, respectively, while k_1 (min^{-1}) and k_2 (g mg^{-1} min^{-1}) are the pseudo-first-order and pseudo-second-order rate constants. Fig. 5a and Table 2 indicate that pseudo-first-order model was not representative to describe the experimental data. This could be due to the fact that pseudo-first-order model is generally applicable only at initial stage of adsorption [34,35]. However, according to Table 2, it is evident that the pseudo-second-order model (Eq. (7)) gave the best fit to the experimental data since $q_{e,exp}$ and $q_{e,model}$ were very close to each other. Thus, the main process resistance could be related to the kinetics of the sorption process [34]. Furthermore, according to the Azizian's theory [31], the sorption fits better to the pseudo-second-order model than to the first-order model when the initial concentration of the adsorbate is not excessively high, which was also the case in this study. The values of the pseudo-second-order rate constants showed faster adsorption kinetics for EDTA-chitosan compared to DTPA-chitosan.

The above theory considers kinetics governed by the rates of the surface reactions. Furthermore, to investigate if film or pore diffusion was the controlling step in the adsorption, a model of intraparticle diffusion was tested as follows:

$$q = k_{id} t^{1/2} + C \tag{8}$$

where k_{id} (mg g^{-1} min$^{-1/2}$) is the rate constant of intraparticle diffusion and C (mg g^{-1}) represents the thickness of the boundary layer. More than one linear portion in the plot of adsorption capacity vs. square root of time (Fig. 5c) indicated that the adsorption of metals by modified chitosans occurred via several steps. The first portion with steep slope represented external surface adsorption or instantaneous adsorption stage. The second portion was the gradual adsorption stage (diffusion in mesopores), where the intraparticle diffusion was rate-controlled. In the third portion (diffusion in micropores) the intraparticle diffusion started to slow down due to the low metal concentration in solution [36].

The values of intraparticle diffusion rate constants: $k_{id,1}$, $k_{id,2}$ and $k_{id,3}$ are given in Table 2. The first two rate constants were higher for EDTA-chitosan than for DTPA-chitosan indicating the faster adsorption processes for EDTA-chitosan both from the bulk phase to the exterior surface of adsorbent and inside the mesopores. The last rate constants were close to zero for EDTA-chitosan supposing the attained equilibrium state. For DTPA-chitosan no plateau was seen indicating the diffusion processes in micropores, which also seemed to be the rate controlling step [36]. Furthermore, Table 2 shows that the rate constant increased as a function of the initial concentration of metal in all three portions. This can be explained by the fact that the intraparticle diffusion model was developed based on the Fick's Law, which states that a rise in the concentration gradient increases the diffusion rate.

Based on the kinetic modeling it was suggested that both intraparticle diffusion and metal binding by the surface ligands affected the metal adsorption by the two adsorbents. Pore diffusion was not the only step that controlled the removal of the metals at the initial stage of the adsorption. This indicated that the external resistance to mass transfer was significant at the early stage of adsorption [37].

3.5.2. Modeling adsorption isotherms for one-component systems

Adsorption isotherms represent the adsorption capacity of the adsorbent as a function of adsorbate concentration in the solution at equilibrium conditions. Langmuir, Freundlich, and their combination Sips model were chosen for equilibrium calculations since they are commonly used in description of liquid–solid systems [38]. Modeling calculations were conducted using Origin software version 8.0 (Microcal Software, Inc.) by means of a nonlinear regression method based on the Levenberg–Marquardt algorithm. Isotherm parameters were determined by minimizing the Sum of the Squares of the Errors (ERRSQ) function across the concentration range studied:

$$\sum_{i=1}^{p} (q_{e,exp} - q_{e,calc})^2 \tag{9}$$

The Langmuir model assumes a monolayer adsorption on a homogenous surface where the binding sites have the same adsorp-

Table 3
Isotherm parameters and error analysis for modeling one-component systems by using the Langmuir and Freundlich models.

Model	Material	Type of metal	$q_{m,exp}$ (mg g^{-1})	q_m (mg g^{-1})	$K_{L/F}$ (L mg^{-1})	n	Chi^2	R^2
Langmuir	EDTA-chitosan	Co(II)	63.0	65.466	0.316		2.443	0.996
		Ni(II)	71.0	77.073	1.066		46.444	0.941
	DTPA-chitosan	Co(II)	49.1	52.866	0.222		0.447	0.999
		Ni(II)	53.1	64.139	0.116		37.027	0.924
Freundlich	EDTA-chitosan	Co(II)	63.0		9610.562	3.105	30.7223	0.947
		Ni(II)	71.0		1029074	3.930	219.166	0.720
	DTPA-chitosan	Co(II)	49.1		4878.553	3.180	32.997	0.911
		Ni(II)	53.1		668.906	2.617	93.637	0.808

tion affinity and no interactions between adsorbates are considered [38,39]:

$$q_e = \frac{q_m K_L C_e}{1 + K_L C_e} \tag{10}$$

where q_e (mg g^{-1}) and C_e (mg L^{-1}) are the adsorption capacity and the equilibrium concentration of the adsorbate, respectively, q_m (mg g^{-1}) is the maximum adsorption capacity of adsorbents, while K_L (L mg^{-1}) represents the energy of the adsorption. Fig. 3 shows that the Langmuir model correlated quite well with the experimental data for Co(II) adsorption but not that for Ni(II). For both adsorbents, the Langmuir model gave a better estimate of the maximum adsorption capacity for Co(II) (Table 3) without considerably affecting the quality of the fit.

The Freundlich model predicts the adsorption on a heterogeneous surface without saturation of adsorbent binding sites [38,39]:

$$q_e = K_F C_e^{1/n_F} \tag{11}$$

where K_F (mg g^{-1}) is a unit capacity coefficient and n_F is the Freundlich parameter related to the degree of system heterogeneity. The parameter n_F is usually greater than unity, and the larger it is, the more heterogeneous is the system [40]. The Freundlich model showed a poor fit to the experimental data with lower R^2 and the higher Chi^2 values (Table 3) in comparison to the Langmuir model. It can be seen from Fig. 3 that the data obtained experimentally formed L type adsorption isotherms providing a concave curve and tending to approach a constant value with increasing metal ion concentration [41]. The Freundlich model, unlike the Langmuir expression, does not show a maximum saturation as the aqueous concentration approaches infinity. Therefore, the equilibrium adsorption data for Co(II) and Ni(II) ion adsorption on modified chitosans were not represented appropriately by the Freundlich model in the concentration range studied.

The Sips model is a hybrid of the Langmuir and the Freundlich isotherms [39]:

$$q_e = \frac{q_m (K_S C_e)^{n_S}}{1 + (K_S C_e)^{n_S}} \tag{12}$$

where K_S (L mg^{-1}) is the Langmuir equilibrium constant and n_S is the Freundlich heterogeneity factor. The Sips isotherm behavior is the same as that of the Freundlich equation with exception of possessing a finite saturation limit when the concentration is sufficiently high. This isotherm is usually applicable where both the Langmuir and the Freundlich models fail [40]. Similar to the previous isotherm equations, the ERRSQ error function was employed to evaluate the fit of the Sips model to the experimental equilibrium data. Since the choice of error function can affect the derived parameters, the isotherm parameters for the Sips model were additionally determined by minimizing the Derivative of Marquardt's Percent Standard Deviation (MPSD) error [39]:

$$\sum_{i=1}^{p} \left(\frac{q_{e,exp} - q_{e,calc}}{q_{e,exp}} \right)^2 \tag{13}$$

A detailed error analysis was carried out to compare the calculation quality for both error functions (ERRSQ and MPSD). The isotherm parameters obtained, along with the standard deviation (σ), mean error, Chi^2 test, and correlation factor (R^2) are listed in Table 4. The comparison of the values obtained indicated that the application of different error functions resulted in different values of the Sips constants as well as the calculation errors. Based on the correlation factor R^2 a better approximation was achieved for ERRSQ. This presumption was partially confirmed by Chi^2 test. The estimated q_m values were very close to the experimentally obtained maximum metal uptake, with the exception of Co(II) adsorption on EDTA-chitosan. For this adsorbent, a slightly higher q_m value was estimated for Co(II) than for Ni(II) (70.59 and 69.90 mg g^{-1}, respectively), as opposite to that observed experimentally. The miniscule lower value of q_m for Ni(II) can result from the approximation to scattered data [42]. On the other hand, based on the standard deviation (σ) and mean error, it is evident that the fit of the Sips

Table 4
Isotherm parameters and error analysis for modeling one-component systems by using the Sips model.

Material	Type of metal	$q_{m,exp}$ (mg g^{-1})	Parameters			Statistical tests			
			q_m (mg g^{-1})	K_S (L mg^{-1})	n_S	σ	Mean error	Chi^2	R^2
ERRSQ									
EDTA-chitosan	Co(II)	63.0	70.585	0.250	0.825	0.827	10.652	0.545	0.999
	Ni(II)	71.0	69.899	1.360	1.985	2.236	7.540	2.821	0.991
DTPA-chitosan	Co(II)	49.1	51.625	0.236	1.08	0.544	3.082	0.122	0.999
	Ni(II)	53.1	53.557	0.173	2.701	1.016	17.664	27.194	0.998
MPSD									
EDTA-chitosan	Co(II)	63.0	62.985	0.370	0.974	0.067	5.297	1.010	0.993
	Ni(II)	71.0	71.520	1.248	1.849	0.101	6.284	3.584	0.987
DTPA-chitosan	Co(II)	49.1	53.008	0.215	1.031	0.038	2.597	0.198	0.999
	Ni(II)	53.1	61.360	0.111	1.502	0.234	17.178	13.091	0.931

equation to the experimental data was better for MPSD. The q_m of adsorbed Ni(II) was larger than that of Co(II) for both EDTA- and DTPA-chitosans. It corresponded to the adsorption order observed experimentally: Ni(II)EDTA > Co(II)EDTA > Ni(II)DTPA > Co(II)DTPA. Nevertheless, for DTPA-chitosan, MPSD function overestimated the real q_m value by 8–15%. All of the preceding remarks indicated that it was incorrect to select the proper error function by comparison of calculation errors when the estimated parameters were highly biased [43].

Further examination of the results represented in Table 4 indicated that the difference between the two error functions was not significant in the case of the estimation of two other Sips constants (K_S, n_S). The K_S indicated the higher affinity of Ni(II) and Co(II) for EDTA-chitosan than for DTPA-chitosan. This is analogous to the relation obtained by other authors [22]. The heterogeneity factor (n_S) values were close to unity for Co(II) adsorption indicating relatively homogenous systems [38,44]. In such a case, the Sips model reduced to the Langmuir that represented a similar extent of fit (Fig. 6a). In the case for Ni(II) adsorption, the Sips equation gave much better approximation of the experimental data, compared to both the Langmuir and the Freundlich models (Fig. 6b). The parameter n_S was greater than unity for Ni(II) adsorption, indicating system heterogeneity.

For both EDTA- and DTPA-chitosan, the heterogeneity factor n_S was higher for Ni(II) than for Co(II). It can be attributed to the structures of the chelates on the surface. The ratio of $CoHEDTA^-$ and CoH_2EDTA chelate is 1.7:1 and the ratio of $NiHEDTA^-$ and NiH_2EDTA chelate is 10.7:1 (MINEQL) at pH 2.1. The speciation in the solution phase indicates that when Ni(II) was bound on the EDTA surface group in 1:1 stoichiometry around 90% of the formed chelates had one unbound negatively charged carboxyl group. This group could have interacted with the surface or participated in binding of another Ni(II) ion. For example, two EDTA groups located close to each other could have bound altogether three Ni(II) ions and in turn increased the heterogeneity factor. In relation to DTPA there is little difference in speciation of Co(II)DTPA and Ni(II)DTPA chelates at pH 2.1. However, unbound carboxyl groups of metal DTPA chelates could have participated in binding other Ni(II) ions rather than Co(II) due to the better overall stability established for Ni(II) carboxylates compared to Co(II) carboxylates [29]. It can be concluded that the surfaces of modified chitosans had adsorption sites that were able to bind Ni(II) but not Co(II) ions.

3.5.3. Modeling adsorption isotherms for two-component systems

From the one-component systems, it was seen that the adsorption capacity of Ni(II) on both modified chitosans was higher than that of Co(II). Same characteristics were seen from adsorption tests in binary systems, where the ratio of initial concentrations of Co(II) and Ni(II) was kept constant (Co:Ni ratio: 1:1, 1:2 and 2:1). The maximum adsorption capacity of Ni(II) was two to five times higher than that of Co(II) in all the studied systems. The selectivity coefficient [45] for Ni(II), which was calculated from the ratio of the distribution constant ($q_{e,Ni}/C_{e,Ni}$) for Ni(II) over the distribution constant for Co(II) ($q_{e,Co}/C_{e,Co}$), varied for EDTA-chitosan from 56 to 102 and for DTPA-chitosan from 37 to 129. Very high values further confirmed that the modified chitosans had better selectivity and affinity for Ni(II) than for Co(II).

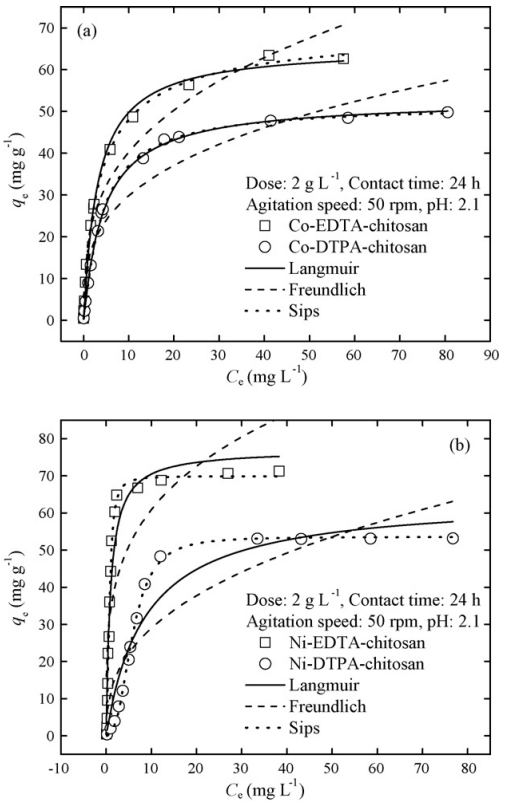

Fig. 6. Modeling of (a) Co(II) and (b) Ni(II) adsorption behavior of EDTA- and DTPA-Langmuir, Freundlich, and Sips equation.

The equilibrium data of two-component systems was modeled by usage of the extended form of the Sips isotherm [46,47]:

$$q_1 = \frac{q_{m1}(K_{S1}C_{e1})^{n_{S1}}}{1 + (K_{S1}C_{e1})^{n_{S1}} + (K_{S2}C_{e2})^{n_{S2}}} \quad (14)$$

$$q_2 = \frac{q_{m2}(K_{S2}C_{e2})^{n_{S2}}}{1 + (K_{S1}C_{e1})^{n_{S1}} + (K_{S2}C_{e2})^{n_{S2}}} \quad (15)$$

where K_{S1} and K_{S2} (L mg^{-1}) are analogous to the Langmuir affinity constants and n_{S1} are n_{S2} are heterogeneity constants. Subscriptions 1 and 2 refer to Co(II) and Ni(II), respectively. The most desirable approach to model multi-component systems is an estimation of competitive isotherm solely on the basis of the corresponding one-component isotherms [46]. However, the individual adsorption constants may not define interactions between com-

Table 5
Isotherm parameters for modeling two-component systems by using the Sips model.

Material	Parameters						Statistical tests			
	q_{m1} (mg g^{-1})	q_{m2} (mg g^{-1})	K_{S1} (L mg^{-1})	K_{S2} (L mg^{-1})	n_{S1}	n_{S2}	σ	Mean error	Chi^2	R^2
ERRSQ, q_m and n_S estimated										
EDTA-chitosan	59.852	75.012	0.250[a]	1.360[a]	0.563	1.582	36.569	74.703	30.392	0.940
DTPA-chitosan	47.983	57.075	0.236[a]	0.173[a]	0.605	3.119	23.311	79.896	19.639	0.941

Subscripts 1 and 2 refer Co(II) and Ni(II), respectively.
[a] Values taken from the one-component systems.

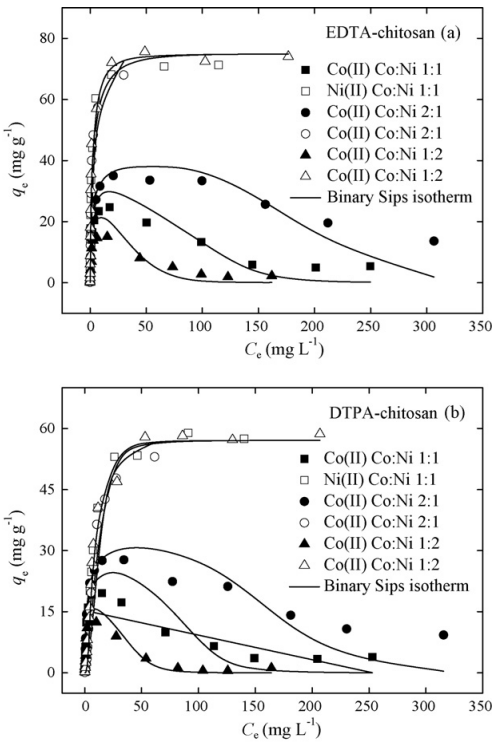

Fig. 7. Modeling of two-component data of (a) EDTA- and (b) DTPA-chitosan using the binary Sips equation. Experimental conditions as in Fig. 6.

petitive ions. The maximum adsorption capacity (q_m) as well as the interaction term (n_S) depend on the concentrations of the other components in the mixture [48]. Thus, in this part of modeling study both parameters were estimated by minimizing the ERRSQ error function (Eq. (9)). The obtained results are depicted in Table 5 and Fig. 7.

Fig. 7 shows that the binary Sips model was fitted reasonable well to the experimental two-component data. Interestingly, estimated q_m values for Ni(II) for both adsorbents were higher than those obtained for one-component systems (Tables 4 and 5). This was seen also experimentally ($q_{m,Ni(II)}$ for EDTA-chitosan 75.6 mg g^{-1} and for DTPA-chitosan 58.9 mg g^{-1} in 1:1 Co:Ni system) and indicated that the presence of Co(II) enhanced the adsorption of Ni(II). Despite of the apparent good fit, statistical tests gave quite high error values (Table 5). Especially high errors were found for low q_e values. Poorer fitting compared to the one-component systems could resulted from the K_S values applied directly from the one-component systems. Thus, it was possible that also K_S's were affected by the presence of competitive ions. On the other hand, it was reasonable to use the same K_S in one- and two-component systems due to the binding groups on the surface were chelating agents having a certain stability constant with each of the metal ions [27]. On the whole, the apparent fit, good R^2 values, and reasonable estimated q_m values supported the applicability of the Sips model also in binary systems.

4. Conclusions

EDTA- and DTPA-modified chitosans were found to effectively adsorb Co(II) and Ni(II) from aqueous solutions. The maximum metal uptake by the EDTA-chitosan was higher (q_m = 63.0 mg g^{-1} for Co(II) and q_m = 71.0 mg g^{-1} for Ni(II)) than that by the DTPA-chitosan (q_m = 49.1 mg g^{-1} for Co(II) and q_m = 53.1 mg g^{-1} for Ni(II)). At metal concentration of 100 mg L^{-1}, the removal of Co(II) and Ni(II) by the modified chitosans ranged from 93.6% to 99.5%. The selectivity sequence of both ions uptake Ni(II)EDTA/DTPA > Co(II)EDTA/DTPA was in accordance with the stability constants of the metal chelates of EDTA and DTPA. Lower metal uptake by DTPA-chitosan was attributed to its crosslinked structure and lower surface coverage of chelating groups. Adsorption kinetics followed a pseudo-second-order model for both modified chitosans, but the rate of the adsorption was also affected by intraparticle diffusion. Modeling of adsorption equilibrium required not only the choice of isotherm equation but also the error function. The quality of the fit was judged by a few statistical tests as well as accurate approximation of the real adsorption capacity (q_m). The Sips isotherm allowed the best approximation of experimental data. Nevertheless, Ni(II) and Co(II) adsorption by modified chitosan occurred under different system behavior. The adsorption studies in two-component systems showed that the modified chitosans had much better affinity for Ni(II) than for Co(II) suggesting that Ni(II) could be adsorbed selectively from the contaminated water in the presence of Co(II). Finally, the two-component equilibrium data was well described by the binary Sips model, which supported further the modeling results obtained for one-component systems.

Acknowledgements

Authors are grateful to the European Commission (Brussels) for the Marie Curie Research Fellowship for Transfer of Knowledge (No. MTKD-CT-2006-042637) and Finnish Funding Agency for Technology and Innovation (TEKES) for financial support.

References

[1] X. Huang, M. Sillanpää, B. Duo, E.T. Gjessing, Water quality in the Tibetan Plateau: metal contents of four selected rivers, Environ. Pollut. 156 (2008) 270–277.
[2] D.M. Manohar, B.F. Noeline, T.S. Anirudhan, Adsorption performance of Al-pillared bentonite clay for the removal of cobalt(II) from aqueous phase, Appl. Clay Sci. 31 (2006) 194–206.
[3] K. Kadirvelu, K. Thamaraiselvi, C. Namasivayam, Adsorption of nickel(II) from aqueous solution onto activated carbon prepared from coirpith, Sep. Purif. Technol. 24 (2001) 497–505.
[4] S.L. McAnally, T. Benefield, R.B. Reed, Nickel removal from a synthetic nickel plating wastewater using sulphide and carbonate for precipitation and coprecipitation, Sep. Sci. Technol. 19 (1984) 191–217.
[5] J. Lu, D.B. Dreisinger, W.C. Cooper, Cobalt precipitation by reduction with sodium borohydride, Hydrometallurgy 45 (1997) 305–322.
[6] K.N. Njau, M.vd. Woude, G.J. Visser, L.J.J. Janssen, Electrochemical removal of nickel ions from industrial wastewater, Chem. Eng. J. 79 (2000) 187–195.
[7] B. Volesky, Detoxification of metal-bearing effluents: biosorption for the next century, Hydrometallurgy 59 (2001) 203–216.
[8] T.A. Kurniawan, G.Y. S. Chan, W.-H. Lo, S. Babel, Physico-chemical treatment techniques for wastewater laden with heavy metals, Chem. Eng. J. 118 (2006) 83–98.
[9] S. Babel, T.A. Kurniawan, Low-cost adsorbents for heavy metals uptake from contaminated water: a review, J. Hazard. Mater. 97 (2003) 219–243.
[10] S. Rengaraj, K.-H. Yeon, S.-Y. Kang, J.-U. Lee, K.-W. Kim, S.-H. Moon, Studies on adsorptive removal of Co(II), Cr(III) and Ni(II) by IRN77 cation-exchange resin, J. Hazard. Mater. 92 (2002) 185–198.
[11] M. Ajmal, R.A.K. Rao, R. Ahmad, J. Ahmad, Adsorption studies on *Citrus reticulata* (fruit peel of orange): removal and recovery of Ni(II) from electroplating wastewater, J. Hazard. Mater. 79 (2000) 117–131.
[12] A. Bhatnagar, M. Sillanpää, Applications of chitin- and chitosan-derivatives for the detoxification of water and wastewater—a short review, Adv. Colloid Interface Sci. 152 (2009) 26–38.
[13] E. Guibal, Interactions of metal ions with chitosan-based sorbents: a review, Sep. Purif. Technol. 38 (2004) 43–74.
[14] M.N.V. Ravi Kumar, A review of chitin and chitosan applications, React. Funct. Polym. 46 (2000) 1–27.
[15] A.J. Varma, S.V. Deshpande, J.F. Kennedy, Metal complexation by chitosan and its derivatives: a review, Carbohydr. Polym. 55 (2004) 77–93.

[16] E.D. van Hullebusch, A. Peerbolte, M.H. Zandvoort, P.N.L. Lens, Sorption of cobalt and nickel on anaerobic granular sludges: isotherms and sequential extraction, Chemosphere 58 (2005) 493–505.
[17] J. Virkutyte, E. Hullebusch, M. Sillanpää, P. Lens, Copper and trace element fractionation in electrokinetically treated anaerobic granular sludge, Environ. Pollut. 138 (2005) 518–529.
[18] J. Rämö, M. Sillanpää, V. Vickackaite, M. Orama, L. Niinistö, Chelating ability and solubility of DTPA, EDTA and β-ADA in alkaline hydrogen peroxide environment, J. Pulp Paper Sci. 26 (2000) 125–131.
[19] M. Sillanpää, M. Orama, J. Rämö, A. Oikari, The importance of ligand speciation in environmental research: a case study, Sci. Total Environ. 267 (2001) 23–31.
[20] K. Pirkanniemi, S. Metsärinne, M. Sillanpää, Degradation of EDTA and novel complexing agents in pulp and paper mill process and waste waters by Fenton's reagent, J. Hazard. Mater. 147 (2007) 556–561.
[21] K. Inoue, K. Ohto, K. Yoshizuka, T. Yamaguchi, T. Tanaka, Adsorption of lead(II) ion on complexane types of chemically modified chitosan, Bull. Chem. Soc. Jpn. 70 (1997) 2443–2447.
[22] S. Nagib, K. Inoue, T. Yamaguchi, T. Tamaru, Recovery of Ni from a large excess of Al generated from spent hydrodesulfurization catalyst using picolylamine type chelating resin and complexane types of chemically modified chitosan, Hydrometallurgy 51 (1999) 73–85.
[23] E. Repo, T.A. Kurniawan, J.K. Warchol, M.E.T. Sillanpää, Removal of Co(II) and Ni(II) ions from contaminated water using silica gel functionalized with EDTA and/or DTPA as chelating agents, J. Hazard. Mater. 171 (2009) 1071–1080.
[24] M. Tülü, K.E. Geckeler, Synthesis and properties of hydrophilic polymers. Part 7. Preparation, characterization and metal complexation of carboxy-functional polyesters based on poly(ethylene glycol), Polym. Int. 48 (1999) 909–914.
[25] Standard Methods for the Examination of Water and Wastewater, 21st ed., American Public Health Association, Washington, DC, USA, 2005.
[26] K. Inoue, K. Yoshizuka, K. Ohto, Adsorptive separation of some metal ions by complexing agent types of chemically modified chitosan, Anal. Chim. Acta 388 (1999) 209–218.
[27] A.E. Martell, R.M. Smith, Critical Stability Constants, vol. 1. Amino Acids, Plenum Press, New York, 1974.
[28] M. Hughes, E. Rosenberg, Characterization and applications of poly-acetate modified silica polyamine composites, Sep. Sci. Technol. 42 (2007) 261–283.
[29] A.E. Martell, R.M. Smith, R.J. Motekaitis, NIST Critically Selected Stability Constants of Metal Complexes Database Version 3.0, Texas A&M, Texas, 1997.
[30] R.-S. Juang, F.-C. Wu, R.-L. Tseng, Adsorption removal of copper(II) using chitosan from simulated rinse solutions containing chelating agents, Water Res. 33 (1999) 2403–2409.
[31] S. Azizian, Kinetic models of sorption: a theoretical analysis, J. Colloid Interface Sci. 276 (2004) 47–52.
[32] W. Rudzinski, W. Plazinski, Kinetics of solute adsorption at solid/solution interfaces: a theoretical development of the empirical pseudo-first and pseudo-second order kinetic rate equations, based on applying the statistical rate theory of interfacial transport, J. Phys. Chem. B 110 (2006) 16514–16525.
[33] W. Rudzinski, W. Plazinski, On the applicability of the pseudo-second order equation to represent the kinetics of adsorption at solid/solution interfaces: a theoretical analysis based on the statistical rate theory, Adsorption 15 (2009) 181–192.
[34] M.S. Chiou, H.Y. Li, Adsorption behavior of reactive dye in aqueous solution on chemical cross-linked chitosan beads, Chemosphere 50 (2003) 1095–1105.
[35] G. McKay, Y.S. Ho, The sorption of lead ions on peat, Water Res. 33 (1999) 578–584.
[36] W.H. Cheung, Y.S. Szeto, G. McKay, Intraparticle diffusion processes during acid dye adsorption onto chitosan, Bioresour. Technol. 98 (2007) 2897–2904.
[37] G. McKay, M.S. Otterburn, J.A. Aga, Intraparticle diffusion process occurring during adsorption of dyestuffs, Water Air Soil Pollut. 36 (1987) 381–390.
[38] D.G. Kinniburgh, General purpose adsorption isotherms, Environ. Sci. Technol. 20 (1986) 895–904.
[39] Y.S. Ho, J.F. Porter, G. Mckay, Equilibrium isotherm studies for the sorption of divalent metal ions onto peat: copper, nickel and lead. Single component systems, Water Air Soil Pollut. 141 (2002) 1–33.
[40] D.D. Do, Adsorption Analysis: Equilibria and Kinetics, Imperial College Press, London, 1998.
[41] G. Limousin, J.-P. Gaudet, L. Charlet, S. Szenknect, V. Barthès, M. Krimissa, Sorption isotherms: a review on physical bases, modeling and measurement, Appl. Geochem. 22 (2007) 249–275.
[42] G.R. Parker, Optimum isotherm equation and thermodynamic interpretation for aqueous 1,1,2-trichloroethene adsorption isotherms on three adsorbents, Adsorption 1 (1995) 113–132.
[43] M. Chutkowski, R. Petrus, J. Warchoł, P. Koszelnik, Sorption equilibrium in processes of metal ion removal from aqueous environment. Statistical verification of mathematical models, Przem. Chem. 87 (2008) 436–438.
[44] S.K. Papageorgiou, F.K. Katsaros, E.P. Kouvelos, N.K. Kanellopoulos, Prediction of binary adsorption isotherms of Cu^{2+}, Cd^{2+} and Pb^{2+} on calcium alginate beads from single adsorption data, J. Hazard. Mater. 162 (2009) 1347–1354.
[45] H.L. Vasconcelos, E. Guibal, R. Laus, L. Vitali, V.T. Fávere, Competitive adsorption of Cu(II) and Cd(II) ions on spray-dried chitosan loaded with Reactive Orange 16, Mater. Sci. Eng. C 29 (2009) 613–618.
[46] S. Al-Asheh, F. Banat, R. Al-Omari, Z. Duvnjak, Predictions of binary sorption isotherms for the sorption of heavy metals by pine bark using single isotherm data, Chemosphere 41 (2000) 659–665.
[47] D. Kumar, A. Singh, J.P. Gaur, Mono-component versus binary isotherm models for Cu(II) and Pb(II) sorption form binary metal solution by the green alga *Pithophora oedogoni*, Bioresour. Technol. 99 (2008) 8280–8287.
[48] R.S. Vieira, E. Guibal, E.A. Silva, M.M. Beppu, Adsorption and desorption of binary mixtures of copper and mercury ions on natural and crosslinked chitosan membranes, Adsorption 13 (2007) 603–611.

Paper III

Heavy metals adsorption by novel EDTA-modified chitosan–silica hybrid materials

Eveliina Repo, Jolanta K. Warchoł, Amit Bhatnagar, Mika Sillanpää

Journal of Colloid and Interface Science 358 (2011) 261-267

Journal of Colloid and Interface Science 358 (2011) 261–267

Contents lists available at ScienceDirect

Journal of Colloid and Interface Science

www.elsevier.com/locate/jcis

Heavy metals adsorption by novel EDTA-modified chitosan–silica hybrid materials

Eveliina Repo [a,b,*], Jolanta K. Warchoł [c], Amit Bhatnagar [d], Mika Sillanpää [a,b]

[a] Laboratory of Green Chemistry, Department of Energy and Environmental Technology, Faculty of Technology, Lappeenranta University of Technology, Patteristonkatu 1, FI-50100 Mikkeli, Finland
[b] Department of Environmental Science, The Faculty of Sciences and Forestry, The University of Eastern Finland, Patteristonkatu 1, FI-50100 Mikkeli, Finland
[c] Rzeszów University of Technology, Department of Water Purification and Protection, 6 Powstańców Warszawy Street, 35-959 Rzeszów, Poland
[d] LSRE – Laboratory of Separation and Reaction Engineering, Departamento de Engenharia Química, Faculdade de Engenharia da Universidade do Porto (FEUP), Rua Dr. Roberto Frias, 4200-465 Porto, Portugal

ARTICLE INFO

Article history:
Received 3 January 2011
Accepted 23 February 2011

Keywords:
EDTA
Chitosan
Silica gel
Hybrid adsorbents
Adsorption
Heavy metals removal

ABSTRACT

Novel adsorbents were synthesized by functionalizing chitosan–silica hybrid materials with (ethylenediaminetetraacetic acid) EDTA ligands. The synthesized adsorbents were found to combine the advantages of both silica gel (high surface area, porosity, rigid structure) and chitosan (surface functionality). The Adsorption potential of hybrid materials was investigated using Co(II), Ni(II), Cd(II), and Pb(II) as target metals by varying experimental conditions such as pH, contact time, and initial metal concentration. The kinetic results revealed that the pore diffusion process played a key role in adsorption kinetics, which might be attributed to the porous structure of synthesized adsorbents. The obtained maximum adsorption capacities of the hybrid materials for the metal ions ranged from 0.25 to 0.63 mmol/g under the studied experimental conditions. The adsorbent with the highest chitosan content showed the best adsorption efficiency. Bi-Langmuir and Sips isotherm model fitting to experimental data suggested the surface heterogeneity of the prepared adsorbents. In multimetal solutions, the hybrid adsorbents showed the highest affinity toward Pb(II).

1. Introduction

The presence of elevated concentrations of heavy metals such as Co(II), Ni(II), Cd(II), and Pb(II) in the environment pose a serious threat to human health and other living beings due to their nondegradability and toxicity. Two main sources, from where these metals enter into waterways, are industrial discharges and particulates in the atmosphere. Especially, Pb(II) is the most widely distributed in the environment. The most severe health effects caused by the toxic metals are brain damage, kidney and liver disorders, and bone damage [1]. It is, therefore, important to reduce the levels of toxic metals or completely remove them from wastewaters before being discharged into the environment.

Adsorption has been proved as one of the most efficient methods for the removal of heavy metals from aqueous media. The most widely applied adsorbent is activated carbon, but its high price makes its use less economical in industrial applications [2]. Therefore, development of alternative adsorbents has been under an intensive study in recent decades. Abundantly available and reasonable low-cost materials such as silica gel and chitosan are of great interest. However, in many cases, these materials do not exhibit high adsorption efficiencies for target metals and therefore their modification has been reported to enhance their adsorption potential [3,4].

Ethylenediaminetetraacetic acid (EDTA) is known to form stable chelates with metal ions [5,6]. Therefore, its immobilization on the different supporting materials for the metal adsorption purposes has received wide attention. For example silica gel [7], chitosan [8], polyamine composites [9], polystyrene [10,11], mercerized cellulose and sugarcane bagasse [12], wood sawdust and sugarcane bagasse [13], rice husk [14], and biomass of baker's yeast [15] have been used as supports for EDTA functionalities. In all of these cases, EDTA—despite its immobilization—was observed to form stable chelates with metals. However, a comparison of the results shows that the adsorption efficiency was significantly influenced by the type of supporting material.

In our previous studies silica gel and chitosan were functionalized with EDTA [7,8]. The adsorption capacity of EDTA–chitosan was three to four times higher for Co(II) and Ni(II) ions than that of EDTA–silica gel, which was attributed to the significantly lower surface coverage of functional groups on the silica gel surface. However, EDTA–chitosan had some drawbacks such as notable swelling in aqueous media and nonporous structure resulting in a very low surface area. Due to these reasons, novel materials were designed to combine the beneficial properties of silica gel and

* Corresponding author at: Laboratory of Green Chemistry, Department of Energy and Environmental Technology, Faculty of Technology, Lappeenranta University of Technology, Patteristonkatu 1, FI-50100 Mikkeli, Finland. Fax: +358 15 336 013.
E-mail address: Eveliina.Repo@lut.fi (E. Repo).

0021-9797/$ - see front matter © 2011 Elsevier Inc. All rights reserved.
doi:10.1016/j.jcis.2011.02.059

chitosan. In this work, chitosan–silica hybrid materials were synthesized following the surface functionalization with EDTA. The synthesized hybrid adsorbents were characterized and their adsorption potential was investigated for the removal of Co(II), Ni(II), Cd(II), and Pb(II) from aqueous solution under varying experimental conditions.

2. Materials and methods

2.1. Synthesis of EDTA-modified adsorbents

Chitosan–silica hybrid materials were synthesized according to the method described by Rashidova et al. [16] by reacting 2 g of chitosan with 15, 30, or 60 mL of 98% tetraethylorthosilicate (TEOS). Chitosan–silica hybrid materials were further functionalized with EDTA according to the chitosan functionalization method [8] by reacting EDTA anhydride with chitosan amino groups in acetic acid methanol solution.

2.2. Characterization of EDTA-modified adsorbents

The amount of silicon in synthesized adsorbents was determined by dissolving 10 mg of adsorbent in a 1:1:1 mixture of HF, HNO_3, and HCl (all suprapure grade). The silicon content was analyzed by an inductively coupled plasma optical atomic emission spectrometer (ICP–OES) Model iCAP 6300 (Thermo Electron Corporation, USA). The specific surface area and total pore volume of the adsorbents were determined with Autosorb-1-C surface area and pore size analyzer (Quantachrome, UK). The surface morphology was further examined using a Hitachi S-4100 scanning electron microscope (SEM). Fourier transform infrared spectroscopy (FTIR) Nicolet Nexus 8700 (USA) was used to identify the surface groups of the synthesized adsorbents.

2.3. Batch adsorption studies

Batch adsorption experiments were conducted at ambient temperature (22 ± 1 °C). Tubes containing metal solution (concentration of metals varied from 0.02 to 7 mM) and the adsorbent (dose: 2 g/L) were agitated for a designed time on a ST5 rotary shaker (CAT M.Zipperer GmbH, Staufen, Germany). After the experiment the adsorbent was separated from aqueous solution using 0.45-μm polypropylene syringe filter and the residual concentrations of metal in the samples were analyzed by ICP–OES. The adsorption capacities (q_e) (mmol/g) of hybrid materials were calculated as

$$q_e = \frac{(C_i - C_e)}{M} V \quad (1)$$

where C_i and C_e are the initial and the equilibrium concentrations (mmol/L) of the metal ions, respectively, while M (g) and V (L) represent the weight of the adsorbent and the volume of the solution respectively.

3. Results and discussion

3.1. Characterization of EDTA-modified adsorbents

The structure of chitosan–silica hybrid material prepared for chromatographic sorbent was presented earlier by Rashidova et al. [16]. It consisted of chitosan–silica network where chitosan moieties were combined through silica groups via both ionic and covalent bonds. The structure also contained free amino groups, which encouraged us to use this material for EDTA binding. The surface properties of synthesized adsorbents are shown in Table 1. Specific surface area of the adsorbent increased with the increasing silicon content. After EDTA modification the surface area of the adsorbent was found to decrease but the total pore volume and average pore size increased. It is important to note here that the changes in surface area could not then be attributed to the pore blocking due to the chemical modification [7], but rather to the loss of silica during the EDTA functionalization. Overall, the surface properties of the prepared adsorbents were rather similar. This was also supported by the SEM analysis, which showed rather similar surface morphologies for different materials (Fig. 1). The adsorbent with the highest chitosan content (EDTA-Chi:TEOS 2:15, 45.4%) showed more grain coalescence than others (Fig. 1b), which can be attributed to the crosslinking between chitosan groups closer to each other [17].

FTIR analysis was used to identify the type of functional groups on the adsorbent surface (Supplementary information, Fig. S1). Similar features were seen for unmodified hybrid materials as was reported earlier [16], i.e., peaks at 1090–1060 cm^{-1} related to Si–O–Si and Si–O–C valent vibrations and at 3400 cm^{-1} related to symmetrical valent vibration of free NH_2 and OH groups. However, after EDTA functionalization bands attributed to the asymmetric and symmetric stretching in carbonyl groups of carboxylates were observed at 1387 and 1560 cm^{-1} and stretching vibrations in carboxyl carbonyl groups at 1734 cm^{-1} [15]. Furthermore, the intensity of these EDTA-related peaks increased as the chitosan content increased, indicating an increasing surface coverage of EDTA groups.

The swelling of EDTA-modified chitosan–silica hybrid materials was compared to the swelling of pure EDTA–silica gel and –chitosan (Supplementary information, Fig. S2). It was observed that there was no pronounced swelling in the case of hybrid materials, indicating that silica gel incorporated in the chitosan thereby increased the rigidity of the structure. Finally, the leaching of silicon at different pH was measured by ICP–OES (Fig. 2). It was noted that only the material with the highest silicon content showed higher Si(II) leaching than EDTA–silica gel. However, at pH 5 its leaching was still below 1% (m/m), indicating the stability of the hybrid adsorbents.

3.2. Adsorption studies

3.2.1. Effect of pH

Adsorption properties of EDTA-modified chitosan–silica hybrid materials were studied by varying pH, contact time, and metal ion concentration. It is well known that pH influences significantly the adsorption processes by affecting both the protonation of the

Table 1
Properties of the chitosan–silica hybrid materials before and after EDTA functionalization.

Adsorbent	Surface area (m^2/g)	Total pore volume (cm^3/g)	Average pore diameter (Å)	Si content (%)
Chi:TEOS 2:60	357.3	0.730	81.8	81.3
Chi:TEOS 2:30	309.7	0.479	61.9	74.4
Chi:TEOS 2:15	268.1	0.407	60.8	59.9
EDTA-Chi:TEOS 2:60	225.6	0.739	121.9	73.4
EDTA-Chi:TEOS 2:30	209.3	0.781	157.7	70.0
EDTA-Chi:TEOS 2:15	168.7	0.552	130.9	54.6

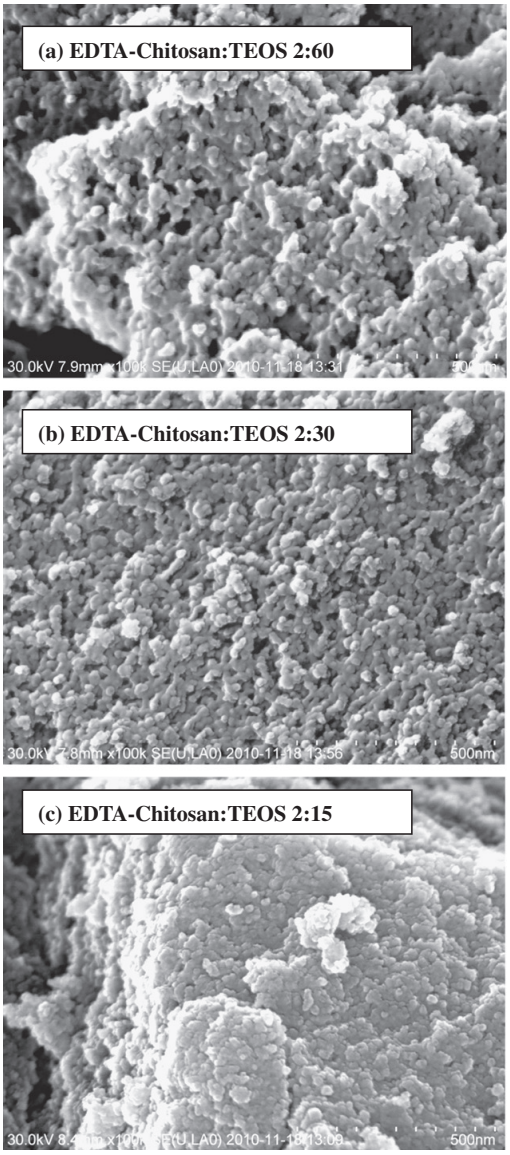

Fig. 1. SEM images of EDTA-modified chitosan–silica hybrid materials.

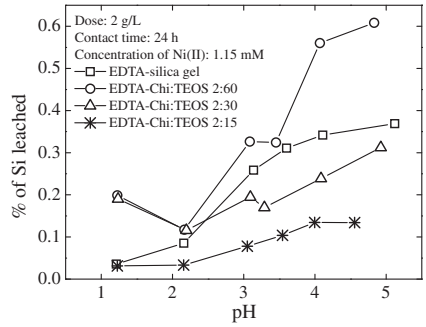

Fig. 2. Leaching of silicon during the adsorption experiments at different pH.

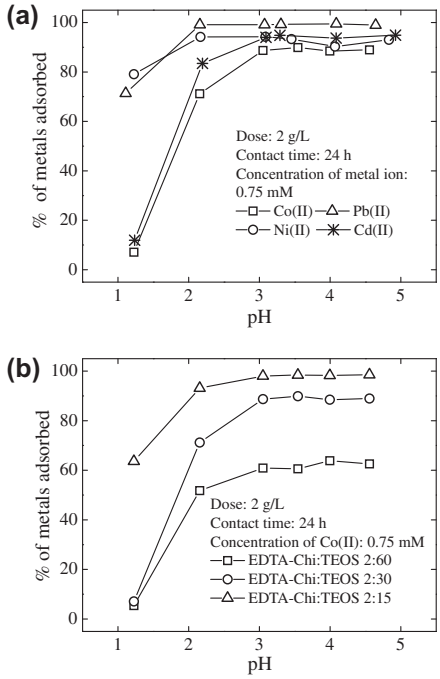

Fig. 3. (a) Effect of pH on the adsorption of different metals by EDTA-Chi:TEOS 2:30. (b) Effect of pH on the adsorption of Co(II) by different EDTA-modified chitosan–silica hybrid materials.

surface groups and the degree of the ionization of the adsorbates [12]. The dependency on the pH followed rather similar trend as obtained earlier for EDTA–silica gel and –chitosan (Fig. 3) [7,8]. Thus, the adsorption efficiency was lowest in acidic media due to the competition between metal ions and protons for adsorption sites. Beyond pH 2, an increasing trend was observed. The optimal pH for all the adsorbents was around 3 (Fig. 3b).

Fig. 3a also shows that Ni(II) and Pb(II) adsorption occurred at lower pH than Co(II) and Cd(II). This can be attributed to the higher stabilities of Ni(II) and Pb(II)EDTA chelates, which at low pH take forms of $Me(II)HEDTA^-$ and $Me(II)H_2EDTA$ (Me═Ni, Pb) [18]. Moreover, the most chitosan-like material (EDTA-Chi:TEOS 2:15) was found to be effective adsorbent at pH near 1, which was earlier observed for pure chitosan modified with EDTA [8]. The metal chelating ability of surface-bound EDTA groups at low pH can be attributed to the inductive effects that decrease the pK_a values of EDTA carboxylic groups [13].

3.2.2. Adsorption kinetics

The effect of contact time on the adsorption of metals by EDTA-modified hybrid materials is shown in Fig. 4. During short contact times, adsorption was fast due to the availability of plenty of active sites on the adsorbent surface. As the active sites were occupied, adsorption slowed down and finally an equilibrium stage was reached. The adsorption kinetics, which can be used for predicting the rate of the adsorption as well as the rate-determining step,

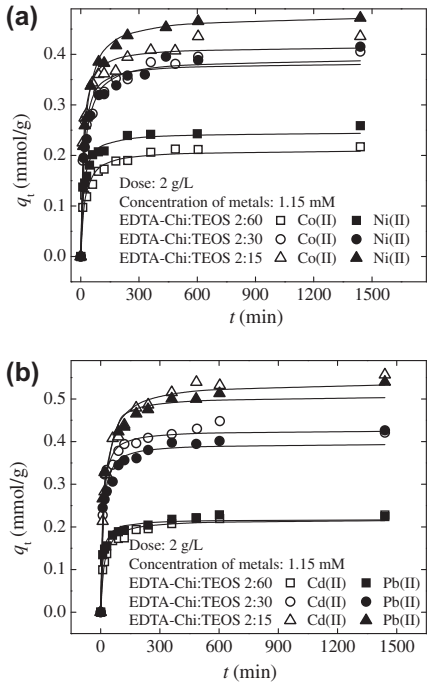

Fig. 4. Pseudo-second-order model fits for the adsorption of (a) Co(II) and Ni(II) and (b) Cd(II) and Pb(II) by EDTA-modified chitosan–silica hybrid materials.

were studied using a pseudo-second-order model and intraparticle diffusion model [8]. The pseudo-second-order model, which assumes that the adsorption process is governed by the surface reaction, has the form

$$q_t = \frac{q_e^2 k_2 t}{1 + q_e k_2 t}, \tag{2}$$

where q_t and q_e (mmol/g) represent the amount of metals adsorbed at time t (min) and at equilibrium, respectively, and k_2 is the pseudo-second-order rate constant. This model was well fitted with the experimental data (R^2 values, 0.93–0.99; average mean error, 5.3%; and simulated q_e values close to the measured ones; Table 2 and Fig. 4), indicating that the surface chelation reaction might have been the rate-limiting step. Calculated rate constants followed an order of EDTA-Chi:TEOS 2:60 > 2:30 > 2:15, indicating that the increasing surface coverage of EDTA did not increase the rate of the adsorption. Instead, it seems that the higher silicon content of the adsorbent made it more rigid, which on its behalf enhanced the adsorption kinetics. The rate constants obtained for hybrid materials were also considerably higher when compared to those of EDTA–silica gel [7], which can be attributed to the smaller particle size of hybrid materials (Supplementary information, Fig. S3).

Due to the mesoporous structure of the adsorbents, diffusion was also expected to influence the rate of the adsorption. The effect of diffusion was studied using the intraparticle diffusion model,

$$q_t = k_d t^{1/2} + C, \tag{3}$$

where k_d (mmol/g min$^{1/2}$) is the diffusion rate constant and C (mmol/g) represents the thickness of the boundary layer. Fig. 5 shows the intraparticle diffusion plots for Pb(II). Several linear portions were observed. The first slopes were attributed to the film diffusion; hence the rate constants calculated from the slopes increased linearly with the increasing metal concentration (Table 3) [19]. The rates of the film diffusion were clearly higher for EDTA-Chi:TEOS 2:30 and 2:15 when compared to those of EDTA-Chi:TEOS 2:60, most likely due to the lower surface coverage of the latter. The highest film diffusion rates were obtained for Pb(II), which can be attributed to its smallest hydration number [20]. The rates of the metal diffusion inside the adsorbent pores (second and third slopes in Fig. 5) were the fastest for EDTA-Chi:TEOS 2:15, which might be attributed to the higher amount of active sites inside the pores attracting metals and enhancing their diffusion rates.

As a summary of the kinetic studies, even though the pseudo-second-order model showed a quite good correlation with the experimental data, the porous structure of the adsorbents and intraparticle model plots indicated the significance of the pore diffusion. It was also seen that the film diffusion was important during the initial stage of the adsorption.

Table 2
Pseudo-second-order kinetics parameters for metal adsorption on EDTA-modified chitosan–silica hybrid materials, pH 3.

Metal	C_0 (mmol/L)	$q_{e,exp}$ (mmol/g)	q_e (mmol/g)	k_2 (g mmol/min)	Chi^2 * 10^{-5}	R^2	Mean error (%)
EDTA-Chi:TEOS 2:60							
Co(II)	0.28	0.13	0.13	0.54	2.2	0.984	3.86
	0.81	0.21	0.22	0.24	18.3	0.967	6.43
	1.21	0.22	0.21	0.26	14.2	0.963	7.05
Ni(II)	0.33	0.16	0.15	0.47	10.9	0.947	7.73
	0.79	0.24	0.22	0.30	27.6	0.934	8.03
	1.31	0.26	0.25	0.31	17.0	0.966	5.48
Cd(II)	0.15	0.07	0.07	2.42	0.1	0.998	1.16
	0.47	0.21	0.19	0.26	20.9	0.936	8.60
	1.23	0.22	0.22	0.28	11.4	0.974	4.81
Pb(II)	0.25	0.12	0.12	0.88	1.4	0.989	2.67
	0.32	0.16	0.15	0.55	3.7	0.983	4.31
	1.09	0.22	0.22	0.51	12.2	0.970	5.30
EDTA-Chi:TEOS 2:30							
Co(II)	1.15	0.41	0.38	0.22	43.6	0.964	5.85
Ni(II)	1.15	0.42	0.39	0.14	28.9	0.977	4.89
Cd(II)	1.23	0.42	0.42	0.27	22.9	0.985	3.06
Pb(II)	1.09	0.43	0.40	0.27	48.7	0.961	5.31
EDTA-Chi:TEOS 2:15							
Co(II)	1.15	0.44	0.42	0.22	33.7	0.976	4.40
Ni(II)	1.15	0.51	0.48	0.11	37.8	0.981	4.26
Cd(II)	1.23	0.55	0.54	0.10	39.2	0.986	3.86
Pb(II)	1.09	0.54	0.51	0.18	17.2	0.992	6.30

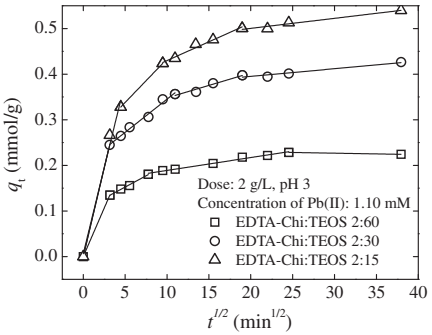

Fig. 5. Intraparticle diffusion model plots for Pb(II) adsorption on EDTA-modified chitosan–silica hybrid materials.

3.2.3. Adsorption isotherms

An adsorption isotherm represents the amount of species adsorbed versus the amount of species left in the solution phase

Table 3
Intraparticle diffusion model parameters for metal adsorption on EDTA-modified chitosan–silica hybrid materials, pH 3.

Metal	C_0 (mmol/L)	$k_{d,1}$ (mmol/g min$^{1/2}$)	$k_{d,2}$ (mmol/g min$^{1/2}$)	$k_{d,3}$ (mmol/g min$^{1/2}$)	$k_{d,4}$ (mmol/g min$^{1/2}$)
EDTA-Chi:TEOS 2:60					
Co(II)	0.28	0.021	0.00613	0.00190	0.00039
	0.81	0.038	0.01107	0.00178	0.00053
	1.21	0.044	0.01040	0.00393	0.00047
Ni(II)	0.33	0.027	0.00660	0.00203	0.00058
	0.79	0.037	0.00855	0.00257	0.00098
	1.31	0.043	0.01420	0.00505	0.00087
Cd(II)	0.15	0.016	0.00432	0.00043	0
	0.47	0.027	0.00750	0.00178	0.00016
	1.23	0.041	0.01493	0.00376	0.00087
Pb(II)	0.25	0.022	0.00526	0.00155	0.00003
	0.32	0.025	0.00656	0.00041	0
	1.09	0.042	0.00988	0.00282	0
EDTA-Chi:TEOS 2:30					
Co(II)	1.15	0.060	0.01130	0.00478	0.00076
Ni(II)	1.15	0.053	0.02130	0.00649	0.00139
Cd(II)	1.23	0.072	0.01097	0.00388	0
Pb(II)	1.09	0.078	0.01460	0.00545	0.00169
EDTA-Chi:TEOS 2:15					
Co(II)	1.15	0.071	0.02470	0.00501	0.00003
Ni(II)	1.15	0.059	0.02780	0.00972	0.00335
Cd(II)	1.23	0.064	0.02696	0.00967	0.00134
Pb(II)	1.10	0.084	0.02374	0.00823	0.00220

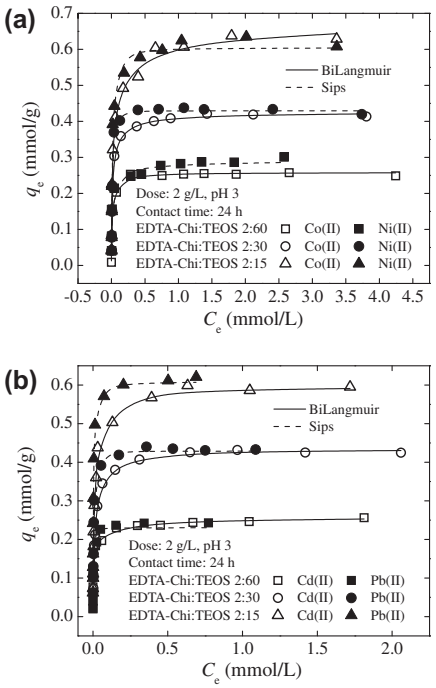

Fig. 6. Adsorption isotherms for (a) Co(II) and Ni(II) and (b) Cd(II) and Pb(II) for EDTA-modified chitosan–silica hybrid materials.

at equilibrium. The plateau at high solution concentrations gives the maximum metal uptake (Fig. 6, Table 4). For chitosan–silica hybrid materials the uptake increased as the chitosan content increased due to the increasing amount of chelating groups on the surface. Otherwise, in one-component systems the maximum adsorption capacities for different metals were rather similar ranging from 0.25 to 0.63 mmol/g (Table 4). For EDTA-Chi:TEOS 2:15 the adsorption percentages from 0.8 mM metal solutions were 93.5% for Co(II), 95.2% for Ni(II), 96.5% for Cd(II), and 99.2% for Pb(II). In addition, EDTA-Chi:TEOS 2:15 showed twice as high metal uptake compared to that of EDTA–silica gel [7], which confirms that the synthesis presented here produced better adsorbents compared to the conventional synthesis based on silanization [4]. Moreover, the adsorption capacities obtained for hybrid adsorbents were higher than those obtained for PS–EDTA resin [10] and EDTA-modified silicapolyallylamine composites [9].

According to the observations in previous studies [7,8], bi-Langmuir and Sips equations were used in modeling of the isotherm data. The bi-Langmuir model assumes that the surface contains two different active sites with different affinities toward target compounds [7]:

$$q_e = \frac{q_{m1} K_{L1} C_e}{1 + K_{L1} C_e} + \frac{q_{m2} K_{L2} C_e}{1 + K_{L2} C_e}. \quad (4)$$

Here q_{m1} and q_{m2} are the maximum adsorption capacities of two different adsorption sites and K_{L1} and K_{L2} are adsorption energies related to these adsorption sites. The Sips model on its behalf is a hybrid of the Langmuir and the Freundlich isotherms [8]:

$$q_e = \frac{q_m (K_S C_e)^{n_S}}{1 + (K_S C_e)^{n_S}}. \quad (5)$$

Here K_S (L/mg) is the Langmuir equilibrium constant and n_S is comparable to the Freundlich heterogeneity factor n_F ($n_S = 1/n_F$). The Sips isotherm behavior is the same as that of the Freundlich equation with the exception of approaching a constant adsorption capacity when the concentration is sufficiently high.

Interestingly, the correlation of the isotherm equation with the experimental data was influenced more by the type of metal than the type of the material (Fig. 6 and Tables 4 and 5). The bi-Langmuir model fitted better for Co(II) and Cd(II) isotherms, indicating the coexistence of two types of active sites on the surface assigned to the different speciations of EDTA at pH 3: R-NH-HEDTA^{2-} and R-NH-H_2EDTA$^-$ (MINEQL software, ver. 2.53). The Sips model fitted better to the isotherms of Ni(II) and Pb(II) (except Ni(II) adsorption on EDTA-Chi:TEOS 2:60) with very high affinity constants, indicating the high affinity of surface groups toward the target metals. It should be noted that n_s values lower than one obtained for Co(II) and Cd(II) suggested a heterogeneous adsorption arising from the solid structural or energetic property (cf. bi-Langmuir model), or the adsorbate property. The modeling results were comparable with the results obtained for EDTA–chitosan [8]. However, the parameters related to the surface affinities obtained by model fitting did not follow the order of stability constants of aqueous metal EDTA chelates (Ni(II) > Pb(II) > Co(II) > Cd(II) [18]). Therefore, it was suggested that the properties of metals, especially the hydration number, played an important role in chelation reaction when EDTA ligands were immobilized.

3.2.4. Adsorption properties of hybrid adsorbents in multimetal systems

To compare the binding affinities further, adsorption tests were also conducted in the solutions containing the same amount of each of the studied metals (Fig. 7, Table 6, and Supplementary information, Fig. S4). Under competing conditions Pb(II) clearly showed the highest adsorption affinity in the case of EDTA-Chi:TEOS 2:60 and 2:30. For EDTA-Chi:TEOS 2:15 the affinities of Pb(II) and Ni(II) were rather similar due to the availability of higher active sites available on the adsorbent surface. Pb(II) was most likely

Table 4
Bi-Langmuir parameters for metal adsorption on EDTA-modified chitosan–silica hybrid materials, pH 3.

Material	Metal	$q_{m,exp}$ (mg g^{-1})	q_{m1} (mg g^{-1})	K_1 (L mg^{-1})	q_{m2} (mg g^{-1})	K_2 (L mg^{-1})	Chi$^2 * 10^{-5}$	R^2	Mean error
EDTA-Chi:TEOS 2:60	Co(II)	0.25	0.16	393.31	0.10	18.54	4.12	0.995	5.42
	Ni(II)	0.30	0.23	447.14	0.10	1.05	50.85	0.954	18.04
	Cd(II)	0.26	0.19	1268.30	0.07	7.02	4.10	0.995	5.07
	Pb(II)	0.24	0.22	744.40	0.03	7.26	41.50	0.942	22.62
EDTA-Chi:TEOS 2:30	Co(II)	0.42	0.38	92.54	0.05	2.53	5.26	0.997	3.92
	Ni(II)	0.44	0.44	75.98	0.00	0.00	73.1	0.969	14.65
	Cd(II)	0.43	0.27	157.99	0.16	20.75	19.1	0.989	5.06
	Pb(II)	0.43	0.44	185.38	0.00	0.00	52.0	0.976	9.54
EDTA-Chi:TEOS 2:15	Co(II)	0.63	0.48	82.50	0.19	2.05	52.4	0.989	12.42
	Ni(II)	0.61	0.60	61.07	0.02	61.00	143	0.972	17.62
	Cd(II)	0.60	0.40	40.78	0.20	632.76	30.3	0.992	3.63
	Pb(II)	0.62	0.62	266.62	0.00	0.00	199	0.958	12.75

Table 5
Sips parameters for metal adsorption on EDTA-modified chitosan–silica hybrid materials, pH 3.

Material	Metal	$q_{m,exp}$ (mg g^{-1})	q_m (mg g^{-1})	K_S (L mg^{-1})	n_S (mg g^{-1})	Chi$^2 * 10^{-5}$	R^2	Mean error
EDTA-Chi:TEOS 2:60	Co(II)	0.25	0.26	35.08	0.73	5.96	0.993	10.31
	Ni(II)	0.30	0.29	26.10	0.64	76.7	0.931	51.04
	Cd(II)	0.26	0.26	23.76	0.55	15.3	0.980	13.90
	Pb(II)	0.24	0.23	3479.21	1.23	38.7	0.946	18.51
EDTA-Chi:TEOS 2:30	Co(II)	0.42	0.42	48.65	0.91	9.70	0.995	5.27
	Ni(II)	0.44	0.43	1239.58	1.58	7.45	0.997	3.47
	Cd(II)	0.43	0.44	35.69	0.83	18.5	0.989	5.20
	Pb(II)	0.43	0.43	1714.21	1.39	22.0	0.990	4.93
EDTA-Chi:TEOS 2:15	Co(II)	0.63	0.64	15.31	0.75	88.6	0.982	16.39
	Ni(II)	0.61	0.60	145.50	1.18	111	0.978	13.15
	Cd(II)	0.60	0.62	23.53	0.71	22.6	0.994	3.73
	Pb(II)	0.62	0.61	590.79	1.13	166	0.965	9.26

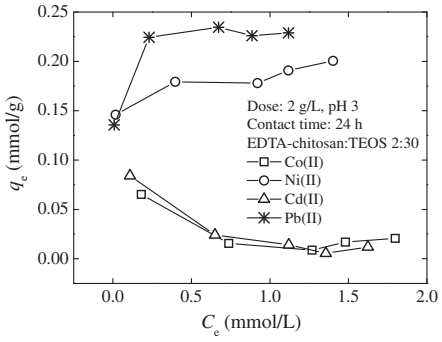

Fig. 7. Adsorption of metals from multicomponent systems for EDTA-Chi:TEOS 2:30.

Table 6
Distribution ratios for different metals calculated from the ratio of the distribution constant ($q_{e,metal1}/C_{e,metal1}$) for metal (1) (vertical) over the distribution constant ($q_{e,metal2}/C_{e,metal2}$) for metal (2) (horizontal), pH 3.

	Co(II)	Ni(II)	Cd(II)	Pb(II)
EDTA-Chi:TEOS 2:60				
Co(II)	1	0.1	0.5	0.04
Ni(II)	7.2	1	3.9	0.3
Cd(II)	1.8	0.3	1	0.07
Pb(II)	27.3	4.0	15.0	1
EDTA-Chi:TEOS 2:30				
Co(II)	1	0.04	0.5	0.02
Ni(II)	28	1	15.3	0.6
Cd(II)	1.8	0.07	1	0.04
Pb(II)	50.5	1.8	27.6	1
EDTA-Chi:TEOS 2:15				
Co(II)	1	0.04	0.5	0.02
Ni(II)	42.3	1	19.5	0.8
Cd(II)	2.2	0.05	1	0.04
Pb(II)	51.2	1.2	23.6	1

the easiest ion to capture by the surface EDTA groups due to its smallest hydration number. This was also supported by the highest values of affinity constants obtained for Pb(II) in one-component systems (Table 5). The second highest adsorption efficiency of Ni(II) in multimetal systems can be attributed to its high stability constant with EDTA ligand [18]. As a conclusion, measurements in multimetal systems suggested that Ni(II) and Pb(II) could be separated from Co(II) and Cd(II) using EDTA-modified chitosan–silica hybrid materials. Based on the pH effects, separation should be even more evident at pH lower than 3 (Fig. 3).

4. Summary

Novel adsorbents for heavy metal removal were synthesized by functionalizing chitosan–silica hybrid materials with EDTA. The synthesized adsorbents combined successfully the beneficial properties of silica gel and chitosan. Materials were porous and rigid like silica gel and had high coverage of functionalities due to the chitosan groups. Furthermore, the adsorption efficiency of hybrid materials could easily be affected by changing the silica content in the synthesis. The novel materials were shown to be effective adsorbents for Co(II), Ni(II), Cd(II), and Pb(II) with adsorption efficiency varying from 93% to 99% from 0.8 mM single metal solutions. The maximum adsorption capacities ranged from 0.25 to 0.63 mmol/g. The material with the highest chitosan content and thus the highest surface coverage of EDTA showed the best adsorption properties. Isotherm fits of bi-Langmuir and Sips models indicated the surface heterogeneity and kinetics modeling suggested the importance of pore diffusion. Adsorption experiments in mul-

timetal systems suggested a possible separation of Ni(II) and Pb(II) from Co(II) and Cd(II). On the whole, the novel EDTA-modified hybrid adsorbents showed their potential to be applied in different water treatment applications for the removal of heavy metals.

Acknowledgments

The authors are grateful to the European Commission (Brussels) for the Marie Curie Research Fellowship for Transfer of Knowledge (No. MTKD-CT-2006-042637) and TEKES/EAKR Moniwater project for financial support. Marcin Ołpiński is acknowledged for his contribution in performing experiments in the laboratory.

Appendix A. Supplementary material

Supplementary data associated with this article can be found, in the online version, at doi:10.1016/j.jcis.2011.02.059.

References

[1] J.E. Girard, Principles of Environmental Chemistry, Jones and Bartlett, USA, 2005, pp. 413–418.
[2] S. Babel, T.A. Kurniawan, J. Hazard. Mater. 97 (2003) 219.
[3] A.J. Varma, S.V. Deshpande, J.F. Kennedy, Carbohydr. Polym. 55 (2004) 77.
[4] P.K. Jal, S. Patel, B.K. Mishra, Talanta 62 (2004) 1005.
[5] J. Rämö, M. Sillanpää, V. Vickackaite, M. Orama, L. Niinistö, J. Pulp Pap. Sci. 26 (2000) 125.
[6] M. Sillanpää, M. Orama, J. Rämö, A. Oikari, Sci. Total Environ. 267 (2001) 23.
[7] E. Repo, T.A. Kurniawan, J.K. Warchol, M.E.T. Sillanpää, J. Hazard. Mater. 171 (2009) 1071.
[8] E. Repo, J.K. Warchol, T.A. Kurniawan, M.E.T. Sillanpää, Chem. Eng. J. 161 (2010) 73.
[9] M. Hughes, E. Rosenberg, Sep. Sci. Technol. 42 (2007) 261.
[10] L.Y. Wang, L.Q. Yang, Y.F. Li, Y. Zhang, X.J. Ma, Z.F. Ye, Chem. Eng. J. 163 (2010) 364.
[11] L.Q. Yang, Y.F. Li, L.Y. Wang, Y. Zhang, X.J. Ma, Z.F. Ye, J. Hazard. Mater. 180 (2010) 98.
[12] O. Karniz Júnior, L.V.A. Gurgel, R.P. Freitas, L.F. Gil, Carbohydr. Polym. 77 (2009) 643.
[13] F.V. Pereira, L.V.A. Gurgel, L.F. Gil, J. Hazard. Mater. 176 (2010) 856.
[14] S.-T. Ong, W.-N. Lee, P.-S. Keng, S.-L. Lee, Y.-T. Hung, S.-T. Ha, Int. J. Phys. Sci. 5 (2010) 582.
[15] J. Yu, M. Tong, X. Sun, B. Li, Bioresour. Technol. 99 (2008) 2588.
[16] S. Sh. Rashidova, D. Sh. Shakarova, O.N. Ruzimuradov, D.T. Satubaldieva, S.V. Zalyalieva, O.A. Shpigun, V.P. Varlamov, B.D. Kabulov, J. Chromatogr. B 800 (2004) 49.
[17] A. Bernkop-Schnurch, M.E. Krajicek, J. Controlled Release 50 (1998) 215.
[18] R.M. Smith, A.E. Martell, R.J. Motekaitis, NIST Standard Reference Database 46.6, National Institute of Standards and Technology, US Department of Commerce, Gaithersburg, MD, 2007.
[19] F. Helfferich, Ion Exchange, Dover, New York, 1995, p. 285.
[20] P. Trivedi, L. Axe, Environ. Sci. Technol. 35 (2001) 1779.

Supplementary material for

Heavy metals adsorption by novel EDTA-modified chitosan-silica hybrid materials

Eveliina Repo[1,4*], Jolanta K. Warchoł[2], Amit Bhatnagar[3] and Mika Sillanpää[1,4]

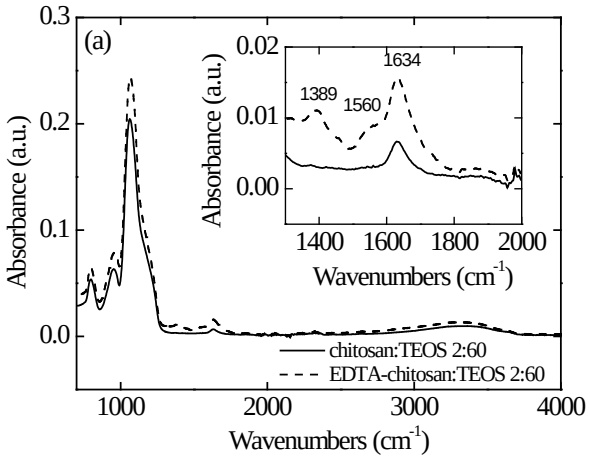

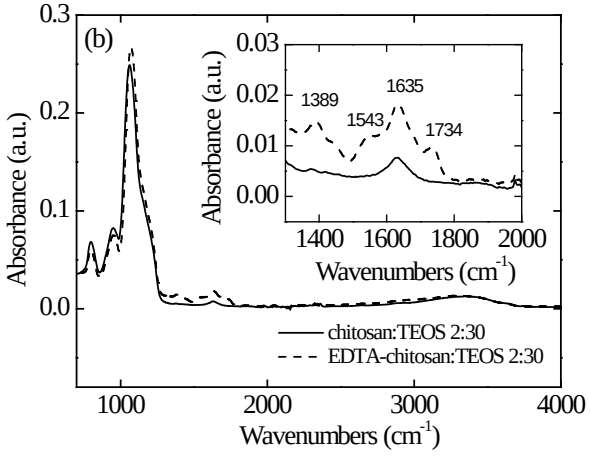

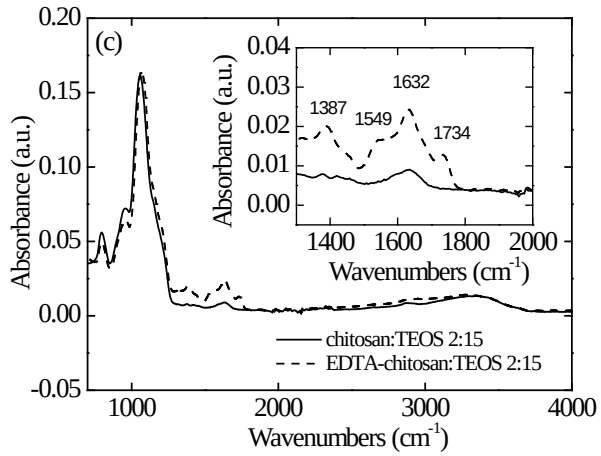

Figure S1. FTIR-spectra of unmodified and modified chitosan-silica hybrid materials.

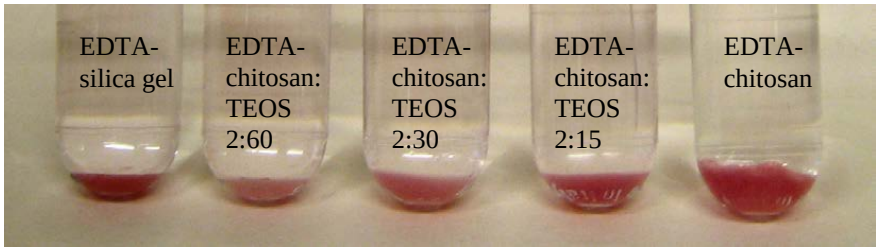

Figure S2. Swelling of EDTA-modified adsorbents in 3.4 mmol/L Co(II) solution.

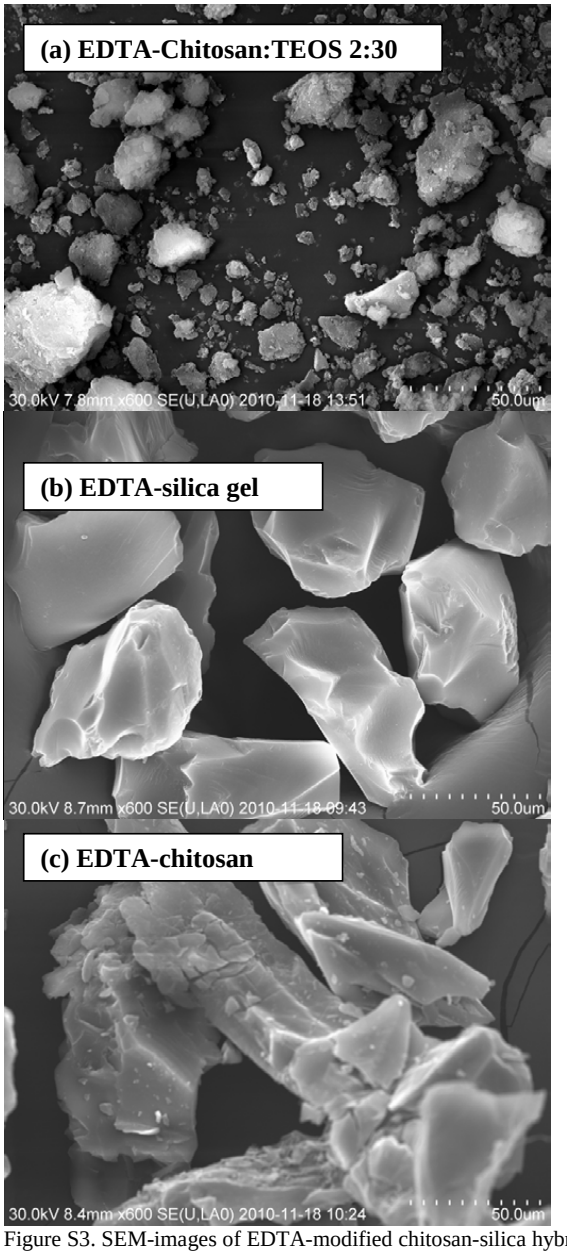

Figure S3. SEM-images of EDTA-modified chitosan-silica hybrid material, EDTA-silica gel, and EDTA-chitosan

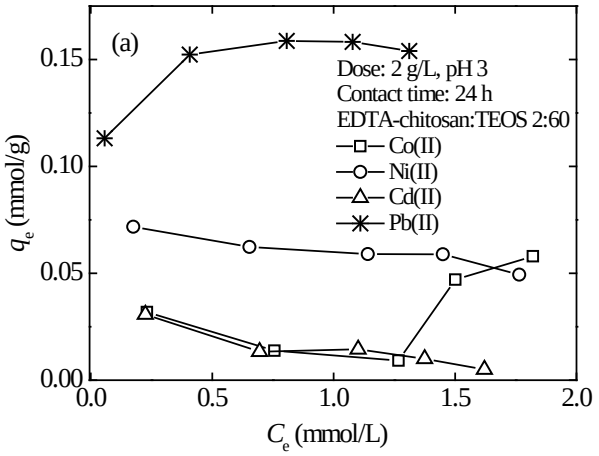

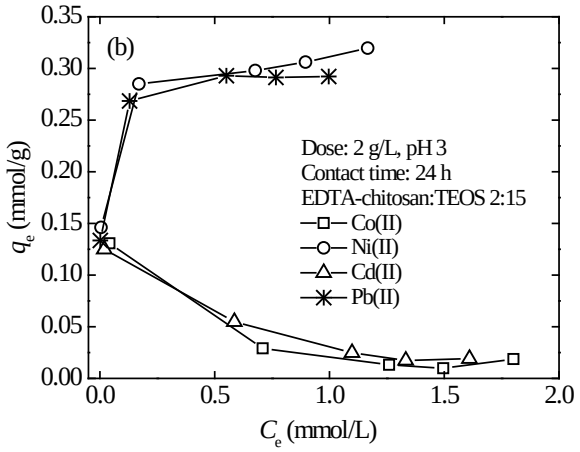

Figure S4. Adsorption of metals from multi-component systems by EDTA-modified chitosan-silica hybrid materials. (a) EDTA-Chi:TEOS 2:60, (b) EDTA-Chi:TEOS 2:15.

Paper IV

Equilibrium studies on the adsorption of Co(II) and Ni(II) by modified silica gels: one-component and binary systems

Eveliina Repo, Roman Petrus, Mika Sillanpää, Jolanta K. Warchoł

Chemical Engineering Journal (2011) (in press)

Equilibrium studies on the adsorption of Co(II) and Ni(II) by modified silica gels: one-component and binary systems

Eveliina Repo[1,3,*], Roman Petrus[2], Mika Sillanpää[1,3] and Jolanta K. Warchoł[2]

[1] Laboratory of Green Chemistry, Department of Energy and Environmental Technology, Faculty of Technology, Lappeenranta University of Technology , Patteristonkatu 1, FI-50100 Mikkeli, Finland, mika.sillanpaa@lut.fi

[2] Rzeszów University of Technology, Department of Water Purification and Protection, 6 Powstańców Warszawy Street., 35-959 Rzeszów, Poland

[3] Department of Environmental Science, The Faculty of Sciences and Forestry, The University of Eastern Finland, Patteristonkatu 1, FI-50100 Mikkeli, Finland

*E-mail: eveliina.repo@lut.fi (Corresponding author)

Abstract

The BiLangmuir and Redlich-Peterson models as well as their extended equations were tested for the modeling of one- and two-component adsorption equilibrium of Co(II) and Ni(II) ions on EDTA- and DTPA-modified silica gel. An approach consisting in initialization of parameter values and non-linear parameter estimation by minimization of two objective functions (MPSD and ERRSQ) was proposed to assure that equilibrium parameters obtained related to the global minimum. A usage of the experimentally obtained value of maximum adsorption capacity as an initial guess made an iteration procedure well-posed and independent of the K_i guess values. None of the parameters obtained for one-component systems satisfactorily helped in prediction of the two-component adsorption equilibrium. The application of the extended Bilangmuir model identified the coexistence of low- and high-energy active sites on EDTA/DTPA-silica gel that showed an unequal ability for Co(II) and Ni(II) adsorption.

Keywords: adsorption isotherm, one-component, two-component, modeling, chelating agent

1. Introduction

Mesoporous silica-based adsorbents have been increasingly attracting the attention of researchers over the last decades due to their large, easy-to-modify surface areas [1,2]. Preliminary modification is usually done by a simple silylating agent such as (3-aminopropyl)triethoxysilane (APTES) or (3-iodopropyl)trimethoxysilane. After that an increase of the organic chain with a variety of organic molecules, such as amines and amides [1,3], aromatics [4,5], phosphonic acids [6], polyaminocarboxylates [7,8], and Schiff base ligands [9], is possible. Immobilization of active chemical groups results in a substantial increase of binding capacity of silica gels for variety of metal ions: Cr(III), Co(II), Ni(II), Cu(II), Zn(II), Hg(II), U(VI), Fe(III), Mn(II). This opens up a possibility to achieve promising and effective alternatives for expensive conventional sorbents [10]. The main challenge of the modified silica gel

application is the proper design of a continuous process for multi-metal systems. Knowledge of the adsorption isotherms is mandatory, since the parameters obtained can greatly help in the mathematical description of kinetics and dynamic processes as well as in further process optimization [11].

The adsorption equilibrium reflects the dependence of the amount of adsorbed species on the liquid phase composition at constant temperature [12]. In order to get access to these quantities the usage of mass balance considerations in a form of the mathematical relationship is required. Despite of large numbers of equilibrium models available [13-17], their appropriate and efficient application is still far from being routine. Most models were derived from gas-solid systems and were fully empirically adapted to the liquid-solid ones. Thus, the physical meaning of the parameters is not always clear. Moreover, there are some numerical problems with these equations. The non-linear regression is a mathematically rigorous method [12], but still the choice of an error function assessment can affect the parameters derived [15]. It is also well known that the initial value of the parameters (the initial guess) may not converge to a global minimum during the optimization process [18]. Most of the equilibrium studies reported in literature give only parameter values and the strength of the relationship between experimental and calculated values without any evidence that the best set of estimated parameters was obtained. Consequently, even for a small residual error, the adopted equations can yield an unacceptable match of the data and highly biased parameters [19,20].

The modeling of multi-component equilibrium is more complicated than the one-component one in relation to modeling itself and to interpretation of the results due to their multi-dimensional nature. Applied equations exemplify further modifications or extensions of one-component models derived by adding one more adsorption intensity and concentration term [21]. The verification of multi-component model fit requires provision of a wide combination of isotherm points representing an adsorption of the target ion at varying concentrations of each competitive ion in the mixture. To reduce the experimental efforts, Myers and Prausnitz [22] put forward a theory that allowed adjustment of the multi-component adsorption solely from the one-component data. This approach was proven to be reasonable in numerous applications such as multi-component adsorption on pine bark [23], green alga [21,24], Ca-Alginate [25], and activated carbon [26]. As the parameters applied directly from one-component systems do not define the exact multi-component adsorption behavior [27], the extended models can lead to doubtful prognosis after extrapolation over too wide concentration ranges [28]. To make competitive isotherms more flexible and to handle the un-ideality of the system, new equations have additional adjustable parameters [29]. Obviously, there is somehow a risk that while the model having a large number of fitting parameters could well correlate with experimental results, it would not conform to the actual physical behavior of the adsorption system [30]. So far the choice of an optimum multi-component isotherm has based on the literature data or on the trial and error method. However, the evaluation procedure requires a critical examination of the extent to which the model with best correlation represents the one-component system. Thus, the achievement of the optimal values of equilibrium parameters by assuring the minimization of the

objective function to the global minimum is required. Unfortunately, until recently, such an approach has been completely neglected.

The models most extensively used to describe the equilibrium characteristic of one-component adsorption, are the Langmuir and Freundlich ones [14]. The Freundlich isotherm is derived by assuming a heterogeneous surface and a nonuniform distribution of adsorption heat over the surface, whereas in the Langmuir theory the basic assumption is that the sorption takes place at specific homogenous sites within the adsorbent [15,16]. Recently reported results demonstrated that neither model could be used to represent one-component adsorption equilibrium of Co(II) and Ni(II) on EDTA- and DTPA-modified silica gels (EDSG and DTSG). Instead, the BiLangmuir isotherm (two-site Langmuir) gave excellent representations of experimental data [8].

The aim of this work was to investigate the competitive adsorption of Co(II) and Ni(II) ions on EDSG and DTSG. Besides its importance for practical applications, the determination of two-component equilibrium can give important information on the properties of modified silica gel surfaces. The competition between ionic species leads to nonideal behavior of the overall solid-liquid system [30]. Therefore, the widths of the modes of the adsorption energy distribution can affect the heterogeneous nature of active sites. To check the validity of this hypothesis, we tested the applicability of an extended form of the Redlich-Peterson equation and the BiLangmuir equation to model two-component equilibrium by using parameters of the one-component systems. However, as the parameters applied directly from one-component systems do not take into account the effects of competitive ion, the approaches, where a few or all of the parameters were let to vary, were applied as well. Since the validation of the parameter values cannot be totally proven by nonlinear regression, it was essential to find out whether the parameters corresponded to the global minimum of the objective function. In this contribution, we examined both models sensitivities to an initial guesses of estimated parameters as well as an error function assessment.

2. Materials and methods

2.1. Chemicals

As-received silica gel type LiChroPrep®, supplied by Merck (Finland), was provided in a powder form. All chemicals used in this study were of analytical grade and were supplied by the same company. Stock solutions of 1,000 mg/L containing only Co(II) or Ni(II) or mixture of these two metals were periodically prepared by dissolving appropriate amounts of Co(II) and Ni(II) nitrate salts in double deionized water. Working solutions were prepared from the stock solutions. Adjustment of pH was undertaken using 0.1 M NaOH or 0.1 M HNO_3.

2.2. Synthesis and characterization of modified silica gels

As previously presented, EDSG and DTSG were synthesized by reacting EDTA- and/or DTPA-anhydrides with aminopropyl-modified silica gels (APSG) in ethanol/acetic acid solution (Fig.1., [8]). The

characterization of the products was conducted by elemental analysis, surface area and pore size analysis as well as zeta potential analysis. The examined properties of the modified silica gels are presented in Table 1.

2.3. Adsorption studies

Adsorption of Ni(II) and Co(II) by modified silica gels were studied at ambient temperature using batch experiments. Based on the previous studies [8] a contact time of 50h and the adsorbent dose of 2 g/L were used. Agitation with the speed of 50 rpm was conducted with a rotary shaker, type ST5 (CAT M.Zipperer GmbH, Staufen, Germany).

The initial metal concentration in one- and two-component systems were varied from 1 to 300 mg/L to generate a relatively evenly spaced distribution of ions along the adsorption isotherm. To obtain the competitive effect of Co(II) and Ni(II) adsorption, nine experimental sets were performed for two-component systems. In each set, the initial concentration of both metal ions was varied so as to maintain the constant mass ratio of Co:Ni ions: 1:1, 1:3, 3:1, 2:3, 3:2, 1:4, 4:1, 1:9, and 9:1. On the basis of batch tests carried out, to maximize the removal of metal ions by the adsorbents, pH of each solution was adjusted to the value of 3.0 by using 0.1 M HNO_3 [8].

After each adsorption test, the adsorbent was separated from the solution using a 0.45 μm polypropylene syringe filter. The metal contents were analyzed by an inductively coupled plasma optical atomic emission spectrometer (ICP-OES) model iCAP 6300 (Thermo Electron Corporation, USA) before and after adsorption tests. Co(II) was analyzed at a wavelength of 228.616 nm and Ni(II) of 231.605 nm. The detection limits were 0.4 and 0.8 μg/L and quantification limits 1.5 and 2.8 μg/L for Co(II) and Ni(II), respectively. The amount of metal ions adsorbed per unit mass of modified silica gel (mg/g) was calculated as follows:

$$q_e = \frac{(C_i - C_e)}{M} V \quad (1)$$

where C_i and C_e (mg/L) are the initial and the equilibrium ion concentrations, respectively, M (g) represent the weight of the adsorbent, and V (L) is the volume of the solution.

3. Theoretical approach

3.1. Equilibrium models

The *BiLangmuir* model is a linear superposition of two Langmuir isotherms. It assumes the coexistence of two kinds of active sites associated with monolayer adsorption ($q_{m,1}$ and $q_{m,2}$). Both sites behave independently and have different stabilities of the adsorbed complexes formed between sites and metal ions (K_1 and K_2). Thus, this two-site population is heterogeneous to a degree and the Bilangmuir equation can be considered as the simplest case of heterogeneous models [31]:

$$q_e = \frac{q_{m,1} K_1 C_e}{1 + K_1 C_e} + \frac{q_{m,2} K_2 C_e}{1 + K_2 C_e} \quad (2)$$

where $q_{m,1}$ and $q_{m,2}$ are the maximum adsorption capacities of two different adsorption sites while K_1 and K_2 are energies of the adsorption related to adsorption sites 1 and 2 respectively. In the case of two component systems, the extended BiLangmuir model is given as:

$$q_{e1} = \frac{q_{m,1,1} K_{1,1} C_{e1}}{1 + K_{1,1} C_{e1} + K_{2,1} C_{e2}} + \frac{q_{m,1,2} K_{1,2} C_{e1}}{1 + K_{1,2} C_{e1} + K_{2,2} C_{e2}} \quad (3)$$

$$q_{e2} = \frac{q_{m,2,1} K_{2,1} C_{e2}}{1 + K_{1,1} C_{e1} + K_{2,1} C_{e2}} + \frac{q_{m,2,2} K_{2,2} C_{e2}}{1 + K_{1,2} C_{e1} + K_{2,2} C_{e2}} \quad (4)$$

where $q_{m,1,1}$ and $q_{m,1,2}$ are the maximum adsorption capacities of the component 1 on adsorption sites 1 and 2, respectively and $K_{1,1}$ and $K_{1,2}$ are adsorption energies related to the adsorption of the component 1 on adsorption sites 1 and 2, respectively. Accordingly, $q_{m,2,1}$, $q_{m,2,2}$, $K_{2,1}$ and $K_{2,2}$ are corresponding parameters related to the adsorption of component 2. In this model, both competitive ions form a mixed monolayer on every kind of sites, with a different affinity toward the target compound. It should be noticed that, when a given active site has adsorbed one ion, another ion cannot be adsorbed at the same site.

The *Redlich-Peterson* model incorporates three parameters and can be applied to both the homogeneous and heterogeneous systems [32]. This empirical isotherm (Eq. 5) combines elements from both the Langmuir and the Freundlich isotherm. Mechanism of adsorption is a hybrid and does not follow ideal monolayer adsorption.

$$q_e = \frac{q_m K_{RP} C_e}{1 + K_{RP} C_e^{\,n_{RP}}} \quad (5)$$

where q_m represents the maximum adsorption capacity of adsorbents (mg/g), K_{RP} is a Redlich-Peterson constant and n_{RP} is the dimensionless exponent, which reflects heterogeneity of the binding surface and lies between 1 and 0. This model becomes the Langmuir equation when n_{RP}=1 and the Henry's Law equation when n_{RP}=0. The extended Redlich-Peterson model is a six-parameter model and is given as:

$$q_{e1} = \frac{q_{m1} K_{RP1} C_{e1}}{1 + K_{RP1} C_{e1}^{\,n_{RP1}} + K_{RP2} C_{e2}^{\,n_{RP2}}} \quad (6)$$

$$q_{e2} = \frac{q_{m2} K_{RP2} C_{e2}}{1 + K_{RP1} C_{e1}^{\,n_{RP1}} + K_{RP2} C_{e2}^{\,n_{RP2}}} \quad (7)$$

Where definitions of parameters are same than for one-component equation, but subscript 1 denotes parameters related to component 1 and subscript 2 those related to component 2.

3.2. Determination of isotherm parameters

Modeling of adsorption equilibrium was conducted using nonlinear least squares technique, which reverted to the problem of finding the corresponding adsorption capacity (q_e) such that the deviations between the experimental and the calculated values were small. The isotherm parameters were determined by minimizing one of two objective functions across the concentration range studied:
the Derivative of Marquardt's Percent Standard Deviation (MPSD):

$$\sum_{i=1}^{n}\left(\frac{q_{e,exp}-q_{e,calc}}{q_{e,exp}}\right)_i^2 \quad (8)$$

and the Sum of the Squares of the Errors (ERRSQ):

$$\sum_{i=1}^{n}\left(q_{e,exp}-q_{e,calc}\right)_i^2 \quad (9)$$

where n is the number of experimental data points, $q_{e,exp}$ and $q_{e,calc}$ are experimental and the calculated equilibrium concentration in solid phase, respectively. The Levenberg-Marquardt algorithm was used as an optimization procedure [33]. This method may converge to a local minimum, which gives an unacceptable match of equilibrium data if a poor initial guess is used. An iterative procedure was selected to find the desired solution (global minimum) for this study. This approach implied the evaluation of the objective function (Eq.8 or Eq.9) for different set of the equilibrium model parameters. The value of each of them was changed one at a time (0.0001, 0.001, 0.01, 0.1, 1.0, etc.), keeping the values of the others constant. The border range of optimization was from 1×10^{-10} to 1×10^{10}. This procedure was repeated until the objective function achieved the lowest value.

The relationship between two variables (experimental and theoretically predicted) was assessed by: the coefficient of determination (correlation coefficient squared R^2), standard deviation (σ), and mean error (%) [34].

4. Results and discussion

4.1. Modeling of one-component equilibrium

In order to reduce the calculation error caused by scattering points or by incomplete isotherm curve [35], an effort was made to increase the quality and quantity of experimental data presented in a previous work [8]. It allowed us to obtain an optimal smooth of experimental points along the isotherm range from the near origin of the plot (q_e versus C_e) to the equilibrium plateau (q_m).

The search for an appropriate set of initial model parameters, which converges the optimization procedure to the global minimum, was started with a random value of equilibrium model parameters. For any modification of a given value, the influence on the estimated parameters was examined. Although this approach was tedious and required a certain patience, it allowed for determining a few sets of initial guesses for which a minimum of objective function was achieved for the four-parameter BiLangmuir model. In the three-parameter Redlich-Peterson model case, one minimum of a given objective function was obtained, independently of the initial guess set. Thus, a lower number of adjustable parameters provides a higher robustness of model (global minimum localization).

Tables 3 and 4 summarize the study of the BiLangmuir model sensitivity for two different sets of initial parameter guesses as well as two different objective function assessments (Eq.8 or Eq.9). The capital

letter A relates to the evaluation of an objective function for the set of guess value parameters $q_{m,1}$, K_1, $q_{m,2}$, K_2 equal to 0.3, 1.0, 0.3, 1.0 respectively, where $q_{m,1}$ and $q_{m,2}$ correspond to the experimentally obtained values of maximum adsorption capacity (q_m) (plateau in an equilibrium graph). The capital letter B relates the set of random value of $q_{m,1}$, K_1, $q_{m,2}$, K_2 equal to 0.1, 1.0, 1.0, 1.0 respectively. The initial set A gave the best fit for the BiLangmuir model indicating the importance of using q_m values close to experimental ones as initial guesses (see further discussion in this section). Furthermore, it is worth noting that with exception of the modeling set for Co(II) adsorption on DTSG, neither the statistics concepts depicted in Tables 3 and 4 nor the overlapped line for set A and B presented in Fig. 3A and B, gave any indication that the evaluation of the MPSD objective function was effected by the initial guess parameters. Thus, the coefficient of determination (R^2), standard deviation (σ), and mean error did not give enough evidence to assure that the parameter values corresponded to the global minimum of the objective function [36].

The difficulty in the calculation of the affinity distribution function from an experimental adsorption isotherm is a well known ill-posed problem of the least-squares optimization. The objective function has very small derivatives in several directions, and there are many affinity distributions that all lead to an equally good approximation of the data [37,38]. An iteration procedure showed that use of the experimentally obtained value of maximum adsorption capacity (q_m) as an initial guess (set A) made the problem well-posed and independent of the K_i guess values.

Fig. 2-3 are graphical expressions of modeling fits for one-component adsorption of metal ions on EDSG and DTSG. In figures, the points are taken from the experimental data while the lines denote the modeling results obtained by minimizing the MPSD Eq. (8) or the ERRSQ Eq. (9) objective functions. Visually, the best fit for both the Redlich-Peterson and the BiLangmuir model (for BiL the set A of initial guess), gave the minimization of the ERRSQ error function. This could be due to the fact that a magnitude of the errors and thus the ERRSQ increased the model fit toward data obtained at the high concentration range [16,39] but at the expense of higher variance of the mean error values observed. Better results for ERRSQ function were further confirmed by the lowest values of the standard deviation (σ) and the correlation coefficient squared (R^2) (Tables 2-4).

To make a meaningful comparison between both objective functions, the obtained parameter values were compared with the experimental ones. Based on the previous study it was identified that two different adsorption groups coexisted on the adsorbent surface. These groups were assigned to different speciations of EDTA and DTPA (MINEQL, ver. 2.53, [40]). The mathematical equation of the Redlich-Peterson model does not give any evidence of the number of adsorption sites. However, the value of heterogeneity coefficients (n_{RP}) close to 1 (Table 2) accounted for the fact that a real surface was not completely homogenous and the widths of the corresponding modes of the adsorption energy distribution were not equal to 0. The adsorption fitting parameters for the BiLangmuir model and minimization of the MPSD objective function (Tables 3 and 4) identified either the lack of the low-energy sites for the set B of initial guess or an equal number of the low- and high-energy sites for the set A of initial guess. None of

them corresponded to the experimental findings. Instead, the data obtained for BiLangmuir model and minimization of the ERRSQ objective function for set A of initial guesses (Tables 3 and 4) showed that the value of q_{m2} obtained correlated well with the calculated amount of high affinity groups. To be concluded, the experimental data clearly supported a better applicability of ERRSQ error function in this study.

4.2. Modeling of two-component equilibrium

For practical reasons, it is unfeasible to experimentally determine the partition behavior of all species in a multi-element system for all possible solution compositions. The experimental study should include a border concentration related to Co:Ni concentration ratios equal 1:0 and 0:1 as well. In other words, one-component systems are specific cases of the two-component one when the amount of the competitive ion in the system equals zero. In this study, 11 experimental sets were conducted to check the interactive effect of competitive ions, comprising a total of 165 equilibrium points with respect to both EDSG and DTSG. To the best of our knowledge, the experimental data as wide as here has never been used in binary modeling.

The simultaneous adsorption data of Co(II) and Ni(II) from the two-component systems were fitted to the extended BiLangmuir (Eq. 3,4) and the extended Redlich-Peterson models (Eq. 6,7). In the first instance, the competitive isotherms were estimated solely on the basis of the corresponding one-component isotherm parameters (Tables 2-4). Although the isotherms determined with this method may appear to be correct, it should be emphasized that parameters derived from one-component systems do not take into account the interactions of competitive ions. The value of the maximum adsorption capacity (q_m) in one-component systems is related only to a given cation adsorbed from liquid phase without any competition (Tables 2-4). The adsorption in two-component systems can be affected by competition, interaction, or displacement effects [25]. Consequently, both applied extended models showed a poor fit to the experimental data (see the statistical values depicted in the first rows in Tables 5 and 6).

Accordingly, in the next step, both maximum adsorption capacities (q_{mi}) as well as the coefficient of system heterogeneity (n_{RPi}) (in the Redlich-Peterson model case) associated with the certain adsorption sites, were estimated by minimizing the ERRSQ objective function (Eq. 9). The best parameter sets obtained for one-component systems were used as an initial guess in the two-component equilibrium calculation procedure. It allowed the inclusion of all solutions related to the local minimum of the objective function. The statistical indicators depicted in Tables 5 and 6 (in the second rows) show improvement of the quality of fitting. The obtained results identified that due to an occurrence of other metals in the solution, the maximum uptake (q_m) did not remain constant. Therefore, q_{mi} in two-component system should be treated as adsorption capacity for a given ion in the presence of another competitive ion in the system [41]. This statement was supported by further experimental findings. As can be seen in Fig 4, despite the materials used, they had a little differences in affinity for the metals studied (Co(II) 0.302, Ni(II) 0.329 and Co(II) 0.294, Ni(II) 0.348 mmol/g for EDSG and DTSG, respectively) but exhibited great

differences in affinity for the metal pairs. Based on previous studies, both metal adsorption, and hence availability, depend on the adsorbent properties as well as on the nature of metals involved and their competition for adsorption sites [8,42]. In two-component systems, metal ion uptake is influenced by the presence of another metal ion competing for the same adsorption sites. Thus, the adsorption of both ions is lower than in their one-component systems.

It is quite frequently observed that the presence of another metal in the solution affects not only the maximum uptake of each component but also the shape of the isotherm curve, due to changes in apparent metal affinity for the active sites [25]. Accordingly, in the last approach all isotherm parameters were estimated. The rationale for this method is that the deviations caused by an interaction between competitive ions in liquid and solid phase are far too complicated to be mathematically described by any empirical equation. The model is considered to be purely predictive if the parameters used are obtained from one-component systems [27]. On the other hand, even if the parameters obtained for one-component systems do not reflect the complexity of multi-component one, they can be used as good initial values in the multi-elements equilibrium calculation procedure [43].

The adsorption fitting parameters for the extended Redlich-Peterson and the extended BiLangmuir model are depicted in Tables 5 and 6 (the third rows) respectively. The presented results show that the increase of involving adjustable parameters lead to better approximation of experimental data as substantiated by statistical correlations [29]. However, in both adsorbent cases, the extended Redlich-Peterson model overestimated the maximum Ni(II) uptake. An examination of results (Table 5) also showed that the heterogeneity factor (n_{RP}) values for the extended Redlich-Peterson model approached unity. This indicated that a material with relatively homogeneous binding sites had similar adsorption affinity toward competitive ions [25]. However, latter disagreed with the experimental findings. Fig. 4 shows that although the competition reduced the adsorption of both metals, the magnitude of this effect was different for both of them. The selectivity coefficient for Ni(II) was calculated from the ratio of the distribution constant ($q_{e,Ni}/C_{e,Ni}$) for Ni(II) over the distribution constant for Co(II) ($q_{e,Co}/C_{e,Co}$). For EDSG the selectivity constants for Ni(II) varied from 10 to 20 and for DTSG from 6 to 15. Very high values confirmed the modified silica gels having better selectivity and affinity for Ni(II) than for Co(II), which can be attributed to the higher stability constants of Ni(II)EDTA/DTPA chelates compared to the corresponding Co(II) chelates [8] as well as a smaller hydrated radius of Ni(II) [44].

The three-dimensional Fig. 5A and B compare the experimental and modeling data obtained for the extended BiLangmuir model by minimizing the ERRSQ objective function (Eq. 9), when all the parameters were adjusted. In the figures, an equilibrium concentration of given metal in adsorbent phase (*z*-axis) is plotted as a function of the equilibrium concentrations of the two metal ions in liquid phase (*x*- and *y*-axis). The relationships illustrated in all figures demonstrate that the extended BiLangmuir model could be successfully used for the estimation of the adsorption behavior of Co(II) and Ni(II) from two-component mixtures on the EDSG/DTSG. However, a quite big mean error values (Table 6) made the model applicability a bit doubtful. To have a deeper insight into the quality of the model fit, single sets of two-

component adsorption data were presented in two-dimensional graphs. Fig. 6 presents comparison of the experimental and modeling data obtained for two sets of competitive adsorption for Co:Ni ratios of 1:9 and 9:1 as an example. The calculated curves clearly show the deviations from the experimental points. Obviously, this effect originated from the presence of relatively strong ion interactions that were able to change the behavior of isotherm model in a qualitative way. It was further confirmed by the mean error values that represent the average of absolute difference between experimental and modeling data. On the other hand, after removing only one equilibrium point obtained for the lowest concentration of competitive ions from each experimental set, the mean error values reduced over a half (data not shown). This is most likely due to the fact that the lowest concentration range was saddled with the highest analytical error (see ERRSQ properties above), especially for high difference between the concentrations of the competitive ions. In such a case, minor changes of the experimental values can lead to enormous changes in the determined parameters and increase the calculation error [38]. Although some doubts presented above, extended BiLangmuir model provided a rather good fit to the experimental two-component data supported by the one-component results.

Last but not least, the calculation procedure can also hold shares in quality of optimization. As long as the number of estimated parameters was limited to only a few (in one-component systems), the simple approach of minimization (Eq. 8 and Eq. 9) was enough to give satisfactory results. In the eight parameter cases (two-component systems) the data might have been "overfitted" meaning that the points of random variations caused by the experimental errors were also fitted by the model. In this case, the resulting values of objective functions became very small and statistically very unlikely [38].

5. Conclusions

In this work the BiLangmuir and the Redlich-Peterson models as well as their extended equations were tested for the modeling of one- and two-component adsorption equilibrium of Co(II) and Ni(II) ions on modified silica gels. In the simulations, the effect of the initial guessed parameters and two objective functions (MPSD and ERRSQ) were tested. In contrast to the three-parameter Redlich-Peterson model, the optimal solution of nonlinear parameter estimation for the four-parameter BiLangmuir equation depended mostly on the initial guess of parameter values. The best correlation with the experimental data was obtained using initial guesses of maximum adsorption capacities (q_{m}) corresponding to the experimentally obtained ones (plateau in an equilibrium graph). In this case, the Levenberg-Marquardt algorithm converged to a global minimum. This indicated that even though the experimentally obtained q_{m} might not exactly link to the value of maximum adsorption level, it still often has at least some quantitative knowledge about the parameter magnitude. This may give important insight into the proper design of adsorption systems. From objective functions ERRSQ gave the better overall fit to the experimental data

than MPSD. This was supported by both statistical analysis (except mean error values) and experimental observations.

The competition in the two-component systems revealed complex phenomena, where standard behavior was not observed. Thus, none of the parameters obtained for one-component systems could satisfactorily help in predicting the two-component adsorption equilibrium. The application of the extended Bilangmuir model confirmed the coexistence of low- and high-energy active sites on EDSG and DTSG that showed an unequal ability for Co(II) and Ni(II) adsorption. However, the overlapping parts of the resulting isotherms presented in the three-dimensional graphs could not provide a useful evaluation of the accuracy of the fit. The obtained result gave ground to the assumption that the modeling of multi-component equilibrium without knowledge of the nature of the phenomenon involved is always fraught with the danger of matching an inadequate multi-component model.

Acknowledgements

The authors gratefully acknowledge the European Commission (Brussels) for the Marie Curie Research Fellowship for Transfer of Knowledge (No.MTKD-CT-2006-042637) and Finnish Funding Agency for Technology and Innovation (TEKES) for the financial support. Karina Kwiecińska is acknowledged for her great contribution in performing experiments in laboratory.

References

[1] P.K. Jal, R.K. Dutta, M. Sudarshan, A. Saha, S.N. Bhattacharyya, S.N. Chintalapudi, B.K. Mishra, Extraction of metal ions using chemically modified silica gel: a PIXE analysis, Talanta 55 (2001) 233–240.

[2] P.K. Jal, S. Patel, B.K. Mishra, Chemical modification of silica surface by immobilization of functional groups for extractive concentration of metal ions, Talanta 62 (2004) 1005–1028.

[3] K.A. Venkatesan, V. Sukumaran, M.P. Antony, P.R. Vasudeva Rao, Extraction of uranium by amine, amide and benzamide grafted covalently on silica gel, J. Radioanal. Nucl. Chem. 260 (2004) 443-450.

[4] A.R. Sarkar, P.K. Datta, M. Sarkar, Sorption recovery of metal ions using silica gel modified with salicylaldoxime, Talanta 43 (1996) 1857–1862.

[5] B.S. Garg, R.K. Sharma, J.S. Bist, N. Bhojak, S. Mittal, Separation and preconcentration of metal ions and their estimation in vitamin, Talanta 48 (1999) 49–55.

[6] J.S. Kim, J.C. Park, J. Yi, Zinc ion removal from aqueous solutions using modified silica impregnated with 2-ethylhexyl-2-ethylhexyl phosphonic acid, Sep. Sci. Tech. 35 (2000) 1901–1916.

[7] I.M. El-Nahhal, F.R. Zaggout, M.A. Nassar, N.M. El-Ashgar, J. Maquet, F. Babonneau, M.M. Chehimi, Synthesis, characterization and applications of immobilized iminodiacetic acid-modified silica, J. Sol-Gel Sci. Tech. 28 (2003) 255–265.

[8] E. Repo, T.A. Kurniawan, J.K. Warchol, M.E.T. Sillanpää, Removal of Co(II) and Ni(II) ions from contaminated water using silica gel functionalized with EDTA and/or DTPA as chelating agents, J. Hazard. Mat. 171 (2009) 1071–1080.

[9] A.N. Kursunlu, E. Guler, H. Dumrul, O. Kocyigit, I.H. Gubbuk, Chemical modification of silica gel with synthesized new Schiff base derivates and sorption studies of cobalt (II) and nickel (II), Appl. Surf. Sci. 255 (2009) 8798–8803.

[10] Y. Shiraishi, G. Nishimura, T. Hirai, I. Komasawa, Separation of Transition Metals Using Inorganic Adsorbents Modified with Chelating Ligands, Ind. Eng. Chem. Res. 41 (2002) 5065–5070.

[11] D.M. Ruthven, Principles of adsorption and adsorption process. Wiley-Interscience, New York 1984, p.108.

[12] A. Seidel-Morgenstern, G. Guiochon, Modelling of the competitive isotherms and the chromatographic separation of two enantiomers, Chem. Eng. Sci. 48 (1993) 2787–2797.

[13] G. Limousin, J.-P. Gaudet, L. Charlet, S. Szenknect, V. Barthe, M. Krimissa, Sorption isotherms: A review on physical bases, modeling and measurement, Appl. Geochem. 22 (2007) 249–275.

[14] D.G. Kinniburgh, General purpose adsorption isotherms, Environ Sci. Technol. 20 (1986) 895–904.

[15] Y.S. Ho, J.F. Porter, G. McKay, Equilibrium isotherm studies for the sorption of divalent metal ions onto peat: copper, nickel and lead single component systems, Water Air Soil Pollut. 141 (2002) 1–33.

[16] S.J. Allen, G. Mckay, J.F. Porter, Adsorption isotherm models for basic dye adsorption by peat in single and binary component systems, J. Colloid. Interface Sci. 280 (2004) 322–333.

[17] K.V. Kumar, K. Porkodi, Relation between some two- and three-parameter isotherm models for the sorption of methylene blue onto lemon peel, J. Hazard. Mater. 138 (2006) 633–635.

[18] P. Seferlis, A.N. Hrymak, Sensitivity analysis for chemical process optimization, Computers Chem. Eng. 20 (1996) 1177–1200.

[19] P. Misaelides, D. Zamboulis, P. Sarridis, J. Warchoł, A. Godelitsas, Chromium (VI) uptake by polyhexamethylene-guanidine-modified natural zeolitic materials, Micropor. Mesopor. Mater. 108 (2008) 162–167.

[20] K.V. Kumar, S. Sivanesan, Prediction of optimum sorption isotherm: Comparison of linear and non-linear method, J. Hazard. Mater. B126 (2005) 198–201.

[21] D. Kumar, A. Singh, J.P. Gaur, Mono-component versus binary isotherm models for Cu(II) and Pb(II) sorption form binary metal solution by the green alga *Pithophora oedogoni*, Bioresour. Technol. 97 (2008) 8280–8287.

[22] A.L. Myers, J.M. Prausnitz, Prediction of the adsorption isotherm by the principle of corresponding states, Chem. Eng. Sci. 20 (1965) 549–556.

[23] S. Al-Asheh, F. Banat, R. Al-Omari, Z. Duvnjak, Predictions of binary sorption isotherms for the sorption of heavy metals by pine bark using single isotherm data, Chemosphere 41 (2000) 659-665.

[24] R. Apiratikul, P. Pavasant, Sorption isotherm model for binary component sorption of copper, cadmium, and lead ions using dried green macroalga, *Caulerpa lentillifera*, Chem. Eng. J. 119 (2006) 135–145.

[25] S.K. Papageorgiou, F.K. Katsaros, E.P. Kouvelos, N.K. Kanellopoulos, Prediction of binary adsorption isotherms of Cu^{2+}, Cd^{2+} and Pb^{2+} on calcium alginate beads from single adsorption data, J. Hazard. Mater. 162 (2009) 1347–1354.

[26] B. Xiao, K.M. Thomas, Competitive adsorption of aqueous metal ions on an oxidized nanoporous activated carbon, Langmuir 20 (2004) 4566-4578.

[27] R.S. Vieira, E. Guibal, E.A. Silva, M.M. Beppu, Adsorption and desorption of binary mixtures of copper and mercury on natural and crosslinked chitosan membranes, Adsorption 13 (2007) 603–611.

[28] B. Al-Duri, A review in equilibrium in single and multicomponent liquid adsorption systems, Rev. Chem. Eng. 11 (1995) 101–143.

[29] F. Pagnanelli, M. Trifoni, F. Beolchini, A. Esposito, L. Toro, F. Veglio, Equilibrium biosorption studies in single and multi-metal systems, Process. Biochem. 37 (2001) 115–124.

[30] L. Asnin, K. Kaczmarski, G. Guiochon, Empirical development of a binary adsorption isotherm based on the single-component isotherms in the framework of a two-site model, J. Chrom. A 1138 (2007) 158–168.

[31] G. Guiochon, A. Felinger, D.G. Shirazi, A.M. Katti, Fundamentals of preparative and nonlinear chromatography. Elsevier, NY, 2006.

[32] O. Redlich, D.L. Peterson, A useful adsorption isotherm, Z. Phys. Chem. 63 (1959) 1024–1026.

[33] D.W. Marquardt, An algorithm for least-square optimization of non linear parameter, J. Soc. Ind. Appl. Math. 11 (1963) 431–441.

[34] S.C. Chapra, R.P. Canale, Numerical methods for engineers, 2nd ed., McGraw Hill International, USA, 1990.

494 [35] K.V. Kumar, S. Sivanesan, Equilibrium data, isotherm parameters and process design for partial and
495 complete isotherm of methylene blue onto activated carbon, J. Hazard. Mater. B134 (2006) 237–244.
496
497 [36] M. Chutkowski, R. Petrus, J. Warchol, P. Koszelnik, Sorption equilibrium of heavy metals removal
498 from aqueous solutions. Statistical verification of mathematical models. Przemysl. Chem. 87 (2008) 436-
499 438.
500
501 [37] F. Zhang, A.C. Reynolds, D.S. Oliver, An initial guess for the Levenberg-Marquardt algorithm for
502 conditioning a stochastic channel to pressure data, Mathematical Geology 35 (2003) 67–88.
503
504 [38] M. Cernik, M. Borkovec, J.C. Westall, Regularized least-Squares methods for the calculation of
505 discrete and continuous affinity distributions for heterogeneous sorbents. Environ. Sci. Technol. 29 (1995)
506 413–425.
507
508 [39] K.Y. Foo, B.H., Hameed, Insight into the modeling of adsorption isotherm systems. Chem. Eng. J. 156
509 (2010) 2–10.
510
511 [40] E. Repo, L. Malinen, R. Koivula, R. Harjula, M. Sillanpää, Capture of Co(II) from its aqueous EDTA-
512 chelate by DTPA-modified silica gel and chitosan, accepted manuscript in J. Hazard. Mater.
513
514 [41] R. Petrus, J.K. Warchol, Heavy metal removal by clinoptilolite. An equilibrium study in multi-
515 component systems, Water Res. 39 (2005) 819–830.
516
517 [42] V. Antoniadis, C.D. Tsadilas, D.J. Ashworth, Monometal and competitive adsorption of heavy metals
518 by sewage sludge-amended soil, Chemosphere 68 (2007) 489–494.
519
520 [43] K. Kaczmarski, D. Zhou, M. Gubernak, G. Guiochon, Equivalent models of indanol isomers
521 adsorption on cellulose tribenzoate, Biotechnol. Prog. 19 (2003) 455–463.
522
523 [44] S. Triantafyllou, E. Christodolou, P. Neou-Syngouna, Removal of nickel and cobalt from aqueous
524 solutions by Na-activated bentonite, Clays Clay Miner. 47 (1999) 567–572.
525

Table 1. Properties of modified silica gels.

Adsorbents	Particle size (μm)	EDTA/ DTPA (mmol/g)	Specific surface area (m^2/g)	Total pore volume (cm^3/g)	Point of zero-charge
EDSG	40-63	0.32	384	0.48	4.0
DTSG	40-63	0.23	328	0.41	4.0

Table 2. Redlich-Peterson constants for the one-component adsorption of Co(II) and Ni(II) ions on EDSG and DTSG.

Sorbent	Objective function	metal	$q_{m,exp}$ (mmol/g)	q_m (mmol/g)	n	K_{RP} (L/mmol)	R^2	σ	ME (%)
EDSG	ERRSQ	Co	0.302	0.277	0.909	82.220	0.9939	0.011	21.795
	MPSD	Co	0.302	0.296	0.997	19.644	0.9786	0.293	15.622
	ERRSQ	Ni	0.329	0.312	0.916	84.481	0.9840	0.020	46.664
	MPSD	Ni	0.329	0.369	1.084	7.348	0.9661	0.419	22.698
DTSG	ERRSQ	Co	0.294	0.273	0.923	97.928	0.9968	0.008	12.010
	MPSD	Co	0.294	0.281	0.986	40.016	0.9875	0.212	11.508
	ERRSQ	Ni	0.348	0.298	0.879	73.123	0.9869	0.018	52.316
	MPSD	Ni	0.348	0.379	1.088	4.673	0.9638	0.439	24.218

Table 3. BiLangmuir constants for the one-component adsorption of Co(II) and Ni(II) ions on EDSG.

	metal	$q_{m,exp}$ (mmol/g)	q_{m1} (mmol/g)	K_{BiL1} (L/mmol)	q_{m2} (mmol/g)	K_{BiL2} (L/mmol)	R^2	σ	ME (%)	Surface coverage of high affinity groups*
Guess value A			0.3	1.0	0.3	1.0				
ERRSQ	Co	0.302	0.132	1.883	0.193	110.671	0.9962	0.009	20.827	0.178
MPSD	Co	0.302	0.148	19.610	0.148	19.610	0.9780	0.301	15.726	0.178
ERRSQ	Ni	0.329	0.142	2.328	0.215	118.205	0.9869	0.019	46.605	0.194
MPSD	Ni	0.329	0.180	7.833	0.180	7.833	0.9699	0.434	22.234	0.194
Guess value B			0.1	1.0	1.0	1.0				
ERRSQ	Co	0.302	0.102	$1.75*10^9$	0.274	1.568	0.9161	0.040	79.447	0.178
MPSD	Co	0.302	bcl	bcl	0.296	19.610	0.9780	0.301	15.726	0.178
ERRSQ	Ni	0.329	0.111	$1.67*10^9$	0.303	1.750	0.9153	0.046	93.546	0.194
MPSD	Ni	0.329	bcl	bcl	0.360	7.833	0.9699	0.434	22.235	0.194

bcl – beyond calculation limit

* High affinity groups were $SiO2\text{-}NH\text{-}HEDTA^{-2}$, of which amount was calculated using MINEQL software, ver. 2.53,

Table 4. BiLangmuir constants for the one-component adsorption of Co(II) and Ni(II) ions on DTSG.

	metal	$q_{m,exp}$ (mmol/g)	q_{m1} (mmol/g)	K_{BiL1} (L/mmol)	q_{m2} (mmol/g)	K_{BiL2} (L/mmol)	R^2	σ	ME (%)	Surface coverage of high affinity groups*
Guess value A			0.3	1.0	0.3	1.0				
ERRSQ	Co	0.294	0.116	2.784	0.190	137.372	0.9980	0.006	11.692	0.168
MPSD	Co	0.294	0.140	39.674	0.140	39.674	0.9839	0.219	12.088	0.168
ERRSQ	Ni	0.348	0.171	1.118	0.208	86.902	0.9882	0.018	51.612	0.198
MPSD	Ni	0.348	0.183	5.021	0.183	5.021	0.9702	0.455	23.549	0.198
Guess value B			0.1	1.0	1.0	1.0				
ERRSQ	Co	0.294	0.102	$2.96*10^9$	0.259	1.724	0.9029	0.042	76.239	0.168
MPSD	Co	0.294	0.009	$2.17*10^9$	1.996	0.370	0.9124	0.467	29.743	0.168
ERRSQ	Ni	0.348	0.098	$1.65*10^9$	0.318	1.580	0.9367	0.040	93.373	0.198
MPSD	Ni	0.348	bcl	bcl	0.366	5.021	0.9702	0.455	23.549	0.198

bcl – beyond calculation limit

* High affinity groups were SiO2-NH-H_2DTPA^{-2}, of which amount was calculated using MINEQL software, ver. 2.53.

Table 5. Redlich-Peterson constants for the two-component adsorption of Co(II) and Ni(II) ions on EDSG and DTSG.

Sorbent	q_{mCo} (mmol/g)	K_{RPCo} (L/mmol)	n_{Co}	q_{mNi} (mmol/g)	K_{RPNi} (L/mmol)	n_{Ni}	R^2	σ	ME (%)
EDSG	n.e.	n.e.	n.e.	n.e.	n.e.	n.e.	0.7516	0.076	90.808
	0.191	n.e.	0.950	0.396	n.e.	0.952	0.8440	0.062	117.944
	0.312	13.952	1.003	0.317	120.230	0.929	0.9801	0.023	105.621
DTSG	n.e.	n.e.	n.e.	n.e.	n.e.	n.e.	0.7548	0.071	117.719
	0.191	n.e.	0.978	0.376	n.e.	0.928	0.8436	0.058	104.873
	0.308	15.851	1.033	0.297	98.063	0.918	0.9791	0.022	138.100

n.e. – non estimated

Table 6. BiLangmuir constants for the two-component adsorption of Co(II) and Ni(II) ions on EDSG and DTSG. Error function ERRSQ

Sorbent	q_{mCo1} (mmol/g)	q_{mCo2} (mmol/g)	K_{BiLCo1} (L/mmol)	K_{BiLCo2} (L/mmol)	$q_{m\,Ni1}$ (mmol/g)	$q_{m\,Ni2}$ (mmol/g)	K_{BiLNi1} (L/mmol)	$K_{BiLNi\,2}$ (L/mmol)	R^2	σ	ME (%)
EDSG	n.e.	n.e.	n.e.	n.e.	n.e.	n.e.	n.e.	n.e.	0.7639	0.074	138.983
	0.047	0.158	n.e.	n.e.	0.220	0.238	n.e.	n.e.	0.8565	0.060	110.941
	0.099	0.238	0.529	70.084	0.098	0.229	492.982	13.907	0.9864	0.018	106.953
DTSG	n.e.	n.e.	n.e.	n.e.	n.e.	n.e.	n.e.	n.e.	0.7097	0.078	128.386
	0.064	0.312	n.e.	n.e.	0.124	0.240	n.e.	n.e.	0.9542	0.031	132.280
	0.065	0.242	0.667	81.245	0.087	0.219	397.411	12.567	0.9870	0.017	85.997

n.e. – non estimated

Figures

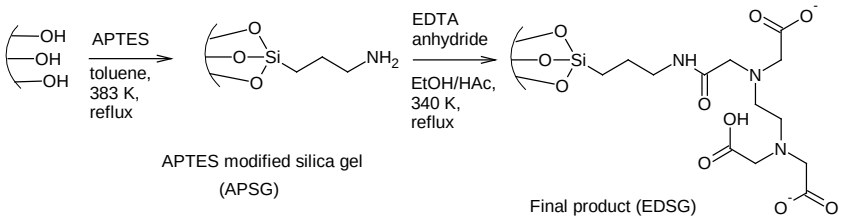

Fig. 1. Synthesis of EDSG.

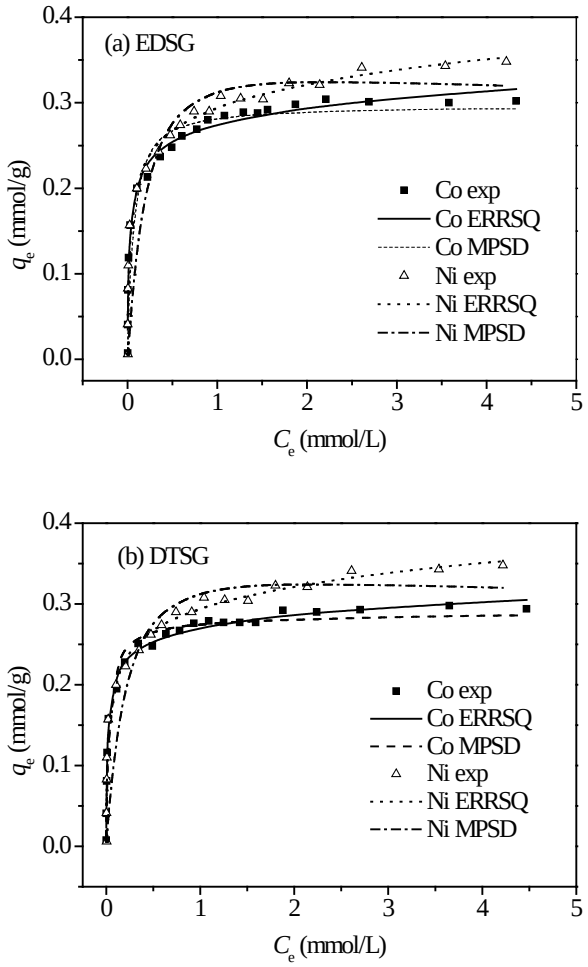

Fig. 2. Comparison between the Redlich-Peterson model and experimental data obtained for Co(II) and Ni(II) adsorption on (a) EDSG and (b) DTSG.

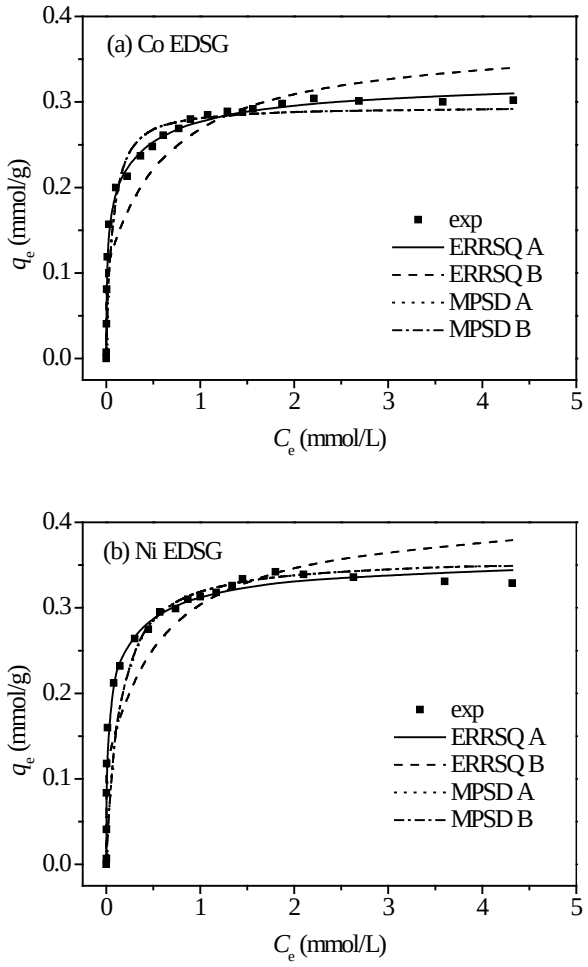

Fig. 3A. The effect of guess values and error function on one-component systems' optimization for the BiLangmuir model for EDSG. Set A relates to the guess value of parameters $q_{m,1}$, $q_{m,2}$, K_1, K_2 equal 0.3, 1.0, 0.3, 1.0, respectively. Set B relates to the guess value of parameters $q_{m,1}$, $q_{m,2}$, K_1, K_2 equal 0.1, 1.0, 1.0, 1.0, respectively.

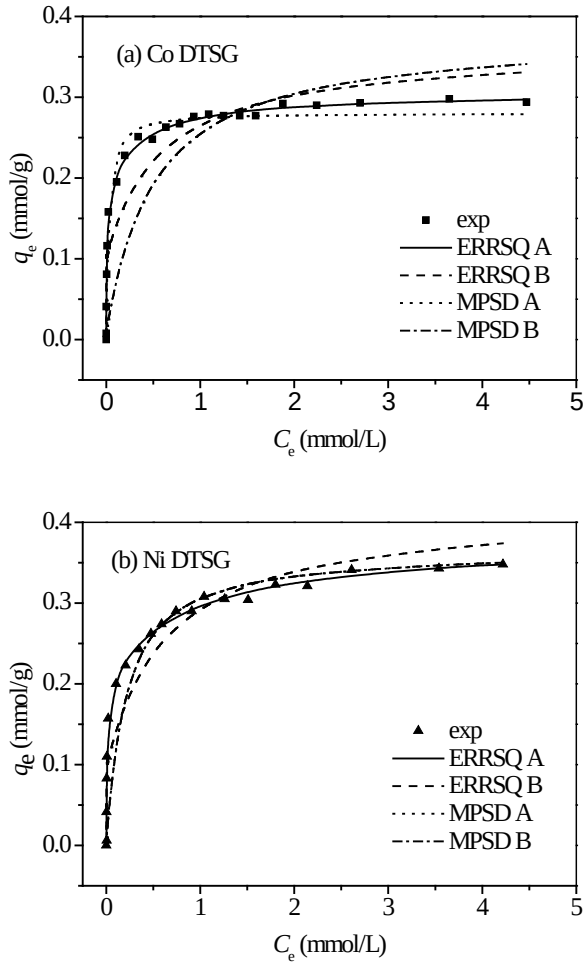

Fig. 3B. The effect of guess values and error function on one-component systems' optimization for the BiLangmuir model for DTSG. Set A relates to the guess value of parameters $q_{m,1}$, $q_{m,2}$, K_1, K_2 equal 0.3, 1.0, 0.3, 1.0, respectively. Set B relates to the guess value of parameters $q_{m,1}$, $q_{m,2}$, K_1, K_2 equal 0.1, 1.0, 1.0, 1.0, respectively.

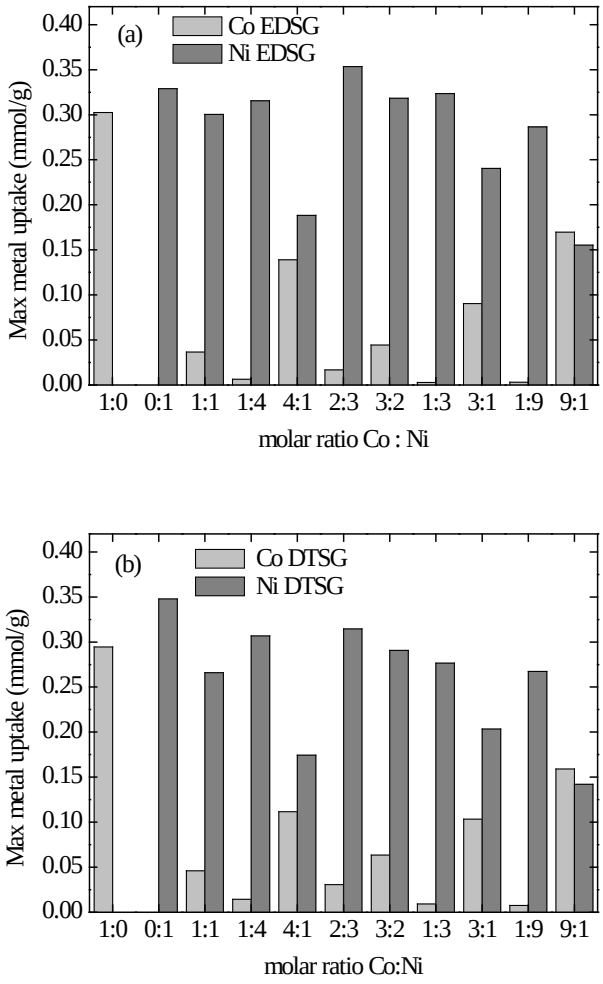

Fig.4. Comparison of metal uptake in two-component systems. (a) EDSG and (b) DTSG.

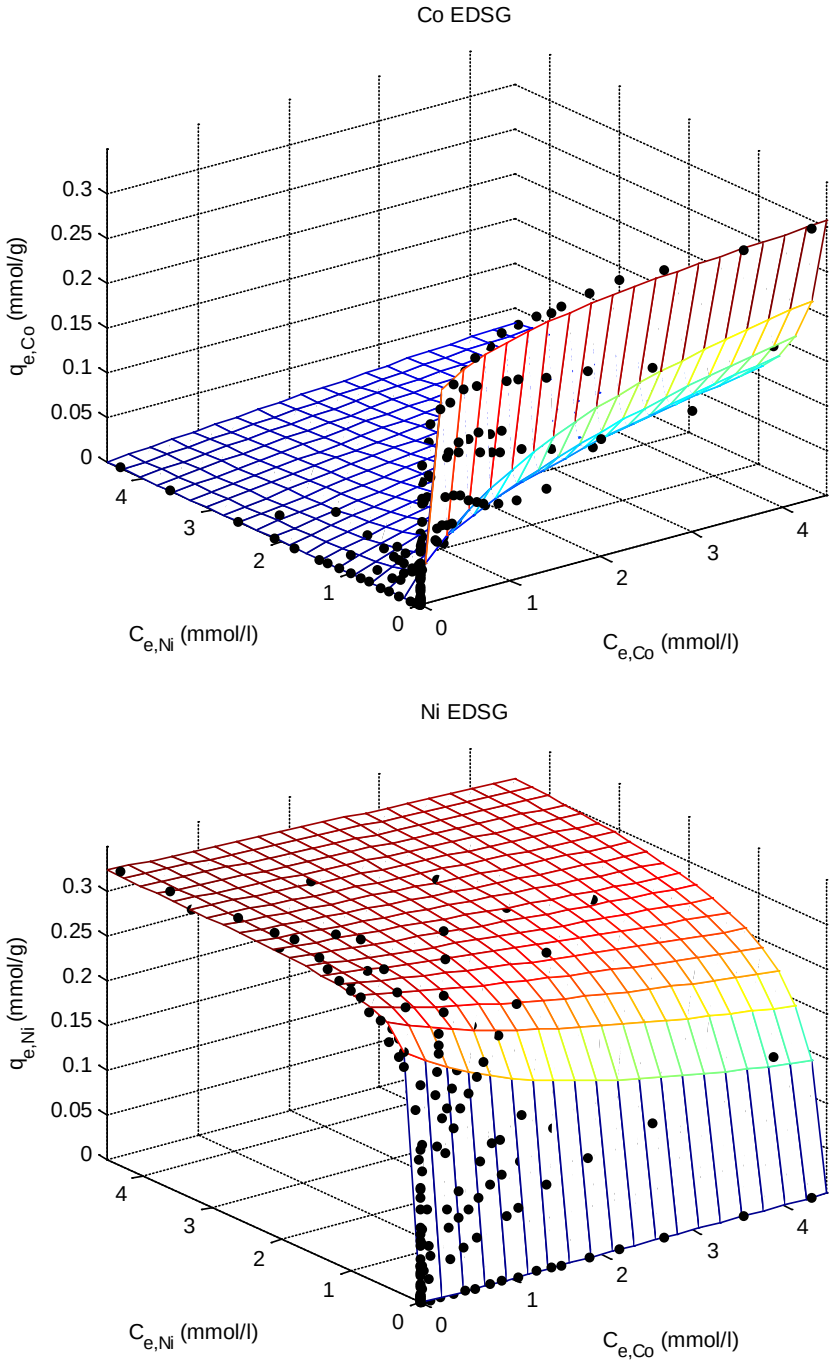

Fig.5A. Comparison between the extended BiLangmuir model and experimental data obtained for Co(II) and Ni(II) adsorption on EDSG.

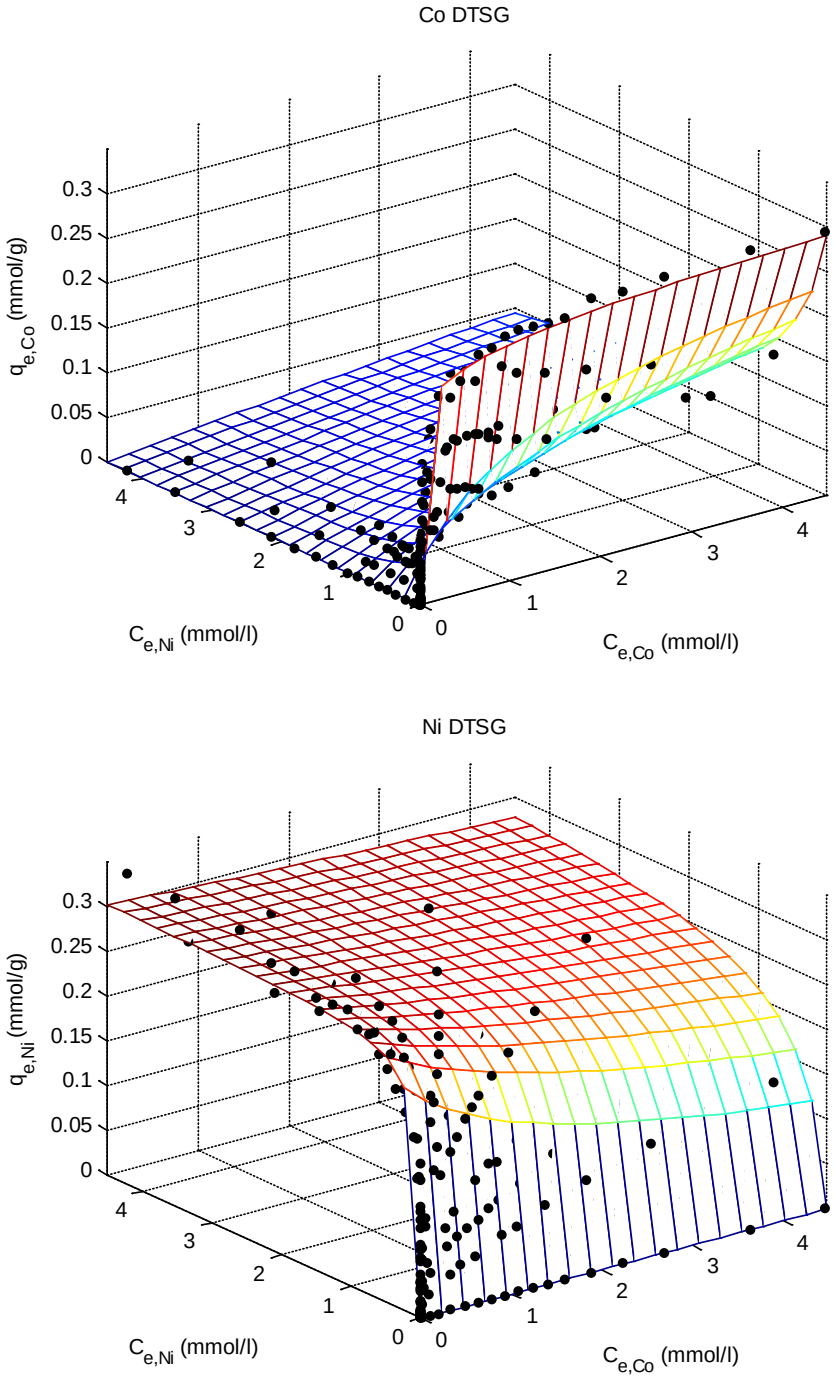

Fig.5B. Comparison between the extended BiLangmuir model and experimental data obtained for Co(II) and Ni(II) adsorption on DTSG.

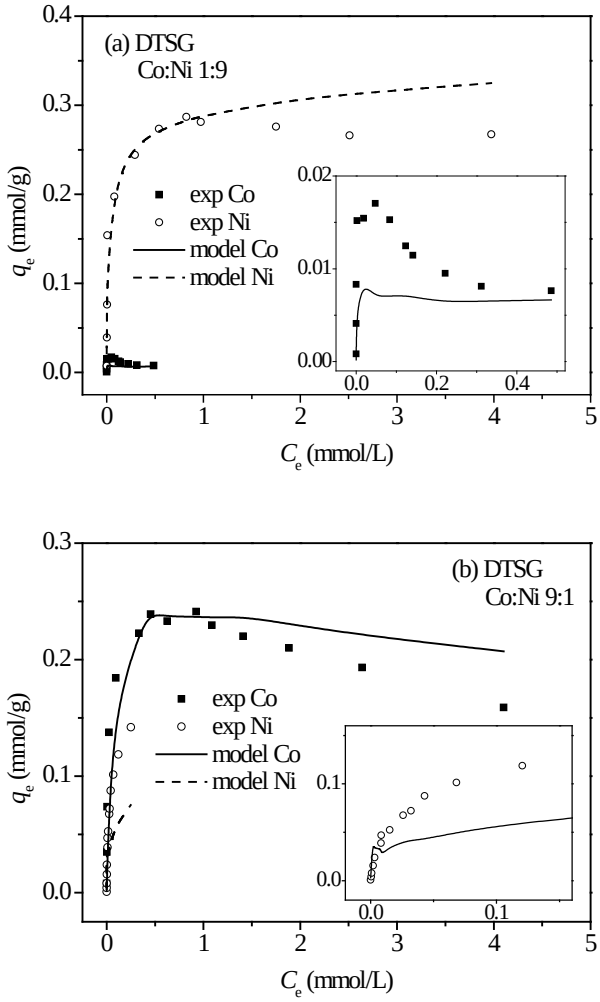

Fig.6 Comparison between the extended BiLangmuir model and experimental data obtained for experimental set for Co:Ni ratio of (a) 1:9 (b) 9:1.

Paper V

Capture of Co(II) from its aqueous EDTA-chelate by DTPA-modified silica gel and chitosan

Eveliina Repo, Leena Malinen, Risto Koivula, Risto Harjula, Mika Sillanpää

Journal of Hazardous Materials 187 (2011) 122–132

Journal of Hazardous Materials 187 (2011) 122–132

Contents lists available at ScienceDirect

Journal of Hazardous Materials

journal homepage: www.elsevier.com/locate/jhazmat

Capture of Co(II) from its aqueous EDTA-chelate by DTPA-modified silica gel and chitosan

Eveliina Repo[a,c,*], Leena Malinen[b], Risto Koivula[b], Risto Harjula[b], Mika Sillanpää[a,c]

[a] Laboratory of Green Chemistry, Department of Energy and Environmental Technology, Faculty of Technology, Lappeenranta University of Technology, Patteristonkatu 1, FI-50100 Mikkeli, Finland
[b] Laboratory of Radiochemistry, Department of Chemistry, University of Helsinki, P.O. Box 55, FI-00014 Helsinki, Finland
[c] Department of Environmental Science, The Faculty of Sciences and Forestry, The University of Eastern Finland, Patteristonkatu 1, FI-50100 Mikkeli, Finland

ARTICLE INFO

Article history:
Received 15 September 2010
Received in revised form 2 December 2010
Accepted 30 December 2010
Available online 6 January 2011

Keywords:
EDTA
DTPA
Silica gel
Chitosan
Water treatment

ABSTRACT

The adsorption of Co(II) by diethylenetriaminepentaacetic acid (DTPA)-modified silica gel and chitosan in the presence of EDTA and other interfering species was studied. Co(II) removal ranged from 93% to 96% from the solutions where Co(II) was totally chelated by EDTA. The amount of oxalate or Fe(II) did not affect the adsorption of Co(II) in the case of DTPA-chitosan. However, increasing the amount of oxalate enhanced the adsorption performance of DTPA-silica gel, probably due to the formation of new active sites on the silica gel surface. DTPA-chitosan was also effective in simulated decontamination solutions. For DTPA-silica gel, the rate of adsorption of free Co(II) was controlled by pore diffusion, but the rate of adsorption of Co(II)EDTA was controlled by the surface chelation reaction, which was attributed to the inhibited diffusion of Co(II)EDTA inside the silica gel mesopores. However, the macroporous structure of DTPA-chitosan enabled pore diffusion of both Co(II) and Co(II)EDTA. The equilibrium isotherms of DTPA-silica gel were best described by a BiLangmuir model, in which there are two different adsorption sites on the silica gel surface assigned to different speciations of DTPA. For DTPA-chitosan, the data fit best with a Sips model, which indicates system heterogeneity. Finally, measurements with capillary electrophoresis showed an increase in dissolved EDTA during adsorption, demonstrating the ability of DTPA-modified adsorbents to release Co(II) from its EDTA chelate. This promising result can provide a basis for applying the studied materials to the treatment of water effluents containing Co(II) chelated by EDTA by a simple one-step adsorption process.

1. Introduction

Ethylenediaminetetraacetic acid (EDTA) is a chelating agent that is widely used in industrial cleaning, the nuclear industry, pharmaceuticals, and manufacturing of textile leather, rubber, and paper [1–6]. The main reason for using EDTA in many of these applications is to clear pipes and reactors of metal ions or prevent their precipitation through chelation [7]. Chelating agents and their salts are not toxic as such, but environmental concerns arise due to the potential for EDTA to remobilize the metals from sediments and decrease the efficiency of heavy metal elimination in wastewater treatment processes [8,9]. Moreover, EDTA contains about 10% nitrogen, which causes eutrophication in the aquatic environment.

Low-level radioactive waste (LLRW) arising from the operation of nuclear power plants (NPPs) and medical use of radioactive isotopes accounts for more than 90% of the volume but only 1% of the radioactivity of all radioactive waste [10]. However, this waste is still hazardous and has to be treated and stored properly. Many of the liquid waste streams from NPPs contain chelating agents, such as EDTA, originating from cleaning solutions used to decontaminate NPP structures [11]. Treatment of radioactive waste containing chelating agents by conventional methods like non-specific ion exchangers, precipitation or mixing with cement produces large amounts of waste to treat and dispose of [12,13]. Combined treatment of radioactive waste involving destruction of chelant before adsorption has been shown to be useful but additional treatment steps usually increase the cost and time spent for the whole process [14]. Thus, a one-step method that is both economical and reduces the amount of LLRW is needed. Selective ion-exchangers may be the most promising solution to this problem.

Various ion exchange materials have been tested for metal adsorption from solutions containing EDTA or other complexing agents. Such materials are, for example, titanium antimonates [11], clay minerals [15], commercial anion exchangers [7,16], commercial cation exchangers [17], copolymers with amino groups

* Corresponding author. Tel.: +358 15 355 3707; fax: +358 15 336 013.
E-mail addresses: eveliina.repo@lut.fi (E. Repo), mika.sillanpaa@lut.fi (M. Sillanpää).

0304-3894/$ – see front matter © 2011 Elsevier B.V. All rights reserved.
doi:10.1016/j.jhazmat.2010.12.113

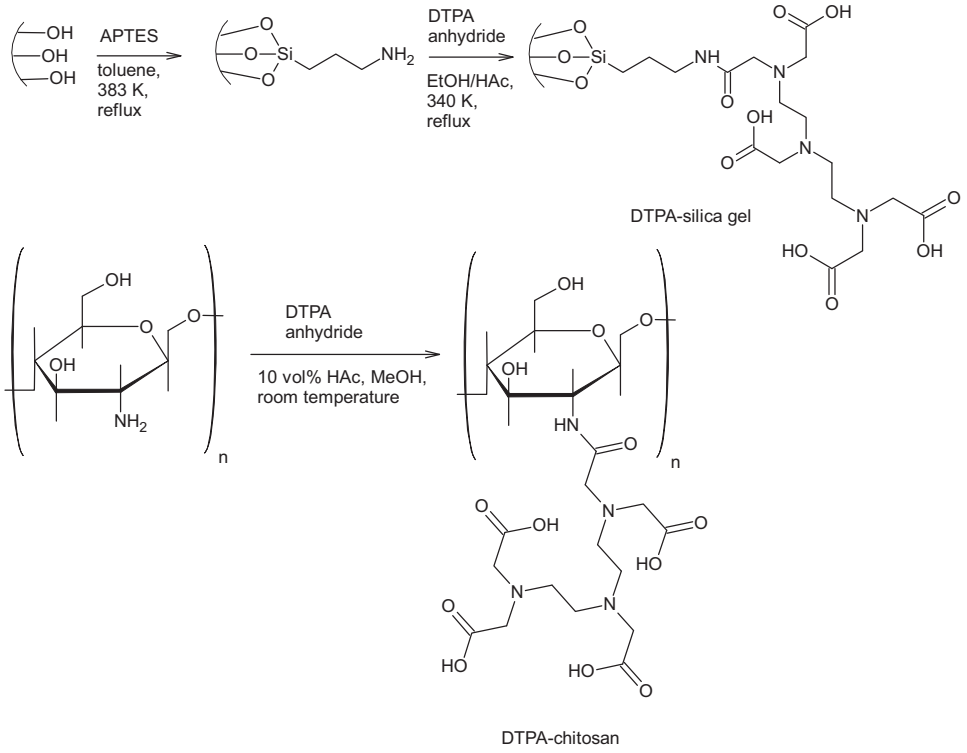

Fig. 1. Synthesis of DTPA-modified adsorbents.

[18], polyethyleneimine-agarose [19], and chitosan [20–23]. The studies above were based on either cation exchange between a dissolved metal–EDTA chelate and the ion exchanger or anion exchange where the whole metal–EDTA chelate was adsorbed. For the treatment of radioactive waste, cation exchange is preferred due to the fact that EDTA may enhance the leaching of radionuclides from the disposal sites. New, effective cation exchangers should contain chelating agents with higher binding affinities towards target metals than EDTA. Such a chelating agent is, for example, diethylenetriaminepentaacetic acid (DTPA).

The aim of this work was to study the applicability of DTPA-functionalized silica gel and chitosan [24,25] to the adsorption of Co(II) in the presence of EDTA. Co(II) was selected as the target metal because its radioactive isotope ^{60}Co is one of the most problematic waste nuclides, with quite a long half-life (5.2 years) and high gamma decay energy [11]. DTPA-modified silica gel [24] and chitosan [25] have been found to be effective adsorbents for Co(II) from pure metal solutions. These studies included only fundamental investigations of metal solutions without any interfering species. However, in this work, the adsorption properties of DTPA-modified adsorbents in the Co(II) solutions containing EDTA as a strong chelating agent as well as some other interfering ions such as oxalate, calcium, permanganate, and iron were studied. Moreover, the release of EDTA during the Co(II) adsorption was experimentally confirmed. To the best of our knowledge, there are not many reports about possible separation of metals from their aqueous EDTA chelates using only cation exchange [11,17].

2. Materials and methods

2.1. Materials

As received, silica gel type LiChroPrep® (Merck) was provided in powder form (diameter: 63–200 μm, surface area: 540 m^2/g). Chitosan flakes >85% deacetylated (Sigma–Aldrich) had a molecular weight ranging from 190,000 to 375,000 g/mol. All chemicals used in this study were of analytical grade and supplied by Sigma–Aldrich. A Co(II) stock solution of 1000 mg/L was prepared from its nitrate salt. The radioactive tracer, ^{57}Co, was obtained from Eckert & Ziegler Isotope products. The ^{57}Co concentration in trace solutions was $<3 \times 10^{-14}$ M. Before use, prepared solutions were allowed to equilibrate for at least 24 h by mixing in the dark. Adjustment of pH was done using 0.1 M NaOH and 0.1 M HNO_3.

2.2. Methods

2.2.1. Chemical modification of silica gel and chitosan

The silica gel was modified as previously described [24]. Briefly, aminopropyltriethoxysilane (APTES) and silica gel were first allowed to react in toluene in order to attach APTES groups covalently to the silica surface. Then the surface-bound amino groups were allowed to react with DTPA-anhydride in an ethanol and acetic acid solution. Chitosan was also modified as described earlier [25] by allowing chitosan to react with DTPA-anhydride in a solution of acetic acid and methanol (Fig. 1).

The formation of functional groups on the adsorbent surface was confirmed using a FTIR-spectroscope Nicolet Nexus 8700 (USA). The

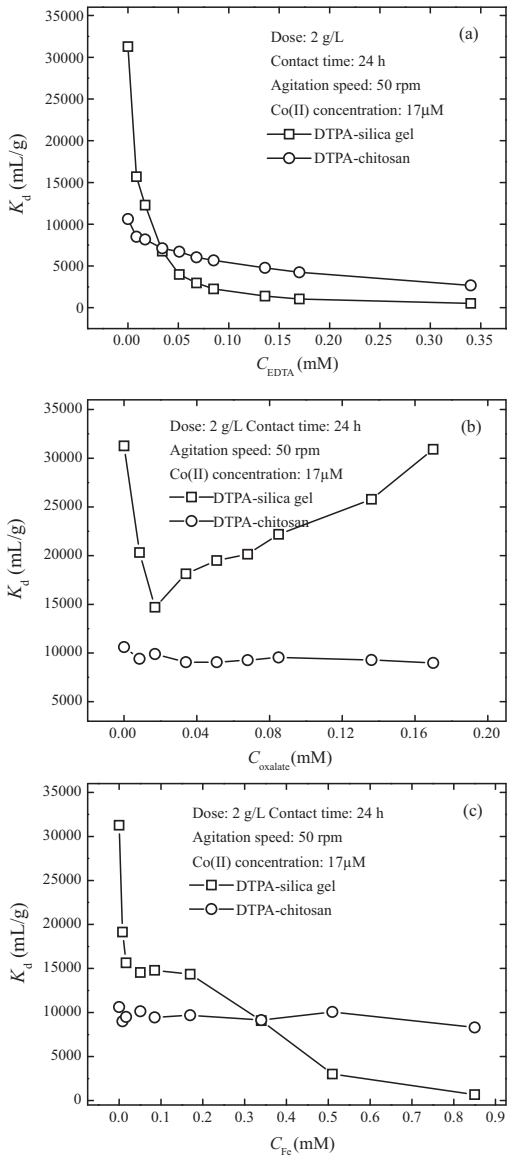

Fig. 2. Effects of (a) EDTA, (b) oxalate, and (c) iron on the adsorption of Co(II) by DTPA-modified adsorbents. pH 3 (DTPA-silica gel) and pH 2 (DTPA-chitosan).

peaks at wavenumbers of 1631 and 1398 cm^{-1} for DTPA-silica gel and 1731 and 1643 cm^{-1} for DTPA-chitosan indicated the formation of carboxylic groups on the adsorbent surfaces. The surface coverages of DTPA-groups analyzed by elemental analysis [24,25] and Boehm titration [26] were 0.22–0.26 mmol/g for DTPA-silica gel and 0.90–0.96 mmol/g for DTPA-chitosan. The specific surface area, total pore volume, and average pore size of DTPA-silica gel were 309 m^2/g, 0.34 cm^3/g, and 49 Å, respectively, and those of DTPA-chitosan were 0.36 fm^2/g, 0.74×10^{-3} cm^3/g, and 552 Å, as determined by Autosorb-1-C (Quantachrome, The UK).

2.2.2. Studied solutions

The adsorption of Co(II) by DTPA-modified adsorbents was tested in different solution matrices. The effects of EDTA, oxalate, and iron on Co(II) adsorption were separately studied, since these ions are often found in the target waste streams. Other solutions were selected to examine the influence of salts, acids and oxidizing agents (Table 1). The studied solutions were an aqueous solution containing oxalate, EDTA, and calcium (EOC), simulated floor drain water (FDW) [27], and simulated decontamination solutions (DEs). In addition, a few adsorption tests were carried out on the Co(II) solutions with trace radioactive ^{57}Co isotope. In LLRW solutions Co(II) can be found at the nanomolar level, but to get reliable results from ICP analysis, a Co(II) concentration of 17 μM (1 mg/L) was selected for most of the studies. Furthermore, at low Co(II) concentrations, the adsorption efficiency of both modified adsorbents was found to be highly dependent on pH [24,25] and the pH was thus adjusted to 3 for DTPA-silica gel and 2 for DTPA-chitosan to obtain maximum adsorption efficiency.

2.2.3. Batch adsorption studies

Batch experiments were conducted at ambient temperature (22 ± 1 °C) by mixing Co(II) solution and adsorbent (dose: 2 g/L) for a designated time in a rotary shaker, type ST5 (CATM.Zipperer GmbH, Staufen, Germany). The adsorbent was separated from the solution using a 0.45 μm polypropylene syringe filter. The samples were analyzed by an inductively coupled plasma optical atomic emission spectrometer (ICP-OES), model iCAP 6300 (Thermo Electron Corporation, USA). Co(II) concentrations were analyzed at a wavelength of 228.616 nm and the detection limit was 0.007 μM. The amount of radiocobalt (^{57}Co) was determined using an automatic gamma counter (Wallac 1480 Wizard^{TM} 3). The quantity of the adsorbed metal per unit mass of modified silica gel (mmol/g) was calculated as follows:

$$q_e = \frac{(C_i - C_e)}{M} V \quad (1)$$

where C_i and C_e are the initial and the equilibrium concentrations (mmol/L), while M and V represent the weight of the adsorbent (g) and the volume of the solution (L), respectively. The distribution ratio (mL/g), which describes the distribution of adsorbate between the solution and the adsorbent at equilibrium, was calculated using Eq. (2):

$$K_d = 1000 \frac{mL}{L} \times \frac{q_e}{C_e} \quad (2)$$

2.2.4. Capillary electrophoresis measurements

Capillary electrophoresis (CE) enables simultaneous detection of EDTA and its metal complexes in aqueous solutions [28]. CE measurements (Beckman Coulter, USA) were conducted to determine the amount of free EDTA in the solution after adsorption experiments [29]. A solution of 25 mM phosphate buffer (pH 7) and 0.5 mM tetradecyltrimethylammonium bromide (TTAB, Aldrich) was used as carrier electrolyte. TTAB changed the direction of the electro-osmotic flow in the fused silica capillary (75 μm diameter, 60 cm length to the detector) by making the wall charge positive. The power supply was changed to negative, generating net fluid movement towards the detector. The injection time of samples was 10 s and the run voltage 19 V. Between runs the capillary was washed with 0.1 M NaOH and water. Between every five samples the capillary was also rinsed with TTAB-buffer solution.

2.2.5. Regeneration studies

The regeneration of DTPA-modified adsorbents was studied previously in pure metal ion solutions [24,25]. Both of the adsorbents lasted several regeneration cycles without losing their adsorption efficiency. However, to study the effect of EDTA on regeneration

Table 1
Co(II) adsorption from waters containing different interfering species.

Solution	Composition	K_d (mL/g)/ads% for DTPA-silica gel	K_d (mL/g)/ads% for DTPA-chitosan
Co1	17 μM Co^{2+}, pH: 3	31270/98.5	
Co2	17 μM Co^{2+}, pH: 2	5726/92.1	10620/95.5
EOC	17 μM Co^{2}, 51 μM EDTA, 51 μM oxalate, 1.25 mM Ca^{2+}, pH: 3	3946/89.0	5985/92.4
FDW	17 μM Co^{2+}, 34 μM EDTA, 1.74 mM Na^{+}, 0.21 mM K^{+}, 25 μM Ca^{2+}, 2.3 M H_3BO_3, pH: 3	4950/90.9	
DE1	17 μM Co^{2+}, 90 μM Fe^{2+}, 0.01 M oxalic acid, pH: 2	1537/75.9	5756/92.1
DE2	17 μM Co^{2+}, 34 μM EDTA, 90 μM Fe^{2+}, 0.01 M oxalic acid, pH: 2	649/57.4	1499/75.5
DE3	17 μM Co^{2+}, 90 μM Fe^{2+}, 1 mM $KMnO_4$, 0.01 HNO_3, pH: 2	241/33.4	316/39.1
DE4	17 μM Co^{2+}, 34 μM EDTA, 90 μM Fe^{2+}, 1 mM $KMnO_4$, 0.01 HNO_3, pH: 2	270/35.5	389/44.5
DE5	17 μM Co^{2+}, 90 μM Fe^{2+}, 0.01 HNO_3, pH: 2	1219/72.0	8518/94.7
DE6	17 μM Co^{2+}, 34 μM EDTA, 90 μM Fe^{2+}, 0.01 HNO_3, pH: 2	980/67.1	4554/90.6
R1	10 μM Co(II) and 20 μM EDTA traced with ^{57}Co, 0.01 M $NaNO_3$, pH: 3	11730/96.0	
R2	10 μM Co(II) and 20 μM EDTA traced with ^{57}Co, 0.01 M $NaNO_3$, pH: 2	3254/86.6	6413/92.8

properties, adsorbents were first mixed with 1 mM Co(II):EDTA (1:2) following regeneration with 2 M HNO_3.

3. Results and discussion

3.1. Effects of various ions on Co(II) adsorption by DTPA-modified adsorbents

Water effluents to be treated before discharge contain not only target metals but also organic and inorganic compounds that may inhibit the adsorption of metal ions. One of the aims of this study was to investigate the possibility of using DTPA-modified adsorbents in the treatment of LLRW solutions produced by NPPs and the solution matrices were selected accordingly (Section 2.2.2, Table 1). The adsorption efficiencies were compared using both distribution ratio (K_d, Eq. (2)) and percentage removal of Co(II).

3.1.1. Effect of EDTA

The main goal of this study was to investigate how EDTA affects the adsorption of Co(II) by DTPA-modified adsorbents. Fig. 2a shows that when EDTA was not present in the solution or the amount of EDTA was less than two-fold the concentration of Co(II), DTPA-silica gel had a higher K_d value than DTPA-chitosan. However, the effectiveness of Co(II) adsorption decreased steeply in the case of DTPA-silica gel, and in Co(II):EDTA 1:10 solution the K_d was four times higher for modified chitosan. The Co(II) removal efficiencies of DTPA-silica gel and -chitosan in the Co(II):EDTA 1:2 solution were 96.3% and 93.8%, and in 1:10 solution they were 67.8% and 90.2%, respectively. For comparison, 97% removal of Co(II) was achieved by Malinen et al. [11] using titanium antimonates in the Co(II):EDTA 1:2 system, while only 7% removal was obtained using CoTreat in a Co(II):EDTA 1:1 system [30].

Based on the speciation calculations (MINEQL, ver. 2.53), in the Co(II):EDTA 1:10 solution over 99% of Co(II) is chelated by EDTA at pH 3 and over 90% at pH 2. Thus, it is obvious that, besides binding Co(II) ions, DTPA-silica gel and -chitosan were able to bind either Co(II)EDTA-chelates or capture Co(II) from dissolved metal EDTA species (see Sections 3.3 and 3.4). This result is promising because the highly Co(II) specific adsorption material CoTreat can bind Co(II) only in ionic form [11,30].

3.1.2. Effect of oxalate

Besides EDTA, oxalate is a commonly found chemical in NPP liquid waste [31]. Oxalate addition did not show any significant effect on the Co(II) adsorption of DTPA-chitosan (Fig. 2b). However, in the case of DTPA-silica gel, an increasing amount of oxalate at first inhibited but then enhanced the adsorption efficiency of Co(II). This could be explained by oxalate ion adsorption on the surface. A previous study showed that there were still free amino groups on the DTPA-silica gel surface after DTPA immobilization [24]. These amino groups were positively charged at pH 3 [21] and might have bound negatively charged oxalate ions on the surface, forming more favorable binding sites for Co(II).

3.1.3. Effect of iron

A very common metal contaminant on NPP's reactor walls and piping is iron. That is why the spent decontamination solutions used in cleaning can contain varying amounts of iron. For DTPA-silica gel, increasing the concentration of iron decreased the adsorption efficiency of Co(II) (Fig. 2c). However, DTPA-chitosan adsorbed approximately the same amount of Co(II) when there was no iron as when the Co(II):Fe(II) molar ratio was 1:50. The difference between modified silica gel and -chitosan can be explained by the higher surface coverage of DTPA-ligands on the surface of chitosan compared to silica gel. While DTPA-chitosan had enough adsorption sites for both Co(II) and Fe(II), Fe(II) was able to occupy some of the adsorption sites of DTPA-silica gel. The overall favorable binding of Co(II) over Fe(II) for both DTPA-modified adsorbents can be explained by the higher stability constant of Co(II)DTPA chelate ($pK = 20.95$) compared to the corresponding Fe(II)DTPA chelate ($pK = 18.35$) [32].

3.1.4. Solutions with mixed ions

Table 1 shows the distribution ratios and adsorption efficiencies for Co(II) removal by DTPA-modified adsorbents from both pure Co(II) solutions and solutions containing different interfering species. At the optimal pH, for DTPA-silica gel the K_d value was three times higher than that of DTPA-chitosan (Table 1). However, at higher Co(II) concentrations the adsorption efficiency of DTPA-chitosan was better than that of DTPA-silica gel due to its higher ligand loading [24,25]. The unusual behavior at low concentrations was attributed to the crosslinking of DTPA-groups on the surface of chitosan due to its branched structure [25]. When solutions contained high amounts of metals, chelating with the surface groups occurred before crosslinking.

The first solution with mixed ions contained both EDTA and oxalate along with 1.25 mM Ca(II). Table 1 shows that distribution ratios of Co(II) decreased significantly for both modified adsorbents but nonetheless adsorption efficiencies of around 90% were obtained. The adsorption performance of DTPA-silica gel in simulated FDW, where the most abundant interfering agent was boric acid, was also lower than in pure Co(II) solutions, but at pH 3 an adsorption efficiency of around 90% was achieved. However, in real applications the pH of FDW is around 8, where both of the adsorbents studied here were shown to be ineffective. This highlights the importance of pH adjustment.

Decontamination solutions (DEs) are used to clean reactors and pipes in NPPs. These solutions contain, for example, nitric acid, boric acid, or fluoroboric acid and in some cases permanganate as an oxidizing agent. In this study the removal of Co(II) from six different

DE-solutions was studied. DTPA-silica gel had low adsorption efficiency in all of the solutions (Table 1). This is because pH 2 was not optimal for DTPA-silica gel. However, even when the pH was optimal for DTPA-chitosan, the adsorption efficiency was clearly affected by the solution matrix. The most notable effect was seen in the solutions containing permanganate ions. This is not surprising since permanganate is known to oxidize polyaminocarboxylic acids [33], which would result in degradation of surface-bound DTPA groups. The effect of the type of acid was also evident in the case of the DE-solutions. The K_d value was around 1.5 times higher in nitric acid than in oxalic acid for DTPA-chitosan in the solutions without EDTA (DE1 and DE5). In similar solutions with EDTA (DE2 and DE6), the K_d value was three times higher in nitric acid. This can be explained by the chelating ability of oxalate ion, which could have interrupted metal binding on the surface groups.

Finally, the adsorption properties of DTPA-modified adsorbents were tested in solutions containing 10 μM Co(II) and 20 μM EDTA with ^{57}Co tracer. K_d values obtained were over 10 000 mL/g for DTPA-silica gel and over 6000 mL/g for DTPA-chitosan. For comparison, the K_d value for CoTreat was below 580 mL/g in the solution where Co(II) was chelated by EDTA [34]. Thus, the reasonably high adsorption efficiency of both DTPA-modified adsorbents in the ^{57}Co(II)EDTA solutions indicated their potential for use in the treatment of LLRW effluents.

3.2. Effect of EDTA on kinetics of Co(II) adsorption

When Co(II) is chelated by EDTA both its diffusion properties and chemical reactions on surfaces are affected. The best way to study these effects is comparison of adsorption kinetics in both Co(II) and Co(II)EDTA solutions. The kinetics of the chelation reaction was investigated using a pseudo-second-order model, which was previously found to describe Co(II) and Ni(II) adsorption well on both DTPA-silica gel and DTPA-chitosan [24,25]. However, non-linear regression (Origin software version 8.0, Microcal Software) was used here instead of linear regression in order to avoid the changes in error distributions caused by the linearization technique [35]. The non-linear pseudo-second-order model has the following form:

$$q_t = \frac{q_e^2 k_2 t}{1 + q_e k_2 t} \quad (3)$$

where q_t and q_e (mmol/g) represent the amount of Co(II) adsorbed at time t (min) and at equilibrium, respectively.

The plots of the pseudo-second-order equation are shown in Fig. 3a and estimated parameters in Table 2. Fig. 3a shows that the non-linear pseudo-second-order model did not describe adsorption kinetics of Co(II) on DTPA-modified adsorbents from pure Co(II) solutions as well as was expected based on the linear fittings [24,25]. However, the kinetic data obtained from Co(II)EDTA solutions fit better, indicating that the chelation reaction was the rate limiting step (Table 2). A possible explanation is that Co(II)EDTA-chelates reacted with outermost surface groups but could not diffuse inside the pores due to their bulky structure and negative charge. In contrast, the adsorption kinetics of free Co(II) seemed to be limited by diffusion. Despite the goodness of fit, parameters pre-

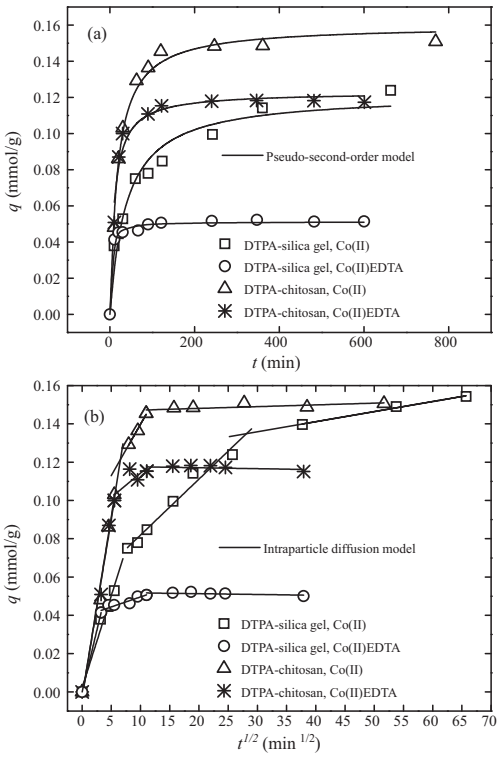

Fig. 3. (a) Adsorption kinetics of Co(II) and Co(II)EDTA (1:2) by DTPA-modified adsorbents. Agitation speed: 50 rpm; Co(II) concentration: 0.34 mM; dose: 2 g/L; pH 3 (DTPA-silica gel), pH 2 (DTPA-chitosan). (b) Intraparticle diffusion plots for the results presented in (a).

Table 2
Pseudo-second-order rate constants for DTPA-modified adsorbents in Co(II) and Co(II)EDTA 1:2 solutions: non-linear regression.

$C_{0,Co}$ (mM)	T (°C)	Co(II):EDTA molar ratio	$q_{e,exp}$ (mmol/g)	q_e (mmol/g)	k_2 (g/mmol min)	R^2
DTPA-silica gel						
0.017	22 ± 1	1:0	0.008	0.008	34.48	0.985
0.017	22 ± 1	1:2	0.008	0.008	17.09	0.988
0.34	22 ± 1	1:0	0.154	0.122	0.24	0.934
0.34	22 ± 1	1:2	0.051	0.051	7.01	0.992
0.14	22 ± 1	1:2	0.036	0.037	2.12	0.987
0.34	35	1:2	0.057	0.056	8.47	0.997
0.34	10	1:2	0.049	0.047	3.23	0.941
DTPA-chitosan						
0.017	22 ± 1	1:0	0.009	0.009	8.55	0.948
0.017	22 ± 1	1:2	0.009	0.009	10.49	0.914
0.34	22 ± 1	1:0	0.151	0.160	0.35	0.976
0.34	22 ± 1	1:2	0.118	0.123	0.78	0.932
0.85	22 ± 1	1:2	0.229	0.233	0.47	0.978
0.34	35	1:2	0.119	0.118	1.50	0.995
0.34	10	1:2	0.116	0.131	0.26	0.950

Table 3
Diffusion rate constants for DTPA-modified adsorbents in Co(II) and Co(II)EDTA 1:2 solutions.

$C_{0,Co}$ (mM)	T (°C)	Co(II):EDTA molar ratio	$k_{d,1}$ (mmol/g min$^{1/2}$)	$k_{d,2}$ (mmol/g min$^{1/2}$)	$k_{d,3}$ (mmol/g min$^{1/2}$)
DTPA-silica gel					
0.017	22 ± 1	1:0	0.0019		4.41×10^{-5}
0.017	22 ± 1	1:2	0.0014		3.05×10^{-5}
0.34	22 ± 1	1:0	0.0101	0.0029	52.4×10^{-5}
0.34	22 ± 1	1:2	0.0128	0.0011	≈ 0
0.14	22 ± 1	1:2	0.0054	0.0029	28.2×10^{-5}
0.34	35	1:2	0.0118	0.0023	16.2×10^{-5}
0.34	10	1:2	0.0104	0.0011	14.6×10^{-5}
DTPA-chitosan					
0.017	22 ± 1	1:0	0.0012		0.85×10^{-5}
0.017	22 ± 1	1:2	0.0010		1.02×10^{-5}
0.34	22 ± 1	1:0	0.0190	0.0054	50.9×10^{-5}
0.34	22 ± 1	1:2	0.0156	0.0025	≈ 0
0.85	22 ± 1	1:2	0.0372	0.0096	8.65×10^{-5}
0.34	35	1:2	0.0236	0.0119	30.8×10^{-5}
0.34	10	1:2	0.0125	0.0046	≈0

sented in Table 2 can be used to compare the adsorption kinetics of Co(II) species on the modified silica gel and chitosan. In most of the cases, the pseudo-second-order rate constant was lower for DTPA-chitosan than for DTPA-silica gel. This could be attributed to the rigid structure of the silica gel where adsorption sites were easily available.

The effect of chelate formation on diffusion was studied using an intraparticle diffusion model:

$$q_t = k_d t^{1/2} + C \quad (4)$$

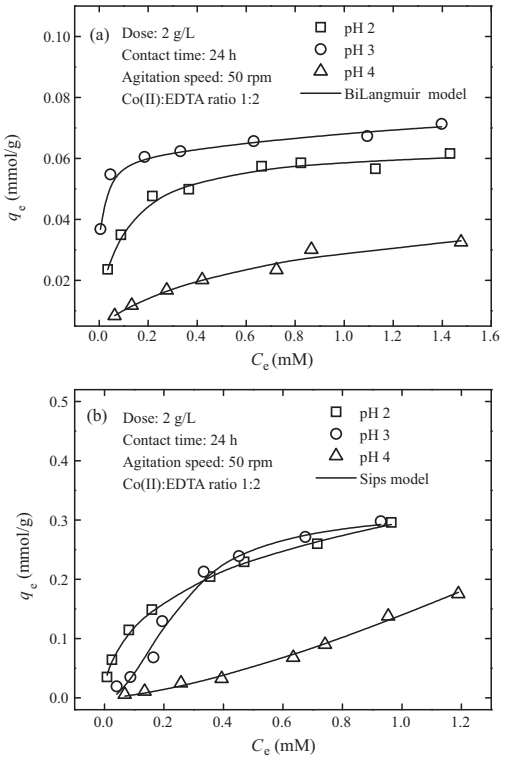

Fig. 4. The effect of pH on the Co(II) adsorption isotherms of (a) DTPA-silica gel and (b) DTPA-chitosan.

where k_d (mmol/g min$^{1/2}$) is the diffusion rate constant and C (mmol/g^{-1}) represents the thickness of the boundary layer. Fig. 3b shows that an intraparticle model plot had more than one linear region. These regions can be attributed to the different stages of diffusion. The first region, with a steep slope, represented diffusion in the bulk phase to the exterior surface of the adsorbent or film diffusion, the second represents the gradual adsorption stage (diffusion into mesopores or macropores), and the third region represents diffusion into micropores or the equilibrium state [36].

The diffusion rate constants obtained from the slopes of the intraparticle model plots are presented in Table 3. In 17 μM Co(II) and Co(II)EDTA solutions only the linear region prior to the equilibrium state represented diffusion from the bulk phase to the surface of the adsorbent or film diffusion. This is not surprising because the outermost surface areas of both adsorbents contained enough adsorption sites for all the metal ions at low concentrations. The most apparent effect of Co(II) chelation was seen in the case of DTPA-silica gel when the concentration of Co(II)/Co(II)EDTA was 0.34 mM. For free Co(II) more diffusion stages were observed than for Co(II)EDTA. This could be attributed to the fact that Co(II) ions were able to diffuse into the silica gel pores (pore diameter: 49 Å) due to their small size and the attraction of negatively charged carboxyl groups. However, the pore diffusion of Co(II)EDTA was limited due to its size and negative charge. Therefore, it rather reacted with the outermost DTPA groups. In the case of DTPA-chitosan, this effect was not seen due to its higher surface coverage and macroporous structure (pore diameter: 552 Å), and both Co(II) and Co(II)EDTA were equally able to reach the active sites. It is interesting to note that the diffusion rate constants from bulk to surface ($k_{d,1}$, Table 3) of DTPA-chitosan were directly proportional to the initial Co(II) concentration, which is consistent with the concept of surface "film diffusion" [37].

Besides ambient temperature, kinetic experiments were also conducted at 10 and 35 °C. Table 2 shows that adsorption was clearly slower at 10 °C than at the other two temperatures. This further indicates that the chelation reaction had the main role in the adsorption kinetics of Co(II) from EDTA-containing solutions. In the case of DTPA-silica gel the adsorption capacity increased slightly as a function of temperature indicating the endothermic nature of the surface reaction (Table 2 and Supplementary information: Figures S1 and S2).

3.3. Effect of EDTA on Co(II) adsorption isotherms

It is evident that the addition of EDTA affected the adsorption of Co(II) by DTPA-modified adsorbents. In addition, the speciation

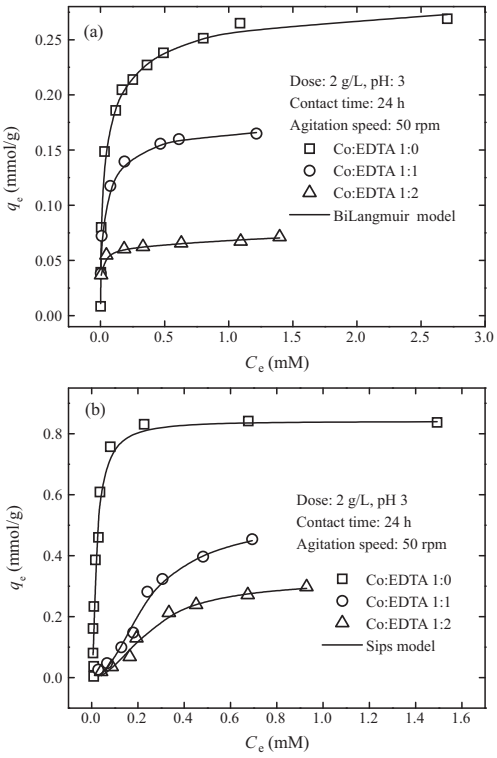

Fig. 5. The effect of EDTA on the Co(II) adsorption isotherms of (a) DTPA-silica gel and (b) DTPA-chitosan.

of both surface bound DTPA and Co(II)EDTA in the solution were pH dependent. Therefore, the adsorption equilibrium was studied in solutions containing Co(II) and EDTA at molar ratios of 1:0, 1:1, and 1:2 and varying in pH from 2 to 4.

It is useful to look first at the overall effects of pH and EDTA on Co(II) adsorption by DTPA-modified adsorbents (Figs. 4 and 5). Fig. 4a shows that in the Co(II):EDTA 1:2 solutions, the best adsorption performance of DTPA-silica gel was obtained at pH 3 and the worst at pH 4. In the case of DTPA-chitosan (Fig. 4b), pH 4 also gave the poorest performance, but near the equilibrium the adsorption capacities were rather similar at pH 2 and pH 3. That the poorest adsorption performance was seen for both materials at pH 4 can be attributed to the speciation of both surface DTPA-groups and Co(II)EDTA-species in the solution (MINEQL, ver. 2.53). At this pH the predominant compound in the solution was Co(II)EDTA^{2-} and the dominant surface compounds were R–NH–H_2DTPA^{2-} and R–NH–HDTPA^{3-} (R = silica gel or chitosan, simplified presentation). Thus, there was electrochemical repulsion between the negatively charged groups. The increase in positive surface charge with decreasing pH allowed a better surface approach of Co(II)EDTA-chelates at pH 2 and pH 3. Fig. 4b also shows that pH had a clear effect on the shape of the isotherm curve, which is discussed later in this section. Furthermore, it should be noted that without EDTA, the pH only slightly affected the maximum Co(II) adsorption (Tables 4 and 5) even if the effect at low Co(II) concentrations was significant.

The effect of Co(II):EDTA molar ratio on the adsorption of Co(II) species is presented in Fig. 5. The adsorption performance of DTPA-modified materials decreased as the EDTA content in the solution increased, and this was evident over the whole studied pH range (Tables 4 and 5). This was attributed to the enhanced competition for Co(II) ions between dissolved EDTA and surface DTPA-groups.

To obtain a deeper understanding of the adsorption equilibrium, theoretical isotherm models were fitted to the experimental data using non-linear regression (Origin software). The BiLangmuir and Sips models were selected based on previous results [24,25]. The BiLangmuir model is given as

$$q_e = \frac{q_{m1}K_{L1}C_e}{1+K_{L1}C_e} + \frac{q_{m2}K_{L2}C_e}{1+K_{L2}C_e} \quad (5)$$

where q_{m1} and q_{m2} are the maximum adsorption capacities of two different adsorption sites while K_1 and K_2 are the energies of adsorption for these adsorption sites. The Sips model is a combination of Langmuir and Freundlich models:

$$q_e = \frac{q_m(K_S C_e)^{n_S}}{1+(K_S C_e)^{n_S}} \quad (6)$$

where K_S (L mmol^{-1}) is the Langmuir equilibrium constant and n_S is the Freundlich heterogeneity factor.

As presented earlier, the BiLangmuir model fit rather well to the equilibrium curves obtained for DTPA-silica gel (Figs. 4a and 5a and Table 4). Even though the adsorption system was relatively complex, the K_L parameters presented in Table 4 can give some insight into the adsorption mechanism by which Co(II) ions are bound by surface DTPA-groups. At pH 3 and $4K_{L1}$ values were clearly higher than K_{L2} values. At pH 3 these values were also related to the binding sites with higher adsorption capacity (q_{m1}). This indicates that these adsorption sites were surface DTPA-groups, which were able to capture Co(II) from its EDTA chelate. However, the results at pH 4 indicated that lower affinity binding sites had higher adsorption capacity in the solution without EDTA. This cannot be explained by the suggestion that the high affinity groups were DTPA-moieties and the low-affinity groups amino-moieties [24]. Instead, it is most likely that high- and low-affinity groups denoted different speciations of the surface-bound DTPA. At pH 4, 74.9% of DTPA is found as R–NH–H_2DTPA^{2-} and 18.5% as R–NH–HDTPA^{3-} (MINEQL, ver. 2.53, R = silica gel). The group with the higher negative charge should clearly have higher affinity for the positive Co(II) ions. However, the surface concentration of this group was also lower, giving lower adsorption capacity. Similarly, at pH 3 high-affinity surface groups could be assigned to R–NH–H_2DTPA^{2-} (50.3%) and low-affinity groups to R–NH–H_3DTPA^{-} (42.7%).

Table 5 and Figs. 4b and 5b show that the Sips model fit better with the experimental data obtained for DTPA-chitosan than the BiLangmuir model. Only at pH 2 did the BiLangmuir model fit well, but the parameters obtained indicated that there was only one kind of binding site on the surface, thus the BiLangmuir equation became a simple Langmuir equation. Moreover, the model overestimated the q_m values. The poor fit of the BiLangmuir/Langmuir model to the data obtained for DTPA-chitosan could be attributed to system heterogeneity. It can be seen from Figs. 4b and 5b that the shape of the isotherm curve was highly affected by both pH and EDTA content, unlike the isotherm of DTPA-silica gel. This indicates that DTPA-chitosan has a much more complex structure than DTPA-silica gel.

Table 5 shows that the heterogeneity factor n_S of the Sips model was greater than one when solution pH was 3 or the Co(II):EDTA ratio was 1:2. Thus, these systems were highly heterogeneous, which was also seen from the S-shape isotherm curves. This type of curve is typically formed when there is a weak interaction between the surface and adsorbate at low adsorbate concentrations, but once some adsorption takes place, adsorbent–adsorbate interactions increase [38]. In the case of DTPA-chitosan, weak surface affinities at low Co(II)EDTA concentrations could be attributed to crosslink formation [25]. Due to the more rigid structure of the

Table 4
Isotherm parameters for DTPA-silica gel.

	Co:EDTA ratio	$q_{m,exp}$ (mmol/g)	q_{m1} (mmol/g)	K_{L1} (L/mmol)	q_{m2} (mmol/g)	K_{L2} (L/mmol)	R^2
Two-site Langmuir model							
pH 2	1:0	0.23	0.09	31.82	0.16	2.77	0.997
	1:1	0.12	0.06	22.10	0.15	0.65	0.991
	1:2	0.06	0.02	58.70	0.04	7.19	0.977
pH 3	1:0	0.27	0.16	193.36	0.13	3.83	0.998
	1:1	0.16	0.10	270.92	0.08	7.31	0.999
	1:2	0.07	0.06	330.26	0.03	0.65	0.991
pH 4	1:0	0.25	0.07	540.89	0.21	5.19	0.992
	1:2	0.03	0.01	78.56	0.04	1.18	0.952

	Co:EDTA ratio	$q_{m,exp}$ (mmol/g)	q_m (mmol/g)	K_S (L/mmol)	n_S	R^2
Sips model						
pH 2	1:0	0.23	0.26	10.78	0.73	0.998
	1:1	0.12	0.27	1.59	0.53	0.991
	1:2	0.06	0.07	18.03	0.73	0.992
pH 3	1:0	0.27	0.30	37.30	0.27	0.993
	1:1	0.16	0.19	48.27	0.16	0.995
	1:2	0.07	0.08	85.16	0.07	0.976
pH 4	1:0	0.25	0.32	18.80	0.56	0.984
	1:2	0.03	0.08	3.18	0.56	0.962

oxide substrate, a similar effect was not seen in the case of DTPA-silica gel.

3.4. Reaction mechanism

In order to understand the reaction mechanism it was important to find out whether EDTA is released during Co(II) adsorption. The speciation of free EDTA and Co(II)EDTA was accomplished using CE. The calibration curves (Supplementary information, Figure S3) of EDTA were not affected by pH unlike those of Co(II)EDTA. This can be explained by Co(II)EDTA speciation, which was seen as split peaks in electopherograms (Fig. 6). However, the total amount of Co(II)EDTA-species could be determined by CE as well as ICP.

It is evident from Fig. 6 that the EDTA content in the solution increased as Co(II) was adsorbed on the DTPA-modified surface. Furthermore, the amount of EDTA released correlated well with the amount of Co(II) adsorbed (Fig. 7), indicating that surface DTPA-groups were able to capture Co(II) from its dissolved EDTA chelates.

The speciation of Co(II)EDTA at different pH values is presented in the supplementary information (Tables S1 and S2). At pH 2 there were some free Co^{2+} ions in the Co(II):EDTA 1:1 solution, but in the other systems the amount of free Co^{2+} was insignificant compared to the amount of chelated Co(II). This further confirmed that Co(II)EDTA-chelates were dissociated due to the high-affinity DTPA-groups. The adsorption efficiency varied from 38% to 96% at pH 2 and 3 depending on the total Co(II) concentration. DTPA-chitosan could remove over 50% of Co(II) from the 1.7 mM Co(II)EDTA 1:2 solution, whereas DTPA-silica gel had a better adsorption performance in the lower concentration range, reaching 96% removal from 85 μM Co(II)EDTA solution.

Determination of the reaction mechanism of the system presented here is complicated due to the fact that DTPA and EDTA as well as their Co(II) chelates have different speciations at different pH values. Mechanisms can be suggested based on the speciation calculations. The most abundant surface group after Co(II) chelation in the studied pH range was R–NH–Co(II)$DTPA^{2-}$ and the solution chelate, which donated Co(II), was expected to be the one with the lowest stability constant (Table S2). Based on this, the reaction mechanisms can be written as

$$Co(II)HEDTA^- + R\text{–}NH\text{–}H_3DTPA^- \leftrightarrow R\text{–}NH\text{–}Co(II)DTPA^{2-} + H_4EDTA \quad (7)$$

$$Co(II)HEDTA^- + R\text{–}NH\text{–}H_2DTPA^{2-} \leftrightarrow R\text{–}NH\text{–}Co(II)DTPA^{2-} + H_3EDTA^- \quad (8)$$

$$Co(II)EDTA^{2-} + R\text{–}NH\text{–}H_2DTPA^{2-} \leftrightarrow R\text{–}NH\text{–}Co(II)DTPA^{2-} + H_2EDTA^{2-} \quad (9)$$

$$Co(II)HEDTA^- + R\text{–}NH\text{–}HDTPA^{3-} \leftrightarrow R\text{–}NH\text{–}Co(II)DTPA^{2-} + H_2EDTA^{2-} \quad (10)$$

Table 5
Isotherm parameters for DTPA-chitosan.

	Co:EDTA ratio	$q_{m,exp}$ (mmol/g)	q_{m1} (mmol/g)	K_{L1} (L/mmol)	q_{m2} (mmol/g)	K_{L2} (L/mmol)	R^2
Two-site Langmuir model							
pH 2	1:0	0.83	0.90	13.08	–	–	0.998
	1:1	0.43	0.51	2.18	0.11	50.86	0.999
	1:2	0.30	0.37	1.06	0.02	42.96	0.999
pH 3	1:0	0.84	0.92	31.82	–	–	0.881
	1:1	0.45	1.04	1.24	–	–	0.919
	1:2	0.30	0.45	2.12	–	–	0.899
pH 4	1:0	0.86	0.92	19.92	–	–	0.440
	1:2	0.18	–	–	–	–	–

	Co:EDTA ratio	$q_{m,exp}$ (mmol/g)	q_m (mmol/g)	K_S (L/mmol)	n_S	R^2
Sips model						
pH 2	1:0	0.83	0.88	12.43	1.08	0.999
	1:1	0.43	0.81	5.60	0.66	0.999
	1:2	0.30	0.31	0.18	2.18	0.982
pH 3	1:0	0.84	0.84	35.18	1.79	0.950
	1:1	0.45	0.49	0.18	2.26	0.981
	1:2	0.30	0.31	0.18	2.18	0.982
pH 4	1:0	0.86	0.92	19.92	1.01	0.502
	1:2	0.18	–	–	–	–

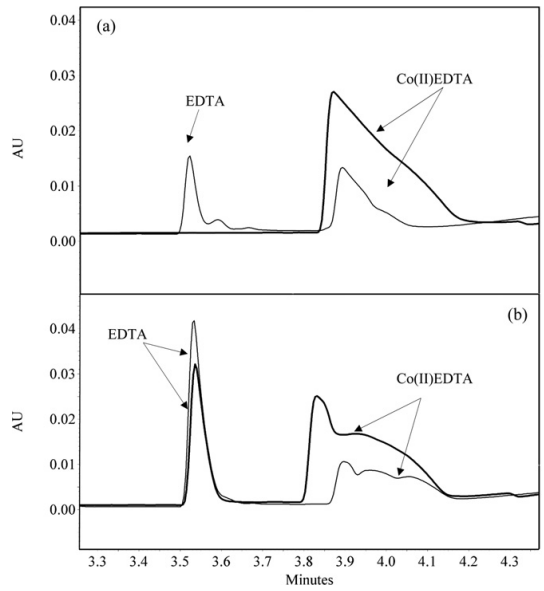

Fig. 6. Comparison of electropherograms before (bold line) and after (thin line) adsorption of Co(II) in (a) Co(II)EDTA 1:1 and (b) Co(II)EDTA 1:2 systems, pH 3. Co(II) concentration: 0.85 mM.

$$Co(II)EDTA^{2-} + R\text{–}NH - HDTPA^{3-} \leftrightarrow R\text{–}NH\text{–}Co(II)DTPA^{2-} + HEDTA^{3-} \quad (11)$$

of which Eq. (7) is suggested to be the main mechanism at pH 2 and (9) at pH 3. At pH 4 all the reactions except (7) may occur. The idea behind the mechanisms presented here was that the most unstable solution chelate reacted with the surface group with the highest affinity towards positive metal ions. It was also assumed that DTPA surface groups formed rather similar coordination compounds with Co(II) ions as they would have formed in the solution phase [39], and the above equations are simplified presentations of coordination. If the stability constant of surface DTPA-groups was assumed to be near that of the solution species (p*K*: 26.53 [32]) the previous mechanisms would also be favorable since the stability constants of Co(II)EDTA-chelates varied from 18 to 23.5 [32], [Table S2]. However, it should be emphasized that the system under investigation was very complex and, besides binding free Co(II) released from EDTA chelates, whole Co(II)EDTA-chelates or free EDTA could have been bound by the surface amino groups [19,20]. On the other hand, in this study, both results with CE and fittings to the BiLangmuir model indicated that most of the Co(II) was bound to the DTPA-modified surfaces in the ionic form.

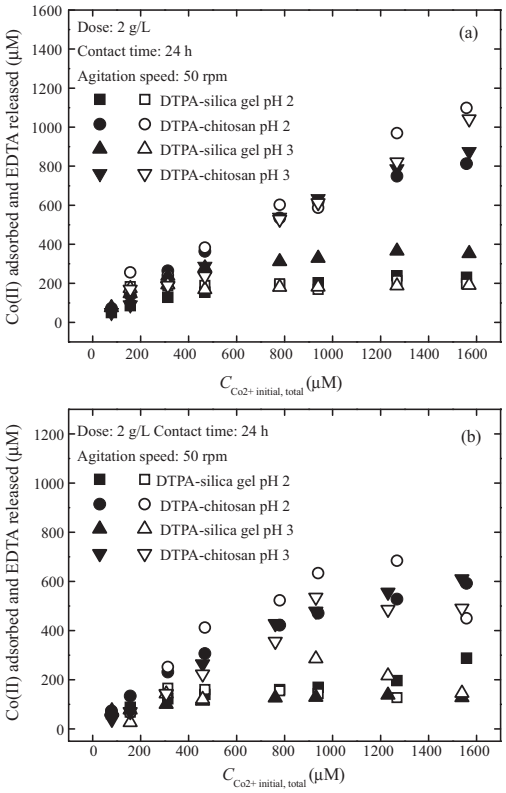

Fig. 7. The relationship between the amount of Co(II) adsorbed and EDTA released as a function of total initial concentration of Co(II). (a) Co(II):EDTA 1:1 and (b) Co(II):EDTA 1:2. Filled symbols: Co(II) adsorbed; open symbols: EDTA released.

3.5. Regeneration and stability of the adsorbents

Earlier studies showed that DTPA-modified silica gel and chitosan were regenerable using 1–2 M HNO_3 when adsorption tests were done in pure metal solutions [24,25]. The regeneration results after adsorption tests in 1 mM Co(II)EDTA solutions are presented in Table 6. For DTPA-chitosan, adsorption efficiency was not affected by regeneration. However, for DTPA-silica gel, adsorption capacity increased after the first regeneration cycle, indicating that some EDTA groups became attached to the surface and increased the ligand loading. Overall, regeneration studies confirmed the stability of the DTPA-groups in the Co(II)EDTA solutions.

Table 6
Regeneration of DTPA-silica gel and -chitosan by 2 M HNO_3. Adsorption from 1 mM Co(II)EDTA (1:2)-solution, pH 3.

Type of adsorbent	No. of cycles	Adsorption capacity of Co(II)EDTA		
		Before regeneration (mg/g)	After regeneration (mg/g)	Regeneration efficiency (%)
DTPA-silica gel	1	8.56	8.01	136.5
	2	8.56	8.16	132.5
	3	8.56	8.09	138.2
	4	8.56	8.38	114.2
DTPA-chitosan	1	2.35	2.18	102.3
	2	2.35	2.18	102.3
	3	2.35	2.25	101.3
	4	2.35	2.26	101.2

DTPA leaching at different pH values was further examined by CE-measurements. A small peak assigned to dissolved Co(II)DTPA chelate was observed in the case of DTPA-chitosan after adsorption experiments at pH 3 and 4 (Figure S4). When the peak was calibrated for Co(II)DTPA, the leached amount was found to be around 10 μM, i.e. 0.5 mol% of the total amount of functional groups. A Co(II)DTPA peak was not observed for DTPA-silica gel, demonstrating its stability, which has also been seen with analysis of leached silicon [24].

4. Conclusions

The DTPA-modified silica gel and chitosan were found to be promising materials for Co(II) adsorption in the presence of organic complexants such as EDTA and oxalate or inorganic species such as Ca(II) and Fe(II). The two adsorbents performed differently depending on the solution pH and the concentration of Co(II). Both modified adsorbents could remove Co(II) even if it was totally chelated by EDTA. DTPA-silica gel was more effective when the EDTA was present in less than two-fold excess, after which the modified chitosan showed better adsorption performance. An excess of oxalate ions or Fe(II) did not influence the Co(II) adsorption by DTPA-chitosan due to its high ligand loading. However, adsorption of Co(II) was enhanced by oxalate in the case of DTPA-silica gel, which was attributed to the oxalate binding on the surface creating more adsorption sites for Co(II). Furthermore, DTPA-chitosan was an efficient adsorbent in simulated decontamination solutions and both adsorbents showed good adsorption properties in solutions traced with radiocobalt ^{57}Co.

The effect of EDTA on Co(II) adsorption was studied by both kinetic and equilibrium experiments. Kinetic experiments showed that the adsorption of free Co(II) on DTPA-silica gel was controlled by intraparticle diffusion, but adsorption of Co(II)EDTA by surface chelation reaction. This was attributed to the large size of Co(II)EDTA and electrochemical repulsion between negatively charged DTPA-groups and Co(II)EDTA. In the case of DTPA-chitosan, a similar effect was not seen due to its macroporous structure, which enabled both Co(II) and Co(II)EDTA diffusion into the adsorbent pores.

The equilibrium studies showed that the BiLangmuir model was most accurate in the case of DTPA-silica gel and the Sips model in the case of DTPA-chitosan. The latter was due to the high heterogeneity of the DTPA-chitosan surface, which was also apparent from the S-shaped isotherm plots. The BiLangmuir model suggested that there were two kinds of active sites on the DTPA-silica gel surface. Based on the K_L/q_m values these sites were attributed to the different speciation of surface DTPA-groups.

Finally, the measurements with CE showed that DTPA-modified adsorbents were able to capture Co(II) from its EDTA chelate, as demonstrated by the increase in dissolved EDTA as Co(II) was adsorbed on the surface. This demonstrated the applicability of the studied adsorbents to treatment of effluent streams containing both Co(II) and EDTA.

Acknowledgements

The authors are grateful to the Finnish Funding Agency for Technology and Innovation (TEKES) for financial support. Dr. Mary Metzler is thanked for language revision.

Appendix A. Supplementary data

Supplementary data associated with this article can be found, in the online version, at doi:10.1016/j.jhazmat.2010.12.113.

References

[1] M. Sillanpää, Review: environmental fate of EDTA and DTPA, Rev. Environ. Contam. Toxicol. 152 (1997) 85–111.
[2] J. Rämö, M. Sillanpää, V. Vickackaite, M. Orama, L. Niinistö, Chelating ability and solubility of DTPA, EDTA and β-ADA in alkaline hydrogen peroxide environment, J. Pulp Paper Sci. 26 (2000) 125–131.
[3] J. Rämö, M. Sillanpää, The degradation of EDTA by hydrogen peroxide in alkaline conditions, J. Clean. Prod. 9 (2001) 191–195.
[4] M. Sillanpää, J. Rämö, Decomposition of β-alaninediacetic acid and diethylenetriaminepentaacetic acid by hydrogen peroxide in alkaline conditions, Environ. Sci. Technol. 35 (2001) 1379–1384.
[5] M. Sillanpää, M. Orama, J. Rämö, A. Oikari, The importance of ligand speciation in environmental research: a case study, Sci. Total Environ. 267 (2001) 23–31.
[6] K. Pirkanniemi, S. Metsärinne, M. Sillanpää, Degradation of EDTA and novel complexing agents in pulp and paper mill process and wastewaters by Fenton's reagent, J. Hazard. Mater. 147 (2007) 556–561.
[7] D. Kołodyńska, H. Hubicka, Z. Hubicki, Sorption of heavy metal ions from aqueous solutions in the presence of EDTA on monodisperse anion exchangers, Desalination 227 (2008) 150–166.
[8] M. Sillanpää, A. Oikari, Assessing the impact of complexation by EDTA and DTPA on heavy metal toxicity using microtox bioassay, Chemosphere 32 (1996) 1485–1497.
[9] J. Sorvari, M. Sillanpää, Influence of metal complex formation on heavy metal and free EDTA and DTPA acute toxicity determined by *D. magna*, Chemosphere 33 (1996) 1119–1127.
[10] I. Hore-Lacy, Nuclear waste management, http://www.eoearth.org/article/Nuclear_waste_management, December 2009.
[11] L.K. Malinen, R. Koivula, R. Harjula, Sorption of radiocobalt and its EDTA complex on titanium antimonates, J. Hazard. Mater. 172 (2009) 875–879.
[12] K. Omata, K. Shibata, Y. Shirai, S. Ichikawa, Method of treating chelating agent solution containing radioactive contaminants, US Patent 5832393 (1998).
[13] International Atomic Energy Agency, Application of ion exchange processes for the treatment of radioactive waste and management of spent ion exchangers. Technical reports series no. 408, Vienna (2002).
[14] R.D. Burack, W.J. Stenger, C.R. Wolfe, Apparatus for waste disposal of radioactive hazardous waste, US Patent 5832393 (1992).
[15] O. Abollino, M. Aceto, M. Malandrino, C. Sarzanini, E. Mentasti, Adsorption of heavy metals on Na-montmorillonite. Effect of pH and organic substances, Water Res. 37 (2003) 1619–1627.
[16] R.-S. Juang, L.D. Shiau, Ion exchange equilibria of metal chelates of ethylenediaminetetra-asetic acid (EDTA) with Amberlite IRA-68, Ind. Eng. Chem. Res. 37 (1998) 555–560.
[17] D. Kołodyńska, E. Skwarek, Z. Hubicki, W. Janusz, Effect of adsorption of Pb(II) and Cd(II) ions in the presence of EDTA on the characteristics of electrical double layers at the ion exchanger/NaCl electrolyte solution interface, J. Colloid Interface Sci. 33 (2009) 448–456.
[18] C.-C. Wang, C.-C. Wang, Adsorption characteristics of metal complexes by chelated copolymers with amino group, React. Funct. Polym. 66 (2006) 343–356.
[19] W. Maketon, C.Z. Zenner, K.L. Ogden, Removal efficiency and binding mechanisms of copper and copper–EDTA complexes using polyethyleneimine, Environ. Sci. Technol. 42 (2008) 2124–2129.
[20] R.-S. Juang, C.-Y. Ju, Equilibrium sorption of copper(II)–ethylenediaminetetraacetic acid chelates onto cross-linked, polyaminated chitosan beads, Ind. Eng. Chem. Res. 36 (1997) 5403–5409.
[21] R.-S. Juang, F.-C. Wu, R.-L. Tseng, Adsorption removal of copper(II) using chitosan from simulated rinse solutions containing chelating agents, Water Res. 33 (1999) 2403–2409.
[22] F.-C. Wu, R.-L. Tseng, R.-S. Juang, Role of pH in metal adsorption from aqueous solutions containing chelating agents on chitosan, Ind. Eng. Chem. Res. 38 (1999) 270–275.
[23] A. Bhatnagar, M. Sillanpää, Applications of chitin- and chitosan-derivatives for the detoxification of water and wastewater—a short review, Adv. Colloid Interface Sci. 152 (2009) 26–38.
[24] E. Repo, T.A. Kurniawan, J.K. Warchol, M.E.T. Sillanpää, Removal of Co(II) and Ni(II) ions from contaminated water using silica gel functionalized with EDTA and/or DTPA as chelating agents, J. Hazard. Mater. 171 (2009) 1071–1080.
[25] E. Repo, J.K. Warchol, T.A. Kurniawan, M.E.T. Sillanpää, Adsorption of Co(II) and Ni(II) by EDTA- and/or DTPA-modified chitosan: kinetic and equilibrium modeling, Chem. Eng. J. 161 (2010) 73–82.
[26] H.P. Boehm, E. Diehl, W. Heck, R. Sappok, Surface oxides of carbon, Angew. Chem. Int. Ed. Engl. 3 (1964) 669–677.
[27] R. Harjula, J. Lehto, A. Paajanen, L. Brodkin, E. Tusa, Testing of highly selective CoTreat ion exchange media for the removal of radiocobalt and other activated corrosion product nuclides from NPP waste waters, Proceeding of Waste Management, Tucson, AZ, United States (1999) 2079–2091.
[28] M. Sillanpää, M.-L. Sihvonen, Analysis of EDTA and DTPA, Talanta 44 (1997) 1487–1497.
[29] C.S. Burgisser, A.T. Stone, Determination of EDTA, NTA, and other amino carboxylic acids and their Co(II) and Co(III) complexes by capillary electrophoresis, Environ. Sci. Technol. 31 (1997) 2656–2664.
[30] L.K. Malinen, R. Koivula, R. Harjula, Removal of radiocobalt from EDTA-complexes using oxidation and selective ion exchange, Water Sci. Technol. 60 (2009) 1097–1101.

[31] E. Ketusky, T. Huff, C. Sudduth, S. Jones, J. Remark, T. Kurniawan, M. Sillanpää, Enhanced chemical cleaning: effectiveness of the UV lamp to decompose oxalates, Waste Management Symposium, SRR-STI-2010-00015.
[32] R.M. Smith, A.E. Martell, R.J. Motekaitis, NIST Standard Reference Database 46.6, National Institute of Standards and Technology, U.S. Department of Commerce, Gaithersburg, MD, 2007.
[33] H.-S. Chang, G.V. Korshin, J.F. Ferguson, Investigation of mechanisms of oxidation of EDTA and NTA by permanganate at high pH, Environ. Sci. Technol. 40 (2006) 5089–5094.
[34] M. Semelova, J. John, F. Sebesta, R. Harjula, A. Paajanen, Separation of radiocobalt from NPP evaporator concentrate, Czech. J. Phys. 56 (2006) D617–D622.
[35] K.V. Kumar, S. Sivanesan, Selection of optimum sorption kinetics: comparison of linear and non-linear method, J. Hazard. Mater. B134 (2006) 277–279.
[36] W.H. Cheung, Y.S. Szeto, G. McKay, Intraparticle diffusion processes during acid dye adsorption onto chitosan, Biores. Tech. 98 (2007) 2897–2904.
[37] F. Helfferich, Ion Exchange, Dover Publications, New York (1995) p. 285.
[38] S. Andini, R. Cioffi, F. Montagnaro, F. Pisciotta, L. Santoro, Simultaneous adsorption of chlorophenol and heavy metal ions on organophilic bentonite, Appl. Clay Sci. 31 (2006) 126–133.
[39] A.R. Jalilian, P. Rowshanfarzad, Y. Yari-Kamrani, M. Sabet, A. Majdabadi, Preparation and evaluation of [55Co](II)DTPA for blood cell labeling, Open Inorg. Chem. J. 3 (2009) 21–25.

Supplementary information for

Capture of Co(II) from its aqueous EDTA-chelate by DTPA-modified silica gel and chitosan

This file contains two tables and four figures

Tables S1 and S2 show the amount of EDTA released vs. the amount of Co(II) adsorbed at different pH and different Co(II) concentrations.
Figures S1 and S2 show the effects of temperature on the adsorption kinetics for DTPA-modified adsorbents in 0.34 mM Co(II)EDTA (1:2) solution.
Figure S3 shows the calibration curves for EDTA and Co(II) EDTA at different pH measured by capillary electrophoresis.
Figure S4 shows the leaching of DTPA at pH 3 and pH 4 measured by capillary electrophoresis.

Table S1. The speciation of Co(II) species in Co(II):EDTA 1:1 solution before adsorption and the amount of Co(II) adsorbed and EDTA released in equilibrium.

pH 2

Initial					Equilibrium, silica gel	DTPA-	Equilibrium, chitosan	DTPA-
Total Co(II)	Free Co(II)	Co(II) $EDTA^{-2}$ pK: 18.16	Co(II) $HEDTA^{-1}$ pK: 21.59	Co(II) H_2EDTA pK: 23.49	Co(II) adsorbed	$EDTA^{-4}$ released	Co(II) adsorbed	$EDTA^{-4}$ released
78.78	16.42	2.89	40.46	19.01	50.57	-	72.20	-
157.17	23.91	6.18	86.47	40.61	85.51	183.70	139.23	256.30
313.10	34.81	12.92	180.61	84.75	128.48	187.16	264.43	240.61
467.54	97.44	14.56	250.28	146.68	154.51	189.64	364.08	383.04
779.70	73.57	25.08	429.58	251.47	190.15	197.76	534.70	602.30
939.67	81.21	30.55	522.33	305.58	202.69	168.80	618.77	586.93
1268.37	95.06	41.89	714.11	417.29	238.41	213.91	749.42	969.60
1558.14	106.43	52.40	890.58	519.92	230.88	198.00	813.39	1099.08

pH 3

Initial					Equilibrium, silica gel	DTPA-	Equilibrium, chitosan	DTPA-
Total Co(II)	Free Co(II)	Co(II) $EDTA^{-2}$ pK: 18.16	Co(II) $HEDTA^{-1}$ pK: 21.59	Co(II) H_2EDTA pK: 23.49	Co(II) adsorbed	$EDTA^{-4}$ released	Co(II) adsorbed	$EDTA^{-4}$ released
78.78	2.03	24.72	49.00	3.01	76.36	-	50.34	-
157.17	2.89	49.90	98.34	6.04	148.54	174.04	90.23	168.80
313.10	4.13	100.64	196.32	12.01	237.38	193.03	184.73	188.88
467.54	5.09	151.57	293.01	17.87	279.91	168.80	288.10	236.70
779.70	6.67	256.10	487.36	29.57	311.69	180.50	538.63	527.54
939.67	7.36	310.41	586.41	35.49	328.94	181.85	633.81	612.09
1268.37	8.64	423.32	788.88	47.53	365.75	188.14	786.70	821.21
1569.33	9.70	528.11	973.11	58.41	352.96	190.69	875.23	1041.23

Table S2 . The speciation of Co(II) species in Co(II):EDTA 1:2 solution before adsorption and the amount of Co(II) adsorbed and EDTA released in equilibrium.

pH 2								
Initial					Equilibrium, silica gel		DTPA-Equilibrium, chitosan	DTPA-
Total Co(II)	Free Co(II)	Co(II) $EDTA^{-2}$ pK: 18.16	Co(II) $HEDTA^{-1}$ pK: 21.59	Co(II) H_2EDTA pK: 23.49	Co(II) adsorbed	$EDTA^{-4}$ released	Co(II) adsorbed	$EDTA^{-4}$ released
81.50	9.88	1.90	40.23	29.49	61.72	-	72.70	-
158.78	10.48	3.93	83.33	61.05	87.55	67.65	133.58	66.51
313.84	10.93	8.05	170.23	124.63	122.37	165.55	231.77	252.16
465.54	6.28	16.29	279.36	163.60	140.17	160.27	306.17	412.50
777.93	6.43	27.52	469.52	274.47	160.02	155.07	422.44	523.12
940.10	8.66	28.89	546.00	356.55	169.21	143.85	470.37	633.70
1243.24	8.63	38.49	724.05	472.08	196.63	127.39	527.87	684.60
1555.98	8.71	48.47	907.82	590.98	287.62	-	591.84	450.33
pH 3								
Initial					Equilibrium, silica gel		DTPA-Equilibrium, chitosan	DTPA-
Total Co(II)	Free Co(II)	Co(II) $EDTA^{-2}$ pK: 18.16	Co(II) $HEDTA^{-1}$ pK: 21.59	Co(II) H_2EDTA pK: 23.49	Co(II) adsorbed	$EDTA^{-4}$ released	Co(II) adsorbed	$EDTA^{-4}$ released
79.80	0.08	21.83	53.75	4.14	74.64	-	38.92	-
157.06	0.07	43.32	105.56	8.11	78.03	26.39	69.72	-
306.47	0.08	85.65	205.08	15.66	100.92	142.85	141.58	143.60
457.97	0.07	129.45	305.26	23.19	113.59	120.64	263.95	223.12
761.12	0.08	219.19	503.82	37.95	126.48	-	427.55	355.78
930.57	0	270.20	614.21	46.09	129.02	285.43	478.54	534.72
1231.17	0	362.78	808.10	60.22	137.69	216.19	555.99	485.45
1538.87	0	459.37	1004.99	74.44	127.55	145.40	610.03	490.78
pH 4								
Initial					Equilibrium, silica gel		DTPA-Equilibrium, chitosan	DTPA-
Total Co(II)	Free Co(II)	Co(II) $EDTA^{-2}$ pK: 18.16	Co(II) $HEDTA^{-1}$ pK: 21.59	Co(II) H_2EDTA pK: 23.49	Co(II) adsorbed	$EDTA^{-4}$ released	Co(II) adsorbed	$EDTA^{-4}$ released
80.00	0	63.78	16.09	0.12	32.38	35.22	11.70	68.05
157.15	0	125.87	31.04	0.24	46.76	24.35	22.24	15.04
309.21	0	249.25	59.50	0.45	74.07	37.88	51.80	47.70
460.43	0	372.92	86.85	0.66	91.29	150.47	66.30	84.03
770.98	0	628.96	140.96	1.06	110.29	86.31	136.30	221.74
927.51	0	758.89	167.38	1.24	112.91	78.59	185.81	298.38
1241.14	0	1020.63	218.90	1.61	121.85	103.32	287.28	376.78
1541.18	0	1272.77	266.47	1.94	122.46	106.84	351.64	406.67

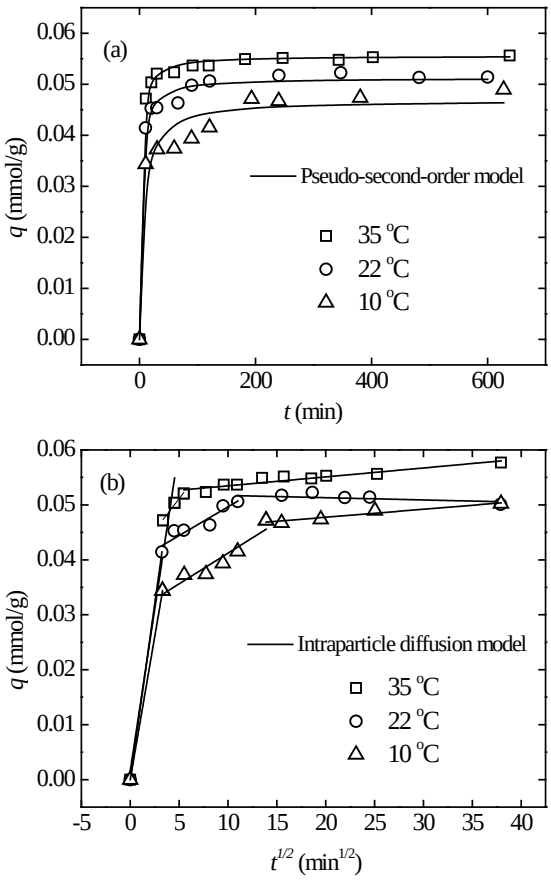

Figure S1. (a) Effect of temperature on adsorption kinetics for DTPA-silica gel in Co(II)EDTA (1:2) solution. Agitation speed: 50 rpm, Co(II) concentration: 0.34 mM, dose: 2g/L, pH 3. (b) Intraparticle diffusion plots for the results presented in Figure (a).

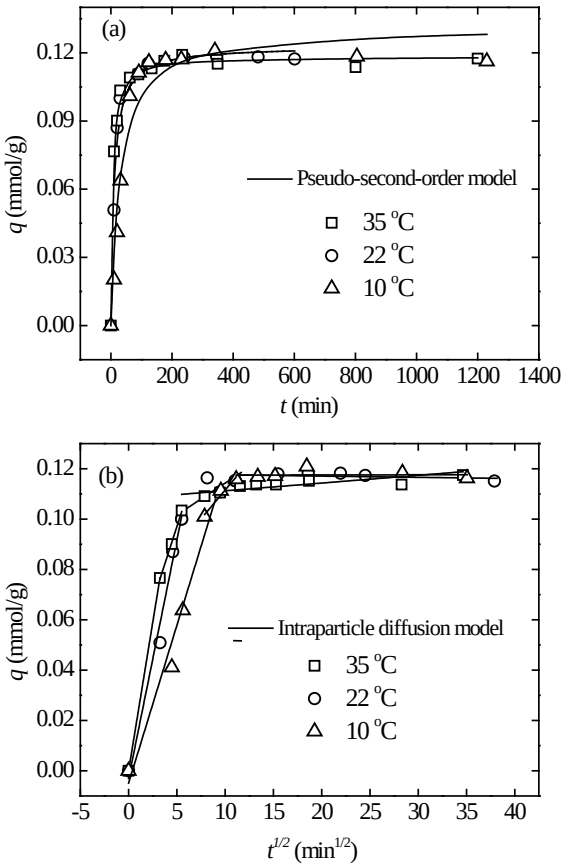

Figure S2. (a) Effect of temperature on adsorption kinetics for DTPA-chitosan in Co(II)EDTA (1:2) solution. Agitation speed: 50 rpm, Co(II) concentration: 0.34 mM, dose: 2g/L, pH 2. (b) Intraparticle diffusion plots for the results presented in Figure (a).

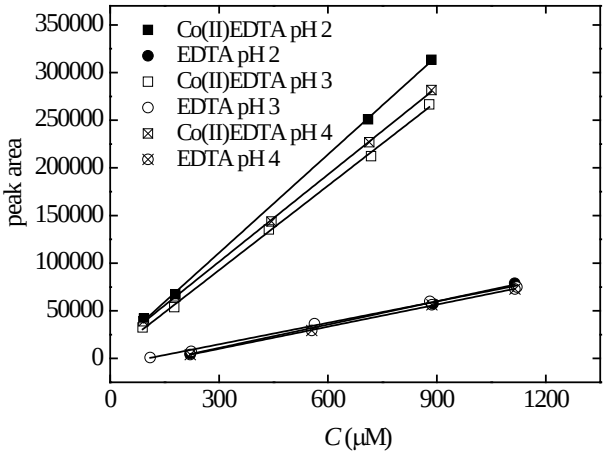

Figure S3. The effect of pH on the calibration curves of Co(II)EDTA and EDTA in Co(II):EDTA 1:2 system.

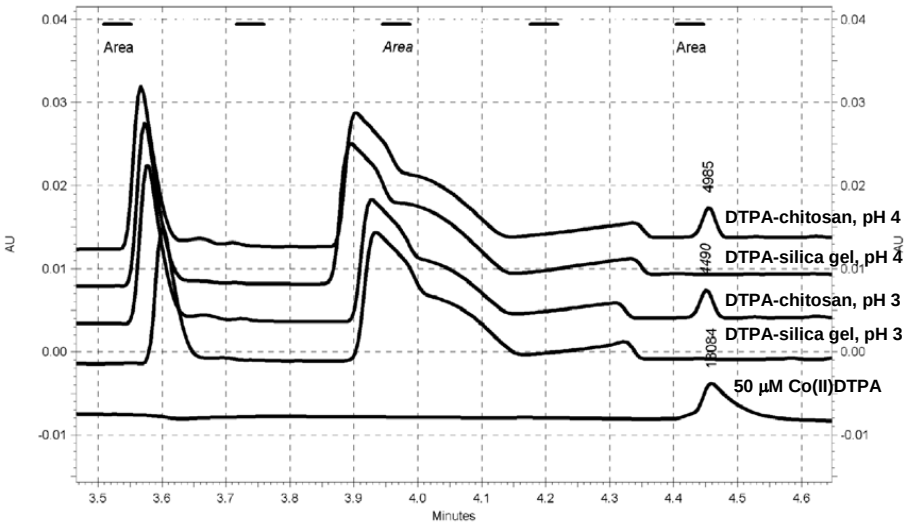

Figure S4. Leaching of DTPA at pH 3 and pH 4 measured by capillary electrophoresis.

ACTA UNIVERSITATIS LAPPEENRANTAENSIS

394. VIROLAINEN, ILKKA. Johdon coaching: Rajanvetoja, taustateorioita ja prosesseja. 2010. Diss.

395. HONG, JIANZHONG. Cultural aspects of university-industry knowledge interaction. 2010. Diss.

396. AARNIOVUORI, LASSI. Induction motor drive energy efficiency – Simulation and analysis. 2010. Diss.

397. SALMINEN, KRISTIAN. The effects of some furnish and paper structure related factors on wet web tensile and relaxation characteristics. 2010. Diss.

398. WANDERA, CATHERINE. Performance of high power fiber laser cutting of thick-section steel and medium-section aluminium. 2010. Diss.

399. ALATALO, HANNU. Supersaturation-controlled crystallization. 2010. Diss.

400. RUNGI, MAIT. Management of interdependency in project portfolio management. 2010. Diss.

401. PITKÄNEN, HEIKKI. First principles modeling of metallic alloys and alloy surfaces. 2010. Diss.

402. VAHTERISTO, KARI. Kinetic modeling of mechanisms of industrially important organic reactions in gas and liquid phase. 2010. Diss.

403. LAAKKONEN, TOMMI. Distributed control architecture of power electronics building-block-based frequency converters. 2010. Diss.

404. PELTONIEMI, PASI. Phase voltage control and filtering in a converter-fed single-phase customer-end system of the LVDC distribution network. 2010. Diss.

405. TANSKANEN, ANNA. Analysis of electricity distribution network operation business models and capitalization of control room functions with DMS. 2010. Diss.

406. PIIRAINEN, KALLE A. IDEAS for strategic technology management: Design of an electronically mediated scenario process. 2010. Diss.

407. JOKINEN, MARKKU. Centralized motion control of a linear tooth belt drive: Analysis of the performance and limitations. 2010. Diss.

408. KÄMÄRI, VESA. Kumppanuusohjelman strateginen johtaminen – Monitapaustutkimus puolustushallinnossa. 2010. Diss.

409. KARJALAINEN, AHTI. Online ultrasound measurements of membrane compaction. 2010. Diss.

410. LOHTANDER, MIKA. On the development of object functions and restrictions for shapes made with a turret punch press. 2010. Diss.

411. SIHVO, VILLE. Insulated system in an integrated motor compressor. 2010. Diss.

412. SADOVNIKOV, ALBERT. Computational evaluation of print unevenness according to human vision. 2010. Diss.

413. SJÖGREN, HELENA. Osingonjakopäätökset pienissä osakeyhtiöissä. Empiirinen tutkimus osakeyhtiölain varojenjakosäännösten toteutumisesta. 2010. Diss.

414. KAUPPI, TOMI. Eye fundus image analysis for automatic detection of diabetic retinopathy. 2010. Diss.

415. ZAKHVALINSKII, VASILII. Magnetic and transport properties of $LaMnO_{3+\delta}$, $La_{1-x}Ca_xMnO_3$, $La_{1-x}Ca_xMn_{1-y}Fe_yO_3$ and $La_{1-x}Sr_xMn_{1-y}Fe_yO_3$. 2010. Diss.

416. HATAKKA, HENRY. Effect of hydrodynamics on modelling, monitoring and control of crystallization. 2010. Diss.

417. SAMPO, JOUNI. On convergence of transforms based on parabolic scaling. 2010. Diss.

418. TURKU. IRINA. Adsorptive removal of harmful organic compounds from aqueous solutions. 2010. Diss.

419. TOURUNEN, ANTTI. A study of combustion phenomena in circulating fluidized beds by developing and applying experimental and modeling methods for laboratory-scale reactors. 2010. Diss.

420. CHIPOFYA, VICTOR. Training system for conceptual design and evaluation for wastewater treatment. 2010. Diss.

421. KORTELAINEN, SAMULI. Analysis of the sources of sustained competitive advantage: System dynamic approach. 2011. Diss.

422. KALJUNEN, LEENA. Johtamisopit kuntaorganisaatiossa – diskursiivinen tutkimus sosiaali- ja terveystoimesta 1980-luvulta 2000-luvulle. 2011. Diss.

423. PEKKARINEN, SATU. Innovations of ageing and societal transition. Dynamics of change of the socio-technical regime of ageing. 2011. Diss.

424. JUNTTILA, VIRPI. Automated, adapted methods for forest inventory. 2011. Diss.

425. VIRTA, MAARIT. Knowledge sharing between generations in an organization – Retention of the old or building the new 2011. Diss.

426. KUITTINEN, HANNA. Analysis on firm innovation boundaries. 2011. Diss.

427. AHONEN, TERO. Monitoring of centrifugal pump operation by a frequency converter. 2011. Diss.

428. MARKELOV, DENIS. Dynamical and structural properties of dendrimer macromolecules. 2011. Diss.

429. HÄMÄLÄINEN, SANNA. The effect of institutional settings on accounting conservatism – empirical evidence from the Nordic countries and the transitional economies of Europe. 2011. Diss.

430. ALAOUTINEN, SATU. Enabling constructive alignment in programming instruction. 2011. Diss.

431. ÅMAN, RAFAEL. Methods and models for accelerating dynamic simulation of fluid power circuits. 2011. Diss.

432. IMMONEN, MIKA. Public-private partnerships: managing organizational change for acquiring value creative capabilities. 2011. Diss.

433. EDELMANN, JAN. Experiences in using a structured method in finding and defining new innovations: the strategic options approach. 2011. Diss.

434. KAH, PAUL. Usability of laser - arc hybrid welding processes in industrial applications. 2011. Diss.

435. OLANDER, HEIDI. Formal and informal mechanisms for knowledge protection and sharing. 2011. Diss.

436. MINAV, TATIANA. Electric drive based control and electric energy regeneration in a hydraulic system. 2011. Diss.